The University Of Sheffield.

The genetics and evolution of iridescent structural colour in *Heliconius* butterflies

Melanie N. Brien

A thesis submitted in partial fulfilment of the requirements for the degree of Doctor of Philosophy

The University of Sheffield
Faculty of Science
Department of Animal & Plant Sciences

Submission Date
August 2019

Abstract

The study of colouration has been essential in developing key concepts in evolutionary biology. The *Heliconius* butterflies are well-studied for their diverse aposematic and mimetic colour patterns, and these pigment colour patterns are largely controlled by a small number of homologous genes. Some *Heliconius* species also produce bright, highly reflective structural colours, but unlike pigment colour, little is known about the genetic basis of structural colouration in any species. In this thesis, I aim to explore the genetic basis of iridescent structural colour in two mimetic species, and investigate its adaptive function. Using experimental crosses between iridescent and non-iridescent subspecies of *Heliconius erato* and *Heliconius melpomene*, I show that iridescent colour is a quantitative trait by measuring colour variation in offspring. I then use a Quantitative Trait Locus (QTL) mapping approach to identify loci controlling the trait in the co-mimics, finding that the genetic basis is not the same in the two species. In *H. erato*, the colour is strongly sex-linked, while in *H. melpomene*, we find a large effect locus on chromosome 3, plus a number of putative small effect loci in each species. Therefore, iridescence in *Heliconius* is not an example of repeated gene reuse. I then show that both iridescent colour and pigment colour are sexually dimorphic in *H. erato* and *H. sara*, pointing to differing selection pressures on the sexes. Structural colour, and to a lesser extent pigment colour, are condition dependent, suggesting the trait could be used as a signal of condition in mate choice. Together this work provides an understanding of the evolution of structural colour in *Heliconius*, in terms of its genetic control and its function as a signal and mimetic warning pattern.

Acknowledgements

Firstly, I would like to thank my supervisor Nicola Nadeau for the opportunity to work on this project and for her ongoing support and guidance for more than four years. It has been an amazing project to be involved with, in no small part due to her supervision, and I have learnt so much.

Thanks to my wonderful fellow lab members, Emma Curran, Juan Enciso-Romero and Vicky Lloyd, for making this project so enjoyable and for many breaks for cake during thesis writing. I am fortunate to be part of a supportive group of PhD students in the Animal & Plant Sciences department, and to have friends in Sheffield and further afield who are always willing to help, or just go to the pub.

A large part of this thesis was possible thanks to Patricio Salazar and Carlos Morochz, who organised field work in Mashpi, and Gabriela Montejo-Kovacevich who allowed me to join her field trip across Ecuador. I am grateful to Andrew Parnell for sharing his expertise and ideas for the physics side of the project, and to Jon Slate, Roger Butlin and Pasi Rastas who all gave useful advice on analyses.

Finally, thank you to my family for their endless support on this career path, especially when I said I was going to live in a jungle for three months.

Table of Contents

Abstract **3**

Acknowledgements **4**

1. General Introduction **9**

1.1 The study of structural colouration: mechanisms and functions 9

1.2 Sexual selection and condition dependence of colour traits 13

1.3 Structural colour in the *Heliconius* butterflies 15

1.4 Repeatability of colour pattern genetics 19

1.5 Outline of thesis 21

1.6 Contributions made to this thesis 22

2. Using phenotypic variation in crosses to explore the genetic basis of iridescent colour in *Heliconius erato* and *Heliconius melpomene* **23**

2.1 Summary 23

2.2. Introduction 24

2.3 Methods 27

2.3.1 Crossing Experiments 27

2.3.2 Phenotypic Analysis 29

2.4 Results 32

2.4.1 Colour variation in Heliconius erato 32

2.4.2 Colour variation in Heliconius melpomene 39

2.5 Discussion 45

2.6 Supplementary Information 49

3. Investigating the genetic basis of iridescent structural colour in the co-mimics *Heliconius erato* and *Heliconius melpomene* using Quantitative Trait Locus mapping **53**

3.1 Summary 53

3.2 Introduction 54

3.3 Methods 57

3.3.1 Experimental cross design and phenotyping 57

3.3.2 DNA extraction and sequencing 59

3.3.3 Sequence data processing 59

3.3.4 Genetic map construction 60

3.3.5 Quantitative Trait Locus mapping 61

3.4 Results 63

3.4.1 Genetic map construction 63

3.4.2 Mapping Cr and Yb/Sb genotypes 65
3.4.3 QTL scans for iridescent colour in H. erato 67
3.4.4 QTL scans for iridescent colour in H. melpomene 72
3.4.5 Comparison of maternal alleles 77
3.5 Discussion 80
3.6 Supplementary Information 85
4. Condition dependence and sexual dimorphism of *Heliconius* structural and pigment colour 103
4.1 Summary 103
4.2 Introduction 104
4.3 Methods 107
4.3.1 Butterfly specimens 107
4.3.2 Thermal stress experiments 108
4.3.3 Optical Reflectance Spectroscopy 108
4.3.4 Analysis of spectral data 110
4.3.5 Visual modelling 110
4.3.6 Scanning Electron Microscopy 112
4.3.7 Inbreeding effects 112
4.4 Results 113
4.4.1 Sexual dimorphism 113
4.4.2 Condition dependence 123
4.4.3 Scale morphology 136
4.5 Discussion 138
4.6 Supplementary Information 145
5. General Discussion 153
5.1 Research summary 153
5.2 Further research on *Heliconius* structural colour: finding genes and testing the function 154
5.3 Determining the genetic basis of condition dependent traits 157
5.4 What next for colour research? 157
References 159
Appendix 174

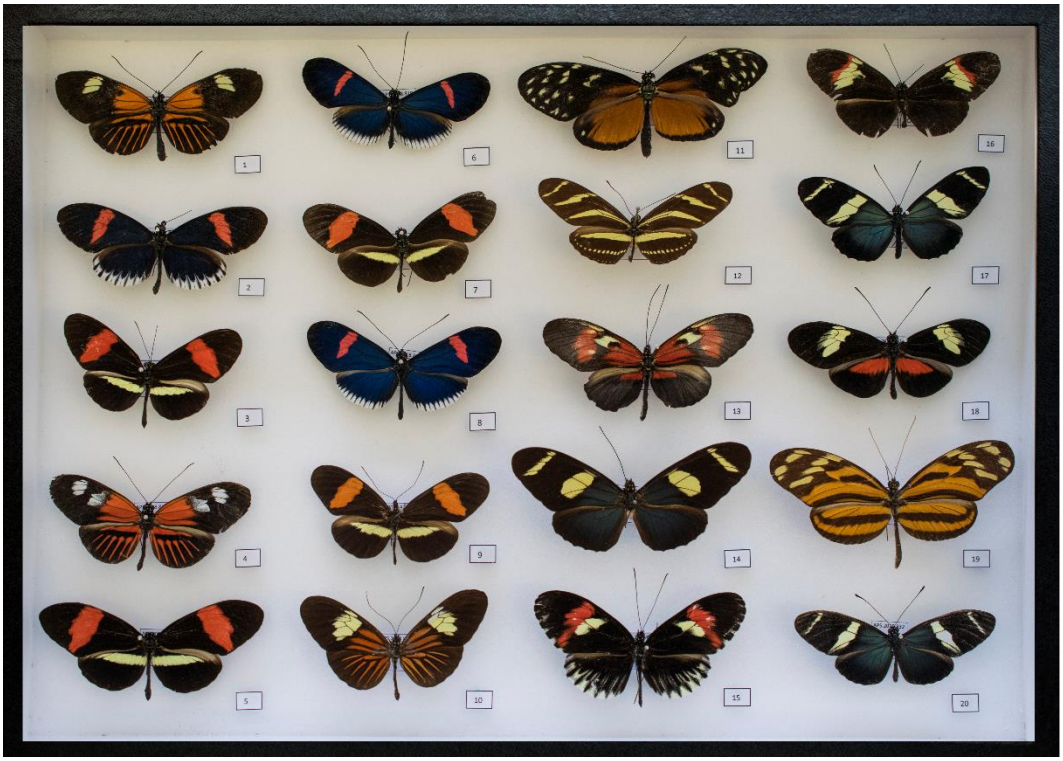

The *Heliconius* collection, Alfred Denny Museum, Sheffield, UK

Top row: *Heliconius melpomene malleti, Heliconius erato cyrbia, Heliconius hecale, Heliconius melpomene hybrid.*

Second row: *Heliconius melpomene cythera, Heliconius erato demophoon, Heliconius charithonia, Heliconius sara.*

Third row: *Heliconius melpomene rosina, Heliconius erato cyrbia, Heliconius melpomene hybrid, Heliconius himera.*

Fourth row: *Heliconius melpomene malleti, Heliconius erato colombina, Heliconius wallacei, Heliconius ismenius telchinia.*

Bottom row: *Heliconius melpomene rosina, Heliconius erato lativitta, Heliconius melpomene hybrid, Heliconius sara.*

1. General Introduction

1.1 The study of structural colouration: mechanisms and functions

The study of colouration has been crucial in understanding key concepts in evolution and genetics. Early studies on seed and flower colour in experimental crosses formed the basis of Mendelian genetics (Mendel 1865; Wheldale 1907), while others used colour variation to look at natural and sexual selection in wild populations (Kettlewell 1955; Endler 1984). More recently, advances in sequencing technology have allowed the genetic basis of colour traits to be uncovered (reviewed in Hoekstra, 2006; San-Jose and Roulin, 2017). Many of these studies have focussed on pigment colours (Hofreiter and Schöneberg 2010; Hubbard et al. 2010), but colour can also be produced by the reflection of light from nanostructures and these are known as structural colours. These form some of the most vivid and striking colours seen in nature. They are widespread and can be found on bird feathers, scales of insects and fish, and leaves of plants (Figure 1.1). One of the first major studies on structural colour in insects dates back to 1927 (Mason 1927).

Structural colours are produced from a variety of mechanisms including, but not limited to, thin-film interference, scattering and diffraction. With thin-film interference, colour is both reflected and refracted between upper and lower layers of a structure. For example, layers of keratin and air produce UV/blue colour in satin bowerbird feathers (Doucet 2006). In many butterfly species, including the bright blue *Morpho* butterflies, blue and green structural colours are produced by layered structures of chitin and air (Ghiradella 1989; Vukusic et al. 1999).

In scattering structures, light is scattered in all directions by irregularities or granules in or under a surface. The colour produced can depend on the size of the granules relative to the wavelengths of light. Coherent scattering, often found on bird feathers and butterfly scales, produces colour when structures are spaced at distances comparable to wavelengths of light, leading to reflectance of a particular wavelength (Prum et al. 1998; Prum 2006). Diffraction occurs when different

wavelengths from a ray of light are bent at varying degrees, splitting white light into its spectral colours and creating a rainbow effect. This is responsible for structural colour in a number of beetle families, shrimps and flowers (Chapman 1998; Seago et al. 2009; Sun et al. 2013).

Structural colour can be intensified by the presence of pigments, often melanin. A layer of melanin underlying the reflectors allows the formation of green colours on the elytra of *Calloodes grayanus* beetles (Parker et al. 1998). In *Heliconius doris*, blue-reflecting structures together with yellow pigments produce a green colour (Wilts et al. 2017).

Structural colours have unique properties which make them ideal for signalling – either for an individual to communicate with conspecifics or to avoid predation. Reflectance of structural colours is generally much brighter than pigment colours (Osorio and Ham 2002). High chromatic and achromatic contrast of structural colour allows it to stand out in a complex habitat, such as a dense forest where the natural background is dark vegetation or bark. In a comparative study by Douglas et al. (2007), species with polarised iridescence were more likely to inhabit forests with complex light environments. In butterflies, colour is important as a long-range signal to recognise conspecifics, while scent likely takes over as a close-range signal (Rutowski 1991). *Morpho* butterflies use their bright blue iridescence as a long-range signal and are reported to be easily seen from low-flying aircraft (Silberglied 1984). Iridescent colours are directional and angle-dependent, allowing for flashes of colour or targeting of signals to specific receivers (Vukusic 2001; Vukusic et al. 2002).

Nanostructures can reflect UV wavelengths as well as wavelengths in the human visible spectrum, and this is important when considering the visual system of the signal receiver. UV can be used as a private communication channel if a species' predators cannot see these short wavelengths (Cummings et al. 2003). Structures also allow the production of blue colours and nearly all blue colours in nature are structurally produced (reviewed in Bagnara, Fernandez and Fujii, 2007). Blue structural colour is used for species recognition within groups of related butterflies (Silberglied and Taylor 1978; Bálint et al. 2012). In another example of species

recognition, male guppies (*Poecilia reticulata*) have more iridescent spots in low-predation populations compared to high-predation populations, and females use this, along with other traits, to choose males from their own population (Endler and Houde 1995).

To avoid predation, some animals use structural colour as camouflage. Iridescent green leaf beetles use their colour to look like water droplets on a leaf, which is cryptic in the foliage of a rainforest (Parker et al. 1998). As green pigments are rare in animals, structural colours can provide efficient and long-lasting camouflage (Seago et al. 2009).

Multiple studies have suggested a role of iridescent colours in mate choice (Silberglied and Taylor 1978; Brunton and Majerus 1995; Andersson et al. 1998; Kemp 2007; Papke et al. 2007). Much of this research has focussed on birds. For example, Velvet Asity, *Philepitta castanea*, males develop a pair of bright blue structurally coloured caruncles above the eyes, which then breakdown completely at the end of the breeding season (Prum and Razafindratsita 1997). Few studies, however, have experimentally tested mate choice of these signals. Nevertheless, sexual selection could be important in the evolution of such colours.

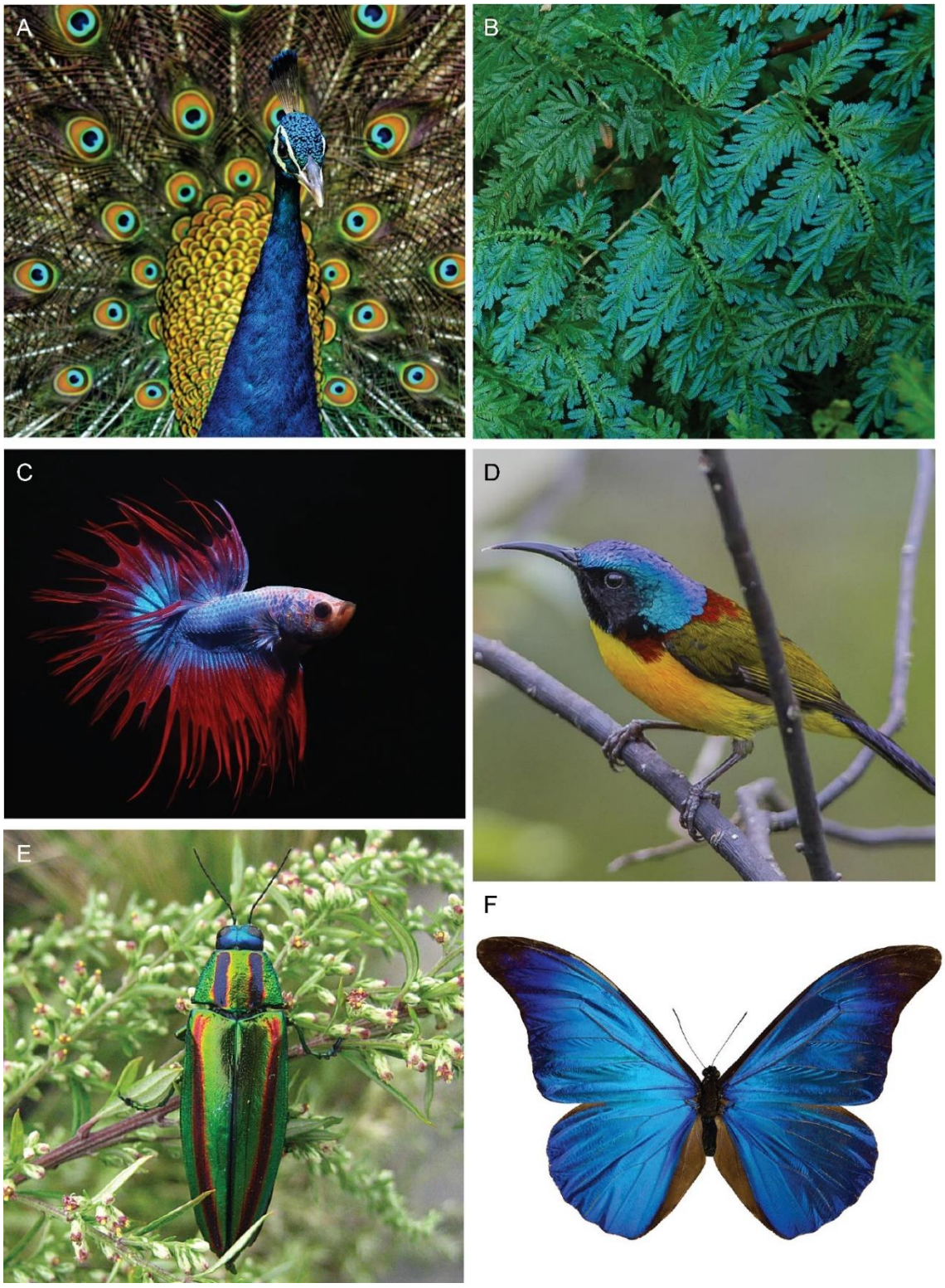

Figure 1.1 Examples of structural colour found in nature. **A.** Male peacock, *Pavo cristanus* (credit: Jatin Sindhu). **B.** Leaves of the tropical *Selaginella* plant (credit: L. Shyamal). **C.** Siamese fighting fish, *Betta splendens*. **D.** Green-tailed sunbird, *Aethopyga nipalensis* (credit: Dibyendu Ash). **E.** Jewel beetle, *Chrysochroa fulgidissima* (credit: Brian Adler). **F.** *Morpho* butterfly *Morpho rhetenor* (credit: Didier Descounes).

1.2 Sexual selection and condition dependence of colour traits

Colour is used as a secondary sexual signal in numerous systems. Darwin (1874) described many examples, showing that these traits are exaggerated in the sex which needs to attract a mate, usually the male, but only later were the mechanisms of sexual selection fully explored (Fisher 1930; Williams 1966; Zahavi 1975). If the trait has a survival advantage, males with this trait will be selected by females so that the offspring will inherit the genes for the trait and the fitness advantage. Genes for female preference of the trait will also be passed to the next generation. As the trait becomes selected for, and female preference spreads, the trait evolves further, eventually reaching a point when it becomes detrimental. This balance between reduced survival and increased mating frequency maintains the presence of the trait.

Male secondary sexual traits are generally not directly beneficial to males themselves but are linked to some benefit to the female and/or her offspring, leading to survival of her own genes, such as food, protection or parental care. There are numerous benefits to choosing the 'best' mate – they may have better fecundity, be more able to provide food, provide better parental care, offer better territory or provide protection from predators (Andersson 1994). As well as these direct benefits, mates may also be selected for traits which signal their genetic quality, an indirect benefit, leading to the production of offspring of higher genetic quality (Andersson and Simmons 2006). Historically much of the literature on mate choice has focussed on female choice, but male choice is widespread, particularly among insects (Bonduriansky 2001). Male mate choice is common when there is large variation in female fecundity, which is generally positively associated with body size (Honěk 1993; García-Barros 2000; Allen et al. 2010).

Along with within-species variation, sexual selection of traits can lead to sexual dimorphism – differences in morphology, behaviour, physiology or life history traits between males and females. Sexual selection is generally reported to be the major selection pressure in the evolution of sexual dimorphism (female choice of the ornament), but natural selection, in the form of increased predation for non-cryptic colouration, for example, will also play some part (Kottler

1980). Sexual dimorphism may also be used for non-sexual functions, such as female-limited mimicry (Kunte 2009). Dimorphism in body size can relate to mating strategy – in an extreme example, male elephant seals weigh three times the females to defend polygamous female groups from other males (Le Boeuf 1974). Some sexually dimorphic traits are used for sex recognition within species (Fisher 1930). More specifically, dichromatic structural colour is seen in many groups, for example, birds (Owens and Hartley 1998) and jumping spiders (Lim and Li 2006).

In many species, certain traits show significant variation and are favoured as sexual signals because they also provide information about an individual's quality. Such traits are condition dependent and are selected because they reflect the ability of a potential mate to provide direct or indirect benefits to the partner. To be an honest signal of condition there must be some cost to producing the trait. This cost could be increased visibility to predators or a physical cost such as loss of mobility, and good health or genetic quality is needed to produce this character and offset the survival disadvantage (Andersson 1994).

Condition dependence of colour has been investigated in numerous ways. The brightness of orange carotenoid spots in guppies increases with the amount of carotenoid in the diet, and so reflects the foraging ability of the male (Endler 1980). Structural plumage colouration in birds can signal nutrition (Keyser and Hill 1999; McGraw et al. 2002), parasite infection (Doucet and Montgomerie 2003; Hill et al. 2005), stress resilience (Taff et al. 2019), and even cognitive ability (Cauchard et al. 2017). In damselflies, hue of the structural colour varies with fat stores, signalling the nutritional status of the male (Fitzstephens and Getty 2000). In fatter males, lamellae are more compressed and so a blue colour is produced via multi-layer interference reflectors. When thinner, the colour produced is green as the lamellae reflect longer wavelengths. To produce bright structural colours, it is likely that good condition is necessary to produce the highly organised nanostructures.

Condition dependent traits are not always sexually selected and although condition dependence is a well-studied theory, Cotton et al. (2004) suggest that many previous studies have made

assumptions that condition dependent traits are sexually selected by not measuring a non-sexual trait as a control, or accounting for body size variation. On the other hand, not all models of sexual selection require traits to be condition dependent (Prum 2010). In sensory bias models for example, pre-existing biases of the sensory or neural systems in animals allow certain traits to be selected for in mate choice, e.g. guppies have an innate preference for the colour orange, possibly linked to food detection (Rodd et al. 2002).

1.3 Structural colour in the Heliconius butterflies

The *Heliconius* butterflies (Nymphalidae: Heliconiini) comprise a group of around 50 species found across the neotropics, from the southern USA to northern Argentina (Jiggins 2017). Their huge diversity in wing colouration and pattern led Henry Walter Bates to develop the theory of mimicry (Bates 1862) and have fascinated many evolutionary biologists since. Colour patterns of hundreds of subspecies show examples of both convergent and divergent evolution, with many species forming mimicry rings. *Heliconius* are toxic due to cyanogenic glucosides which they can synthesise themselves and sequester from *Passiflora*, their larval hostplants. Their bright red, yellow and black pigment colours act as aposematic warning signals to predators, and thus are an example of Müllerian mimicry.

Heliconius also display structural colour, and in comparison to the well-studied pigment colours, very little is known about the development and genetic basis of these. Structural colour has evolved multiple times within the *Heliconius* genus (Kozak et al. 2015). In some species, all subspecies have iridescent colour. In particular, one monophyletic group contains seven iridescent specialists – *Heliconius antiochus, H. leucadia, H. hewitsoni, H. sapho, H. congener, H. eleuchia* and *H. sara* (Figure 1.2). Iridescence is thought to have arisen in the common ancestor of this group 2-5 million years ago (Kozak et al. 2015; Parnell et al. 2018). Other species such as *H. cydno* and *H. wallacei* have evolved the colour more recently, possibly under selection pressure to mimic other species.

Heliconius erato and *Heliconius melpomene* are two co-mimicking species which diverged around 10-13Mya (Kozak et al. 2015) with each evolving around 25 different colour pattern races (Sheppard et al. 1985) (Figure 1.3). Most of the different colour patterns are produced by pigment colours, but subspecies found west of the Andes in Ecuador and Colombia also have an iridescent blue structural colour. *H. erato cyrbia* and *H. melpomene cythera* found in Western Ecuador have the brightest iridescence. The Panamanian subspecies *H. erato demophoon* and *H. melpomene rosina* have only pigment colour. A hybrid zone forms between the iridescent and non-iridescent groups where they meet near the border between Panama and Colombia, and here subspecies with intermediate levels of iridescence can be found (Curran 2018).

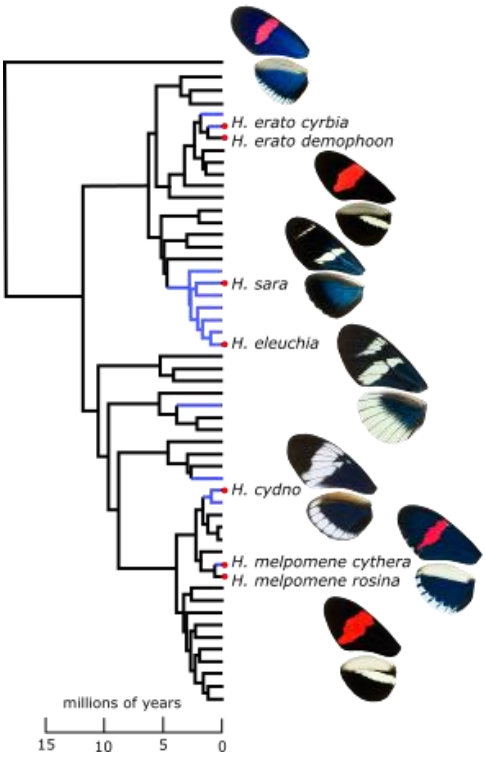

Figure 1.2: Phylogeny of some of the iridescent *Heliconius* species and subspecies. Blue branches indicate the inferred presence of blue iridescent colour. From Parnell et al. (2018).

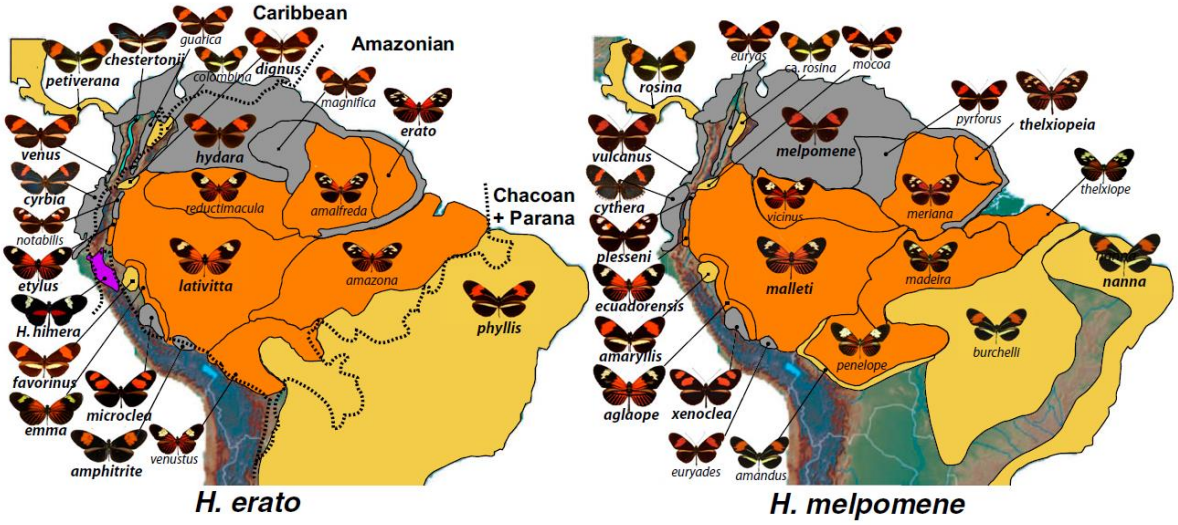

Figure 1.3: Distribution of mimetic colour pattern races in *H. erato* and *H. melpomene* in Central and South America. From Hines et al. (2011).

Butterfly wing scales develop during the first few days of the pupal stage. Each scale forms from a specialised epidermal cell as a long, flattened extension of the cuticle (Nijhout 1991). Densely packed F-actin filaments elongate to form thick bundles which are regularly spaced and precisely orientated. In the later pupal stages, the scale cells die leaving a chitin structure (Dinwiddie et al. 2014). There are two types of scales on butterfly wings, cover and ground, both around 100µm long. The upper surfaces of scales are composed of longitudinal ridges connected by cross-ribs (Figure 1.4). These ridges can be made up of layered lamellae and micro-ribs. The upper surface is connected to the lower lamina by trabeculae (Ghiradella and Radigan 1976). To date, two main mechanisms have been shown to produce structural colour in *Heliconius* scales. Thin-film interference from the lower laminae produces a blue colour in *H. doris*, while multi-layered lamellae produce the colour in other species including *H. erato* and *H. sara* (Wilts et al. 2017). In these layered ridge reflectors, ridge spacing is correlated with brightness of iridescence, with narrower spacing between ridges producing brighter colour. Compared to non-iridescent scales,

lamellae on iridescent scales are layered, producing chitin/air interfaces, resulting in constructive interference (Parnell et al. 2018).

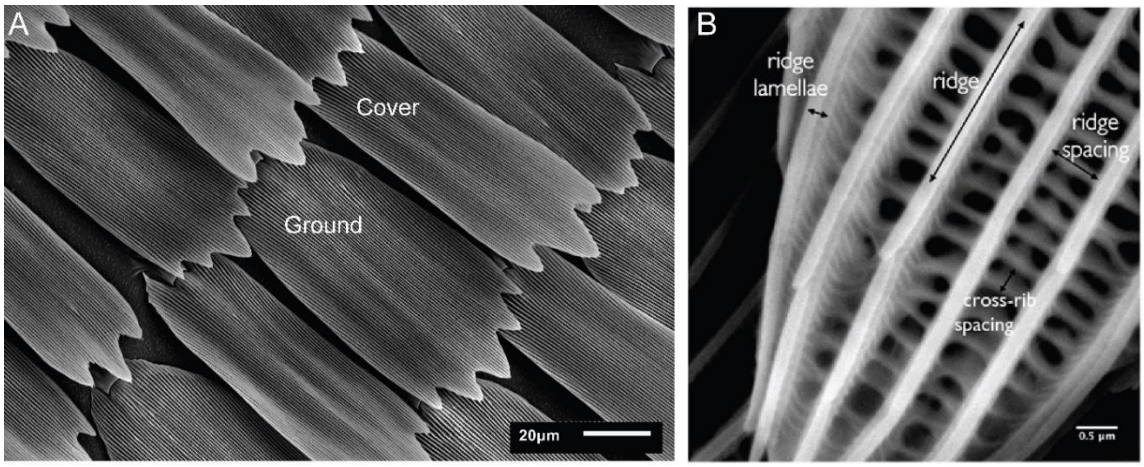

Figure 1.4: **A.** Scanning electron microscope image of a *Heliconius* scale. Cover and ground scales slightly overlap, with cover scales forming the uppermost layer. **B.** Longitudinal ridges run down the length of the scale. These are made up of ridge lamellae and joined by perpendicular cross-ribs.

The ecological function of iridescent colour is becoming more widely investigated in *Heliconius*. Polarised light (Sweeney et al. 2003) and UV/yellow wing patterns (Bybee et al. 2012) seem to be important in allowing butterflies to recognise conspecifics while still mimicking colour patterns of other species. McCulloch et al. (2016) found that the *H. erato* compound eye is sexually dimorphic in that females express a duplicated UV opsin, meaning they are better able to discriminate colours in the shorter wavelengths than males, who express only one UV opsin. This suggests that UV reflectance may be particularly important as a signal in *Heliconius* and that these signals are being used differently by the sexes (Thurman and Seymoure 2016).

The use of colour and pattern as sexually selected signals may conflict with selection for mimicry. In mating trials, co-mimics *H. erato* and *H. melpomene* spent similar time courting each species, suggesting that mimicry reduces species recognition (Estrada and Jiggins 2008). However, assortative mating was shown between divergent colour patterns (Merrill et al. 2014). In these trials, iridescent *H. erato cyrbia* males were more likely to approach conspecifics than

heterospecific *H. himera*. Divergence in warning colour patterns and in mate preference can also lead to reproductive isolation and speciation, making colour pattern a 'magic trait' (Merrill et al. 2012; Thilbert-Plante and Gavrilets 2013). Strong genetic associations between colour pattern mating cues and mate preference have been found in *Heliconius* (Merrill et al. 2019), suggesting these traits will facilitate speciation despite gene flow.

1.4 Repeatability of colour pattern genetics

A fundamental question in evolutionary biology asks how repeatable is evolution? If evolving traits are restricted to certain genetic pathways, then this will limit the number of ways a phenotype can evolve. To investigate this question we can use organisms that have evolved convergent traits. These are phenotypes that have evolved in independent lineages in response to similar selection pressures. A number of reviews suggest that mutations are restricted to certain genes, creating hotspots of evolution (Stern and Orgogozo 2009; Nadeau and Jiggins 2010), and so mutations are not found randomly across the genome. For example, the gene which encodes the melanocortin-1 receptor (*Mc1r*) is involved in melanin pigmentation and colour variation in birds (Mundy et al. 2004; Corso et al. 2016), mammals (Nachman et al. 2003; McRobie et al. 2009) and reptiles (Rosenblum et al. 2006). Convergent evolution is often separated from the term parallel evolution. Whereas convergent evolution refers to similar traits independently evolving in distantly related species, parallel evolution can be used for traits repeatedly evolving in closely related species and using similar genetic pathways. However, genetic studies have shown that similar traits can evolve using the same or different genetic mechanisms, independent of relatedness, and so these two terms are often used interchangeably. Thus Arendt & Reznick (2008) suggest using the term convergent evolution in all cases.

In *Heliconius*, pigment colour patterns are largely determined by a small number of genes which are homologous across species. Extensive research has uncovered a 'toolkit' of five loci which control much of the colour pattern variation in *Heliconius* species, and some other Lepidoptera (reviewed in Nadeau, 2016). In *Heliconius*, the gene *cortex* controls yellow and white colour

pattern elements (Nadeau et al. 2016). This gene has also been shown to regulate melanin pigmentation in the peppered moth (van't Hof et al. 2016). At the same genomic location, a supergene controlling multiple colour patterns was found in *Heliconius numata* (Joron et al. 2006). The transcription factor *optix* is responsible for most red and orange colour pattern elements in *H. erato* and *H. melpomene*, as well as *H. cydno*, a species closely related to *melpomene* (Reed et al. 2011). The *WntA* gene controls various colour pattern characteristics by controlling the size and shape of black pattern elements, which in turn affects the appearance of the yellow and white areas (Martin et al. 2012). A further locus, *K*, switches between white and yellow colour elements and this was recently shown to be due to a duplication of the transcription factor *aristaless*, found on chromosome 1 (Westerman et al. 2018). Finally, the locus *Ro* controls rounding and shape of the forewing band (Sheppard et al. 1985; Nadeau et al. 2014), and this is thought to be the gene *ventral veins lacking* (Van Belleghem et al. 2017; Morris et al. 2019).

These examples have all focussed on phenotypes controlled by a single gene but less is known about gene reuse for complex traits. We can use crosses between different populations to determine the genetic basis of a phenotypic trait, and this is important as the genetic architecture of a trait determines how it can evolve. Quantitative Trait Locus (QTL) mapping can be used to look for associations between genomic regions and phenotypic variation, and determine the effect size of each locus. This is a 'forward genetics' approach which starts with a trait of interest, then identifies the loci controlling the trait. For example, a QTL analysis in *H. erato* and *H. himera* crosses confirmed that a set of major effect loci control most colour pattern variation and that a single locus controlled 87% of the variation in the amount of white or yellow scales on the forewing (Papa et al. 2013). For other traits, such as the amount of red in the forewing band, they found five QTL which together explained 88% of the variation. More large-scale mapping studies are needed to uncover the minor effect QTL which modify the colour pattern elements controlled by the large effect loci.

With mimetic colour patterns, two or more species will converge on the same phenotype. We can say that mimicry is a type of convergence in which the optimal phenotype is determined by a phenotype already present, rather than the result of an environmental challenge (Jiggins 2017). The breadth of work on *Heliconius* colour pattern fits with the 'two-step model' of mimicry (Nicholson 1927; Turner 1977), in which an initial mutation produces a large enough change to protect against predation, but a second set of smaller mutations are needed to perfect the mimicry (Papa et al. 2013).

1.5 Outline of thesis

While the properties and physical nanostructures of structural colours have been well-studied, we know very little about their genetic architecture. In this thesis, I aim to explore iridescent colour in *Heliconius* butterflies in terms of convergent evolution in co-mimics and its adaptive function, to link phenotype, genotype and function.

Chapters 2 and 3 make use of crosses between iridescent and non-iridescent races of *H. erato* and *H. melpomene* to look at the genetic basis of iridescent colour in these co-mimics. In Chapter 2, I compare phenotypic variation in the offspring of the crosses, using a method of measuring blue iridescent colour from photographs. I demonstrate continuous variation in colour and look for patterns of segregation with Mendelian colour pattern loci. I use these results to estimate the number and distribution of loci controlling iridescence and compare this between the two species. Part of this chapter has been published in the journal Interface Focus. This paper can be found in the Appendix.

In Chapter 3, I aim to determine the genetic basis of iridescent colour in the same crosses. I ask whether this convergent phenotype is driven by the same genetic architecture. Making use of high-quality reference genomes and RAD-sequencing, I use a Quantitative Trait Locus (QTL) mapping approach to determine genomic regions associated with iridescence. I look at how the

distribution of these loci compares between the two mimetic species and if this provides evidence for gene reuse in parallel evolution of this quantitative trait.

Chapter 4 looks at the possible adaptive function of iridescence in *Heliconius* and evidence for its use as a signal in sexual selection. Here I focus on two species, *Heliconius sara* which has blue/green structural colour in all its races, and *H. erato*, which has blue structural colour in a small number of races. Firstly, I look for sexual dimorphism in both structural and pigment colour, measuring reflectance of UV and visible wavelengths using optical spectroscopy. Within-species variation of structural and pigment colour has not previously been investigated in multiple *Heliconius* species. I then use thermal stress experiments to determine if iridescence is a condition dependent trait. I measure the impact of stressful environmental conditions during development on structural colour, pigment colour and body size. I use visual modelling to assess whether butterflies and their predators can distinguish differences in colour between sexes and treated groups. Lastly, I begin to explore how temperature is affecting scale structure morphology.

Finally, Chapter 5 discusses the main findings of this thesis and identifies some unanswered questions about *Heliconius* structural colour evolution.

1.6 Contributions made to this thesis

A large part of this thesis focuses on experimental crosses which were undertaken at Mashpi Reserve, Ecuador. This work was organised by Patricio Salazar, Carlos Morochz and Nicola Nadeau, with help from Darwin Chalá, Emma Curran, Juan López, Gabriela Irazábel and staff at Mashpi Lodge. For Chapter 3, the *H. erato* linkage map was made by Pasi Rastas and I used scripts written by Victor Soria-Carrasco for processing of sequence reads. In Chapter 4, some of the *H. erato* reflectance measurements were provided by Adam Gillis, wing length measurements were taken by Hannah Bainbridge and Harriet Smith, and microscopy images were taken with help from Andrew Parnell and Victoria Lloyd. Processing of reflectance data was improved by a python script provided by Juan Enciso-Romero.

2. Using phenotypic variation in crosses to explore the genetic basis of iridescent colour in *Heliconius erato* and *Heliconius melpomene*

2.1 Summary

Heliconius butterflies have been widely studied for their diversity and mimicry of wing colour patterns. Much of this research has focussed on pigment colour and patterning which has been shown to be controlled by a small number of large effect loci that are homologous across species. Some species also produce iridescent structural colours and despite iridescence evolving multiple times in this genus, little is known about the genetic basis of this colour. Here we use crosses between iridescent and non-iridescent races of each of two mimetic species, *Heliconius erato* and *Heliconius melpomene*, to study phenotypic variation in the resulting F2 generation. Using measurements of blue colour from photographs, we find that iridescent colour is a quantitative trait controlled by multiple genes in both species, but that the genomic regions involved are different between species. In *Heliconius erato*, there is strong evidence for large effect loci on the Z sex chromosome, whereas in *Heliconius melpomene* there seem to be loci linked to the region containing the gene *cortex*, which controls pigment colour pattern elements. This is one of the first studies to begin to uncover the genetic control of structural colour in any system.

2.2. Introduction

Understanding the genetic basis of differentiation in traits is vital to deciphering mechanisms of adaptation and speciation. The study of animal colouration and its inheritance has allowed geneticists such as Haldane to determine key genetic concepts (Haldane 1927). Often studies have focussed on colour traits which have a simple genetic architecture involving a single gene with clear inheritance patterns. However, natural populations more frequently exhibit extensive phenotypic variation. Traits that show continuous variation and do not fall into discrete categories are known as complex or quantitative traits because they are controlled by multiple genetic loci and are also often influenced by the environment. The way in which traits evolve and respond to natural selection is determined by their genetic architecture - a term for all the genetic factors which influence a trait, including the number of genes and their relative contribution to the trait (Griffiths et al. 2015).

The fundamental step when studying genetic architecture is to determine whether a trait is controlled by few major effect genes, or a large number of genes with relatively small effects (Lynch and Walsh 1998), and how much variation is controlled by the environment. Genetic approaches to study quantitative traits look for associations between segregating molecular markers and variation in phenotype. A popular method for this is Quantitative Trait Locus (QTL) mapping, which has been used to study continuous phenotypic variation in a number of different contexts (Barton and Keightley 2002; Slate 2005). Classically, geneticists used biometrical genetics methods which involve estimating the number of genes involved in controlling a trait with the use of phenotype distributions across segregating generations (Lynch and Walsh 1998). Experimental genetic crosses between two parental populations are generally used for both of these approaches. They are particularly useful as genes controlling different aspects of a trait can segregate in the F2 generation. Traits that are controlled by a single locus of major effect will segregate according to Mendelian ratios, with 50-100% of individuals in the F2 generation having phenotypes the same as one or other of their parents (depending on dominance of the alleles).

The more individuals there are with intermediate phenotypes, the more loci are likely to be involved, as a greater number of allelic combinations will be possible.

Wing patterns of the butterfly genus *Heliconius* are well-known for their diversity and show examples of both convergent evolution among distantly related species, and divergent evolution between closely related species (Merrill et al. 2015). *Heliconius erato* and *Heliconius melpomene* are two distantly related species that diverged around 10-13 million years ago (Kozak et al. 2015) and have evolved strikingly similar colour patterns within more than 25 parapatric races (Papa et al. 2013; Nadeau et al. 2014). The 'rayed' or 'postman' colour pattern races are an example of Müllerian mimicry and act as brightly-coloured aposematic warnings to predators, mainly insectivorous birds (Joron et al. 2006).

Variation in pigment colour and pattern in *Heliconius* is mostly controlled by a small number of major effect loci. Many of these loci map to the same positions in the genomes of distantly related species (Joron et al. 2006; Baxter et al. 2008; Papa et al. 2013; Nadeau 2016). In *Heliconius erato*, the locus *Cr*, found on linkage group 15, controls the presence or absence of a yellow bar or white margin on the hindwings. In *H. melpomene*, three tightly-linked loci (*Yb*, *Sb* and *N*) map to the same location as *Cr* and control similar colour pattern elements (Mallet 1989; Mallet et al. 1990; Joron et al. 2006). These are likely to be alleles of the gene *cortex* (Nadeau et al. 2016). The transcription factor *optix* on chromosome 18 controls most red and orange elements (Reed et al. 2011), while the gene *WntA* affects the appearance of these elements by controlling the size and shape of the black patterning (Martin et al. 2012). Locus *K*, on linkage group 1, can switch white elements to yellow in *H. melpomene* crosses (Joron et al. 2006; Westerman et al. 2018).

In addition to pigment colour patterns, several species of *Heliconius* exhibit blue iridescent colour. This angle-dependent structural colour is produced by thin-film interference, in which light is reflected from nanostructures on the scales of the wings (Parnell et al. 2018). *H. erato cyrbia* and *H. melpomene cythera* are mimetic subspecies, found in Western Ecuador, which have both evolved iridescent colour. Races found further north in Panama have only pigment colour

and hybrid zones arise between the iridescent and non-iridescent races, where populations with intermediate levels of iridescence can be found. To date, little is known about the genetic basis of iridescent colour, despite it evolving multiple times within the genus. Previous researchers have noted that levels of iridescence vary in F2 hybrid crosses and appears to do so in a continuous manner, but have not attempted to verify this quantitatively (Emsley 1965; Papa et al. 2013). The presence of intermediate forms in hybrid zones suggests that the trait is unlikely to be a Mendelian trait, but rather controlled by more than one gene.

While diversity in *Heliconius* warning colour patterns is caused by a few major effect loci, quantitative traits such as iridescence may show less genetic parallelism. The study of mimicry often focuses on the number of steps and the effect sizes of mutations needed to resemble the future mimic (Papa et al. 2013). Experiments with *Heliconius* have repeatedly shown strong selection against novel patterns in the field (Mallet and Barton 1989; Kapan 2001), meaning the initial steps of mimicry would need to be large enough for an individual to roughly resemble the local phenotype before smaller mutations can refine it. Because of this, the genes controlling iridescence would be expected to follow the same pattern, with a few major effect loci and a larger number of smaller effect.

Although the colour patterns of iridescent *H. erato* and *H. melpomene* mimic each other, the level of iridescence between the two species is not a perfect match. The brightness of the blue is visually not as strong, and the reflectance not as high, in *melpomene* (Parnell et al. 2018), and therefore we would expect there to be some differences in the genetic basis of the trait. The presence or absence of iridescence is genetically determined, as these differences are maintained when individuals are reared under the same conditions. Here we take the first steps in determining the genetic basis of iridescent colour in mimetic *Heliconius erato* and *Heliconius melpomene*. By measuring phenotypic variation in iridescence, we aim to show if it is a quantitative trait controlled by multiple genes. We can determine the approximate location of these genes in the

genome by seeing if iridescence segregates with sex or with the known colour pattern loci in the crosses.

2.3 Methods

2.3.1 Crossing Experiments

Experimental crosses were performed using geographical races of *Heliconius erato* and *Heliconius melpomene*. The non-iridescent races *H. erato demophoon* and *H. melpomene rosina* were collected from Gamboa, Panama (9.12ºN, 79.67ºW) in May 2014, then transported to Mashpi, Ecuador (0.17ºN, 78.87ºW), where they were kept as stocks. Iridescent *H. erato cyrbia* and *H. melpomene cythera* were collected from the area around Mashpi. For *H. melpomene*, *rosina* were crossed with *cythera*, then the F1 generation crossed with each other to produce an F2 generation. Similarly, for *H. erato*, *demophoon* were crossed with *cyrbia*, and the F1 generation crossed, along with the addition of 2 backcrosses between the F1 and *cyrbia* (Figure 2.1). Crosses were reciprocal, so that in roughly half of the F1 crosses the female was the iridescent race and the male non-iridescent, and vice versa. In line with previous studies with intraspecific *Heliconius* hybrids (Mallet 1989; Papa et al. 2013), races readily hybridised and we did not observe any evidence of differing success between the reciprocal crosses. Crosses were performed at the insectary in Mashpi Reserve over a period of 2 years. *Passiflora* species were provided as larval food plants and for oviposition, and butterflies were given *Lantana camara* and other locally collected flowers, plus sugar solution (10%) and pollen to feed. The bodies of the parents and offspring were preserved in NaCl saturated 20% dimethyl sulfoxide (DMSO) 0.25M EDTA solution to preserve the DNA, and the wings stored separately in glassine envelopes.

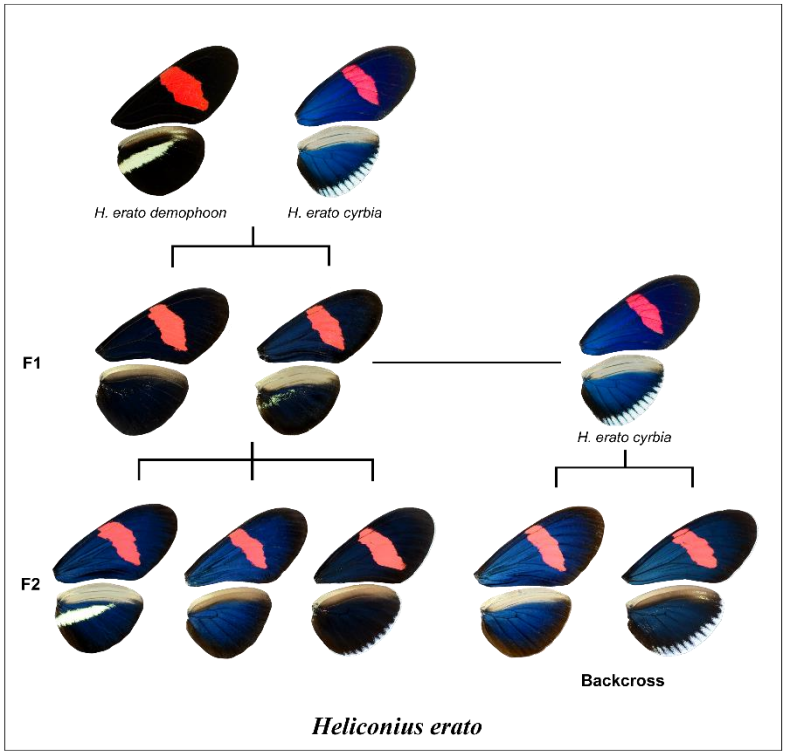

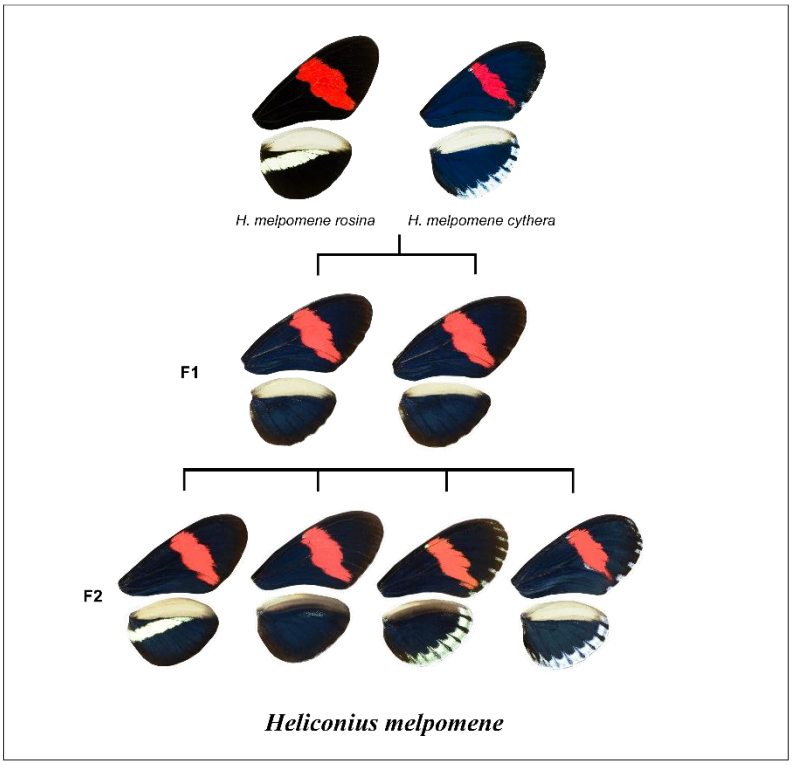

Figure 2.1: Cross design showing the parental, F1, F2, and backcross (BC) generations of *H. erato*, and the parental, F1 and F2 generations of *H. melpomene*. The F2 show examples of colour pattern variation, including the hindwing yellow bar and the white margin, controlled by the *Cr* and *Yb/Sb* loci, and in *H. melpomene*, the yellow hindwing margin.

A total of 302 *H. erato* parents and offspring from 14 crosses and wild caught individuals were used in the analysis (12 *demophoon*, 51 *cyrbia*, 60 F1, 114 F2, 65 backcross). The direction of the F1 and F2 crosses is shown in Table 2.1 (further details of each cross in Table S2.1). A total of 357 *H. melpomene* individuals from 14 crosses were used (12 *rosina*, 22 *cythera*, 109 F1, 214 F2; Table 2.2 and Table S2.2).

Table 2.1. *H. erato* crosses performed and the number of offspring produced from each.

H. erato cross type	Number of crosses	Total number of offspring
F1: *demophoon* ♂ x *cyrbia* ♀	2	32
F1*: cyrbia* ♂ x *demophoon* ♀	3	28
F2: *cyrbia* maternal grandfather	3	100
F2: *demophoon* maternal grandfather	3	14
Backcross: *cyrbia* ♂ x (*demophoon* ♂ x *cyrbia* ♀)	2	16
Backcross: *cyrbia* ♀ x (*cyrbia* ♂ x *demophoon* ♀)	1	49

Table 2.2: *H. melpomene* crosses performed and the number of offspring produced from each.

H. melpomene cross type	Number of crosses	Total number of offspring
F1: *rosina* ♂ x *cythera* ♀	4	55
F1: *cythera* ♂ x *rosina* ♀	5	54
F2: *rosina* maternal grandfather	3	97
F2: *cythera* maternal grandfather	2	117

2.3.2 Phenotypic Analysis

All butterfly wings were photographed flat under standardised lighting conditions using a mounted Nikon D7000 DSLR camera with a 40mm f/2.8 lens set to an aperture of f/10, a shutter speed of 1/60 and ISO of 100. Lights were mounted at a fixed angle of 45 degrees to maximise the observed blue reflection from the iridescent wing regions. All photographs also included an X-Rite Colour Checker to help standardise the colour of the images. RAW format images were standardised using the levels tool in Adobe Photoshop CS2 (Version 9.0). Using the colour histogram plugin in ImageJ (Abramoff et al. 2004; Comeault et al. 2016), red-green-blue (RGB) values were recorded from two sections of the wings and averaged (Figure 2.2). These areas were

chosen because the scales on these sections of the wings close to the body tended to be the least damaged and worn, so a more accurate measurement of the colour could be taken, and the wing venation was used as a marker to allow the same areas to be measured each time.

Blue reflection from the iridescent wing regions was measured as variation in blue-red (BR) colour. This was calculated as (B-R)/(B+R), with -1 being completely red and 1 being completely blue. The level of UV reflectance could not be measured from our photographs. Previous spectral measurements of the wing reflectance show that peak reflectance for *H. erato cyrbia* is just below the visible range at about 360-370nm, with much of the reflectance being within the human visible range, while *H. erato demophoon* reflects very little but tends to show highest reflectance in the red-infrared range (Parnell et al. 2018). Therefore, the colour values will allow variation in colour and reflectance to be measured but will not represent butterfly visual systems. Luminance, the overall brightness of wing colour, was calculated as (R+G+B). Measurements were shown to be repeatable using the repeatability equation of Whitlock and Schluter (2009) and taking 5 measurements each on 5 randomly selected individuals (Table S2.3). This estimates the fraction of total variance that is among groups in a random-effects ANOVA. Ninety-nine percent of variation in blue scores was due to differences between individuals and 1% due to measurement error ($R^2 = 0.99$, $F_{4,20} = 54159$, $p < 0.001$). We used the Castle-Wright estimator:

$$n_e = \frac{[\mu(P_1) - \mu(P_2)]^2 - Var[\mu(P_1)] - Var[\mu(P_2)]}{8Var(S)}$$

where $Var(S) = Var(F_2) - Var(F_1)$, to estimate the effective number of genetic loci (n_e) contributing to variation in the trait (Cockerham 1986; Lynch and Walsh 1998; Otto and Jones 2000). This is the difference between the mean BR values of the parental races squared, then the subtraction of the two variance terms, which corrects for sampling error of the estimates of the parental means (P_1 and P_2).

In *H. erato*, the genotype at the *Cr* locus was scored in 286 individuals based on the presence and absence of the white hindwing margin and the dorsal hindwing yellow bar, under the assumption

that these pattern elements are controlled by alternative alleles of the *Cr* locus (Mallet 1986; Joron et al. 2006). The *demophoon* genotype has the yellow bar present, a white margin indicates the *cyrbia* genotype, and the heterozygous genotype has neither of these elements or a partial yellow bar (Figure 2.1). Similarly, the *Yb/Sb* locus in *H. melpomene* was scored in 213 individuals. The *rosina* genotype has the yellow bar, while the *cythera* genotype has a hindwing margin. In *melpomene* hybrids, this margin can be white, yellow or a mix of both white and yellow scales.

All statistical analyses were carried out in the R statistical package version 3.4.2 (R Core Team 2018). Welch's t-tests were used for analysis of differences between sexes and reciprocal crosses. ANOVA models were used to compare blue values to *Cr* and *Yb/Sb* genotypes. Yellow bar and white margin traits were tested for departures from the expected segregation ratios, based on the above hypothesis of the linkage and Mendelian inheritance, using a chi-squared test.

Figure 2.2: RGB values were measured in the areas highlighted and averaged for each butterfly. Left side wings were used when the right side was too damaged.

2.4 Results

2.4.1 Colour variation in Heliconius erato

H. erato demophoon showed very little blue colour with an average BR value of -0.56 ± 0.08 compared to iridescent *H. erato cyrbia* which had a mean value of 0.97 ± 0.05 (Table 2.3). The mean for the F2 generation fell midway between the two parental races (Figure 2.3), suggesting additive effects of alleles. The mean of the F1 was slightly skewed towards *demophoon*, although the median was in a similar position to the F2 (0.13 and 0.14). The mean BR value of the backcrosses did not fall halfway between that of the F1 and the parental race which they were crossed with, but was skewed towards *cyrbia*, the Ecuadorian race. This suggests that the effects of the alleles are not completely additive, and there may be some dominance of the *cyrbia* alleles or epistatic interactions between loci.

The lack of discrete groups in the F2 generation suggests that variation in the trait is controlled by more than one locus. Using the Castle-Wright estimator, with mean BR values and variances from only one cross direction to reduce variation due to sex linkage (see subsequent results), we obtained an estimate of 4.6 loci contributing to the trait. While this formula assumes that crosses started with inbred lines, it is generally robust to deviations from the assumptions (Lande 1981). However, it likely underestimates the total number of loci as it assumes loci all have equal effects. It is therefore perhaps best interpreted as the likely number of loci with medium to large effects on the phenotype. In addition, the F1 individual wings that we measured were of varying age and condition, which may have increased the variance and decreased the mean value of blue reflectance seen in these individuals relative to the F2 individuals, which were all preserved soon after emergence. This could influence the estimation of the number of loci.

Table 2.3: Summary statistics (mean ± S.D.) for BR and luminance values in each generation of *H. erato.*

Generation	BR value	Variance of BR	Luminance	Sample size
demophoon	-0.56 ± 0.08	0.01	71 ± 14	12
F1	0.13 ± 0.23	0.05	100 ± 24	60
Backcross	0.69 ± 0.28	0.08	130 ± 32	65
F2	0.21 ± 0.30	0.09	104 ± 23	114
cyrbia	0.97 ± 0.05	0.00	162 ± 29	51

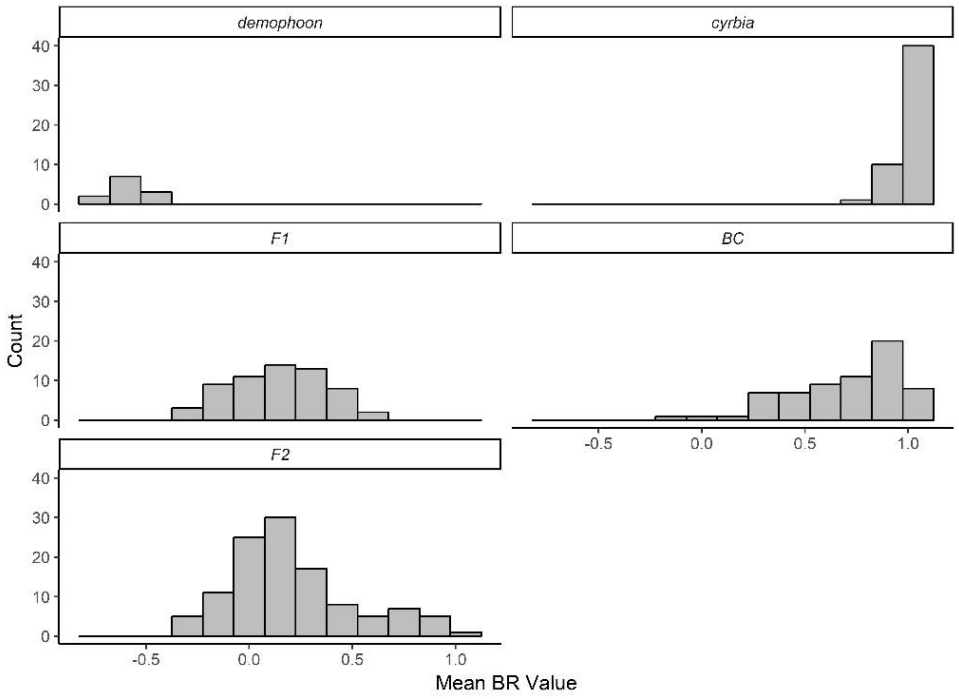

Figure 2.3: Mean BR values across *H. erato* generations. F1 and F2 individuals largely fall between the parental *demophoon* and *cyrbia* races. The backcross generation (BC) are highly skewed towards *cyrbia*, which is the race they were crossed with.

We also looked at the variation in luminance, which is the overall brightness of the colour (Table 2.3). While the distribution of values in the F1 and F2 generations were similar to the BR values, variance was higher in the *cyrbia* race (Figure 2.4). Values were skewed towards *demophoon* in the intercross offspring, suggesting dominance of *demophoon* alleles. This suggests that colour and brightness are being controlled by different loci, or different numbers of loci.

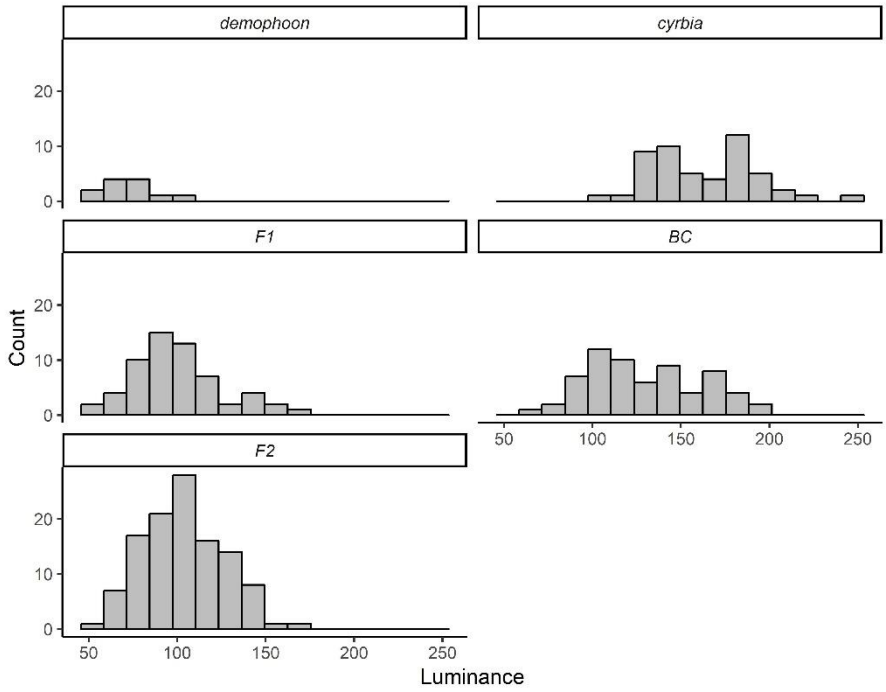

Figure 2.4: Distribution of luminance values for each *H. erato* generation.

Sex linkage

Sex linkage leads to a difference in the trait between reciprocal crosses in the F1 generation, which is confined to the heterogametic sex, and a difference between reciprocal crosses in the F2 generation in the homogametic sex (Mather and Jinks 1982). As in birds, female butterflies are the heterogametic sex; they have ZW sex chromosomes whereas males have ZZ. Differences would occur depending on which parent or grandparent the Z or W is inherited from (Figure 2.5). If the sex difference is present in the parental population, or the pattern is the same in reciprocal crosses, this would indicate a sex-limited trait (i.e. an autosomal trait that is expressed differently between the sexes).

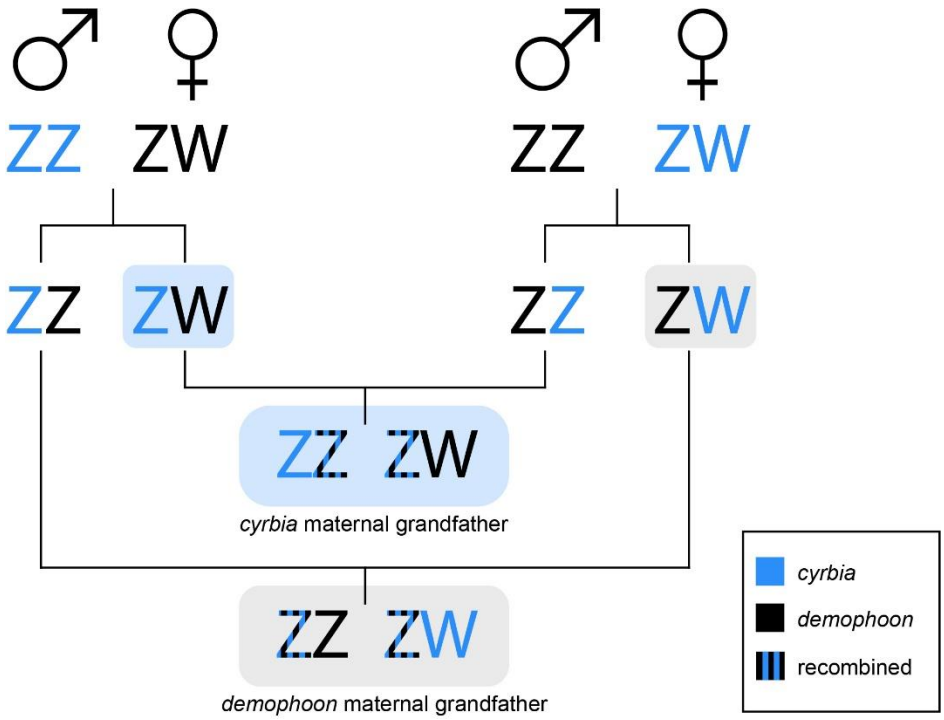

Figure 2.5: If there are loci of interest on the Z chromosome, F1 females with an iridescent *cyrbia* father will be bluer than those with a non-iridescent *demophoon* father because they inherit a "*cyrbia*" Z chromosome. In the F2, males always inherit a complete, non-recombined Z chromosome from their maternal grandfather, so if he is iridescent they will be bluer than offspring from the reciprocal cross. Blue shading shows offspring are, on average, bluer than offspring from the reciprocal cross (shown as grey shading).

Comparing the F1 offspring of reciprocal crosses suggested some sex linkage (Table 2.4; Figure 2.6). Offspring of crosses with a male *cyrbia* parent had significantly higher BR values than those which had a female *cyrbia* parent. Separated by sex, there was no difference between the males from reciprocal F1 crosses, which had means of 0.25 and 0.23 respectively. The variation was amongst the female offspring which had means of 0.26 and -0.03 (Table 2.5). This pattern would be expected if there were one or more loci controlling iridescence on the Z chromosome. In each case, males will be receiving one Z chromosome from an iridescent parent, and the other from a non-iridescent parent. The female offspring, in contrast, will only receive a Z chromosome from their father (Figure 2.5). To confirm that these results were not biased by a particular cross, individual crosses were plotted and the same pattern was found (Figure S2.1).

If blue colour was controlled only by genes on the Z chromosome, we would expect that females from crosses with a non-iridescent father would have the same phenotype as *demophoon* females. However, they are significantly bluer than wild *demophoon* (cross offspring = -0.03 ± 0.2, wild type = -0.56 ± 0.1, t_{25} = -10.6, p<0.001), supporting the hypothesis that the colour is controlled by multiple loci on different chromosomes.

Table 2.4: Comparison of BR values (± S.D.) between females and males in each *H. erato* generation. Males are bluer than females in crosses with a *demophoon* father or *cyrbia* maternal grandfather (MGF). Males are also bluer in backcrosses with a *cyrbia* MGF. There are no differences in the parental races.

Generation	**Female BR value**	**Female sample size**	**Male BR value**	**Male sample size**	**t**	**df**	**p**
demophoon	-0.56 ± 0.1	6	-0.56 ± 0.1	6	-0.06	9.0	0.96
All F1	0.10 ± 0.3	46	0.24 ± 0.2	14	-2.37	28.9	0.03
F1 *cyrbia* father	0.26 ± 0.2	21	0.25 ± 0.2	7	0.17	8.4	0.87
F1 *demo.* father	-0.03 ± 0.2	25	0.23 ± 0.1	7	-3.80	13.3	0.002
All F2	0.10 ± 0.3	63	0.33 ± 0.3	51	-4.28	96.4	<0.001
F2 *cyrbia* MGF	0.12 ± 0.3	53	0.35 ± 0.3	47	4.00	92.1	<0.001
F2 *demo.* MGF	0.02 ± 0.2	10	0.15 ± 0.4	4	-0.72	3.5	0.51
All BC	0.60 ± 0.3	35	0.79 ± 0.2	30	-2.93	62.9	0.005
BC *cyrbia* MGF	0.58 ± 0.3	24	0.83 ± 0.2	25	-3.86	42.7	<0.001
BC *demo.* MGF	0.65 ± 0.4	11	0.62 ± 0.4	5	0.16	7.6	0.88
cyrbia	0.98 ± 0.02	16	0.97 ± 0.1	35	0.79	48.2	0.43

Table 2.5: Comparison of BR values for offspring from reciprocal F1 crosses, which had either an iridescent mother or iridescent father, and for F2 crosses, which had either an iridescent maternal grandfather or grandmother. Mean values and sample sizes are shown in Table 2.4.

F1 *cyrbia* or *demophoon* father				**F2 *cyrbia* or *demophoon* maternal grandfather**			
	t	df	p		t	df	p
Female	-5.55	43.6	<0.001	Female	-1.64	19.5	0.12
Male	-0.19	10.8	0.85	Male	-1.06	3.4	0.36
All	-4.67	56.8	<0.001	All	-2.53	20.2	0.02

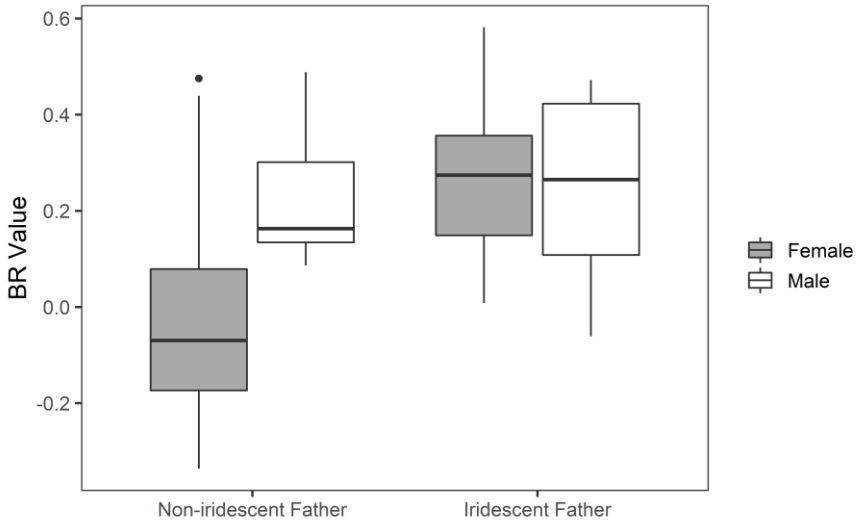

Figure 2.6: F1 females with a *H. e. cyrbia* father were significantly bluer than those with a *H. e. cyrbia* mother. There were no differences in males.

In the F2 generation, sex linkage would be shown as males with an iridescent maternal grandfather being more blue than those with an iridescent maternal grandmother. The results point towards this pattern, however the differences between the male groups are not significant, possibly due to small sample sizes in the first group (Figure 2.7; Table 2.5). There was little difference in females. Overall, however, offspring with an iridescent maternal grandfather were bluer than those with a black maternal grandfather. This is consistent with sex linkage, due to the greater number of "*cyrbia"* Z chromosomes present in the F2 offspring with an iridescent maternal grandfather (Figure 2.5). Within the offspring with an iridescent maternal grandfather, males were bluer than females, while this was not the case for crosses with a black maternal grandfather, also supporting Z linkage (Table 2.4). In summary, F1 females were bluer than males when they had an iridescent father, and males were bluer in the F2 when they had an iridescent maternal grandfather. We did not find any difference in blue score between the sexes in pure *H. erato cyrbia* or in *H. e. demophoon* (Table 2.4), demonstrating that the difference between the sexes in the crosses is not due to autosomally mediated sexual dimorphism. These results support the presence of loci controlling iridescence on the Z chromosome.

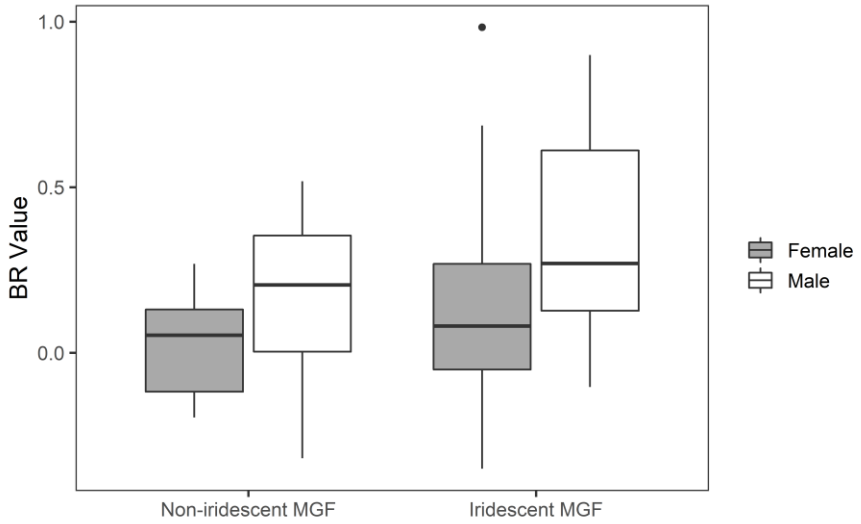

Figure 2.7: Mean BR value for males with an iridescent maternal grandfather were higher than those with an iridescent maternal grandmother, although not significantly. Females in both groups had similar BR values.

Links to other colour pattern loci

In *H. erato*, the *Cr* locus controls the presence of a yellow forewing bar in *demophoon* and a white margin in *cyrbia*. There were 3 observed phenotypes in the F2 generation – yellow bar present, white margin present, and both absent (Figure 2.1). Consistent with the hypothesis that these two features are controlled by recessive, tightly linked loci or are alternative alleles of the same locus, we did not find any individuals that had both a full yellow dorsal bar and a white margin present. The ratio of these traits was also consistent with a 1:2:1 ratio as expected under the assumption that the individuals lacking both features were heterozygous at this locus (x^2 = 2.1, df = 2, p = 0.35). There was no significant difference in BR values between individuals with different *Cr* genotypes ($F_{2,107}$ = 2.05, p = 0.13) (Figure 2.8), suggesting that *cortex* is not one of the genes controlling iridescence, nor are there any major effect loci linked to this region on *Heliconius* chromosome 15.

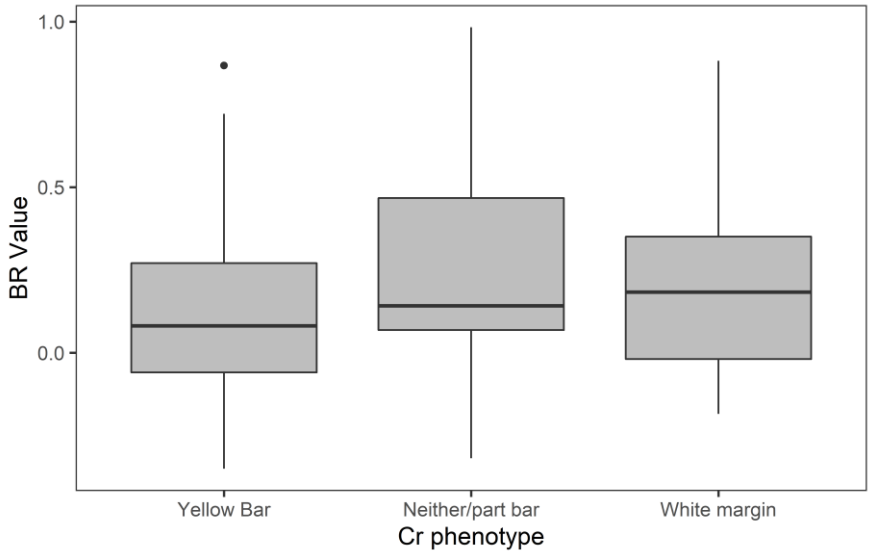

Figure 2.8: In the *H. erato* F2 generation, BR values did not differ with the different *Cr* phenotypes.

2.4.2 Colour variation in Heliconius melpomene

Overall, the blue values in *H. melpomene* were not as high as in *H. erato* (Table 2.6). Values for *H. m. rosina* were similar to the non-iridescent *H. e. demophoon*. The mean of the F1 generation was skewed towards *rosina*. The F2 did not fall midway between the parental races and were also closer to *rosin*a, suggesting dominance of the *rosina* alleles.

Table 2.6: Summary statistics (mean ± S.D.) for BR and luminance values in the *H. melpomene* parental races and F1 and F2 offspring.

Generation	BR value	Variance of BR	Luminance	Sample Size
rosina	-0.63 ± 0.07	0.004	66.5 ± 14	12
F1	-0.20 ± 0.11	0.01	68.3 ± 13	109
F2	-0.13 ± 0.18	0.03	72.6 ± 16	214
cythera	0.45 ± 0.24	0.06	107 ± 20	22

The F1 and F2 measurements did not fall into discrete categories and formed a normal distribution, again suggesting that the trait is being controlled by multiple loci (Figure 2.9). Here the Castle-Wright equation estimated 6.9 loci, suggesting more loci of medium-large effect are contributing to the trait compared to *erato.*

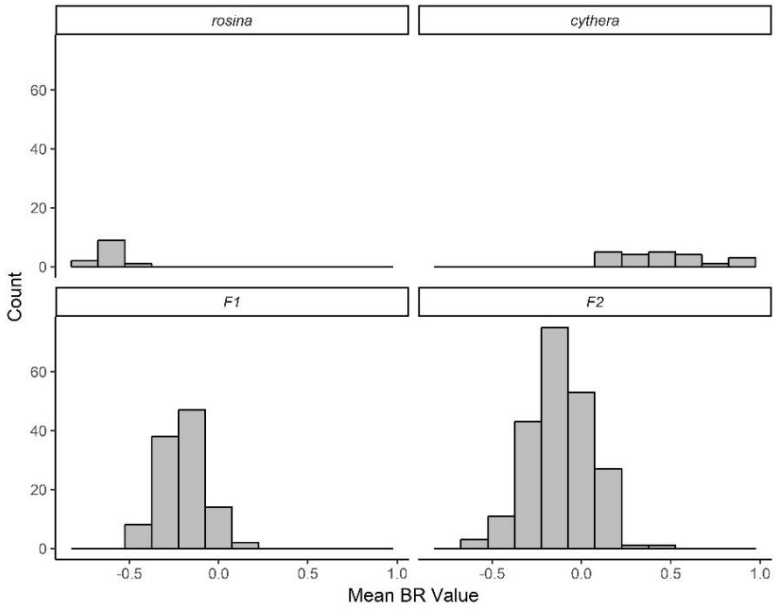

Figure 2.9: Distribution of BR values for each *H. melpomene* generation. High variance in *cythera* is likely due to wear on the wings of wild individuals.

With luminance, there was more variation in the parental races compared to the BR values, and the values of these races overlapped with those of the cross offspring (Figure 2.10; Table 2.6). As in *erato,* luminance values in the F1 and F2 generations were skewed towards the non-iridescent race. These results suggest a complex genetic basis controlling overall brightness of colour.

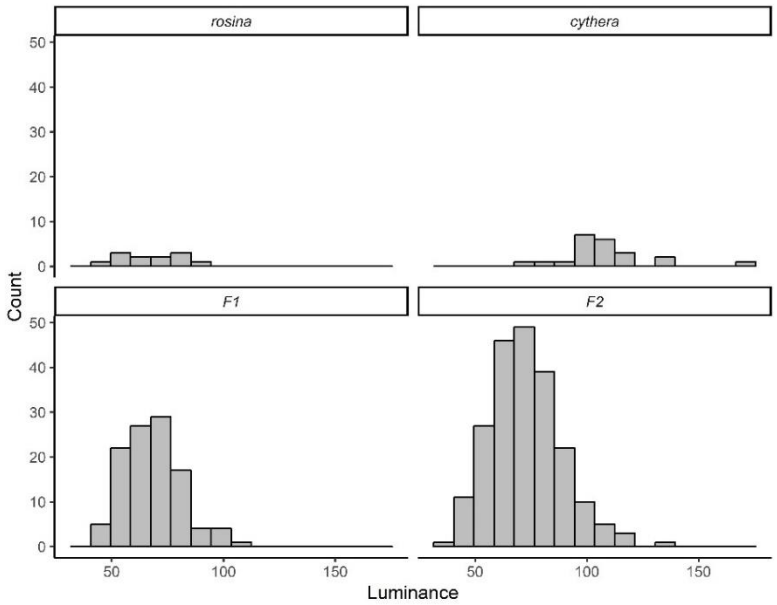

Figure 2.10: Luminance values for each *H. melpomene* generation.

Sex linkage

There was no evidence of sexual dimorphism of blue colour in either of the pure *H. melpomene* races. Males in the F2 generation were significantly bluer than females (Table 2.7). In general, males were also bluer in the F1 and in *cythera*, and the lack of significance may be due to sample sizes.

Table 2.7: Comparison of BR values (± S.D.) between females and males in each *H. melpomene* generation.

Generation	**Female BR value**	**Female sample size**	**Male BR value**	**Male sample size**	**t**	**df**	**p**
rosina	-0.62 ± 0.1	6	-0.64 ± 0.1	6	0.63	8.6	0.54
All F1	-0.21 ± 0.1	66	-0.19 ± 0.1	43	1.38	100.5	0.17
F1 *rosina* father	-0.23 ± 0.1	33	-0.18 ± 0.1	22	-1.36	45.3	0.18
F1 *cythera* father	-0.20 ± 0.1	33	-0.19 ± 0.1	21	-0.26	34.1	0.80
All F2	-0.15 ± 0.2	101	-0.10 ± 0.2	113	-2.13	208.5	0.03
F2 *rosina* MGF	-0.15 ± 0.2	49	-0.12 ± 0.1	48	-1.07	93.2	0.29
F2 *cythera* MGF	-0.16 ± 0.2	52	-0.09 ± 0.2	65	-1.82	110.2	0.07
cythera	0.37 ± 0.3	7	0.49 ± 0.2	15	-0.15	16.8	0.88

Table 2.8: Comparison of BR values for offspring from reciprocal F1 crosses, which had either an iridescent mother or iridescent father, and for F2 crosses, which had either an iridescent maternal grandfather or grandmother. Mean values and sample sizes are shown in Table 2.7.

F1 *rosina* or *cythera* father				**F2 *rosina* or *cythera* maternal grandfather**			
	t	df	p		t	df	p
Female	-1.12	62.0	0.27	Female	0.32	96.2	0.75
Male	0.15	40.0	0.88	Male	-0.78	109.8	0.44
All	-0.70	106.8	0.49	All	-0.44	208.3	0.66

When comparing the F1 offspring of reciprocal crosses, there were no differences between those which had an iridescent mother and those which had an iridescent father (Figure 2.11; Table 2.8). Males in the F2 generation were significantly bluer than females (male = -0.10 ± 0.2, female = -0.15 ± 0.2). However, when the crosses were split according to the race of the maternal grandfather (MGF), there was no difference (Figure 2.12; Table 2.8), although the values do change in the direction we expect. If the colour was sex-linked we would expect that only males with an iridescent maternal grandfather would be bluer.

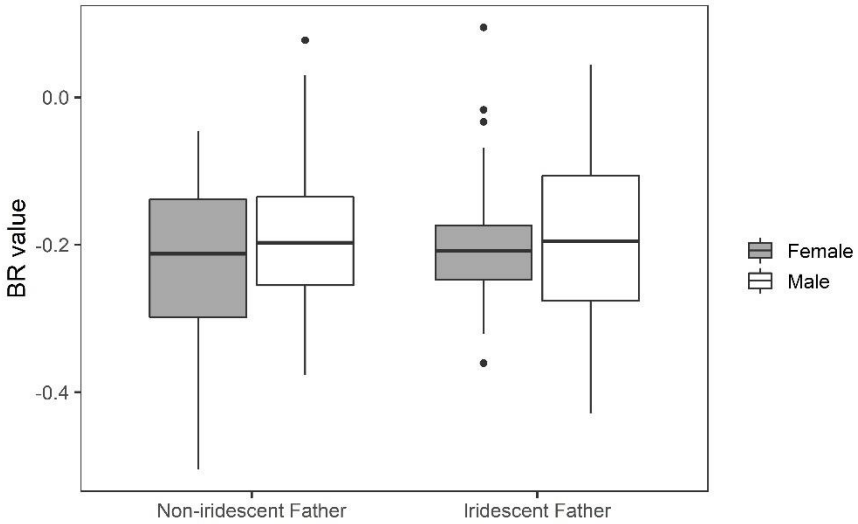

Figure 2.11: BR values for F1 males and females did not differ from each other, or with respect to cross direction, suggesting that here the colour is not sex-linked.

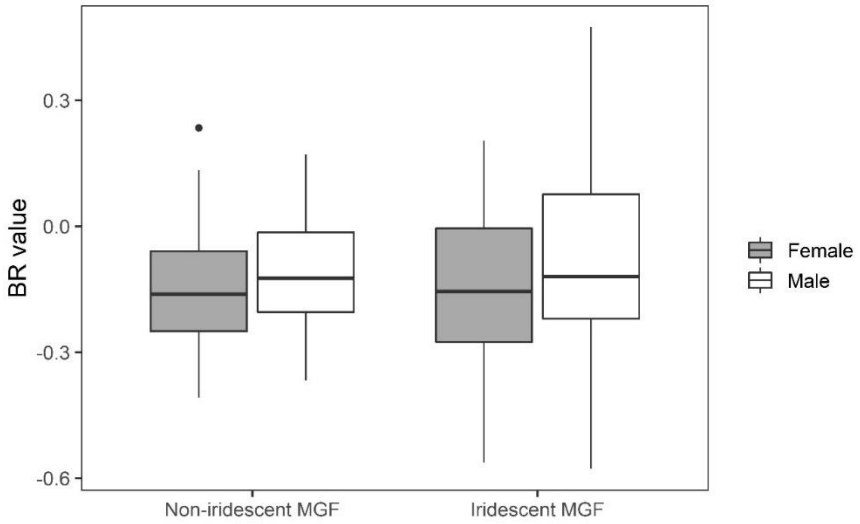

Figure 2.12: The race of the maternal grandfather of the cross did not affect the mean BR values of males and females in the F2 generation.

Links to other colour pattern loci

BR values were compared to other colour pattern elements in *H. melpomene*. The *Yb* locus controls the presence of a hindwing yellow bar in *cythera*, and the tightly linked *Sb* locus controls the presence of a white/yellow margin. BR values significantly differed with *Yb/Sb* genotype ($F_{2,210}$ = 8.46, p<0.001) (Table 2.9; Figure 2.13). This is in contrast to the homologous *Cr* locus in *H. erato.* Individuals with a yellow bar had lower levels of blue compared to those with a white margin and those with the heterozygous genotype. The ratio of these phenotypes is as expected for an F2 generation (1:2:1), where around half of the individuals have neither a yellow hindwing bar or a margin (x^2 = 0.79, df = 2, p = 0.68).

Table 2.9: Mean (± S.D.) BR values for groups of *H. melpomene* individuals with each *Yb/Sb* genotype.

Yb/Sb	**BR values**	**Observed**	**Expected**
Yellow bar	-0.21 ± 0.1	53	53.25
Neither/part bar	-0.11 ± 0.2	114	106.5
White margin	-0.08 ± 0.2	46	53.25

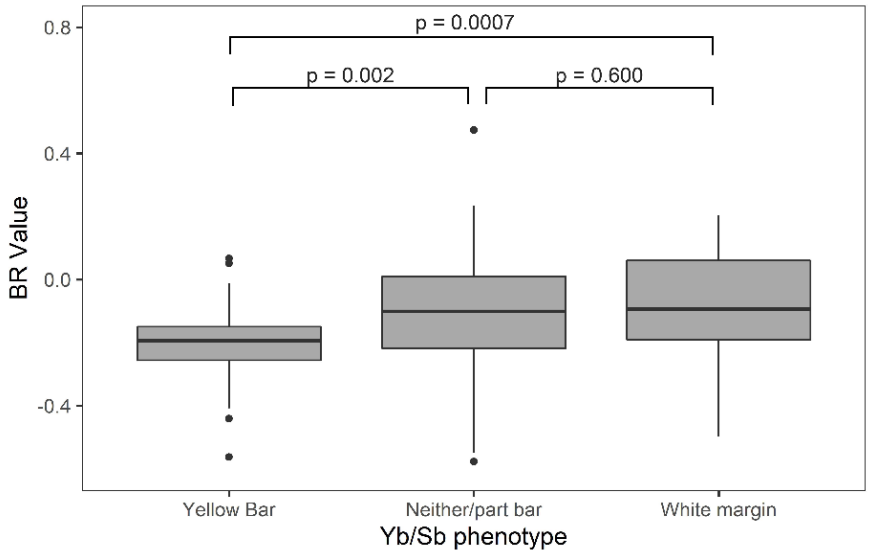

Figure 2.13: *H. melpomene* F2 individuals which had the *cythera* hindwing margin phenotype were significantly bluer than those with the *rosina* yellow bar phenotype. Tukey's test p-values are shown above. Photos of these phenotypes are shown in Figure 2.1.

We also tested for an association between BR colour and the *K* locus in 44 F2 individuals which had a hindwing margin. There was no relationship between the colour of this margin and the BR value ($F_{2,41}$= 0.93, p = 0.40).

2.5 Discussion

Our phenotypic analysis of crosses between iridescent and non-iridescent races show that iridescence is being controlled by multiple loci in both *H. melpomene* and *H. erato*. There is convincing evidence for loci on the Z sex chromosome in *erato*, and in *melpomene* there is evidence for a link to the *cortex* gene which controls other colour pattern elements.

There is an extensive history of using experimental crosses in *Heliconius* to investigate the genes controlling colour and pattern, but although iridescence has been shown to segregate in crosses, the trait has not been investigated due to the difficulty of quantifying the continuous phenotype and measuring the number of different features affecting the colour. We show that the use of standardised photographs and the BR ratio is an effective method of estimating variation in blue iridescent reflectance. As expected, iridescent *H. erato cyrbia* gave the highest blue values, and non-iridescent *H. e. demophoon* and *H. m. rosina* the lowest. The distribution of blue values in both of the F2 generations suggests that variation in the trait is not controlled by a single locus. Luminance, the overall brightness of the colour, is also controlled by multiple genes and further genetic analysis can determine how much the genetic basis of blue colour and brightness are linked.

Sex linkage

The differences in blue values found between sexes in the F1 reciprocal *H. erato* crosses suggest that there could be a major effect locus involved in iridescent colour on the Z chromosome. We may expect that genes on the sex chromosomes will control sexually selected traits (Fairbairn and Roff 2006). Reinhold (1998) calculated that in *Drosophila* around a third of phenotypic variation in sexually selected traits was caused by X-linked genes, and that X-linked genes only influenced traits classified as under sexual selection. Iridescent structural colours are used as sexual signals in many butterfly species (Sweeney et al. 2003; Kemp 2007; Rajyaguru et al. 2013). Work with *Colias* butterflies has found many wing pattern elements are sex-linked, including melanisation,

UV reflectance and yellow wing pigmentation (Silberglied 1979; Ellers and Boggs 2002). These studies found that sex linkage was important in prezygotic isolation and species differentiation. Therefore, sex linkage of iridescence in *Heliconius* may have contributed to the differentiation of this trait between geographical races.

Unlike some Lepidoptera, *Heliconius* do not show complete sex chromosome dosage compensation. Analysis of *H. cydno* and *H. melpomene* gene expression showed a modest dosage effect on the Z chromosome, and overall reduced expression compared to autosomes (Walters et al. 2015). Our results are also consistent with a lack of complete dosage compensation, with some evidence for expression of both Z chromosome alleles in males. A lack of dosage compensation could also favour the build-up of sexually selected or sexually antagonistic loci on the Z chromosome, as these will automatically be expressed differently between the sexes.

In *H. melpomene*, the results for sex linkage are ambiguous. Males were slightly bluer in the F2 crosses with an iridescent maternal grandfather which could suggest the influence of minor effect loci on the Z chromosome, but evidence for this is not as strong as in *H. erato.*

Colour pattern links

H. melpomene offspring with the white/yellow margin phenotype had higher blue values than those with the *rosina* yellow bar phenotype, suggesting there is a locus on chromosome 15 linked to the *Yb/Sb* loci that is contributing to iridescent colour. In contrast, the three *H. erato* phenotypes controlled by the *Cr* locus did not show any correlation with iridescent colour values. The gene *cortex*, found in this genomic region, has been shown to underlie these colour pattern differences (Nadeau et al. 2016). In Lepidoptera and *Drosophila*, *cortex* is a cell-cycle regulator during meiosis (Chu et al. 2001). Therefore, it likely has a broader role in scale cell development, beyond controlling pigmentation, and could play a role in the formation of structural colours. Knockouts of one of the genes that control colour pattern in *Heliconius*, *optix*, resulted in a change in pigmentation in *Junonia coenia* butterflies, and the gain of structural colour (Zhang et al. 2017),

although this was not observed in the same tests with *Heliconius erato*. The *optix* transcription factor in particular is likely to have a role outside of pigment patterning. It is expressed in association with wing traits other than pigment in many species – in basal Heliconiini, *optix* expression is involved in the differentiation of wing scales, marking male-specific vein structures in *Dryas* (Martin et al. 2014).

Linkage between multiple divergently selected loci may also be expected under 'divergence hitchhiking', in which genomic regions around key divergently selected loci are protected from recombination during speciation (Via and West 2008), although theoretical and empirical support for this model is limited (Feder et al. 2012; Yeaman et al. 2016). However, for highly polygenic traits we would expect many loci to be distributed throughout the whole genome, so that for any genetic marker there will be some phenotypic association, however small. This effect would be particularly strong in F2 crosses due to the lack of recombination in females. Individuals with homozygous *Yb/Sb* phenotypes, for example, will have inherited an entire chromosome 15 from either an iridescent or non-iridescent parent. Therefore, the correlation with blue values seen here could be the result of a single major effect locus or multiple smaller effect loci on chromosome 15. There do not seem to be any large effect loci on chromosome 1 influencing blue colour, as this would have been seen as a difference in individuals with a white or yellow margin. The heterogeneous effects that we see with respect to markers on different chromosomes suggest that structural colour is not highly polygenic but controlled by a moderate number of loci in both species. In *H. erato*, one of these appears to be on the Z chromosome, while in *H. melpomene* one is on chromosome 15.

Comparison of mimetic species

In *Heliconius* pigment colour patterns, a small set of major effect genes have been well studied but a larger set of "modifier" loci have also been found which adjust colour pattern (Papa et al. 2013). It is possible that the iridescence genes have a similar distribution of effect sizes, with a small number of major effect genes, including one on the Z chromosome in *erato* and on

chromosome 15 in *melpomene*, and a distribution of other smaller effect genes. This supports the existing evidence of the importance of major effect loci in adaptive change (Joron et al. 2006; Baxter et al. 2008; Papa et al. 2013).

Previous research has shown that spacing of longitudinal ridges on the wing scales, one of the key features of structural colour, is similar in iridescent *erato* and *melpomene* (Parnell et al. 2018). However, there are differences in the curvature of the lamellae that form the ridges between the two species. In *H. melpomene*, ridges are more curved with less uniform layering, explaining the lower brightness levels. It appears that ridge density rapidly evolved to allow mimicry, but lamellae modifications are evolving more slowly. This difference in the physical scale architecture between the species perhaps makes it unsurprising that the genetic architecture of iridescence is different between the species.

Following the two-step process of Müllerian mimicry described by Turner (Turner 1977; 1981), a large effect mutation allows an adaptive phenotypic change large enough for the population to resemble those in the mimicry ring and survive, then smaller changes will produce incremental improvements in mimicry. *H. melpomene* populations in Western Ecuador are estimated to have diverged from the Eastern populations later than the *H. erato* race – 65Kya and 1.5-2Mya respectively (Cuthill et al. 2012) – possibly explaining the lower brightness of the iridescence if *H. melpomene* converged on the *H. erato* phenotype.

Crosses are ideal for investigating the genetic basis of colour and pattern as traits will segregate in the following generations. Crosses of iridescent and non-iridescent *Heliconius* races have allowed us to show that structural colour has a different genetic basis in *H. erato* and *H. melpomene*. While in both species iridescence is controlled by multiple genes, in *erato* there is a large effect locus on the Z chromosome which is not present in *melpomene*.

2.6 Supplementary Information

Table S2.1: 14 *Heliconius erato* crosses which produced offspring were included in the phenotypic analysis. Parents of F2 crosses and backcrosses have the cross they originated from in brackets.

Cross ID	**Cross type**	**Father ID**	**Mother ID**	**Offspring used for colour measurements**
EC01F1	*demophoon* ♂ x *cyrbia* ♀	14N012	14N011	17
EC03F1	*cyrbia* ♂ x *demophoon* ♀	Unknown	14N047	5
EC10F1	*cyrbia* ♂ x *demophoon* ♀	14N065	14N064	15
EC39F1	*cyrbia* ♂ x *demophoon* ♀	14N339	14N338	8
EC45F1	*demophoon* ♂ x *cyrbia* ♀	14N359	14N358	15
EC11BC	*cyrbia* ♂ x (*demophoon* ♂ x *cyrbia* ♀)	14N067	14N066 (EC01)	1
EC12BC	*cyrbia* ♂ x (*demophoon* ♂ x *cyrbia* ♀)	14N069	14N068 (EC01)	15
EC41BC	*cyrbia* ♀ x (*cyrbia* ♂ x *demophoon* ♀)	14N348 (EC10)	14N347	49
EC13F2	*demophoon* maternal grandfather	14N078 (EC01)	14N077 (EC01)	5
EC15F2	*demophoon* maternal grandfather	14N093 (EC01)	14N089 (EC01)	6
EC17F2	*cyrbia* maternal grandfather	14N112 (EC01)	14N111 (EC10)	60
EC18F2	*cyrbia* maternal grandfather	14N114 (EC01)	14N113 (EC10)	16
EC53F2	*cyrbia* maternal grandfather	14N396 (EC39)	14N395 (EC39)	24
EC56F2	*demophoon* maternal grandfather	14N428 (EC39)	14N427 (EC45)	3

Table S2.2: Offspring from 14 *Heliconius melpomene* crosses were used in the colour analysis. Parents of F2 crosses have the cross they originated from in brackets.

Cross ID	Cross type	Father ID	Mother ID	Offspring used for colour measurements
EC05F1	*cythera* ♂ x *rosina* ♀	14N052	14N051	13
EC07F1	*cythera* ♂ x *rosina* ♀	14N059	14N058	13
EC09F1	*rosina* ♂ x *cythera* ♀	14N063	14N062	17
EC26F1	*cythera* ♂ x *rosina* ♀	14N219	14N220	9
EC27F1	*rosina* ♂ x *cythera* ♀	14N221	14N222	12
EC35F1	*cythera* ♂ x *rosina* ♀	Unknown	14N315	4
EC38F1	*rosina* ♂ x *cythera* ♀	14N337	14N336	6
EC48F1	*rosina* ♂ x *cythera* ♀	14N366	Unknown	20
EC49F1	*cythera* ♂ x *rosina* ♀	14N368	14N367	15
EC51F2	*rosina* maternal grandfather	14N379 (EC35)	14N385 (EC38)	55
EC57F2	*rosina* maternal grandfather	14N452 (EC38)	14N451 (EC48)	34
EC63F2	*cythera* maternal grandfather	14N480 (EC48)	14N479 (EC49)	63
EC65F2	*cythera* maternal grandfather	14N563 (EC48)	14N562 (EC49)	54
EC69F2	*rosina* maternal grandfather	14N605 (EC49)	14N604 (EC48)	8

Table S2.3: Repeatability of BR measurements for 5 randomly chosen *H. erato* individuals.

Individual	1	2	3	4	5	Sum	Mean	Variance
14N014	0.854	0.861	0.851	0.847	0.852	4.266	0.853	2.50E-05
15N019	0.978	0.977	0.975	0.977	0.977	4.884	0.977	1.75E-06
15N075	-0.049	-0.038	-0.038	-0.045	-0.049	-0.219	-0.044	3.36E-05
14N203	0.572	0.587	0.580	0.582	0.597	2.919	0.584	8.72E-05
14N345	-0.460	-0.473	-0.467	-0.463	-0.464	-2.327	-0.465	2.74E-05

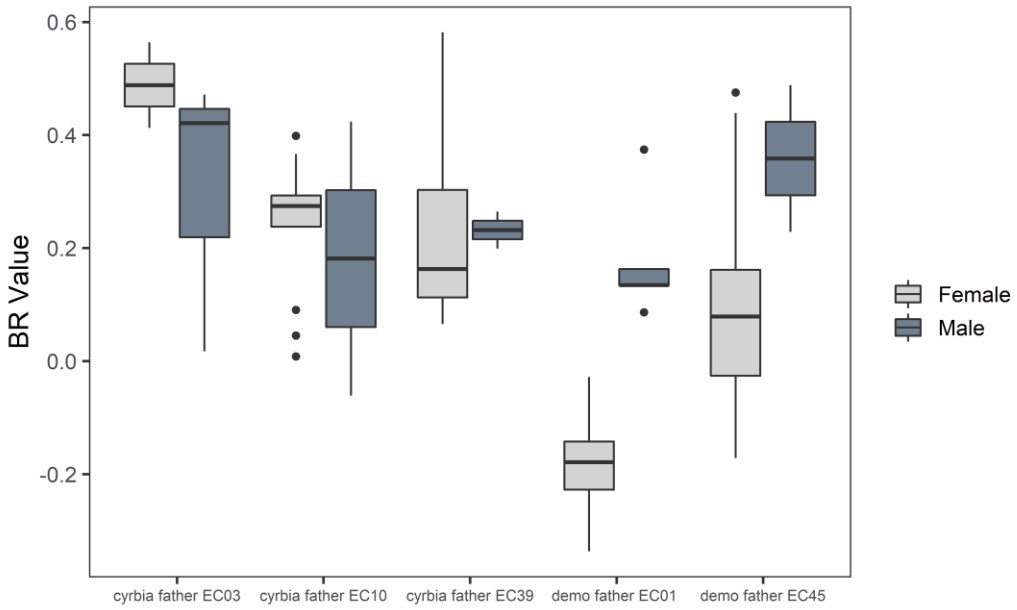

Figure S2.1: Individual *H. erato* F1 crosses split by sex. There were no significant differences between males across all crosses ($F_{4,9} = 0.45$, $p = 0.77$), but females with a *cyrbia* father were bluer than those with a *demophoon* father, showing that this effect was not biased by one particular cross.

3. Investigating the genetic basis of iridescent structural colour in the co-mimics *Heliconius erato* and *Heliconius melpomene* using Quantitative Trait Locus mapping

3.1 Summary

Iridescent structural colour has convergently evolved multiple times within the *Heliconius* genus, but little is known about the genetics of structural colour variation in any species. By comparing the genetic basis of convergent phenotypic traits across distantly related species, we can address the repeatability of evolution and determine if certain genes are more likely to be used. The co-mimics *Heliconius erato* and *Heliconius melpomene* exhibit an iridescent structural colour in some subspecies, in addition to pigment colour patterns. Using crosses between races with and without iridescent colour, we carry out a Quantitative Trait Locus mapping analysis to determine the genetic basis of structural colour in these species. We find that iridescence has a different genetic basis in *H. erato* and *H. melpomene*. Both showed two unlinked loci of medium to large effect, along with putative small effect loci. However, these loci were found at different positions in the genome. Iridescent colour in *H. erato* is strongly associated with the Z sex chromosome. This is not the case in *H. melpomene*, which has large effect locus on chromosome 3. In contrast to pigment colour patterns in *Heliconius*, iridescence is not an example of repeated use of the same genomic loci across distantly related species.

3.2 Introduction

Complex traits such as the compound eye (Gehring and Ikeo 1999; Fernald 2006), echolocation (Liu et al. 2010) and C4 photosynthesis (Heyduk et al. 2019) have convergently evolved across distantly related taxa and species in response to similar environmental selection pressures. Examples of convergent evolution allow us to test whether similar phenotypes have the same underlying genetic architecture and if certain genes are more likely to be repeatedly used across populations, due to increased mutation rates, large effect sizes, epistatic or pleiotropic effects (Conte et al. 2012). Ultimately, we may be able to use this to predict the genetic changes underlying adaptive phenotypic evolution.

Many studies have found convergent phenotypes are produced by the same genes, in some cases even the same mutation within the gene. The genes *Mc1r* and *Agouti* control pigment colour differences across many taxa (reviewed in Manceau et al, 2010 and Hubbard et al, 2010). Similarly, a cytochrome P450 is associated with carotenoid production in birds and spider mites (Wybouw et al. 2019). Another gene, *cortex*, regulates mimetic colour patterns across many species of Lepidoptera (Nadeau et al. 2016). There are also examples where the same phenotype is produced by different genetic pathways. Identical *Caerulein* toxin skin secretions were found to be produced by different precursor genes in two distantly related frog lineages (Roelants et al. 2010).

In a review of repeated evolution studies, gene reuse between taxa undergoing repeated phenotypic evolution was estimated as an average probability of 0.32 in genetic mapping analyses (Conte et al. 2012). When populations have a more recent common ancestor, the probability of gene reuse is higher. Many of these types of studies have focussed on candidate genes which can introduce bias towards previously known genes (Stern and Orgogozo 2009). Genome-wide mapping studies are needed to complement these as they do not rely on functional analyses of candidate genes.

Wing colour patterns have been widely studied in the *Heliconius* butterflies, a group of butterflies with a diverse set of aposematic colour patterns. These patterns show examples of both convergent evolution between distantly related species, and divergent evolution within species. Some species form mimicry rings, in which wing patterning is under strong frequency-dependent selection due to predation (Mallet and Barton 1989). A set of five unlinked loci control most of the pigmentary colour pattern variation across species, including *cortex* which controls mainly yellow and white elements. Another is the gene *optix*, which controls red patterns in multiple *Heliconius* species (Reed et al. 2011) and also further ommochrome wing patterning in other nymphalid groups (Zhang et al. 2017).

Simple pigment colour pattern elements are repeatedly controlled by the same genes, but would we also expect reuse of genes for a quantitative trait? Genetic basis may be less predictable for traits controlled by multiple genes (Conte et al. 2012). We can use *Heliconius* to address this question as some species also produce iridescence, an angle-dependent structural colour formed by nanostructures on the scales of the wings, that has evolved multiple times within the genus (Parnell et al. 2018). Offspring of crosses between subspecies with and without structural colour show high variation in brightness of the colour, suggesting that this trait is not controlled by a single gene with Mendelian inheritance (Chapter 2). Little is known about the genetics of structural colour variation in any species, and the developmental control is poorly understood.

Heliconius erato and *Heliconius melpomene* are distantly related species that mimic both pigmentary and structural colour (Figure 3.1). Subspecies found in Western Ecuador and Colombia produce iridescent colour, whereas those found further north have only pigment colour. There are a number of reasons why we would suspect that iridescent colour is not controlled by the same genes in these two species. *H. erato cyrbia*, an iridescent subspecies, has much brighter iridescence than its co-mimic, *H. melpomene cythera*. Therefore, some differences in the genetics of this trait between the two species are likely. The lack of structural colour in most subspecies

of *erato* and *melpomene* suggests a recent origin of this colour, estimated to be within the last 100,000 years (Kozak et al. 2015). We expect iridescence to be controlled by at least 4 loci in each species, but not to be highly polygenic (Chapter 2), thus it seems less likely that the same genes will have been reused.

Here we use a QTL mapping approach to determine the genetic architecture of iridescent colour in the *Heliconius* co-mimics, *Heliconius erato* and *Heliconius melpomene*. Using RADseq data obtained from crosses between iridescent and non-iridescent races, and by taking advantage of two high-quality reference genomes, we can estimate the number, distribution and effect sizes of loci in the genome that are controlling variation in iridescent colour. Following results from phenotypic analysis of these crosses (Chapter 2), we expect that in both species there will be multiple loci involved but that these will differ in genomic position between species. In *H. erato* a large effect locus on the Z chromosome is likely, while in *H. melpomene* we do not expect a strong effect of the Z, but instead a link to the *cortex* gene on chromosome 15.

Figure 3.1: *Heliconius erato cyrbia* and *Heliconius melpomene cythera* mimic pigmentary and structural wing colour patterning.

3.3 Methods

3.3.1 Experimental cross design and phenotyping

Experimental crosses were performed between races of *Heliconius erato* and *Heliconius melpomene* with and without iridescent colour. Non-iridescent *H. erato demophoon* were crossed with iridescent *H. erato cyrbia* to produce 5 F2 crosses plus one backcross (Table 3.1). *H. melpomene rosina* were crossed with *H. melpomene cythera* and produced 4 F2 broods (Table 3.2). Rearing conditions and further methods can be found in Chapter 2. As previously described, wings were photographed under standardised lighting conditions and RGB values were extracted from photographs. BR values (calculated as (B-R)/(B+R)) were used as a measure of blue iridescent colour. Luminance measured overall brightness and was calculated as (R+G+B). All individuals were scored for the presence or absence of a full hindwing yellow bar (1 or 0) and a white hindwing margin (1 or 0). *Cr* and *Yb* genotypes were described as being homozygous Ecuador-type (with hindwing margin), homozygous Panama-type (with yellow hindwing bar) or heterozygous (neither of these elements, or a few dorsal yellow bar scales only), based on previous analyses of this locus (Chapter 2). A total of 155 *H. erato* individuals were used in the analysis (3 *demophoon*, 3 *cyrbia*, 10 F1, 40 backcross offspring and 99 F2). For *H. melpomene*, data from 228 individuals were used (1 *rosina*, 2 *cythera*, 5 F1 and 219 F2, and 1 unknown).

Table 3.1: Pedigree information for the *H. erato* crosses used in linkage map construction.

Cross ID	Cross type	Father ID	Mother ID	Number of offspring used for linkage map
EC01F1	*demophoon* ♂x *cyrbia* ♀	14N012	14N011	5
EC10F1	*cyrbia* ♂ x *demophoon* ♀	14N065	14N064	3
EC39F1	*cyrbia* ♂ x *demophoon* ♀	14N339	14N338	2
EC41BC	*cyrbia* ♀ x (*cyrbia* ♂ x *demophoon* ♀)	14N348 (EC10)	14N347	40
EC13F2	*demophoon* maternal grandfather	14N078 (EC01)	14N077 (EC01)	3
EC15F2	*demophoon* maternal grandfather	14N093 (EC01)	14N089 (EC01)	5
EC17F2	*cyrbia* maternal grandfather	14N112 (EC01)	14N111 (EC10)	56
EC18F2	*cyrbia* maternal grandfather	14N114 (EC01)	14N113 (EC10)	14
EC53F2	*cyrbia* maternal grandfather	14N396 (EC39)	14N395 (EC39)	21

Table 3.2: Pedigree information for the *H. melpomene* crosses used in linkage map construction.

Cross ID	Cross type	Father ID	Mother ID	Number of offspring used for linkage map
EC48F1	*rosina* ♂ x *cythera* ♀	14N366	Unknown *cythera*	1
EC49F1	*cythera* ♂x *rosina* ♀	14N368	14N367	4
EC63F2	*cythera* maternal grandfather	14N480 (EC48)	14N479 (EC49)	52
EC65F2	*cythera* maternal grandfather	15N563 (EC48)	15N562 (EC49)	54
EC69F2	*rosina* maternal grandfather	15N605 (EC49)	15N604 (EC48)	7
EC70	Unknown maternal grandfather	15N614 (EC49)	15N613	106

3.3.2 DNA extraction and sequencing

Genomic DNA was extracted using the Qiagen DNeasy Blood & Tissue kit following the manufacturer's instructions, with an additional treatment with Qiagen RNase A to remove RNA. Approximately half of the thorax of each individual was used in the extraction. DNA quality and quantity were measured using a Qubit Fluorometer and a Nanodrop spectrophotometer. Single-digest Restriction site-associated DNA (RAD) library preparation and sequencing were carried out by the Edinburgh Genomics facility at the University of Edinburgh. DNA was digested with the enzyme *PstI*, which has a cut site approximately every 10kb. Libraries were sequenced on an Illumina HiSeq 2500 producing 125bp paired-end reads. 16 *H. erato* and 9 *H. melpomene* parents of the crosses were included at 2x higher concentration within the pooled library to produce a higher depth of coverage.

3.3.3 Sequence data processing

The RADpools function in RADtools version 1.2.4 was used to demultiplex the RAD sequences, using the option to allow one mismatch per barcode (Baxter et al. 2011). Quality of all raw sequence reads were checked using FastQC (version 0.11.5, Babraham Bioinformatics). FASTQ files were mapped to the *H. erato* v1 reference genome (Van Belleghem et al. 2017) or the *H. melpomene* v2.5 reference genome (Davey et al. 2017) using bowtie2 v2.3.2 (Langmead and Salzberg 2012). BAM files were then sorted and indexed with SAMtools (v1.3.1). PCR duplicates - a potential source of bias – were removed using Picard tools MarkDuplicates (v1.102). These were possible in our data because our libraries were generated with a single digestion enzyme and random shearing, meaning that each read pair should be unique. Genotype posteriors were called with SAMtools mpileup (Li 2011), set to a minimum mapping quality of 10 and minimum base quality of 10, using Lep-MAP data processing scripts (Rastas 2017). These scripts filtered the SNPs so that there was at least 3x coverage per individual, individuals with lower coverage were limited to 20% of the total and SNPs with rare alleles were excluded.

3.3.4 Genetic map construction

Linkage maps were constructed using Lep-MAP3 (Rastas 2017). Before starting, the sex of each individual was confirmed by comparing the depth of coverage of the Z chromosome against a single autosome. Females have half the depth of coverage on the Z compared to the autosomes, as they only have one copy of the Z. Five *H. melpomene* individuals were removed when the genetic sex did not match the sex inferred from the wings. The IBD module was run to verify the pedigree and a further 5 individuals (1 *erato,* 4 *melpomene)* were removed when the ancestry could not be confirmed.

The ParentCall2 module was used (with options ZLimit=2, removeNonInformative=1) to calculate the most accurate parental genotype posteriors and to obtain missing parental genotypes using information from related parents, grandparents and offspring, provided as a pedigree file. Markers were then filtered to remove those with high segregation distortion (dataTolerance=0.001). Next, markers were assigned to 21 linkage groups with the SeparateChromosomes2 module which calculates LOD scores between all pairs of markers. LOD limits between 10 and 20 were tested within this module. For *H. erato*, a limit of 12 was used as this gave the correct number of linkage groups with an even distribution of markers, and for *H. melpomene* the limit was set to 23. SizeLimit was set to 50 to remove any linkage groups with <50 markers. JoinSingles2all added additional single markers to the existing linkage groups. OrderMarkers2 orders the markers within each linkage group by maximising the likelihood of the data. In this recombination2 was set to 0, because there is no recombination in females (Suomalainen et al. 1973) and male recombination set to 0.05 (following Morris et al. 2019). Using outputPhasedData=1 gives phased data and removes markers with missing information, hyperPhaser was used to improve phasing of markers and minimum error was set as 0.01. OrderMarkers was run 5 times and the output with the highest likelihood was used. An outline of this process is shown in Figure S3.1.

Finally, we used LMPlot to visualise the maps and check for errors in marker order. Any erroneous markers that caused long gaps at the beginning or ends of the linkage groups were manually removed. Genotypes were phased using Lep-MAP's map2genotypes.awk script, and markers were named using the map.awk script and a list of the SNPs used to provide the scaffold name and position. Markers which had grouped to the wrong linkage group based on genomic position were removed (<1% of the total markers).

3.3.5 Quantitative Trait Locus mapping

The R package R/qtl was used for the QTL analysis (Broman et al. 2003). The phased output from Lep-MAP produces 4 genotypes, equivalent to AA, AB, BA, and BB. R/qtl does not accept phased data so BA genotypes were switched to AB. In addition, males were assigned as females and vice versa, because R/qtl assumes an XY sex determination system and Lepidoptera have a ZW system where females are the hemizygous sex.

The R script used for QTL mapping can be found in the supplementary information Script 3.1. For *H. erato*, initially the F2 crosses were analysed together and the backcross analysed separately. Markers on the Z sex chromosome were coded as described in Broman et al. (2006). Genotype probabilities were calculated for these two groups using *calc.genoprob*. We ran standard interval mapping to estimate QTL LOD (logarithm of the odds) scores using the *scanone* function with the Haley-Knott regression method. LOD scores show the likelihood that there is a QTL at the marker position compared to if there are no QTL anywhere in the genome. In the F2 analysis, sex and cross were included as additive covariates, and cross was included as an interactive covariate. Sex was included as a covariate in the backcross analysis. To determine the significance level for the QTL, we ran 1000 permutations, with *perm.Xsp=T* to get a separate threshold for the Z chromosome. The test for linkage on the sex chromosome has 3 degrees of freedom compared to 2 for the autosomes, so more permutation replicates are needed (determined by R/qtl) and the significance threshold is higher for the Z chromosome (Broman et al. 2006). LOD scores above 3.5 were also listed as being 'suggestive' (adapted from previous studies

including Huber et al. 2015). Suggestive QTL are those which may become significant when using larger sample sizes and so may also be classed as minor effect loci. This single QTL model was used to look for QTL for BR colour, luminance, yellow bar, hindwing margin and *Cr* locus genotypes. Confidence intervals for the positions of QTL were determined with the *bayesint* function. To calculate the phenotypic variance that each QTL explained, we used a multiple QTL *fitqtl* model which considers QTL together to increase confidence in individual loci and looks for interactions between them. Finally, LOD scores from the scanone outputs for the F2 crosses and the backcross were added together at each marker position, to allow analysis of all individuals together to increase power, and the permutation level recalculated in R/qtl. Genome scan and genotype plots were made with R/qtl2 (Broman et al. 2019) and linkage group diagrams made with LinkageMapView (Ouellette et al. 2018). Genetic distances in the QTL results are based on the observed recombination rate and expressed in centimorgans (cM), which is the distance between two markers that recombine once per generation. These were related to physical distances using the marker names obtained in Lep-MAP which give the position in the assembled reference genome of each species.

The same method was used to run genome scans for BR colour, luminance and *Yb/Sb* locus genotypes in *H. melpomene*. After sequencing, we discovered that one of the *H. melpomene* broods, referred to as EC70, had an unknown mother that was likely an F2, rather than an F1 hybrid. This meant that the maternal alleles in the offspring could not be assigned as being from either a *cythera* or a *rosina* grandparent. Therefore, in this family only paternal alleles were taken into account (and all maternal alleles set to 'A'), and the cross was treated as if a backcross.

To compare effect sizes of whole chromosomes and allow a comparison of genetic architecture between species, we ran a genome scan in the F2 crosses for BR colour using only maternal alleles as these have no recombination. To do this, paternal alleles were all coded as 'A'.

3.4 Results

3.4.1 Genetic map construction

A total of 155 *H. erato* individuals were used in the analysis (3 *demophoon*, 3 *cyrbia*, 10 F1, 40 backcross offspring and 99 F2). We obtained between 265,931 and 89,854,434 reads per individual (Table S3.1). An average of 70% of reads were mapped to the reference genome. Individuals had between 15 and 55% PCR duplication. Following filtering steps and deduplication, an average of 4,342,764 reads were retained for each individual. 65,892 SNPs were called and used in the Lep-MAP pipeline. The final genetic map contained 5,648 markers spread over 21 linkage groups, with an average spacing of 0.2cM (Figure 3.2; Table S3.2; Figure S3.2).

For *H. melpomene*, data from 228 individuals were used (1 *rosina*, 2 *cythera*, 5 F1 and 219 F2, and 1 unknown). We obtained between 240,778 and 12,135,760 reads per individual, averaging 1,746,094 (Table S3.3), of which 96% mapped to the Hmel2.5 reference genome. 63,224 SNPs were used to produce the linkage map which contained 38,163 markers. Many of these markers had no recombination events between them, so one marker per map position was used. After condensing these markers, the final map had 2,163 markers spanning 1469.9cM, with an average spacing of 0.7cM (Figure 3.3; Table S3.4; Figure S3.3). This is comparable to the *H. melpomene* linkage map created by Davey et al. (2016) which was 1364.2cM. There was no evidence of genotype distortion in either species as genotypes appeared in expected proportions; in the F2 crosses (25% AA, 50% AB and 25% BB), and in the backcross (50% AA and 50% AB) (Figure S3.4; Figure S3.5).

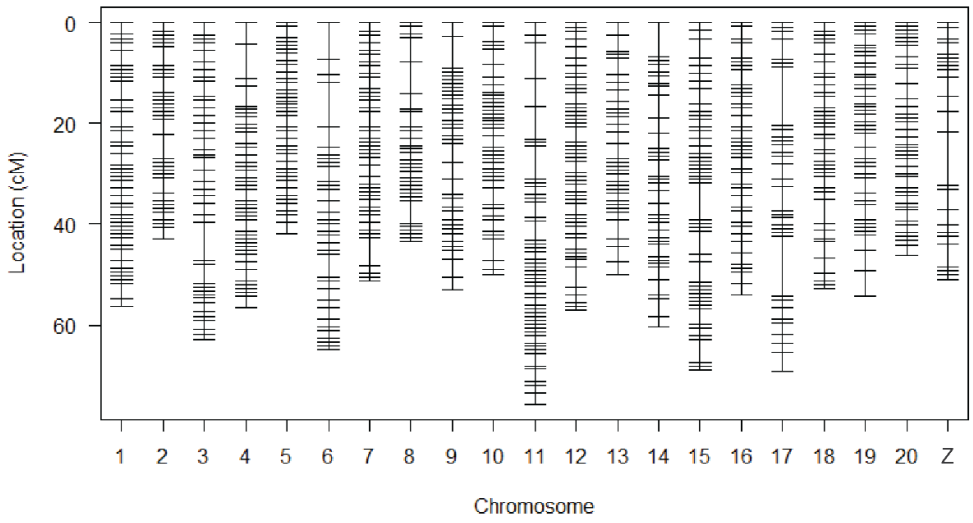

Figure 3.2: Positions of 5,648 makers across 21 *H. erato* chromosomes including the Z sex chromosome, with an average spacing of 0.2cM.

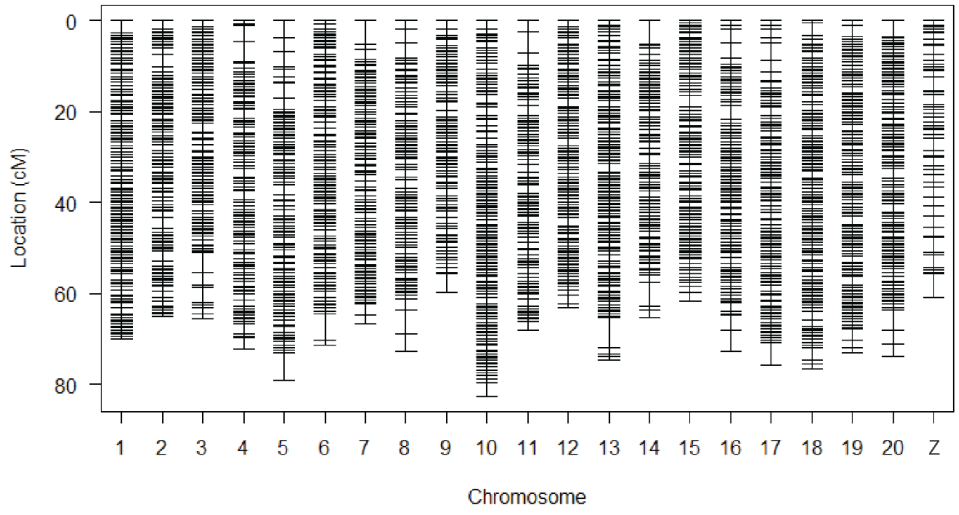

Figure 3.3: Positions of 2,163 markers across 21 *H. melpomene* linkage groups, with an average spacing of 0.7cM. Maximum spacing per linkage group was smaller than in the *H. erato* map.

3.4.2 Mapping Cr and Yb/Sb genotypes

As a validation of the analysis, we ran a QTL scan for the presence/absence of the hindwing yellow bar and the hindwing white margin, which are expected to be associated with the *Cr* locus, previously mapped to chromosome 15. As expected, there was a clear peak on chromosome 15 for both the yellow bar and the white margin (Figure 3.4) which correspond to marker Herato1505_2424998 (11.5cM). Genotype for the *Cr* locus was also estimated using these elements, with heterozygotes having neither element or a partial yellow band. The scan for this also had one significant marker ($p<0.001$) on chromosome 15 but at 4cM. The bayesian intervals (3.25-11.47cM) for this QTL relate to a region of the genome on scaffold Herato1505 covering basepairs 999,965-2,425,053. The gene *cortex* can be found within this region. The genotype x phenotype plot for this marker (Figure 3.4D) is not perfectly associated with predicted *Cr* genotype, suggesting it may be some distance from the causal mutation.

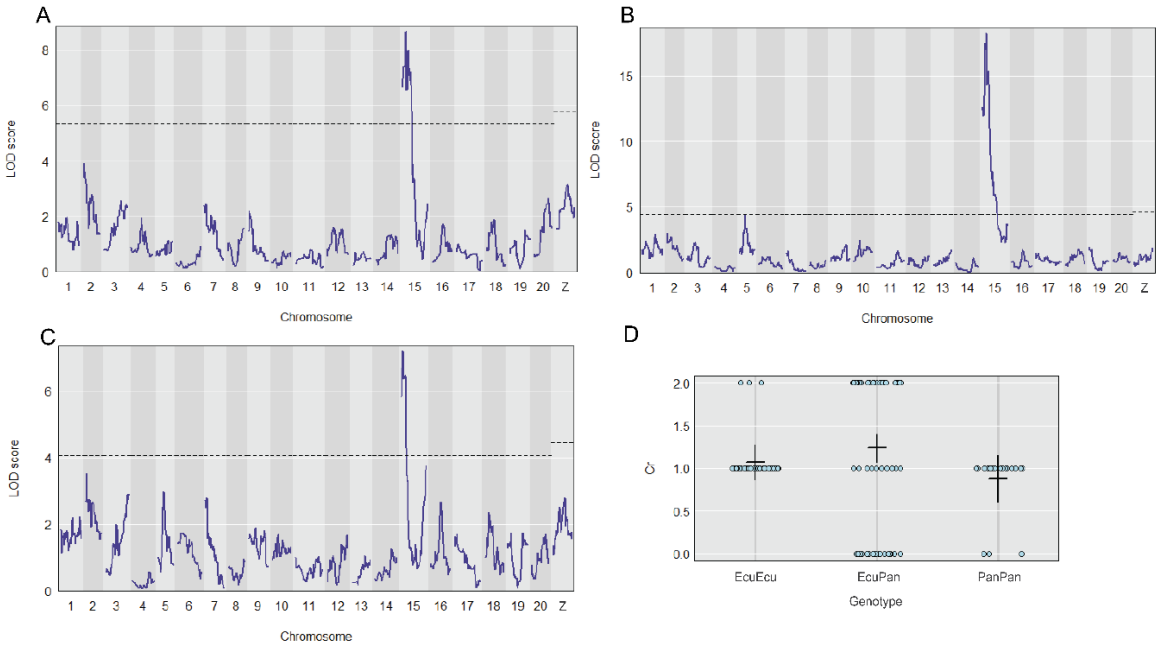

Figure 3.4: *H. erato* QTL scans using all F2 and backcrosses combined for the presence/absence of the yellow bar (**A**), the white margin (**B**), and *Cr* genotypes (**C**). All show a peak on chromosome 15, around the location of the *cortex* gene. (**D**) Genotype x phenotype plot for marker Herato1505_1000078. Alleles inherited from *cyrbia*, the iridescent race from Ecuador are labelled 'Ecu', and those from *demophoon*, the non-iridescent race from Panama, are named

'Pan'. Phenotypes were assigned as 0 (yellow bar, Panama-type), 2 (white margin, Ecuador-type), or 1 (neither element or shadow bar only).

In *H. melpomene*, scans for the presence of the yellow hindwing bar and the hindwing margin both show a large effect locus on chromosome 15. These phenotypes were used to estimate genotypes at the *Yb/Sb* locus and again these are explained by a large effect locus on chromosome 15 (LOD = 28.3, p<0.001) (Figure 3.5). The confidence intervals for this locus span around 1.1Mbp (3.69-8.74cM), which overlaps with the position of the *cortex* gene. The genotype x phenotype plot of the *Yb/Sb* genotypes shows the expected pattern, with homozygous Panama genotypes showing the yellow band and Ecuador genotypes showing the white margin, although again the association is not perfect.

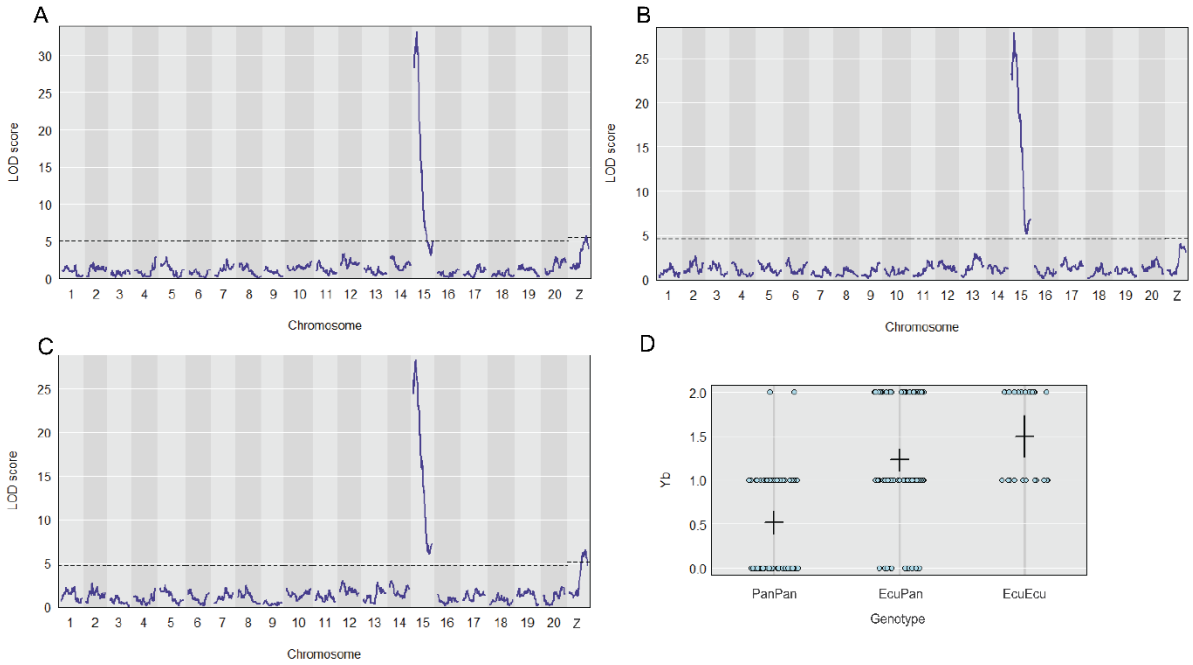

Figure 3.5: In *H. melpomene*, a large effect locus on chromosome 15 explained changes in the *Yb* genotypes as expected. **A.** QTL scan using all families for the presence of the yellow band only. **B.** QTL scan for the hindwing margin only. **C.** Scan for estimated *Yb* genotypes. These were scored as 0 (*rosina* type), 1 (heterozygous) or 2 (*cythera* type). The Z chromosome is also significant but possibly a false positive in this case. **D.** The genotype x phenotype plot of the *Yb* genotypes at marker Hmel215003o_1257868. Alleles inherited from *cythera*, the iridescent race from Ecuador are labelled 'Ecu', and those from *rosina*, the non-iridescent race from Panama, are named 'Pan'. Phenotypes were assigned as 0 (yellow bar, Panama-type), 2 (white margin, Ecuador-type), or 1 (neither element or shadow bar only).

3.4.3 QTL scans for iridescent colour in H. erato

Genome scans using the BR values were first run for the F2 and backcross offspring separately. The F2 scan showed clear peaks on chromosome 20 (LOD = 4.38, p = 0.085) and the Z chromosome (LOD = 4.62, p = 0.182), although these did not reach the significance level (Figure 3.6A). LOD scores in the backcross were low, likely due to the small sample size, so there were no significant peaks (Figure 3.6B). However, the highest LOD score for BR colour was again found on the Z chromosome (LOD = 2.45, p = 0.68).

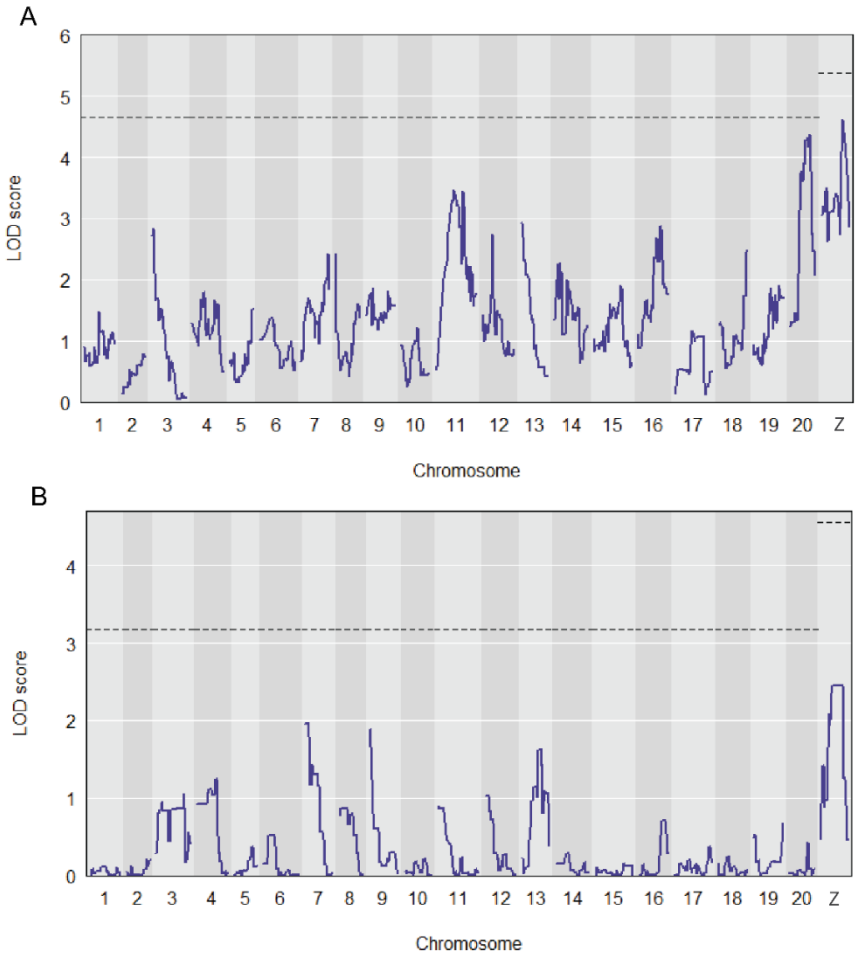

Figure 3.6: *H. erato* genome scans for BR colour did not reveal any significant loci in either the F2 crosses (**A**) or the backcross (**B**). The dotted line shows the 5% significance level.

Scan outputs for the F2 crosses and backcrosses were then combined by adding the LOD scores at each marker position to increase the power, and a new permutation analysis was performed to assess significance in the combined dataset. This combined scan did show two significant QTL on chromosomes 20 and the Z chromosome (Figure 3.7; Table 3.3). Both of these intervals contain around 150 genes. At both markers, individuals with 'Panama-type' genotypes had significantly lower BR values than Ecuador-type and heterozygous genotypes, so following the expected trend. Only two individuals have homozygous Panama-type *demophoon* genotypes at the Z chromosome marker due to the small number of individuals with a *demophoon* maternal grandfather. A further 3 loci had LOD scores above 3.5 (Table 3.3), suggesting a small effect of these loci. The QTL on the Z chromosome explained the largest proportion of the phenotypic variation in BR colour in both the F2 crosses (12%) and the backcross (19%). Together the five QTL explained 27% of variation in colour in the F2 crosses, and 35% in the backcross due a larger effect of chromosome 3 (Table 3.4).

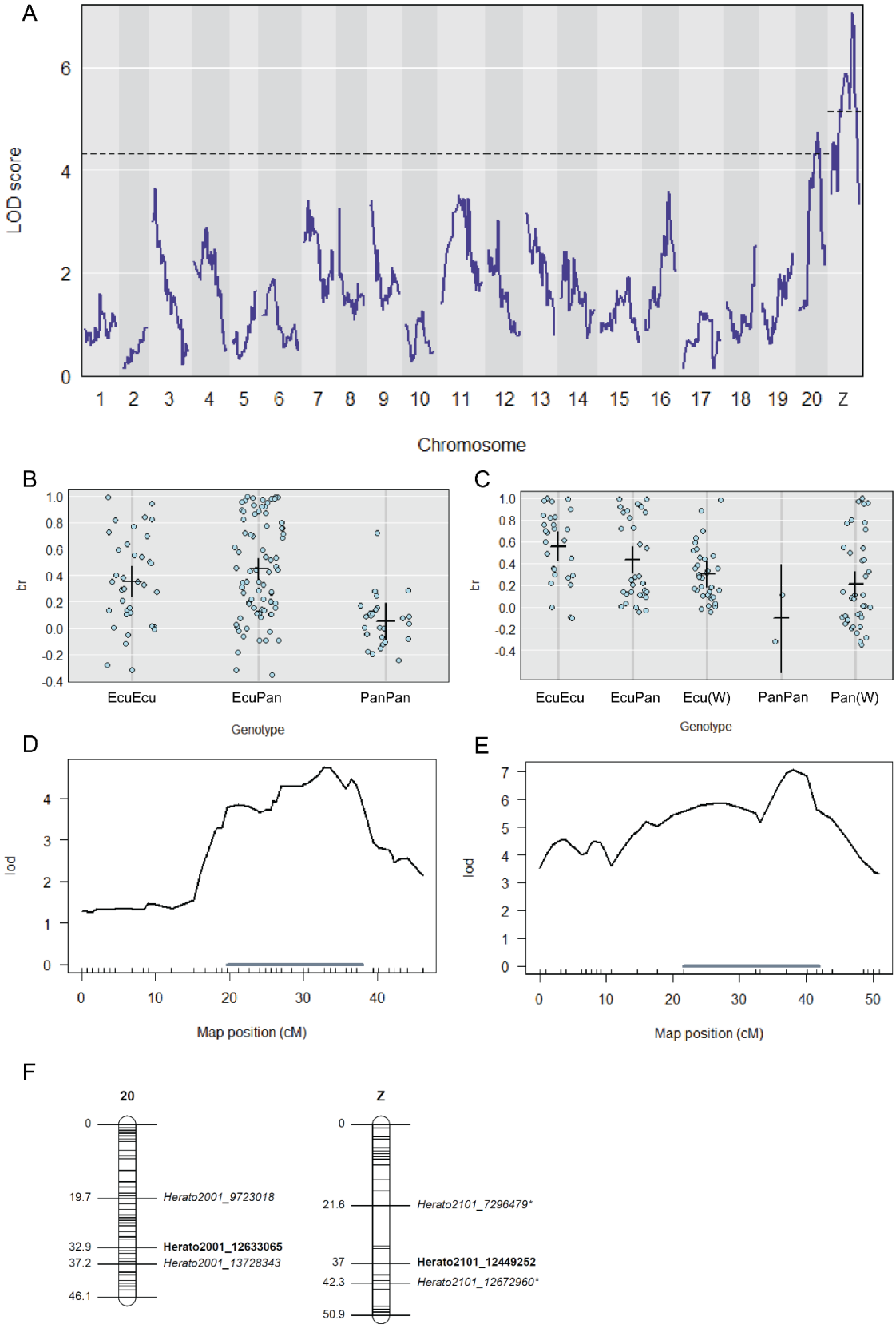
A
LOD score
Chromosome
B
br
EcuEcu
EcuPan
PanPan
Genotype
C
br
EcuEcu
EcuPan
Ecu(W)
PanPan
Pan(W)
Genotype
D
lod
Map position (cM)
E
lod
Map position (cM)
F
20
Herato2001_9723018
Herato2001_12633065
Herato2001_13728343
Z
Herato2101_7296479*
Herato2101_12449252
Herato2101_12672960*

Figure 3.7: **A.** The *H. erato* genome scan for BR colour showed 2 significant QTL on chromosome 20 and the Z chromosome. The black dotted line indicates a 5% significance level determined by 2000 permutations for the autosomes and 43664 permutations for the Z chromosome. Genotype x phenotype plots for QTL on chromosome 20 (**B**) and the Z chromosome (**C**). Alleles inherited from *cyrbia* are labelled 'Ecu', and those from *demophoon* are named 'Pan'. LOD scores for the two chromosomes, 20 (**D**) and Z (**E**), with significant markers. Grey bars indicate the 95% Bayesian confidence interval. **F.** The position of the two significant markers and the confidence intervals on chromosomes 20 and Z. Centimorgan positions are on the left and the marker names on the right. Marker names show the scaffold name and genomic position.

Table 3.3: The combined genome scan using all F2 and backcrosses for *H. erato* BR colour showed two significant markers, and a further 3 markers with suggestive minor effects. P values are genome scan adjusted for each LOD peak. 95% Bayesian credible intervals in cM are indicated. One marker was significantly associated with luminance (R+G+B), which overlapped in 95% CI with one of the significant BR loci.

Marker	**LG**	**Position (cM)**	**LOD**	**p**	**Lower interval cM (LOD score)**	**Upper interval cM (LOD score)**
BR colour						
Herato2101_12449252	Z	38.0	7.07	0.001	21.58 (5.56)	42.0 (5.61)
Herato2001_12633065	20	32.9	4.75	0.022	19.73 (3.79)	38.0 (3.84)
Herato0301_835995	3	4.07	3.65	0.156	0.00 (3.00)	21.55 (2.03)
Herato1605_2359798	16	41.83	3.57	0.183	28.00 (2.09)	52.0 (2.06)
Herato1108_1872853	11	33.96	3.51	0.204	11.07 (2.30)	54.47 (2.42)
Luminance						
Herato2101_12449398	Z	41.6	14.50	<0.001	16.0 (13.04)	44.0 (13.26)

Table 3.4: Output from the *fitqtl* model showing the percentage of phenotypic variation in *H. erato* BR colour that the two most significant QTL explain in the F2 crosses and the backcross. P values are based on the F value.

	QTL location	df	Sum of Squares	LOD	% variation	F value	p
F2	Z	15	0.89	3.82	12.00	0.95	0.518
	20	12	0.57	2.51	7.65	0.75	0.694
	3	2	0.10	0.45	1.23	0.76	0.470
	16	2	0.24	1.11	3.27	1.93	0.151
	11	2	0.18	0.84	2.44	1.44	0.242
Backcross	Z	3	0.36	2.38	19.08	3.26	0.035
	20	1	0.003	0.02	0.014	0.007	0.933
	3	1	0.20	1.43	10.6	5.52	0.025
	16	1	0.06	0.45	3.24	1.66	0.207
	11	1	0.04	0.28	2.00	1.02	0.320

Luminance (overall brightness of the colour) was highly associated with the Z chromosome (Figure 3.8). The significant marker did not map exactly to the same position as for the BR values (Table 3.3) but was apart by only 3.6cM (or just 146bp based on the SNP positions in the genome assembly). Genotypes with Ecuador-type alleles had higher luminance values than those with Panama-type genotypes, and so the effect is in the same direction as for the BR values.

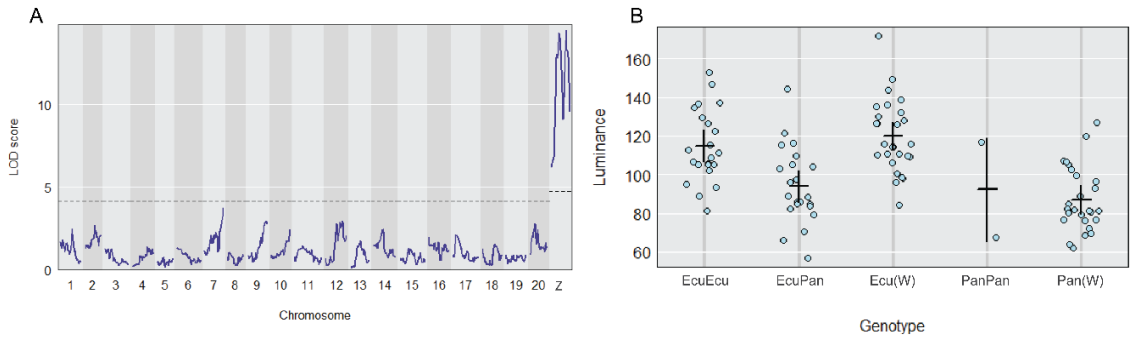

Figure 3.8: **A.** Genome scan for luminance in all *H. erato* crosses shows a significant marker on the Z chromosome. **B.** Genotype x phenotype plot for the Z marker. Alleles inherited from *cyrbia* are labelled Ecuador-type and those from *demophoon* labelled Panama-type. Luminance phenotypes were measured as (R+G+B).

3.4.4 QTL scans for iridescent colour in H. melpomene

For the initial genome scans, the broods were grouped into two – the first group contained the 3 F2 crosses and the second contained the EC70 cross, treated as a backcross. The F2 crosses (Figure 3.9A) showed two clear peaks for BR colour on chromosomes 3 (LOD = 4.04, p = 0.324) and 10 (LOD = 4.41, p = 0.198). The LOD scores for these did not reach the significance threshold, although they were both above 3.5. EC70 (Figure 3.9B) also showed a peak on chromosome 3 which was above the significance level (LOD = 3.82, p = 0.008), but had very low LOD scores (<1) on chromosome 10.

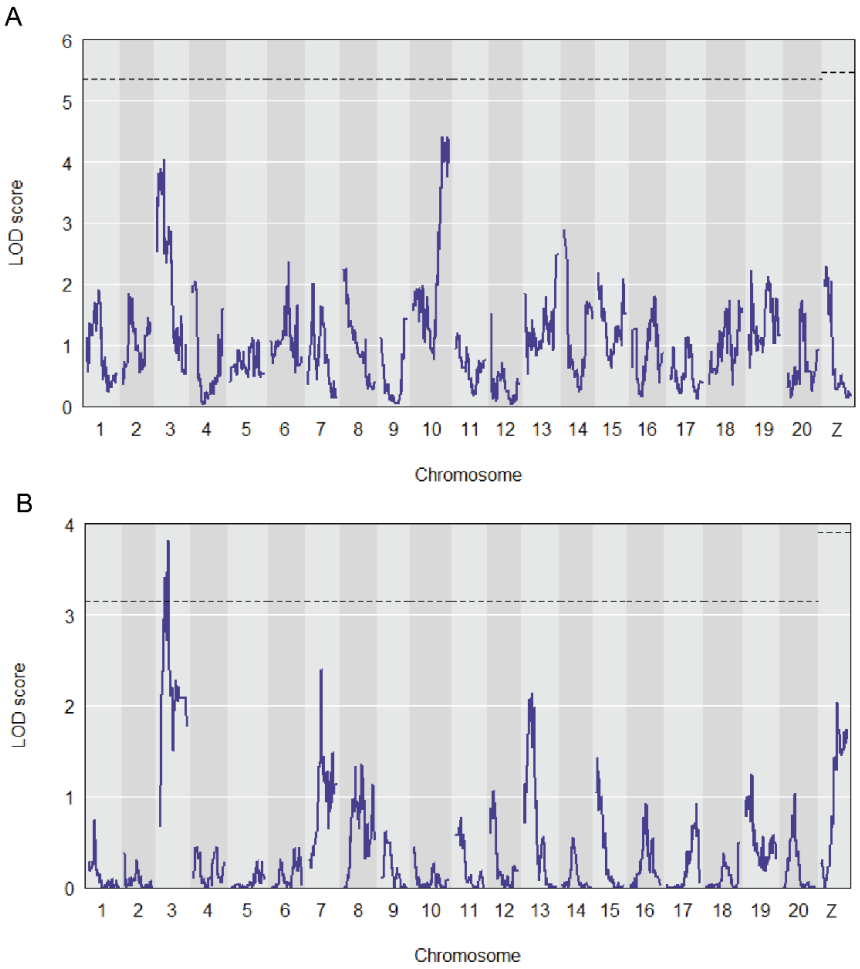

Figure 3.9: **A.** The QTL scan for *H. melpomene* BR colour in the three F2 crosses suggests an effect of loci on chromosomes 3 and 10. Family and sex were included as covariates in the model. Dotted lines show 5% significance level. **B.** The scan for BR colour in the EC70 cross shows a clear effect of a locus on chromosome 3.

After combining the results and running a permutation analysis, the presence of a large effect locus on chromosome 3 became clearer (Figure 3.10A). The interval around this marker relates to a genomic region of approximately 3Mbp and contains 130 genes. A marker on chromosome 10 also shows a high LOD score so is likely to have an effect on the colour, and a further marker on chromosome 7 had a LOD score over 3.5, suggesting a small effect of this locus (Table 3.5).

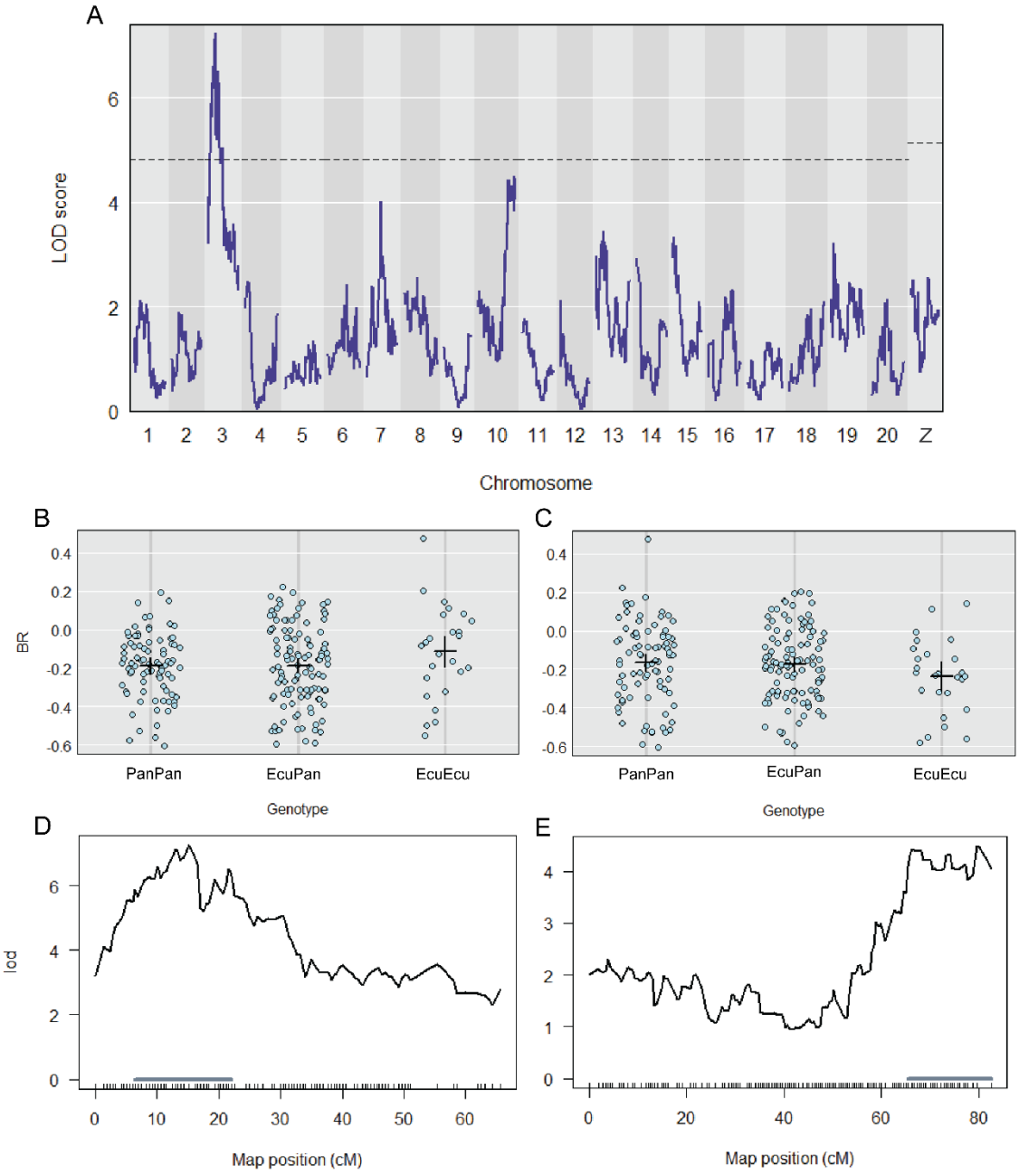

Figure 3.10: **A.** Combining LOD scores for all *H. melpomene* crosses showed a significant locus for BR colour on chromosome 3, and a second locus with a high LOD score approaching significance on chromosome 10. Genotype x phenotype plot for these markers on chromosome 3 (**B**) and 10 (**C**). There are fewer homozygous Ecuador-type genotypes because these are not present in the EC70 brood. Single chromosome plots for chromosomes 3 (**D**) and 10 (**E**). Grey bars show the 95% Bayesian confidence intervals.

Table 3.5: A marker on chromosome 3 was significant for *H. melpomene* BR colour when combining LOD scores from all crosses, and a further two markers had LOD scores over 3.5. Marker name denotes scaffold and position.

Marker	**LG**	**Position (cM)**	**LOD**	**p**	**Lower interval cM (LOD score)**	**Upper interval cM (LOD score)**
BR						
Hmel203003o_2119654	3	15.22	7.26	0.001	6.49 (5.89)	22.10 (6.31)
Hmel207001o_4202577	7	30.60	4.03	0.168	9.93 (2.39)	40.74 (2.22)
Hmel210001o_17693002	10	79.64	4.49	0.085	65.45 (4.10)	82.55 (4.06)
Luminance						
Hmel203003o_2635435	3	17.97	13.61	<0.001	14.39 (12.49)	22.10 (12.84)

The marker on chromosome 10 is on the same chromosome the *WntA* gene controlling pigment colour pattern elements, however the QTL interval does not overlap with this. We also looked at chromosome 15 to look for possible linkage to the *cortex* gene, as expected from results in Chapter 2. A marker with a LOD score of 3.32 is located on chromosome 15 close to the position of the *cortex* gene (Figure 3.11), although the intervals around this marker are large.

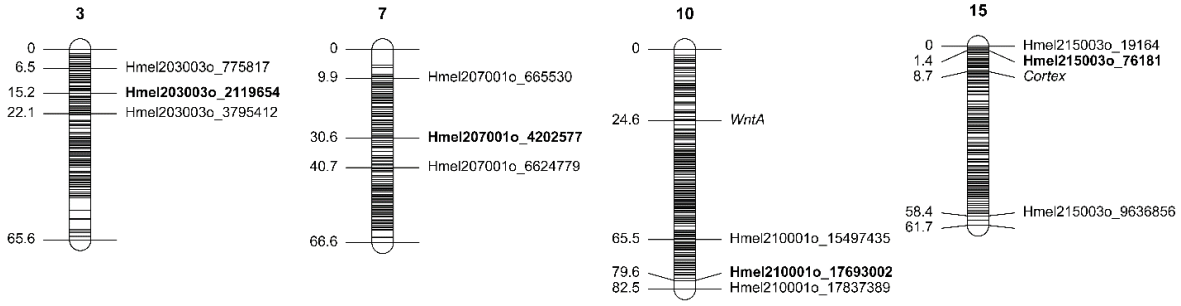

Figure 3.11: *H. melpomene* linkage groups with suggestive markers for blue colour (in bold). Map position (cM) is shown on the left and marker name (scaffold and genomic position) on the right. The marker positions at either end of the 95% Bayesian confidence intervals are shown. The position of *WntA* is also shown on chromosome 10. The marker with LOD = 3.32 on chromosome 15 is included to show possible linkage to the *cortex* gene.

To estimate the amount of phenotypic variation that these markers were explaining, we ran the *fitqtl* model for the combined F2 crosses and the EC70 cross separately (Table 3.6). In the F2 crosses, chromosome 10 had a large effect, explaining 19% of the variation, while the same marker had almost no effect in the EC70 cross. Together the three QTL explain 33% of variation in the F2 crosses, and 22% in the EC70 cross. There was no significant interaction between the markers ($F = 0.005$, $p = 0.95$).

Table 3.6: Output from the *fitqtl* model showing the percentage of phenotypic variation in *H. melpomene* BR colour that each QTL explains in the F2 crosses and the EC70 cross.

	QTL location	**df**	**Sum of squares**	**LOD**	**% variation**	**F value**	**p**
F2	3	2	0.34	2.2	7.89	5.63	0.005
	7	6	0.28	2.15	6.43	1.53	0.176
	10	6	0.80	5.79	18.67	4.44	<0.001
EC70	3	1	0.35	3.12	11.18	14.52	<0.001
	7	2	0.30	2.72	9.66	6.27	0.003
	10	2	0.04	0.41	1.39	0.90	0.408

In the combined analysis of all crosses, luminance was also strongly associated with chromosome 3 (Figure 3.12). The significant marker was 2.75cM (or 515kbp estimating from SNP position) from the marker for BR colour, and the confidence intervals overlap. Directional effect of the alleles was not clear as the homozygous genotypes had similar luminance levels, while heterozygous genotypes were significantly lower ($F_{2,216} = 4.21$, $p = 0.016$).

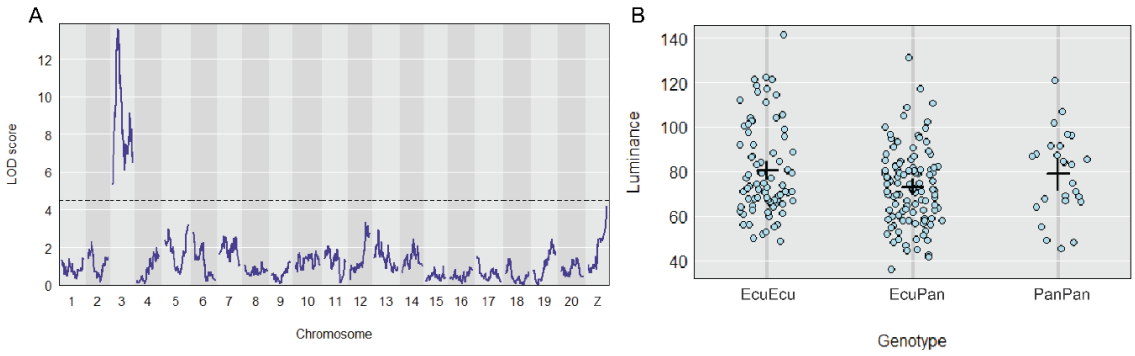

Figure 3.12: **A**. Luminance in *H. melpomene* was strongly associated with linkage group 3 in the combined analysis of all crosses. **B.** Genotype x phenotype plot for the significant marker on chromosome 3.

3.4.5 Comparison of maternal alleles

Comparison of maternal alleles provides further evidence for the differences in the genetic basis of iridescence between *H. erato* and *H. melpomene*. As there is no recombination of maternal chromosomes, we can use maternal markers to investigate chromosome level effects. Scans for BR colour in *erato* show an effect of chromosome 12 (LOD = 3.44, p= 0.020) (Figure 3.13A). Interestingly, this was not seen in the full QTL analysis, suggesting there may be multiple small effect loci on this chromosome. The LOD score for the Z chromosome was low, this is likely because this analysis will have low power to detect Z chromosome effects. As we are limiting our analysis to maternal markers, only males will have a Z chromosome included in the analysis, and as most of the crosses are from a single direction (i.e. *cyrbia* maternal grandfather), there will be very little variation among these. For *melpomene*, the highest LOD score was for chromosome 3 (Figure 3.13B), which follows what is seen in the full scan.

In *H. erato*, total LOD score per linkage group did not correlate with the length of the linkage group as map length (r = -0.21, df = 19, p = 0.356) or as genome length (r = 0.416, df = 19, p = 0.061), and while this p-value may suggest some relationship, this may be driven by the high LOD score of chromosome 12 (Figure S3.6). Likewise, in *H. melpomene*, LOD score did not

correlate with map length (r = -0.18, df = 19, p = 0.426) or genome length (r = -0.15, df = 19, p = 0.514). The chromosomes of these species are highly syntenic and numbered in the same way (Davey et al. 2016; Van Belleghem et al. 2017). Therefore, to test for parallelism in the combined effect of all markers on each chromosome, we compared the variance explained by each chromosome in *erato* and *melpomene* and found no correlation between the species (r = 0.09, df = 19, p = 0.698) (Figure 3.14). The maternal chromosomes explain very little of the overall variation, around 22% in both species. However, this is not unexpected because the most that these maternal genotypes can explain is 50%, with the rest of the genetic variance coming from the paternal markers. For *H. erato*, we might expect even less given that around 20% of the variation in blue colour is controlled by the Z chromosome, which will not be detected. In both species, chromosome 8 explains a comparatively large part of the variation explained by maternal genotypes (2.3% in *erato* and 5.2% in *melpomene*), suggesting there may be small effect loci for blue colour on this chromosome in *erato* and *melpomene*.

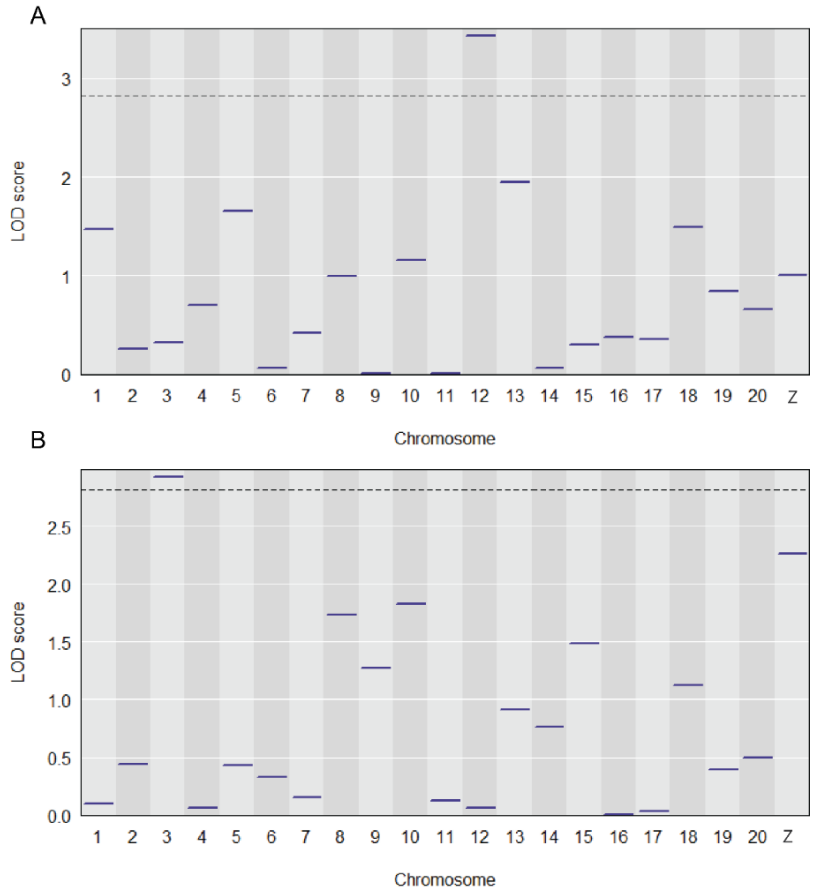

Figure 3.13: **A.** QTL genome scan for BR colour in *H. erato* using only maternal alleles. The high LOD score for chromosome 12 was not seen in the overall scan of all crosses. **B.** Scan for BR colour using *H. melpomene* maternal alleles, with the 3 F2 crosses. Overall, LOD scores were low but the highest association was with chromosome 3. The dotted line shows the 5% significance level.

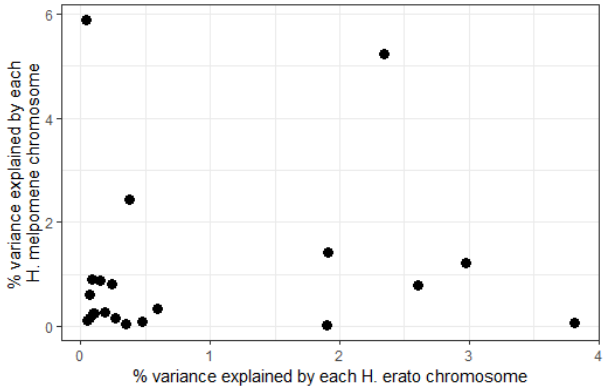

Figure 3.14: No correlation was found between the percentage of variation in BR colour explained by *H. melpomene* chromosomes and *H. erato* chromosomes.

3.5 Discussion

In one of the first studies to look at the genetic basis of structural colour, we have used experimental crosses to show that the same genes are not producing iridescence in the co-mimics *Heliconius erato* and *Heliconius melpomene*. In contrast to many of the loci for pigment colour pattern which are homologous across multiple species, iridescence in *H. erato* and *H. melpomene* is produced by loci located at different positions in the genome, as was expected from the differences in the level of iridescence between species. In both species, iridescence is controlled by multiple genes, with both having two medium to large effect loci, plus a number of putative smaller effect loci.

Iridescence is not an example of convergent evolution controlled by the same genes across distantly related species, unlike the repeated use of loci controlling pigment colour in *Heliconius* and other species. Time since divergence of these species is over 10 million years (Kozak et al. 2015), suggesting a lower likelihood of gene reuse, although the same major effect genes control pigment colour pattern in these species. In a study of sticklebacks in which multiple phenotypic traits diverged in parallel between different species, around half of these traits were associated with the same QTL in each population (Conte et al. 2015). These species had a recent common ancestor around 10,000 years ago suggesting that constraints, such as the number of loci able to produce the phenotype, and genetic biases, such as mutation rate, are more likely to be similar between them (Schluter et al. 2004; Conte et al. 2012). Standing genetic variation may also be shared between closely related species and so lead to repeated use of certain genes (Colosimo et al. 2005; Burke et al. 2014). Parallel changes in fish body size in response to fishing, a polygenic mechanism, were associated with the same allele frequency shifts across lineages, likely linked to pre-existing genetic variation (Therkildsen et al. 2019). Our results do not provide evidence for ancestral variation which allowed the evolution of iridescence in *Heliconius*, because the differences in genetic architecture suggest the trait likely evolved due to multiple, independent genetic mutations. Other colour pattern elements have spread via adaptive introgression (Enciso-

Romero et al. 2017), but this is only seen in more closely related species, and it is thought that *H. erato* and *H. melpomene* are too divergent to hybridise.

In both species, the two largest effect loci together explain 20-30% of the variation in iridescent blue colour. Effect sizes in small samples, said to be less than 500 individuals (Xu 2003), may be overestimated due to the 'Beavis effect'. QTL are only reported once they reach the predetermined significance level which can lead to QTL with high effect sizes from variation in sampling being more likely to reach the significance level (Xu 2003). In practice, this means that the effect sizes of the most significant QTL can be overestimated, while at the same time, smaller effect QTL are not reported. Using a chromosome-level analysis of the maternal alleles allows us to look at the combined effects of small effect loci. For example, if there are many small effect loci on a single linkage group, these may not be detected in the full genome scan but the additive LOD scores could reach significance when comparing effect sizes of whole chromosomes. We can then use this to compare genetic architecture between species. With the iridescent trait, there were no obvious parallels between the two species, again pointing towards a lack of homologous loci between species, but we still cannot rule out smaller effect loci which were not detected in this analysis. Due to the quantitative nature of the trait, we may expect there to be more small effect loci which may be detected if using a larger sample size (Xu 2003). In *H. erato*, chromosome 12 was significant in the analysis of maternal markers but not in the main analysis suggesting there could be a number of small effect loci on this linkage group. If there were many genes of interest on each linkage group, i.e. if the trait is highly polygenic, we would expect to see a correlation between chromosome-level LOD scores and map length, but this was not found. Rather than summing the LOD scores of all markers on a chromosome, the use of maternal alleles is beneficial as there is one marker per chromosome and so we do not need to control for the confounding effect of the number of markers. The limitation of this approach is that only the effects of the maternal markers are analysed, which contribute less than 50% of the total genetic variance (due to the sex chromosome), so small effects may still be hidden.

As discussed in Chapter 2, we may expect the genetic control of iridescence to be linked to previously discovered colour pattern genes, as recent studies have suggested joint control of pigment and structural colouration. In particular, the gene *optix* controls red colour pattern elements in *Heliconius,* but has also been linked to the presence of structural colour in other species (Zhang et al. 2017). In *Junonia* butterflies, artificial selection for iridescence resulted in a thickening of the lower lamina, which is linked to *optix* (Thayer et al. 2019). *Cortex* is a cell-cycle regulator so is also likely to have further roles in scale development (Nadeau 2016). Looking for overlap between known colour pattern genes and the QTL found here for iridescence may provide initial evidence for the role of these genes in structural colour production. On the other hand, as the genetic basis of iridescence seems to be different between species, this overlap may be less likely.

As we expected from the phenotypic analysis of blue colour variation in *H. erato* cross offspring, the QTL analysis confirms the presence of a large effect locus on the Z chromosome. In *Heliconius* studies, the Z chromosome has previously been linked to variation in forewing band shape in *erato* (Mallet 1989) and *melpomene* (Baxter et al. 2009), as well as colour of the forewing band in *erato* and *H. himera* (Papa et al. 2013), and *H. numata* pattern variation (Jones et al. 2012). In contrast, no studies on pigment colour and pattern variation have been linked to chromosome 20. In *H. melpomene,* although we expected to see a locus linked to the *cortex* gene, which was detected in the phenotypic analysis (Chapter 2), there were no significant markers on chromosome 15. However, there was some evidence for a small effect locus located near to this gene, although the interval for this QTL effectively spans the whole linkage group so we are unable to say whether *cortex* itself has a direct effect on iridescence or if it is a linked gene. Forewing band size has been shown to be largely determined by *WntA* (Papa et al. 2013; Mazo-Vargas et al. 2017) which is found on chromosome 10, although it is not located close to the marker we identified for blue colour. This fits with previous results which did not find a link between BR colour and the size of the red forewing band (Brien et al, 2018/Appendix).

BR values were generally lower in the EC70 *melpomene* cross, suggesting more *rosina* alleles in its ancestry. Maternal alleles were not taken into account in this analysis, so this could also cause differences between the crosses. Chromosome 7, on which we found a suggestive QTL, has also been linked to modifier loci controlling forewing red band shape in *melpomene* (Baxter et al. 2009).

Differences in the effect sizes of QTL between the F2 crosses and the backcross in *H. erato* could be due to epistatic effects or dominance. One allele may have a large phenotypic effect in one genetic background but not in another, due to non-additive interactions of alleles. The QTL on chromosome 20 was only significant in the F2 crosses, and if the effect of this allele is only visible when another allele is homozygous for the *demophoon* allele, this effect could not be seen in the backcross. Epistatic interactions produce quantitative colour variation in many systems. Human eye colour (Pośpiech et al. 2011), coat colour in cats (Little 1919) and *Brassica* petal colour (Rahman 2001; Zhang et al. 2002) are all examples. Another possibility is that the *cyrbia* allele for the locus on chromosome 20 could be dominant. In the backcross, all the offspring will be heterozygous or homozygous for the *cyrbia* allele, and so if this allele is dominant, no effect would be observed. The data support this hypothesis as individuals with heterozygous genotypes at the marker have similar levels of blue colour to those homozygous for the *cyrbia* allele, with the phenotypic effect largely seen in homozygous *demophoon* (PanPan) individuals (Figure 3.7B).

The nanostructures which produce structural colours are complex and formed of repeating elements which can vary in thickness and patterning producing different effects (Ghiradella 1989; Nijhout 1991). Independent genes could be controlling different aspects of these structures, for example, ridge spacing, cross-rib spacing or layering of lamellae, which would explain the large variation in colour that is seen. Complex structures such as these could be more difficult to mimic than pigment-based colours and there may be developmental constraints which prevent iridescence in *H. melpomene* from becoming as bright as *H. erato* (e.g. actin production).

Matsuoka & Monteiro (2018) used CRISPR/Cas9 knockouts to show that mutations in the melanin pathway in *Bicyclus* butterflies alter scale morphology, which in turn could affect the production of structural colours. Mutations in the *yellow* gene increased the number of horizontal lamellae while the *DDC* gene led to taller vertical lamellae, suggesting scale morphology is under the control of multiple genes which are also likely having pleiotropic effects.

As with many quantitative traits, we expect that the brightness of the iridescence may also be affected by environmental factors. Kemp et al. (2006) showed that UV reflectance in adult *Colias* butterflies was lower if they had been thermally stressed as pupae, or had been fed on lower quality diets as larvae. Therefore, some of the unexplained variation in iridescence variation could be due to extrinsic factors. Nonetheless, all the individuals used in this study were reared in the same environment and with the same diet.

In conclusion, unlike the major loci controlling pigment colour pattern, iridescent colour in two *Heliconius* co-mimics is not an example of repeated gene use. In both species, iridescence is controlled by two loci with medium-large effects and a number of smaller effect loci but is not a highly polygenic trait. The results suggest that there is less genetic parallelism between quantitative traits in distantly related species and that the genetic basis of such adaptative traits may be harder to predict.

3.6 Supplementary Information

Table S3.1: Number of sequenced *H. erato* reads per individual obtained after initial quality filtering steps. Parents of crosses are in bold.

Individual	Total sequenced reads	Mapped reads	Reads retained after deduplication	% duplication
14N012	**32 322 593**	**22 874 122**	**13 580 236**	**43.23**
14N064	**28 310 085**	**19 577 002**	**12 901 051**	**41.87**
14N065	**14 274 730**	**10 057 200**	**6 460 579**	**38.38**
14N077	**32 767 659**	**23 148 958**	**13 644 737**	**44.42**
14N078	**25 721 592**	**18 359 980**	**11 121 070**	**42.12**
14N093	**25 061 618**	**17 602 926**	**10 784 574**	**41.35**
14N111	**16 391 172**	**11 470 428**	**7 502 551**	**37.61**
14N112	**25 021 843**	**17 677 162**	**10 894 944**	**40.75**
14N113	**30 635 463**	**21 576 324**	**12 714 835**	**44.08**
14N114	**48 405 198**	**34 134 072**	**18 979 823**	**47.04**
14N153	2 774 538	1 912 106	1 484 115	23.75
14N189	11 118 281	7 716 990	5 546 081	29.84
14N190	6 381 640	4 519 566	3 291 150	28.94
14N191	5 425 461	3 807 644	2 796 748	28.26
14N192	5 206 660	3 688 002	2 709 776	28.10
14N194	3 229 746	2 246 744	1 751 305	23.44
14N195	8 785 660	6 069 184	4 883 532	20.84
14N201	5 331 333	3 676 018	2 839 968	24.25
14N204	5 007 896	3 473 386	2 681 115	24.88
14N205	3 076 870	2 141 558	1 601 557	26.91
14N206	8 378 856	5 838 838	4 719 525	20.45
14N207	3 078 180	2 117 620	1 668 055	22.64
14N210	6 571 318	4 537 234	3 389 563	26.87
14N211	2 339 796	1 622 964	1 389 300	15.26
14N212	6 571 086	4 534 640	3 440 377	25.64
14N224	3 132 551	2 209 428	1 893 159	15.18
14N225	4 254 203	2 940 518	2 186 107	27.39
14N227	9 087 392	6 303 494	4 645 340	28.13
14N228	13 991 451	9 726 896	6 751 185	32.52
14N229	6 526 929	4 564 090	3 464 463	25.68
14N230	7 394 221	5 197 710	3 914 813	26.28
14N232	11 181 462	7 853 288	5 495 856	32.05
14N233	9 296 363	6 467 006	4 612 139	30.40
14N235	4 728 567	3 311 472	2 551 413	24.35
14N236	10 747 451	7 578 714	5 359 953	31.08
14N238	5 131 015	3 623 152	2 674 921	27.76
14N240	20 318 128	14 275 044	9 851 822	33.13
14N241	6 539 306	4 515 598	3 430 831	25.46
14N242	14 269 066	9 810 474	7 048 319	30.12
14N243	6 693 273	4 564 184	3 517 425	24.35
14N244	5 609 795	3 912 552	2 987 832	25.43
14N245	7 652 312	5 378 358	3 862 384	29.97
14N246	5 605 290	3 910 890	2 966 578	25.58
14N247	6 841 488	4 839 952	3 640 590	26.41
14N248A	4 969 227	3 463 218	2 575 916	27.22
14N248B	7 097 630	4 926 744	3 904 486	22.03
14N250	4 562 134	3 207 336	2 469 950	24.55
14N252	7 182 379	5 010 810	3 925 637	23.13

14N255	3 827 162	2 666 498	2 080 736	23.54
14N256	5 304 088	3 639 838	2 634 207	29.36
14N257	6 478 516	4 502 628	3 190 655	30.88
14N260	2 156 915	1 500 968	1 103 619	28.26
14N261	5 212 845	3 583 670	2 725 150	25.45
14N262	5 186 602	3 645 452	2 617 940	30.81
14N264	2 273 703	1 611 906	1 173 433	28.83
14N265	5 825 252	4 103 638	2 883 036	31.80
14N273	1 971 458	1 389 508	1 020 717	28.25
14N276	4 829 425	3 425 504	2 440 962	30.64
14N277	5 221 825	3 634 582	2 585 693	30.75
14N278	5 514 848	3 804 204	2 714 770	30.59
14N279	3 652 476	2 528 722	1 831 956	29.45
14N282	4 472 828	3 129 784	2 225 053	30.77
14N283	1 778 020	1 257 644	924 612	28.21
14N284	6 497 099	4 586 408	3 200 795	32.18
14N285	8 946 912	6 311 696	4 382 274	32.49
14N287	9 704 490	6 772 720	4 663 858	32.99
14N288	6 353 047	4 327 658	3 062 092	31.54
14N289	10 004 793	6 973 946	4 795 257	33.09
14N291	7 951 501	5 595 236	4 557 163	19.71
14N293	6 800 962	4 716 792	3 324 106	31.36
14N297	5 547 975	3 840 724	2 702 168	31.60
14N298	7 487 002	5 307 678	3 682 421	32.62
14N299	5 687 313	4 010 704	2 852 610	30.63
14N306	6 719 848	4 737 036	3 325 722	31.72
14N307	5 455 794	3 827 204	2 696 145	31.42
14N308	5 439 796	3 738 000	2 776 274	27.29
14N310	5 170 275	3 571 166	2 632 023	27.89
14N326	4 531 590	3 112 342	2 304 484	27.48
14N328	2 005 472	1 390 516	1 050 179	25.94
14N330	2 640 579	1 882 030	1 420 171	25.95
14N331	11 119 565	7 860 070	5 484 884	32.17
14N333	8 266 979	5 824 746	4 184 174	29.88
14N334	6 133 957	4 347 772	3 170 604	28.67
14N335	2 911 689	2 020 564	1 523 677	26.05
14N338	**42 639 953**	**29 964 370**	**17 007 610**	**46.14**
14N339	**35 345 204**	**24 946 638**	**14 275 134**	**45.71**
14N341	3 592 010	2 495 982	1 861 775	26.94
14N343	2 757 756	1 947 320	1 461 621	26.43
14N344	4 485 001	3 139 794	2 635 642	17.17
14N347	**89 854 434**	**64 476 216**	**31 400 944**	**55.12**
14N348	**47 412 143**	**33 749 872**	**18 699 787**	**47.63**
14N351	9 622 355	6 707 060	4 756 518	31.03
14N372	7 513 792	5 286 808	4 130 718	23.52
14N374	11 488 447	8 080 512	6 165 435	25.21
14N380	10 266 976	7 133 750	5 482 030	24.61
14N390	7 791 557	5 443 306	4 290 677	23.23
14N391	13 302 097	9 240 728	7 178 075	25.47
14N394	4 874 765	3 408 900	2 782 028	20.82
14N395	**28 541 234**	**20 001 188**	**11 846 331**	**43.68**
14N396	**265 931**	**187 520**	**135 204**	**31.60**
14N399	7 121 271	4 939 210	3 881 633	22.94
14N400	13 509 198	9 365 574	7 011 768	26.81
14N401	12 546 656	8 920 858	6 735 207	26.09
14N402	3 164 259	2 195 858	1 917 010	15.29

14N403	10 073 296	6 836 168	5 679 192	20.11
14N412	6 021 576	4 238 474	3 321 254	23.12
14N413	4 325 452	2 996 552	2 507 039	17.43
14N415	4 393 976	3 062 244	2 455 421	21.05
14N426	5 910 302	4 144 054	3 243 738	23.13
14N431	6 006 683	4 170 788	3 285 325	22.63
14N432	3 563 536	2 480 142	2 003 397	20.41
14N436	4 538 384	3 151 286	2 524 941	21.15
14N437	6 434 202	4 475 636	3 499 134	23.28
14N442	4 030 588	2 783 460	2 330 719	17.36
14N447	2 050 519	1 436 544	1 197 549	18.28
14N469	3 389 360	2 352 274	1 899 995	20.49
14N470	2 844 649	1 966 824	1 668 897	16.10
14N471	10 576 900	7 460 478	5 719 792	24.80
14N475	4 475 499	3 126 032	2 490 951	21.65
14N486	10 670 366	7 587 758	5 784 949	25.22
14N487	14 709 875	10 533 920	7 844 269	27.16
14N489	10 764 871	7 510 894	5 667 755	26.20
15N502	7 186 463	5 029 084	3 955 699	22.71
15N503	5 073 889	3 518 824	2 788 227	22.12
15N504	4 631 092	3 239 990	2 602 937	20.90
15N528	2 843 162	1 997 040	1 638 722	19.07
15N529	4 640 866	3 278 828	2 750 395	17.16
15N530	7 667 446	5 415 784	4 195 035	24.02
15N531	6 685 166	4 655 568	3 660 742	22.71
15N532	4 097 897	2 878 844	2 436 771	16.27
15N541	12 275 778	8 655 886	6 455 140	27.16
15N553	6 158 059	4 370 192	3 450 692	22.48
15N554	4 717 957	3 311 148	2 773 131	17.25
15N556	11 371 653	8 127 896	6 251 063	24.55
15N568	4 353 991	3 040 828	2 427 404	21.60
15N573	2 758 367	1 948 422	1 594 979	19.34
15N578	4 147 172	2 929 526	2 373 888	20.18
15N579	5 310 508	3 726 870	2 976 825	21.41
15N596	7 830 872	5 440 894	4 249 073	23.32
15N597	8 208 467	5 727 464	4 438 732	23.92
15N598	1 441 328	1 000 526	851 474	15.90
15N599	5 643 650	3 929 986	3 145 704	21.15
15N600	805 921	569 510	482 583	16.29
15N601	832 918	597 112	506 581	16.16
15N608	8 300 476	5 927 412	4 565 327	24.39
15N609	7 239 666	5 083 984	3 960 460	23.50
15N611	5 775 454	4 114 904	3 270 636	21.74
15N617	3 686 564	2 615 916	2 128 104	19.83
15N629	7 280 151	4 983 274	4 088 972	19.05
15N634	3 745 043	2 589 044	2 175 557	17.03
15N637	2 757 430	1 919 886	1 645 582	15.18
15N638	2 848 769	1 994 300	1 694 148	16.04
15N662	16 701 974	11 788 314	8 832 035	26.67
15N675	4 033 549	2 833 280	2 385 697	16.80
15N702	8 576 226	6 017 234	4 823 992	21.19
Average	8 982 430	6 307 435	4 342 765	26.65
Total	1 140 241 438	990 267 236	681 814 039	

Table S3.2: Genetic map summary for *H. erato*. The *H. erato* genome is 380Mb meaning a centimorgan (cM) in this map has a physical distance of 330Kb on average, and an average of 66Kb (0.2cM) between markers.

Linkage group	**Number of markers**	**Length (cM)**	**Average spacing (cM)**	**Maximum spacing (cM)**
1	303	56.3	0.2	3.9
2	247	42.9	0.2	4.7
3	219	62.8	0.3	7.8
4	438	56.7	0.1	6.8
5	371	41.9	0.1	2.3
6	333	65.0	0.2	9.0
7	228	51.4	0.2	5.5
8	333	43.4	0.1	6.4
9	208	52.9	0.3	6.4
10	373	49.9	0.1	4.5
11	265	75.7	0.3	7.2
12	340	57.0	0.2	3.9
13	244	50.1	0.2	3.9
14	180	60.2	0.3	6.7
15	335	69.0	0.2	7.2
16	229	54.0	0.2	3.1
17	199	69.1	0.3	11.7
18	234	52.7	0.2	4.7
19	299	54.4	0.2	5.3
20	160	46.1	0.3	3.1
Z	110	50.9	0.5	10.8
Overall	**5648**	**1162.4**	**0.2**	**11.7**

Table S3.3: Number of sequenced *H. melpomene* reads per individual obtained after initial quality filtering steps. Parents of crosses are in bold.

Individual	Total sequenced reads	Mapped reads	Reads retained after deduplication	% duplication
14N365	**12 025 732**	**11 585 557**	**7 957 368**	**31.32**
14N366	**6 641 594**	**6 398 730**	**4 956 070**	**22.55**
14N368	**6 777 050**	**6 533 658**	**5 003 340**	**23.42**
14N479	**4 688 912**	**4 528 171**	**3 559 292**	**21.40**
15N546	1 499 198	1 455 941	1 283 549	11.84
15N677	2 291 944	2 221 953	1 880 740	15.36
15N683	2 427 864	2 346 255	2 032 268	13.38
15N694	1 053 398	1 021 841	910 204	10.93
15N703	2 083 626	2 018 189	1 724 111	14.57
15N706	4 160 722	4 025 224	3 251 131	19.23
15N711	856 682	831 092	737 644	11.24
15N712	1 862 638	1 804 590	1 546 319	14.31
15N725	3 124 038	3 021 651	2 590 269	14.28
15N726	3 185 902	3 072 095	2 592 097	15.62
15N731	2 009 046	1 947 479	1 675 623	13.96
15N744	827 006	801 083	711 643	11.16
15N746	1 335 398	1 293 891	1 138 167	12.04
15N748	2 936 432	2 846 492	2 412 073	15.26
15N753	735 034	706 701	638 948	10.32
15N755	546 108	529 279	480 246	9.26
15N758	1 954 466	1 896 930	1 642 086	13.43
15N765	2 016 296	1 955 446	1 679 838	14.09
15N768	1 632 632	1 582 341	1 380 315	12.77
15N784	1 030 890	1 000 495	900 313	10.01
15N787	1 702 362	1 649 743	1 453 374	11.90
15N789	1 470 440	1 427 168	1 265 362	11.34
15N808	689 636	668 737	610 948	8.64
15N822	265 446	257 449	237 368	7.80
15N844	401 524	389 060	357 313	8.16
15N849	2 392 796	2 318 281	2 000 272	13.72
15N855	2 858 816	2 771 286	2 361 024	14.80
15N857	2 091 268	2 014 271	1 743 558	13.44
15N860	4 375 844	4 244 335	3 496 153	17.63
15N864	2 545 156	2 467 642	2 096 038	15.06
15N885	1 033 370	1 003 188	901 977	10.09
15N906	1 281 348	1 242 823	1 110 990	10.61
15N907	4 391 084	4 257 346	3 440 107	19.20
15N910	1 244 220	1 206 930	1 081 392	10.40
15N913	1 256 496	1 170 265	1 036 474	11.43
15N921	697 882	676 951	612 024	9.59

15N932	1 047 688	1 015 684	903 436	11.05
15N933	1 722 480	1 669 191	1 455 896	12.78
15N939	1 365 412	1 324 225	1 187 167	10.35
15N944	1 490 320	1 445 193	1 273 828	11.86
15N945	1 315 892	1 274 846	1 110 810	12.87
15N957	2 409 480	2 155 054	1 858 382	13.77
15N960	2 109 898	2 048 262	1 748 379	14.64
15N964	959 774	930 204	829 311	10.85
15N967	1 322 058	1 278 535	1 118 515	12.52
15N968	623 308	605 002	553 452	8.52
15N969	1 940 306	1 881 338	1 651 618	12.21
15N976	925 380	887 422	796 288	10.27
15N979	1 070 396	1 039 219	935 284	10.00
15N982	1 014 880	984 321	891 298	9.45
15N987	859 356	833 786	761 196	8.71
15N562	**2 961 742**	**2 830 456**	**2 301 018**	**18.71**
15N563	**12 135 760**	**11 750 935**	**8 122 988**	**30.87**
15N1000	1 003 360	972 578	862 422	11.33
15N1003	2 641 820	2 559 149	2 139 545	16.40
15N1004	1 684 160	1 633 671	1 431 683	12.36
15N1007	2 085 386	2 023 763	1 770 293	12.52
15N1012	1 841 166	1 785 028	1 548 621	13.24
15N1017	1 319 006	1 278 610	1 126 975	11.86
15N1019	1 098 140	1 065 044	951 384	10.67
15N1020	1 191 206	1 153 580	1 030 163	10.70
15N1021	527 316	511 248	467 155	8.62
15N1023	1 712 820	1 662 117	1 461 610	12.06
15N1035	1 152 442	1 116 610	989 310	11.40
15N1042	700 126	679 620	615 134	9.49
15N732	390 016	378 408	352 743	6.78
15N736	1 451 620	1 408 123	1 265 414	10.13
15N737	1 345 584	1 304 687	1 154 227	11.53
15N745	1 567 960	1 521 650	1 346 341	11.52
15N747	2 616 274	2 528 858	2 202 911	12.89
15N750	671 176	650 331	596 142	8.33
15N756	1 217 412	1 181 297	1 060 989	10.18
15N760	984 262	953 183	847 620	11.07
15N763	1 756 798	1 701 876	1 472 216	13.49
15N766	1 172 274	1 136 320	1 021 764	10.08
15N778	1 789 462	1 735 376	1 509 449	13.02
15N782	3 647 288	3 538 589	2 965 203	16.20
15N783	2 308 814	2 231 777	1 950 382	12.61
15N799	3 547 148	3 440 070	2 873 808	16.46
15N807	3 031 430	2 931 082	2 523 416	13.91
15N827	4 454 882	4 320 701	3 533 171	18.23
15N841	1 408 672	1 364 812	1 199 629	12.10

15N842	915 362	887 917	784 070	11.70
15N843	650 954	631 359	572 730	9.29
15N863	1 018 186	986 661	901 065	8.68
15N872	1 374 806	1 333 915	1 199 117	10.11
15N876	2 451 296	2 369 672	2 066 675	12.79
15N882	1 015 644	985 363	883 899	10.30
15N889	927 920	899 530	820 078	8.83
15N895	866 514	840 820	757 285	9.93
15N904	731 620	709 910	644 769	9.18
15N914	2 021 292	1 959 804	1 704 866	13.01
15N918	2 738 330	2 654 949	2 267 327	14.60
15N919	868 786	843 324	755 886	10.37
15N926	1 386 770	1 345 195	1 204 103	10.49
15N930	2 367 894	2 296 956	1 996 486	13.08
15N931	3 141 378	3 049 764	2 590 824	15.05
15N943	1 202 150	1 167 530	1 036 433	11.23
15N947	2 227 904	2 158 756	1 847 495	14.42
15N959	1 469 006	1 423 808	1 232 887	13.41
15N965	2 357 180	2 284 465	1 973 729	13.60
15N970	1 826 956	1 771 669	1 545 282	12.78
15N975	2 934 200	2 843 025	2 394 586	15.77
15N980	1 190 576	1 152 940	1 016 437	11.84
15N983	3 743 922	3 626 478	3 002 855	17.20
15N991	1 272 136	1 233 221	1 076 404	12.72
15N994	1 015 806	984 709	881 719	10.46
15N605	**4 099 178**	**3 963 162**	**3 185 931**	**19.61**
15N780	616 434	598 339	548 251	8.37
15N781	1 725 860	1 672 989	1 482 584	11.38
15N785	1 772 020	1 721 882	1 527 076	11.31
15N788	1 397 798	1 353 772	1 179 565	12.87
15N790	1 610 126	1 560 986	1 371 674	12.13
15N794	3 332 602	3 226 519	2 694 297	16.50
15N809	518 064	502 692	458 161	8.86
15N613	**4 937 904**	**4 719 488**	**3 698 506**	**21.63**
15N614	**2 181 162**	**2 114 372**	**1 809 875**	**14.40**
15N1001	1 475 216	1 428 216	1 149 613	19.51
15N1005	3 235 488	3 133 739	2 264 333	27.74
15N1006	985 894	954 400	779 332	18.34
15N1008	974 876	941 426	756 160	19.68
15N1009	1 372 730	1 330 202	1 045 195	21.43
15N1010	2 579 546	2 503 631	1 944 073	22.35
15N1011	913 384	885 275	733 711	17.12
15N1018	1 920 846	1 861 410	1 608 078	13.61
15N1022	1 437 748	1 390 984	1 120 349	19.46
15N1025	1 042 416	1 010 814	839 110	16.99
15N1026	1 356 644	1 315 533	1 048 542	20.30

15N1027	2 046 362	1 985 092	1 540 513	22.40
15N1028	561 902	545 535	464 704	14.82
15N1029	955 440	925 997	751 400	18.86
15N1030	905 456	878 786	722 979	17.73
15N1031	1 723 952	1 671 065	1 319 514	21.04
15N1032	1 093 852	1 060 197	878 137	17.17
15N1034	2 589 324	2 508 305	1 884 813	24.86
15N1039	846 460	820 027	676 009	17.56
15N1040	1 697 600	1 648 563	1 454 499	11.77
15N1041	2 696 928	2 617 708	2 270 358	13.27
15N1043	240 778	233 122	205 096	12.02
15N1044	951 948	924 880	768 359	16.92
15N1047	1 716 886	1 666 636	1 455 711	12.66
15N1050	953 158	924 824	821 258	11.20
15N1051	563 640	547 485	506 526	7.48
15N1052	1 678 514	1 630 222	1 425 775	12.54
15N1053	963 054	933 928	821 391	12.05
15N1055	1 663 782	1 616 528	1 417 292	12.32
15N1056	2 317 564	2 247 987	1 894 287	15.73
15N1059	1 010 634	979 588	876 861	10.49
15N1061	2 099 170	2 039 060	1 749 822	14.18
15N1062	1 190 920	1 155 947	1 007 590	12.83
15N1063	1 536 100	1 488 624	1 293 527	13.11
15N1067	1 608 652	1 563 910	1 377 101	11.95
15N1068	1 520 874	1 474 635	1 272 175	13.73
15N1072	1 014 986	986 530	898 651	8.91
15N1075	1 775 498	1 725 390	1 509 886	12.49
15N797	1 822 382	1 765 194	1 387 445	21.40
15N798	1 014 992	983 834	796 411	19.05
15N801	827 874	802 910	648 337	19.25
15N802	2 232 662	2 164 390	1 680 043	22.38
15N803	1 670 560	1 619 809	1 291 556	20.26
15N804	1 411 172	1 368 170	1 094 127	20.03
15N805	3 304 676	3 200 554	2 324 326	27.38
15N811	1 253 994	1 216 586	974 016	19.94
15N818	1 568 234	1 521 029	1 166 149	23.33
15N821	1 226 218	1 189 733	1 050 813	11.68
15N826	1 110 746	1 077 751	874 319	18.88
15N830	2 472 894	2 400 160	1 797 644	25.10
15N831	2 317 020	2 247 739	1 749 932	22.15
15N835	1 215 796	1 179 444	932 408	20.95
15N837	1 597 544	1 547 951	1 240 934	19.83
15N846	1 104 656	1 071 352	854 009	20.29
15N847	1 032 102	999 224	798 856	20.05
15N848	923 888	895 478	732 424	18.21
15N850	1 208 398	1 171 057	929 684	20.61

15N851	1 489 090	1 442 253	1 116 605	22.58
15N853	1 132 274	1 096 821	884 644	19.34
15N859	3 089 332	2 992 315	2 178 631	27.19
15N861	1 537 012	1 491 137	1 199 308	19.57
15N862	805 652	781 061	666 817	14.63
15N867	865 256	839 258	721 409	14.04
15N868	1 721 496	1 670 095	1 409 836	15.58
15N875	1 208 628	1 173 834	972 112	17.18
15N878	959 986	931 844	779 723	16.32
15N880	1 501 606	1 457 836	1 238 147	15.07
15N886	675 392	656 233	581 056	11.46
15N887	821 478	796 950	691 603	13.22
15N888	2 142 776	2 075 489	1 678 677	19.12
15N891	1 054 062	1 022 831	875 692	14.39
15N894	1 717 726	1 666 945	1 360 090	18.41
15N897	1 154 530	1 119 981	940 239	16.05
15N899	2 078 904	2 015 324	1 647 433	18.25
15N900	2 584 108	2 509 078	2 065 636	17.67
15N901	1 436 848	1 392 903	1 156 407	16.98
15N902	2 027 516	1 969 088	1 647 360	16.34
15N905	1 126 644	1 093 036	891 564	18.43
15N908	827 064	801 674	689 817	13.95
15N912	1 696 122	1 643 914	1 393 328	15.24
15N915	2 165 270	2 098 262	1 697 858	19.08
15N922	1 419 396	1 374 226	1 123 101	18.27
15N923	1 060 830	1 029 917	893 041	13.29
15N924	894 330	866 408	751 666	13.24
15N925	725 166	701 199	601 211	14.26
15N928	1 921 664	1 854 506	1 500 852	19.07
15N934	1 739 604	1 685 795	1 411 845	16.25
15N935	1 179 286	1 143 058	912 858	20.14
15N936	617 930	598 448	523 695	12.49
15N938	1 350 330	1 309 174	1 111 175	15.12
15N940	1 551 354	1 504 356	1 254 239	16.63
15N942	761 902	739 121	635 053	14.08
15N948	1 146 694	1 111 595	952 985	14.27
15N950	1 032 412	1 000 289	837 055	16.32
15N952	1 710 734	1 659 925	1 389 702	16.28
15N955	719 848	697 903	610 702	12.49
15N958	1 585 536	1 537 956	1 301 453	15.38
15N961	1 748 980	1 695 384	1 433 615	15.44
15N966	602 324	583 555	508 893	12.79
15N977	784 034	758 507	646 412	14.78
15N978	2 119 096	2 051 998	1 681 445	18.06
15N984	1 137 040	1 101 781	914 893	16.96
15N985	2 128 472	2 064 582	1 687 629	18.26

15N990	710 960	689 351	605 491	12.17
15N992	1 489 406	1 443 620	1 200 409	16.85
15N996	1 171 212	1 134 521	914 648	19.38
15N956	547 942	531 381	481 842	9.32
Average	1 746 094	1 690 235	1 406 209	14.79
Total	398 109 466	385 373 615	320 615 606	

Table S3.4: The genetic linkage map used for the *H. melpomene* analysis contained 2163 markers across 21 linkage groups.

Linkage group	Number of markers	Length (cM)	Average spacing (cM)	Maximum spacing (cM)
1	123	69.9	0.6	2.8
2	103	65.0	0.6	2.8
3	97	65.6	0.7	4.2
4	100	72.1	0.7	4.4
5	99	79.1	0.8	6.0
6	108	71.2	0.7	5.8
7	100	66.6	0.7	5.3
8	90	72.6	0.8	5.2
9	87	59.7	0.7	3.9
10	134	82.5	0.6	2.9
11	90	68.0	0.8	4.8
12	107	63.1	0.6	1.9
13	122	74.8	0.6	6.5
14	89	65.3	0.7	5.1
15	102	61.7	0.6	2.3
16	99	72.7	0.7	4.6
17	107	75.7	0.7	5.0
18	125	76.5	0.6	2.8
19	119	72.9	0.6	2.5
20	111	73.9	0.7	4.4
Z	51	61.0	1.2	5.3
Overall	2163	1469.9	0.7	6.5

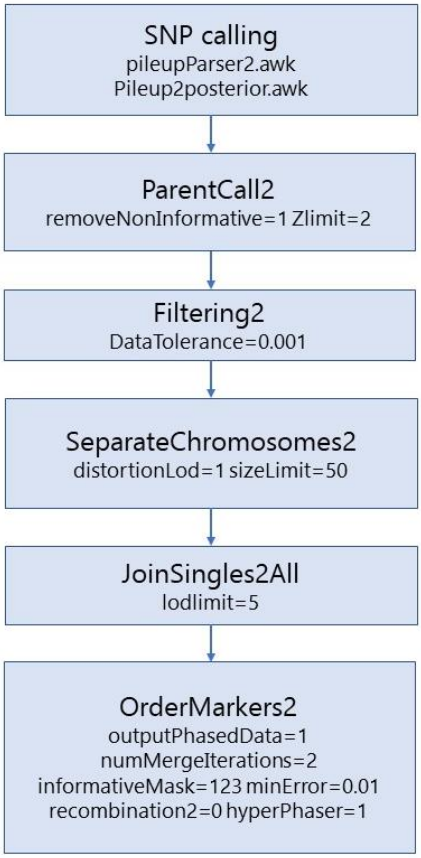

Figure S3.1: Lep-MAP3 modules used for linkage map construction, including values for parameters that were adjusted from the default.

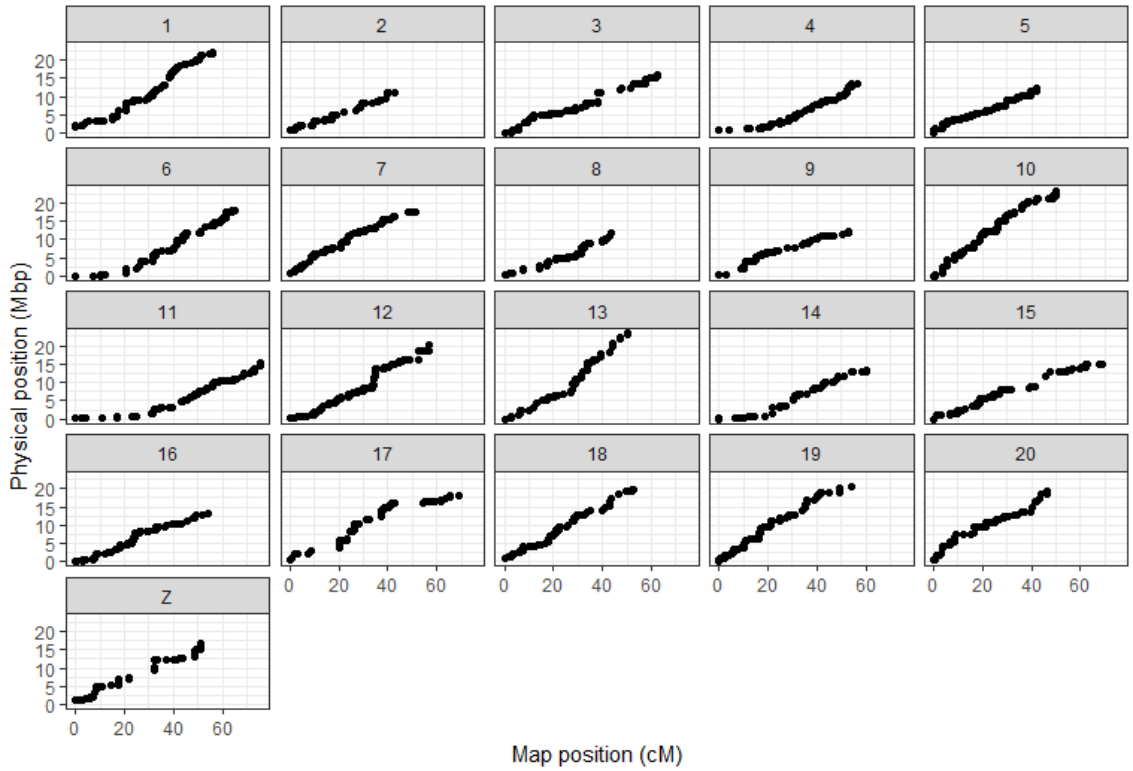

Figure S3.2: Map positions in *H. erato* linkage map against genomic position.

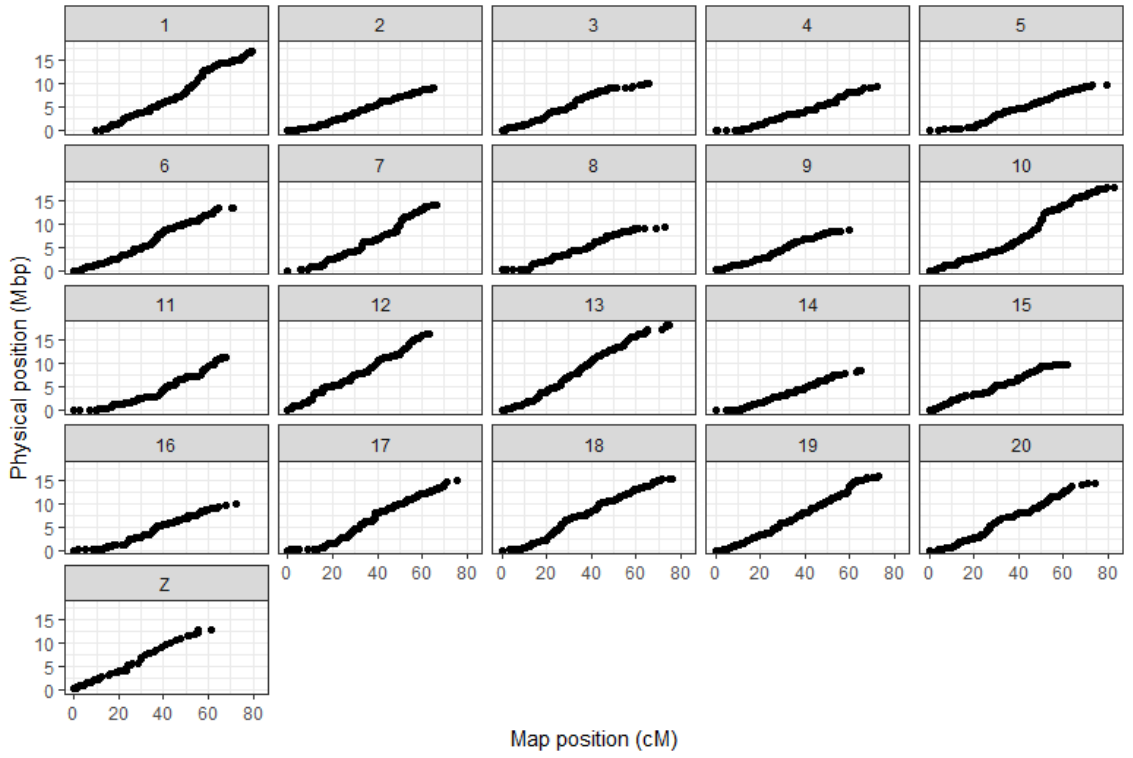

Figure S3.3: Map positions in *H. melpomene* map against genomic positions.

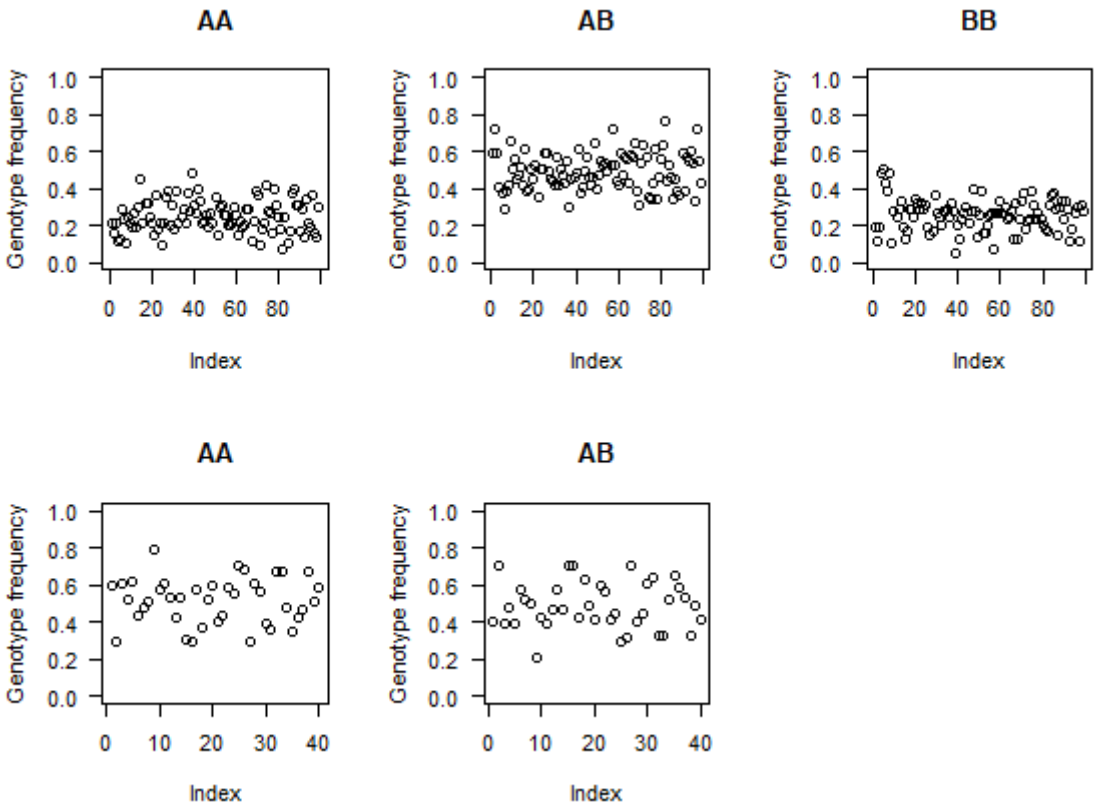

Figure S3.4: Genotype frequencies for all *H. erato* F2 offspring (top) and backcross offspring (bottom). In F2 crosses we expect that AB genotypes will make up approximately 50% of all genotypes, and AA and BB genotypes will make up around 25% each. In the backcrosses, genotypes should be 50% AA and 50% AB. Index represents a list of the individuals.

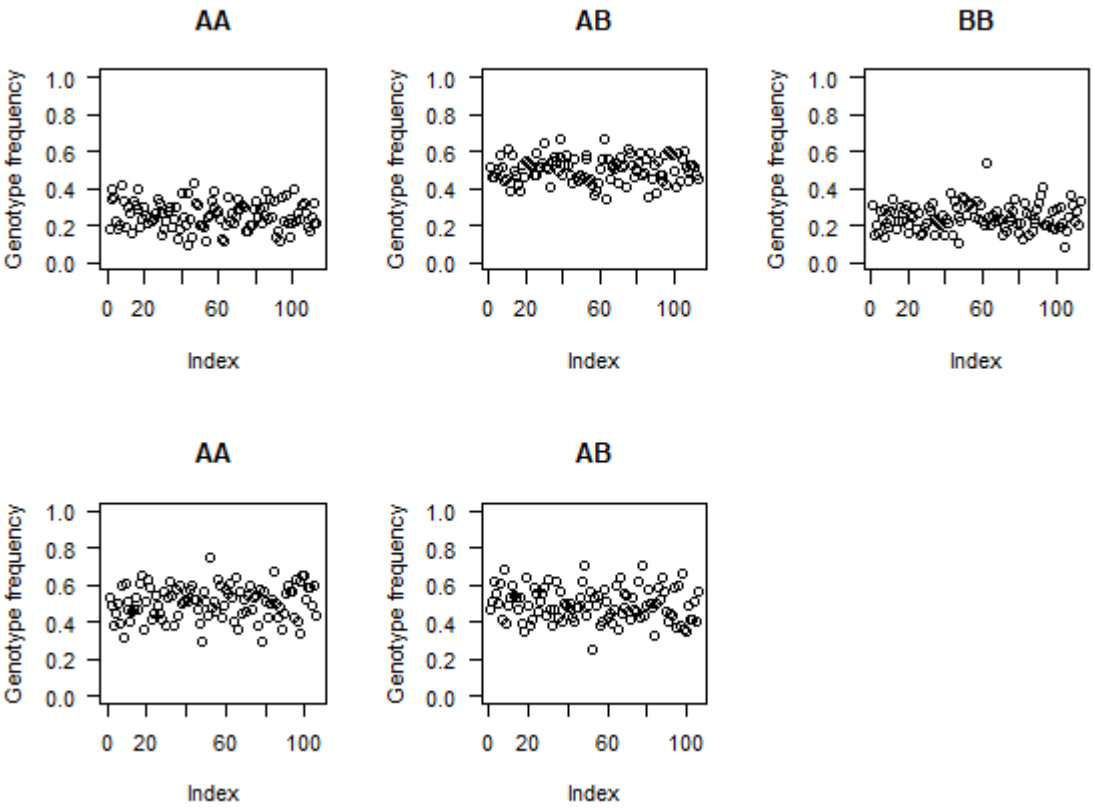

Figure S3.5: Genotype frequencies for all *H. melpomene* F2 offspring (top) and EC70 offspring (bottom). In F2 crosses we expect that AB genotypes will make up approximately 50% of all genotypes, and AA and BB genotypes will make up around 25% each. EC70 was treated as a backcross so genotypes should be 50% AA and 50% AB. Index represents a list of the individuals.

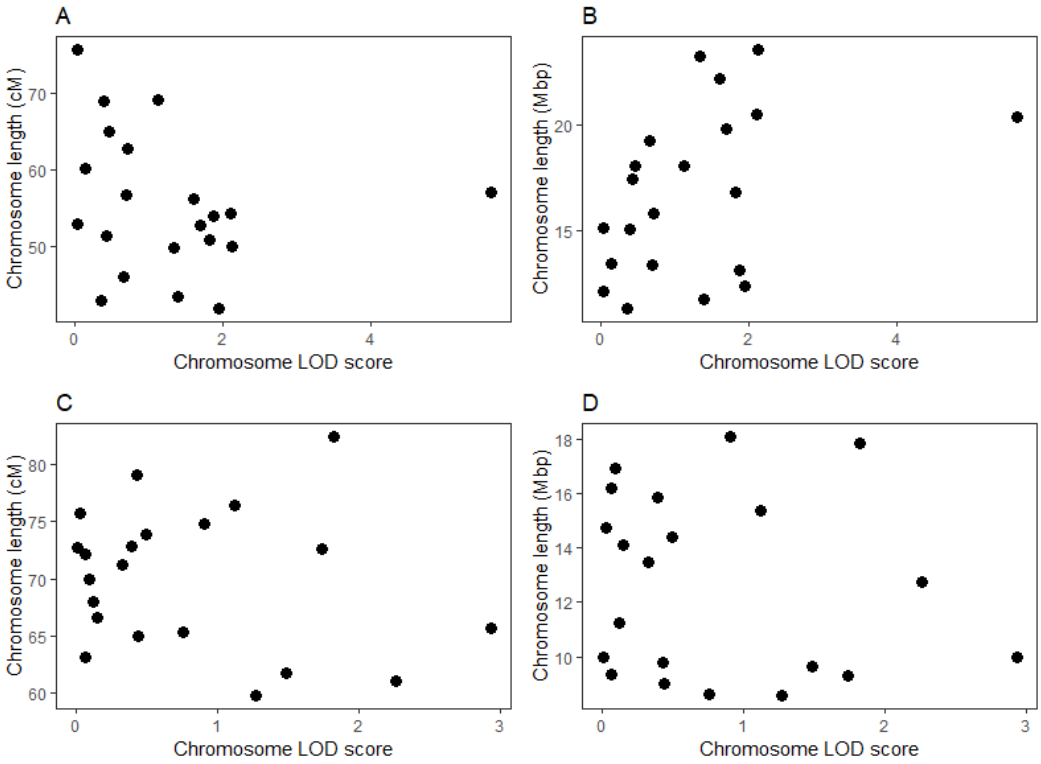

Figure S3.6: Chromosome level LOD score in *H. erato* did not correlate with map chromosome length (**A**) or genome length (**B**). *H. melpomene* chromosome LOD scores also did not correlate with map chromosome length (**C**) or genome length (**D**).

Script 3.1: R script used within the R/qtl package to run QTL mapping analyses for BR, yellow bar and luminance phenotypes in *Heliconius erato* and *Heliconius melpomene*. The example shown here uses F2 and backcrosses. The *H. melpomene* EC70 cross was treated in the same way as a backcross.

Load libraries

```
library(qtl)
```

Load map files

```
# F2 data
f2<-read.cross(format="csv", file="f2.csv", genotypes = c("AA", "AB","BB"), a
lleles = c("A", "B"),  estimate.map = F, convertXdata = T)
# Backcross / EC70 data
bc<-read.cross(format="csv", file="bc.csv", genotypes = c("AA", "AB"), allele
s = c("A", "B"),  estimate.map = F, convertXdata = T)
```

Data checking

```
summary.map(f2)
plot.map(f2)

# estimate recombination fraction
plot1<-est.rf(f2)
plot.rf(plot1)
f2<-clean(f2)

# plot genotype frequencies
g <- pull.geno(f2)
gfreq <- apply(g, 1, function(a) table(factor(a, levels=1:2)))
gfreq <- t(t(gfreq) / colSums(gfreq))
par(mfrow=c(2,3), las=1)
for(i in 1:3)
  plot(gfreq[i,], ylab="Genotype frequency", main=c("AA", "AB", "BB")[i], yli
m=c(0,1))
par(mfrow=c(1,1))
```

Genome scans

```
# calculate genotype probabilities
f2<- calc.genoprob(f2, step=2.0, off.end=0.0, error.prob=1.0e-4, map.function
="haldane", stepwidth="fixed")
bc<- calc.genoprob(bc, step=2.0, off.end=0.0, error.prob=1.0e-4, map.function
="haldane", stepwidth="fixed")

# extract covariates for f2
cross<-as.numeric(pull.pheno(f2, "family"))
sex<-as.numeric(pull.pheno(f2, "sex"))
crossX<-cbind(cross, sex, sex*cross)

# extract covariates for BC/EC70
sex_bc<-as.numeric(pull.pheno(bc, "sex"))

# QTL scan
f2_scan1<- scanone(f2, pheno.col=4, model="normal", method="hk", addcovar=cro
```

```
ssX, intcovar=cross)
bc_scan1<- scanone(bc, pheno.col=4, model="normal", method="hk", addcovar=sex
_bc)
# run permutations to get significance level
perm.f2 <-scanone(f2, pheno.col=4, n.perm=1000, perm.Xsp=T, addcovar=crossX,
intcovar=cross, method="hk")
summary(perm.f2)
perm.bc <-scanone(bc, pheno.col=4, n.perm=1000, perm.Xsp=T, addcovar=sex_bc,
method="hk")
summary(perm.bc)

# plot f2 scan
plot(f2_scan1)
add.threshold(f2_scan1, perms=perm.f2, alpha=0.05, lty=2)
# plot bc scan/EC70
plot(bc_scan1)
add.threshold(bc_scan1, perms=perm.bc, alpha=0.05, lty=2)


# plot combined scans
plot(f2_scan1+bc_scan1)

# significance level for combined scans
perm.all<-c(perm.f2, perm.bc)
summary(perm.all)
```

Extract significant markers

```
# get significant markers
summary(f2_scan1, perms=perm.f2, lodcolumn=1, alpha=0.05, pvalues=T)
summary(bc_scan1, perms=perm.bc, lodcolumn=1, alpha=0.05, pvalues=T)

# get intervals for significant markers
bayesint(f2_scan1, chr=3, prob=0.95)

# plot chromosomes with significant markers
CIchr<- bayesint(f2_scan1, chr=3, prob=0.95)
plot(f2_scan1, chr=3, lodcolumn = 1, main="Chromosome 3")
lines(x=CIchr[c(1,3),2], y=c(0,0), type="l", col="slategrey", lwd=4)
```

Estimate effect sizes

```
sim_f2 <- sim.geno(f2, n.draws=128, step=2, err=0.001)
qtl<- makeqtl(sim_f2, chr=c(3,7, 10), pos=c(15.22, 30.60, 79.64))
out.fq <- fitqtl(sim_f2, pheno.col=4, qtl=qtl, formula=y~Q1+Q2*Q3, forceXcova
r =T)
summary(out.fq)
```

Using R/qtl2 to plot combined scans

```
library(qtl2)
library(qtl2convert)

# combine scans
all_qtl <- scan_qtl_to_qtl2(f2_scan1+bc_scan1)


# plot genome scans
plot(all_qtl$scan1, all_qtl$map)
```

```
add_threshold(all_qtl$map, thresholdA = 4.83, thresholdX = 5.14, lty=2)
add_threshold(all_qtl$map, thresholdA = 4.41, thresholdX = 4.77, lty=2, col="
slategrey")
# genotype x phenotype plots
map_all<- insert_pseudomarkers(all_qtl$gmap, step=1)
all_gp<-calc_genoprob(all_qtl, all_qtl$gmap, error_prob = 0.001)
g<- maxmarg(all_gp, all_qtl$gmap, chr=3, pos=17.97, return_char=T)
plot_pxg(g, all_qtl$pheno[,"BR"], ylab="BR", SEmult=2, sort=F, swap_axes=F)
```

4. Condition dependence and sexual dimorphism of *Heliconius* structural and pigment colour

4.1 Summary

Variation in *Heliconius* colour patterns, and their use as mating cues and warning signals, have been widely studied. However, the possibility that variation in brightness and hue of colour could be used as condition dependent indicators of mate quality, as they are in other animals, has not been considered. We investigated variation in structural and pigment colour within subspecies to determine if these traits are condition dependent and could act as sexually selected signals.

We used spectroscopy to quantify reflectance of structural and pigment colour in *Heliconius sara*, an iridescent specialist with structural colour in all of its range, and *Heliconius erato*, which has iridescence in a small number of its subspecies. Structural colour is sexually dimorphic in both species but in differing directions, suggesting different selection pressures on the sexes, most likely sexual selection. Pigment colour is male-biased in both species.

Thermal stress experiments during pupal development showed that structural colour is condition dependent, particularly in *H. sara*, demonstrating that this colour can potentially be used as an honest signal of condition, and there were some differences in the effects on males and females. Pigment colour is affected by thermal stress to a lesser extent. Visual modelling of butterfly and bird visual systems suggests that both are able to discriminate differences in hue and brightness, meaning iridescence is unlikely to be used as a private communication channel between *Heliconius*. Finally, we show that thermal stress appears to affect the formation of the reflective ridges on the wing scales, which are vital for producing iridescent colour.

4.2 Introduction

Heliconius colour pattern evolution is driven by mimicry and predation, and so Müllerian mimicry is expected to produce uniform patterns. Therefore it follows that natural selection will oppose sexual selection favouring traits which are sexually dimorphic or condition dependent (Sheppard et al. 1985; Andersson 1994). The diversity of pigment colour patterns has been well-studied in *Heliconius* butterflies and we are starting to learn more about differences in structural colours between species (Parnell et al. 2018). While colour patterns have been shown to be cues in mate choice and species recognition (Jiggins et al. 2001; Merrill et al. 2014), sexual selection of colour variation and condition dependence of structural and pigment colours have not yet been tested.

Condition dependent traits can be used as honest signals of condition and can convey information about a potential mate. These are phenotypically plastic traits which are costly to produce so only individuals of the highest fitness or genetic quality will be able to produce them to the maximum level. Condition dependent traits can evolve in response to sexual selection, as they allow the choosing sex (usually females) to determine which mates can provide direct or indirect benefits ('good genes') to their reproductive success (Zahavi 1975; Andersson 1986). For example, in birds, structurally coloured ornaments can signal benefits such as incubation provisioning (Siefferman and Hill 2005), presence of infection (Hill et al. 2005), territory size (Keyser and Hill 2000), and quality of diet (Keyser and Hill 1999). Thus, sexually selected traits are expected to be more condition dependent relative to traits less strongly subject to sexual selection (Cotton et al. 2004; Kemp and Rutowski 2011).

Given that sexual selection often acts more strongly on one sex (usually males), such traits are often sexually dimorphic, e.g. in blue tits, brightness, chroma and hue of UV reflectance are higher in males compared to females (Andersson et al. 1998; Hegyi et al. 2018). In *Heliconius*, one study has looked at sexual dimorphism of colour patterns, finding that there was some variation in the size of colour pattern elements between sexes in *H. erato phyllis* and *H. besckei*

(Klein and de Araújo 2013). However, this study did not look at variation in the brightness or hue of the colour.

In *Heliconius* and *Colias* butterflies, iridescent structural colour is produced by thin-film interference (Silberglied and Taylor 1978; Ghiradella 1989; Parnell et al. 2018). Layered lamellae make up longitudinal ridges, which run down the length of the scale, and these ridges develop from actin bundles which are laid down during pupal development (Dinwiddie et al. 2014). Therefore, it is likely that a stable environment during pupal development is needed for the precise development and formation of the scale structures. In *Heliconius*, red and yellow pigment colours are produced by different types of ommochromes (Reed et al. 2008). These are synthesised *de novo* so we might expect pupal conditions to influence their production, more so than pigments which are acquired from diet, such as carotenoids (Nijhout 1991). Male *Colias eurytheme* butterflies have structural colour on their dorsal wings producing a UV signal which is used in mate choice (Silberglied and Taylor 1978). Using thermal and nutrient stress experiments, both structural and pigment colour were shown to be condition dependent, but variation in structural colour due to limited larval nutrition was much higher than in pigment colour (Kemp 2006; Kemp and Rutowski 2007). Further studies on the effects of heat shock on colour pattern are reviewed by Otaki (2008).

When discussing colour and selection, it is important to consider how colour is perceived by the viewer, particularly when assessing colours outside of the human visible spectrum (Bennett et al. 1997). Visual modelling can determine how well butterflies and their avian predators can discriminate variation in structural colours. Unlike other nymphalids, which have three opsins (ultraviolet, blue and long wavelength), *Heliconius* also express a duplicated UV opsin, allowing them to see shorter UV wavelengths. These opsins have peak sensitivities at 355, 390, 470 and 555nm. However, males in the *erato* and *sara* clades lack expression of the first UV opsin (McCulloch et al. 2016; McCulloch et al. 2017). This suggests that UV-reflecting structural colours could be important in mate choice by females, as females will be more able to

discriminate variation in short wavelength colour (UV and violet). The main avian predators of *Heliconius* are flycatchers (Tyrannidae) and jacamars (Galbulidae) (Pinheiro 1996; Pinheiro 2004). These both have a violet-sensitive visual system that lacks UV sensitivity (Hart 2001). Therefore, variation in UV reflectance should not be discriminated as strongly by the avian visual system compared to the *Heliconius* visual system, particularly females.

Little is known about structural and pigment colour variation within a single *Heliconius* subspecies. Previously, these types of studies have mainly focussed on structural colours in bird species (Keyser & Hill 1999; Shawkey et al. 2003; Doucet 2006; Hegyi et al. 2018), while one study has investigated yellow and red colour variation in *Heliconius melpomene* crosses (Sheppard et al. 1985). Here, we focus on variation within subspecies in structural and pigment colour in two *Heliconius* species, *Heliconius erato* and *Heliconius sara*. Both species are found across Central and South America, and form mimicry rings with other species. *H. sara* produces blue-green structural colour in all of its races, whereas only a small number of *H. erato* races, found in Western Ecuador and Colombia, exhibit blue structural colour. *H. sara* has a yellow pigmented forewing band. This contains 3-hydroxykynurenine (3-OHK) pigment which also reflects UV (Briscoe et al. 2010). *H. erato cyrbia* has a red forewing band containing ommochrome pigments.

We aimed to determine if:

1. structural colour and pigment colour are sexually dimorphic. Sexual dimorphism suggests that different selective pressures are acting on the sexes, most likely due to sexual selection of the colour.
2. structural colour and pigment colour are condition dependent using a thermal stress method (adapted from Kemp et al. 2006). From previous research on structural colour in birds and butterflies, we predict that iridescence can be used as an honest signal of an individual's condition, as only high-quality individuals will be able to produce the precise

nanostructures needed for bright iridescence. We also test if there is a correlation between the brightness of structural and pigment colours.

3. males and females are equally affected by thermal stress. Differences between sexes could again indicate the use of the colour as a sexually selected signal of condition.
4. wing size is sexually dimorphic and/or affected by thermal stress. Wing size and body size have been shown to correlate with fecundity in insects (Horne et al. 2018 and references within), thus if wing size and colour are related, this could give some indication of whether colour can signal fecundity.
5. *Heliconius* and violet-sensitive bird visual systems are able to discriminate between differences in structural colour and brightness between sexes and treated individuals. UV sensitivity in the butterfly visual system suggests that variation in iridescence may be perceived more easily by butterflies compared to avian predators.
6. thermal stress affects the development of structural colour-producing nanostructures. Important factors in the production of *Heliconius* structural colour include ridge spacing and lamellae layering (Parnell et al. 2018). We use Scanning Electron Microscopy to compare scale structures between control and stressed individuals, and compare the angle of peak reflectance which can give us some indication of the slope of the lamellae.

4.3 Methods

4.3.1 Butterfly specimens

Heliconius erato cyrbia were collected from around Pacto, Pichincha, Ecuador (0.15°N, 78.77°W) in February 2018. Females were transported to Sheffield, UK and bred in a controlled greenhouse environment at 25°C with a 16:8hr light-dark cycle. *Heliconius sara* pupae were purchased from Stratford-upon-Avon butterfly farm (UK) and reared in the same conditions. Adults of both species were provided with a 10% sugar solution containing bee pollen, and *Lantana camara* flowers to feed. *H. erato* were provided with *Passiflora biflora* shoots for oviposition, and *H. sara* with *Passiflora auriculata*. Eggs were collected from these shoots and

moved to small tanks in which the larvae were reared. Larvae were fed with *Passiflora biflora* shoots.

4.3.2 Thermal stress experiments

One to two hours after pupation, pupae were alternately assigned to a control or treatment group (Table 4.1). The control group were left to develop in a controlled environment which was set at a constant 25ºC and 75% humidity. The treatment group were given a hot/cold treatment which was a cycle of 1 hour at 32ºC, 1 hour at 15ºC followed by 2 hours at 25ºC (adapted from Kemp et al., 2006). Relative humidity was set at 50% for the first hour (due to constraints of the controlled temperature chamber) and 80% for the remaining 3 hours. Pupae were left in these conditions for the remainder of their developmental period, which in *H. erato* is usually 10 days, and in *H. sara*, 8 days. Development time was recorded to the nearest day. Butterflies were killed 2-3 hours after eclosion. Wings were stored in glassine envelopes, and bodies placed in tubes filled with 100% ethanol and stored at -20°C.

4.3.3 Optical Reflectance Spectroscopy

The right forewings of each butterfly were attached to a microscope slide using adhesive. Reflectance measurements were taken by attaching the sample slide to a rotating mount. For *H. erato*, measurements were taken at 11 different angles on the proximal-distal axis, moving the mount every two degrees from 0 to 22°. The maximum reflectance of *H. sara* wings occurs at a lower angle relative to normal incidence (Parnell et al. 2018), so measurements of *H. sara* were taken every two degrees between 0 and 10°. When rotating the stage, the proximal part of the wings was moved closer to the light source to ensure that the peak reflectance was obtained. Reflectance spectra were recorded using an Ocean Optics USB2000+ spectrometer connected to a light source via a bifuricated fibre-optic probe. The end of the probe was clamped perpendicular to the rotating mount. Measurements were normalised using a diffuse white standard (polytetrafluoroethylene, Labsphere Spectralon 99% at 400–1600 nm). We used the OceanView software (v1.6.7) to record scans, set to average 5 scans, with a boxcar width of 3 and integration

time of 350ms. All *H. erato* wings were measured in the blue region and a smaller subset measured at a point on the red forewing band, to calculate reflectance of structural and pigment colour. *H. sara* wings were measured in the blue region and in the yellow forewing band (Figure 4.1). A custom Python script (Supplementary Information script 4.1) was used to standardise all reflectance measurements against the white standard. For wing size, both forewings were measured at the longest points using digital callipers. Measurements were repeated twice and the average of the four measurements used in the analysis. We use wing size as a proxy for body size as this has previously been shown to correlate with body size in neotropical butterflies (Chai and Srygley 1990).

Table 4.1: Sample sizes of *H. erato* and *H. sara* individuals used for each analysis.

Species	**Treatment**	**Sex**	**Structural colour**	**Pigment colour**	**Wing size**
H. erato	Control	Female	52	9	52
		Male	59	18	58
	Thermal stress	Female	21	20	20
		Male	29	29	29
H. sara	Control	Female	41	41	41
		Male	43	43	43
	Thermal stress	Female	50	50	49
		Male	60	60	60

Figure 4.1: Reflectance was measured at two points on the dorsal side of the right forewing on *Heliconius sara* (left) and *Heliconius erato* (right). One point was close to the proximal edge to measure structural colour, and one point on the forewing band to measure pigment colour.

4.3.4 Analysis of spectral data

The R package PAVO (v2.0, (Maia et al. 2013)) was used for the processing and analysis of spectral data. The reflectance spectra (from 300-700nm) were smoothed using *procspec* with parameters span = 0.25 and fixneg = zero. The angle of maximum reflectance was extracted for each individual. The function *summary* gave information on a number of colour variables including various measurements of brightness, saturation and hue (Montgomerie 2006). We focussed on 6 of these measurements, outlined in Table 4.2. Briefly, they measure total brightness, intensity, saturation, contrast, chroma and hue of the colour. Welch's t-tests were used to determine differences in colour variables between treatments and sexes, and ANOVA models tested for an interaction between treatment and sex. Pearson correlation coefficient was used to look for correlations between reflectance measurements and wing size, as well as generational effects.

Table 4.2: The six colour metrics used throughout this study. Descriptions are taken from Montgomerie (2006).

Colour measurements		
B1	Total brightness	Sum of the relative reflectance over the entire spectral range (area under the curve)
B3	Intensity	Maximum relative reflectance (% reflectance at wavelength of maximum reflectance)
S2	Spectral saturation	Maximum reflectance/Minimum reflectance
S6	Contrast	Maximum reflectance-Minimum reflectance
S8	Chroma	(Maximum reflectance-Minimum reflectance)/Mean brightness
H1	Hue	Wavelength of maximum reflectance

4.3.5 Visual modelling

Following methods in Parnell et al. (2018), visual modelling of bird and butterfly visual systems was carried out using the PAVO package (Supplementary Information script 4.2). The *vismodel* function was used to calculate von Kries-transformed quantum catches which quantifies stimulation of cones and perception of colour under different light conditions. We used illum = "D65" for standard daylight, and illum = "forestshade" to simulate forest shade. In total, four visual systems were tested (Table 4.3). Firstly, for the avian model we used the average violet-

sensitive avian model within PAVO to represent the visual systems of likely *Heliconius* predators (Pinheiro 1996; Hart 2001; Pinheiro 2004). This is tetrachromatic with four photoreceptors with spectral sensitivities at 416, 478, 542 and 607nm. Three different models were used for the *Heliconius* visual system. Type I and III have four photoreceptors (UV1 – 355nm, UV2 - 390nm, B – 470nm and L – 555nm). These were used for *H. erato* female and *H. sara* female vision respectively (McCulloch et al. 2016; Finkbeiner et al. 2017; McCulloch et al. 2017). Type II lacks the UV1 receptor so is trichromatic. This was used for *H. erato* and *H. sara* males. These visual models were then used within *coldist*, along with photoreceptor densities, to calculate colour distances and infer contrast between colours. Just Noticeable Differences (JNDs) were calculated between randomly selected independent pairs to determine if differences in reflectance could be discriminated by bird and butterfly visual systems. Individuals were only included once in these tests to avoid pseudoreplication. Sign tests were used to assess whether JNDs were significantly above 1 or 3. A JND value of 1 is the threshold at which the viewer can distinguish two things side by side in bright lighting. A value of 3 is also used as this represents more natural conditions (Thurman and Seymoure 2016). We tested both chromatic differences (changes in colour/wavelength) and achromatic differences (brightness).

Table 4.3: The four visual systems tested, following values given in Finkbeiner et al. (2017) and McCulloch et al. (2017).

	Peak photoreceptor sensitivities, λmax (nm)	**Relative photoreceptor densities**	**Weber fraction**
Avian Violet sensitive	416, 478, 542, 607	0.25, 0.5, 1 1	0.06
***Heliconius* type I (*erato* female)**	355 (UV1), 390 (UV2), 470 (B), 555 (L)	0.09, 0.07, 0.17, 1	0.05
***Heliconius* type II (*erato* and *sara* male)**	390 (UV), 470 (B), 555 (L)	0.13, 0.2, 1	0.05
***Heliconius* type III (*sara* female)**	355 (UV1), 390 (UV2), 470 (B), 555 (L)	0.06, 0.09, 0.18, 1	0.05

4.3.6 Scanning Electron Microscopy

Scanning electron microscopy (SEM) images were taken of 5 different cover scales from each of 5 *H. sara* control wings and 5 *H. sara* stressed wings, giving a total of 50 images. Samples were prepared by cutting a small area of the forewings from the proximal region, where the iridescence is brightest. These were sputter coated with a few nanometres of gold using vacuum evaporation and imaged on a JEOL JSM-6010LA instrument (Parnell et al. 2018). Images were taken with a voltage of 10-15kV. Ridge spacing was measured using the PeakFinder macro (Vischer 2013) in ImageJ.

4.3.7 Inbreeding effects

To check for possible effects of inbreeding in the stock on the brightness of the iridescent colour, we looked at the wing reflectance measurements over time. Comparing colour variables against emergence date in *H. erato*, there was a slight decrease only in S2 over time ($r = -0.46$, $df = 22$, $p = 0.030$). In *H. sara*, emergence date did not correlate with any of the colour variables. Wing size of the control groups also did not significantly change over time in *erato* ($r = -0.41$, $df = 21$, $p = 0.058$) or *sara* ($r = -0.13$, $df = 81$, $p = 0.221$). Therefore, we infer that there is no strong effect of inbreeding or selection in captivity on colour or size.

4.4 Results

4.4.1 Sexual dimorphism

Structural colour

We began by looking for any sexual dimorphism in structural colour of *H. erato*, using the control group. Males were significantly brighter than females, in terms of intensity of colour (B3), with higher contrast (S6) and chroma (S8). The peak reflectance for all individuals (H1) fell in the violet range (380-450nm) of the spectrum (Figure 4.2; Table 4.4).

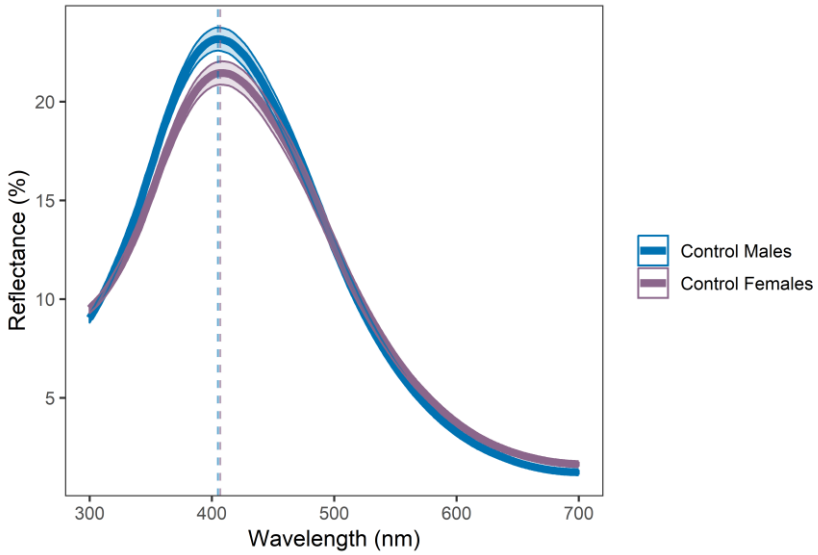

Figure 4.2: Mean relative reflectance and standard error across wavelengths for *H. erato* iridescent colour. At the peak wavelength, males had significantly higher reflectance than females. Dotted lines denote peak wavelength.

Table 4.4: Mean ± standard error colour metrics from female (n = 52) and male (n = 60) *H. erato* iridescent colour.

	Female	**Male**	**t**	**df**	**p**
B1	4363 ± 94	4482 ± 105	-0.84	109.81	0.405
B3	21.87 ± 0.4	23.58 ± 0.6	-2.33	104.97	**0.021**
S2	20.05 ± 3.6	45.38 ± 17.0	1.46	64.38	0.150
S6	20.24 ± 0.4	22.35 ± 0.6	-2.81	104.09	**0.006**
S8	1.87 ± 0.02	1.99 ± 0.03	-3.51	109.94	**<0.001**
H1	407.9 ± 2.1	405.1 ± 1.8	1.03	104.35	0.303

The angle of peak reflectance was not significantly different between sexes (females = 12.9° ± 1.3, males = 12.9° ± 0.6). As angle increased, hue became bluer (Figure S4.1). Wing size was not

sexually dimorphic (female = 34.64 ± 0.3mm, male = 35.10 ± 0.2mm, t = -1.29, df = 99.55, p = 0.200).

In contrast to *H. erato*, female *H. sara* were significantly brighter than males (Figure 4.3). There were no differences in hue, saturation, contrast or chroma (Table 4.5). The peak reflectance fell within the green wavelengths (495-570nm).

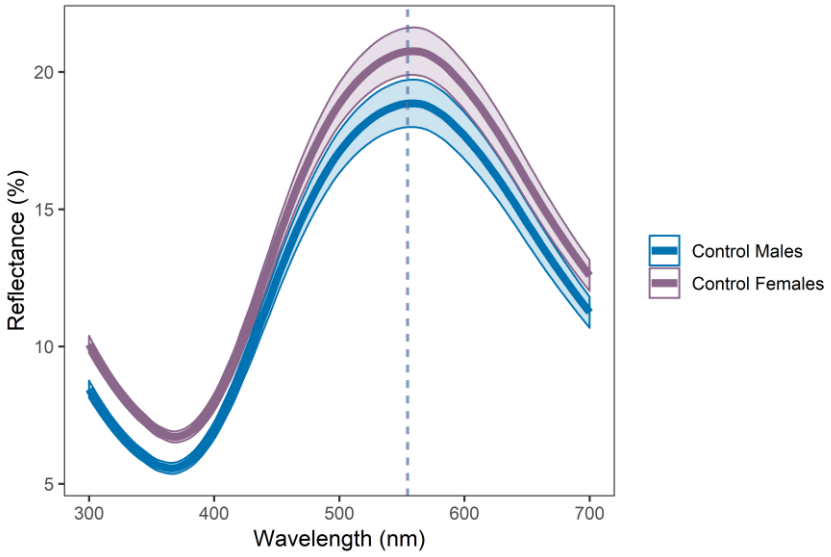

Figure 4.3: Mean relative reflectance and standard error across wavelengths for *H. sara* iridescent colour. Dotted lines denote peak wavelength.

Table 4.5: Mean ± standard error colour metrics for female (n = 41) and male (n = 43) *H. sara* iridescent colour.

	Female	**Male**	**t**	**df**	**p**
B1	5902 ± 236	5158 ± 207	2.37	80.17	**0.020**
B3	21.89 ± 0.9	19.35 ± 0.9	1.98	80.97	**0.051**
S2	3.43 ± 0.1	3.68 ± 0.1	-1.36	79.10	0.179
S6	15.46 ± 0.8	14.03 ± 0.8	1.27	81.87	0.207
S8	1.03 ± 0.02	1.06 ± 0.03	-0.69	79.23	0.490
H1	554.0 ± 4.8	554.7 ± 4.9	-0.10	82.00	0.921

Peak angle of reflectance was significantly higher for males (5.95° ± 0.3) than females (4.83° ± 0.3) in the control group (t = -2.64, df = 79.9, p = 0.010; Figure 4.4). Males were generally greener

than females across all angles, although variation in hue was high. Wing size of females was larger than males in the control group (female = 30.94 ± 0.4mm, male = 29.42 ± 0.4mm, t = 2.72, df = 80.65, p = 0.008).

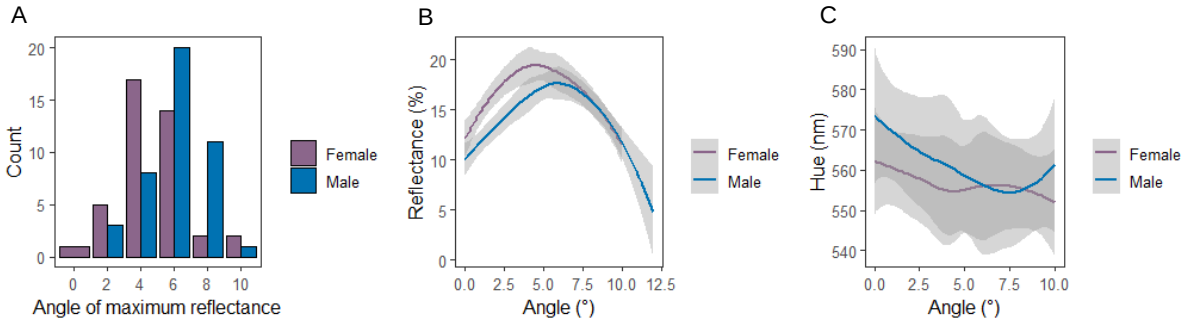

Figure 4.4: Angle of peak reflectance for iridescent colour was on average lower in *H. sara* females. **A.** Differences in angle of peak reflectance between males and females. **B.** Mean reflectance at angles measured every 2°. **C.** Mean hue against each angle. Grey shading shows 95% confidence interval.

Pigment colour

Reflectance measurements of the pigment bands did not differ greatly with angle (Figure S4.2). Because of this, and to limit any effects of overlying structural colour, we used only measurements taken at 0º for analysis of the pigment colour.

As with structural colour, pigment colour was also sexually dimorphic in *H. erato* (Figure 4.5). Saturation, chroma and contrast of colour were significantly higher in males than females (Table 4.6). Brightness was not significantly different although males did have higher maximum reflectance, while females had overall higher brightness, possibly due to higher reflectance of lower wavelengths. Hue was not different between sexes.

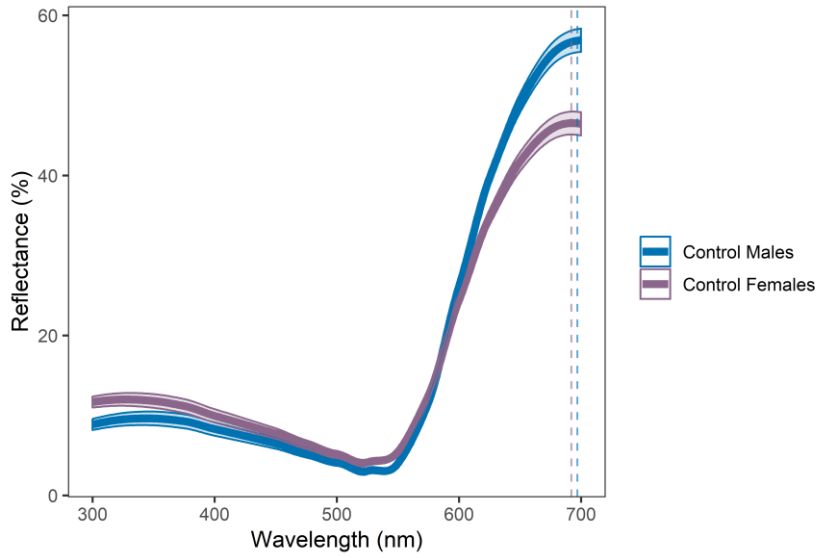

Figure 4.5: Mean ± S.E. relative reflectance of the red pigment band on *H. erato*. Dotted lines denote peak wavelength.

Table 4.6: Mean ± S.E. colour variables for red pigment colour in *H. erato* females (n = 9) and males (n = 18).

	Female	**Male**	**t**	**df**	**p**
B1	7164 ± 521	6886 ± 153	0.51	9.41	0.620
B3	49.0 ± 3.5	55.7 ± 1.3	-1.79	10.14	0.103
S2	12.8 ± 1.0	26.1 ± 3.8	-3.43	19.06	**0.003**
S6	45.0 ± 3.1	52.8 ± 1.5	2.26	11.90	**0.043**
S8	2.53 ± 0.10	3.09 ± 0.1	-4.57	24.22	**<0.001**
H1	694 ± 2.2	698 ± 0.6	-1.91	9.20	0.088

In the yellow forewing band on *H. sara*, there was sexual dimorphism in saturation and hue (Table 4.7). Males had more saturated colour, and hue fell in the lower wavelengths compared to females, in which the hue could be described as more orange. However, brightness, chroma and contrast were not different between sexes (Figure 4.6).

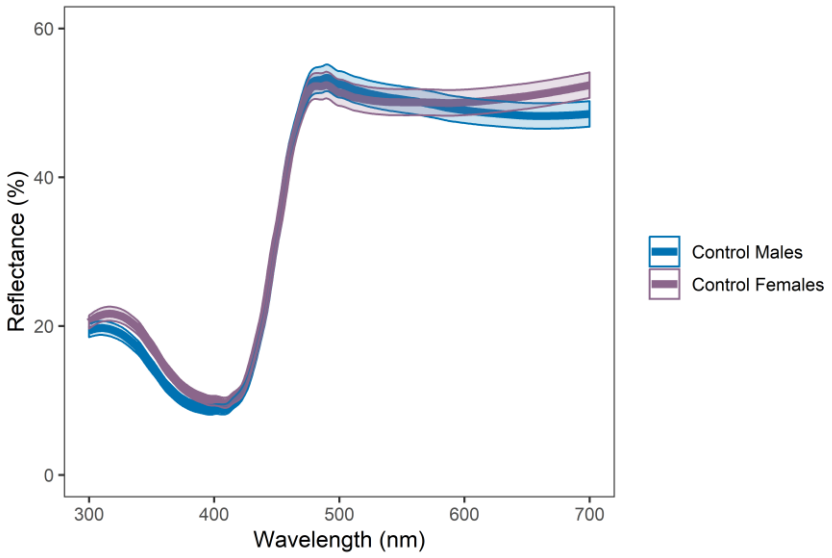

Figure 4.6: Mean ± S.E. relative reflectance of the yellow pigment band on *H. sara*.

Table 4.7: Mean ± S.E. colour variables for yellow pigment colour in *H. sara* females (n = 41) and males (n = 43).

	Female	**Male**	**t**	**df**	**p**
B1	14988 ± 434	14552 ± 456	0.69	81.95	0.491
B3	54.7 ± 1.6	54.6 ± 1.7	0.04	81.71	0.965
S2	6.37 ± 0.4	8.11 ± 0.7	-2.31	64.91	**0.025**
S6	45.2 ± 1.4	46.2 ± 1.8	-0.42	78.68	0.675
S8	1.21 ± 0.02	1.27 ± 0.03	-1.70	72.50	0.094
H1	601 ± 17	533 ± 13	3.18	76.89	**0.002**

Colour variables for the pigment colour did not strongly correlate with values for iridescent colour. In *H. erato*, there was a slight positive correlation between the iridescent blue and pigment colours in saturation and contrast, but no correlation between brightness (Table S4.1). Colour variables for the *sara* yellow band did not correlate with the same measurements for the iridescent blue area (Table S4.1).

Visual modelling

The avian visual model was able to distinguish all chromatic and achromatic differences between iridescent colour in sexes of *H. erato* (Figure 4.7) in the ideal lighting conditions. The mean chromatic JND was also above 1 for both *Heliconius* type I (female) and type II (male), although type I was able to discriminate better than type II, likely due to the duplicated UV opsin. JNDs for the *Heliconius* models were not significantly above 3, suggesting *Heliconius* would have difficulty distinguishing differences in 'natural' conditions (Table 4.8). However, JNDs were higher for the forest shade simulations compared to the daylight conditions. Achromatic JNDs were higher for the avian model compared to the *Heliconius* model in both conditions. Differences in pigment colour were much less likely to be seen. Only the avian model could discriminate chromatic differences and only in ideal conditions, while only the *Heliconius* model could discriminate achromatic differences (Table 4.8).

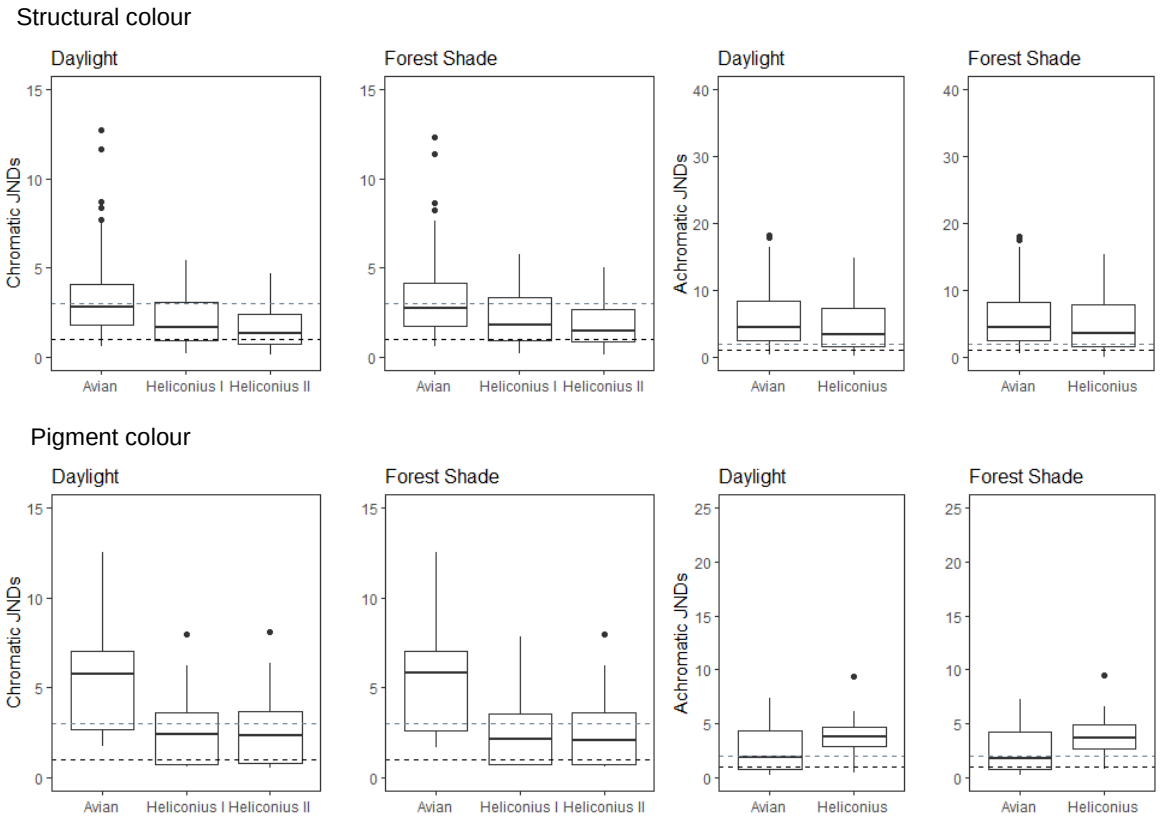

Figure 4.7: Discrimination between *H. erato* male and female wings under daylight and forest shade conditions for structural colour and pigment colour. Pairwise comparisons using only unique pairs (n = 52). Chromatic Just Noticeable Differences (JNDs) between independent pairs for the avian model, *Heliconius* type I (*H. erato* female, tetrachromatic) and *Heliconius* type II (*H. erato* male, trichromatic). Achromatic JNDs for avian and *Heliconius* models. Values above 1 (black dotted line) show that differences can be discriminated under 'ideal' conditions. A threshold of 3 (grey dotted line) is also shown as this represents more natural conditions.

Table 4.8: Chromatic and achromatic Just Noticeable Differences (mean ± S.E.) between independent pairs of male and female *H. erato* for structural colour (n = 52) and pigment colour (n = 9).

Structural colour	**Visual model**	**Chromatic JND**	**Number JNDs >1**	**p**	**Number JNDs >3**	**p**
Daylight	Avian	3.55 ± 0.4	48	**<0.001**	23	0.834
	Heliconius type I	2.04 ± 0.2	36	**0.004**	14	0.999
	Heliconius type II	1.69 ± 0.2	32	0.063	8	0.999
Forest shade	Avian	3.51 ± 0.4	48	**<0.001**	23	0.834
	Heliconius type I	2.20 ± 0.2	38	**<0.001**	15	0.999
	Heliconius type II	1.83 ± 0.2	35	**0.009**	10	0.999
		Achromatic JND	**Number JNDs >1**	**p**	**Number JNDs >3**	**p**
Daylight	Avian	6.15 ± 0.7	49	**<0.001**	36	**0.004**
	Heliconius	4.85 ± 0.6	42	**<0.001**	27	0.445
Forest shade	Avian	6.11 ± 0.7	48	**<0.001**	36	**0.004**
	Heliconius	5.05 ± 0.6	43	**<0.001**	27	0.445
Red pigment colour		**Chromatic JND**	**Number JNDs >1**	**p**	**Number JNDs >3**	**p**
Daylight	Avian	5.71 ± 1.3	9	**0.002**	5	0.500
	Heliconius type I	2.97 ± 0.9	6	0.254	3	0.910
	Heliconius type II	2.97 ± 0.9	6	0.254	3	0.910
Forest shade	Avian	5.71 ± 0.3	9	**0.002**	5	0.500
	Heliconius type I	2.89 ± 0.9	6	0.254	3	0.910
	Heliconius type II	2.89 ± 0.9	3	0.254	3	0.910
		Achromatic JND	**Number JNDs >1**	**p**	**Number JNDs >3**	**p**
Daylight	Avian	2.59 ± 0.8	6	0.254	3	0.910
	Heliconius	4.00 ± 0.9	8	**0.020**	6	0.254
Forest shade	Avian	2.57 ± 0.8	6	0.253	3	0.910
	Heliconius	4.09 ± 0.9	8	**0.020**	6	0.254

The avian model could discriminate between *H. sara* male and female differences in colour and brightness (Figure 4.8). Similar to *H. erato*, *Heliconius* type III (*sara* female) could discriminate colour differences more clearly than *Heliconius* type II (*sara* male), although not as well as the avian model (Table 4.9). However, in contrast to *H. erato*, the *Heliconius* model was more able to discriminate achromatic differences compared to the avian model, in both ideal and natural environments. Similar results were found for pigment colour, with avian models most able to discriminate chromatic differences, and *Heliconius* slightly more able to discriminate achromatic differences.

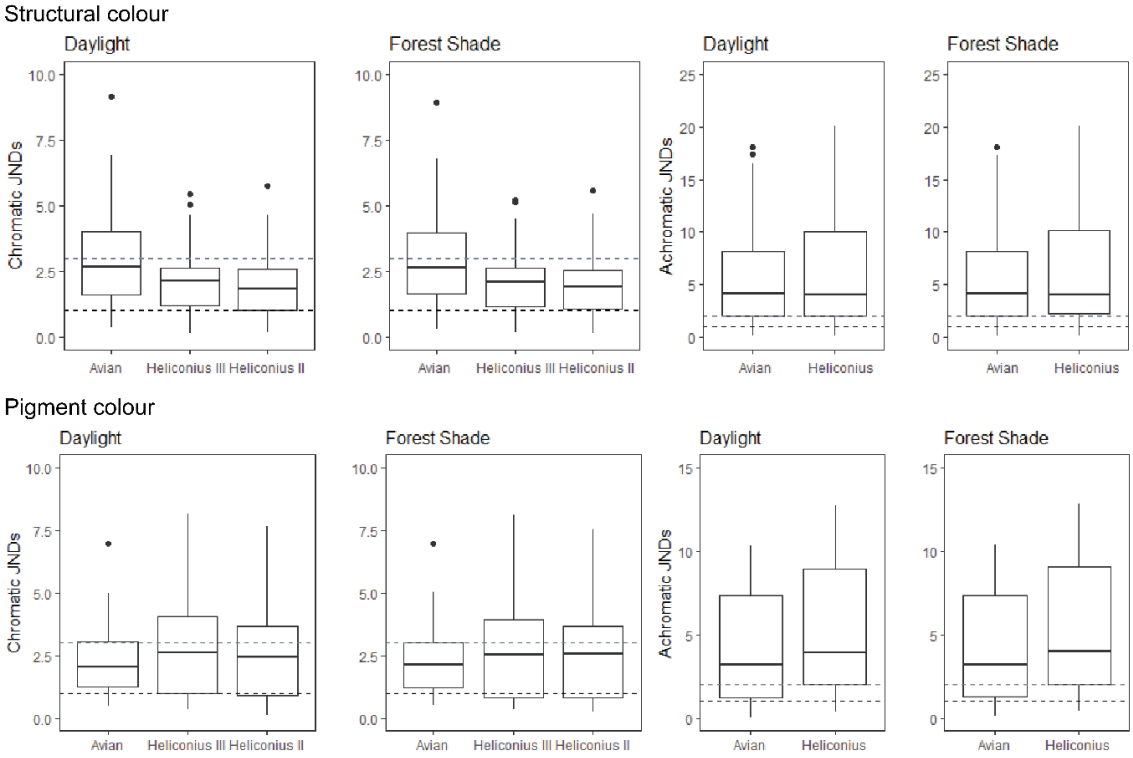

Figure 4.8: Pairwise comparisons between unique pairs of male and female *H. sara* wings (n = 41). Ability of the avian, *Heliconius* type III (*sara* female) and *Heliconius* type II (*sara* male) visual models to discriminate chromatic and achromatic differences between control male and female wings in daylight and forest shade light conditions. The black dotted line shows a JND value of 1, and the grey dotted line a value of 3.

Table 4.9: Chromatic and achromatic Just Noticeable Differences (mean ± S.E.) between independent pairs of male and female *H. sara* for structural and pigment colour. Number of pairs = 41.

Structural colour	**Visual model**	**Chromatic JND**	**Number JNDs >1**	**p**	**Number JNDs >3**	**p**
Daylight	Avian	3.03 ± 0.3	35	**<0.001**	17	0.894
	Heliconius type II	1.92 ± 0.2	32	**<0.001**	6	1.000
	Heliconius type III	2.15 ± 0.2	34	**<0.001**	7	1.000
Forest shade	Avian	2.97 ± 0.3	35	**<0.001**	17	0.894
	Heliconius type II	1.93 ± 0.2	31	**<0.001**	6	1.000
	Heliconius type III	2.17 ± 0.2	34	**<0.001**	7	1.000
		Achromatic JND	**Number JNDs >1**	**p**	**Number JNDs >3**	**p**
Daylight	Avian	5.85 ± 0.8	36	**<0.001**	25	0.106
	Heliconius	6.29 ± 0.9	35	**<0.001**	27	**0.030**
Forest shade	Avian	5.85 ± 0.8	37	**<0.001**	25	0.106
	Heliconius	6.33 ± 0.9	35	**<0.001**	27	**0.030**
Yellow pigment colour		**Chromatic JND**	**Number JNDs >1**	**p**	**Number JNDs >3**	**p**
Daylight	Avian	2.27 ± 0.2	35	**<0.001**	11	0.999
	Heliconius type II	2.56 ± 0.3	29	**0.006**	18	0.826
	Heliconius type III	2.96 ± 0.3	30	**0.002**	18	0.826
Forest shade	Avian	2.29 ± 0.2	35	**<0.001**	12	0.998
	Heliconius type II	2.58 ± 0.3	29	**0.006**	17	0.894
	Heliconius type III	2.91 ± 0.3	30	**0.002**	18	0.826
		Achromatic JND	**Number JNDs >1**	**p**	**Number JNDs >3**	**p**
Daylight	Avian	4.03 ± 0.5	32	**<0.001**	22	0.378
	Heliconius	5.11 ± 0.6	38	**<0.001**	26	0.059
Forest shade	Avian	4.04 ± 0.5	32	**<0.001**	22	0.378
	Heliconius	5.15 ± 0.6	38	**<0.001**	26	0.059

4.4.2 Condition dependence

Structural colour in Heliconius erato

Thermal stress did not affect overall mortality of *H. erato* pupae – the mortality rate for control pupae was 19.6%, and 17.3% for stressed pupae ($x^2 = 0.02$, df = 1, p = 0.90). Developmental time of pupae also did not differ between treatment groups (control = 9.5 ± 0.1 days, stressed = 9.7 ± 0.1 days, t = -1.26, df = 38.7, p = 0.216).

Between the control and stressed groups, there were large differences in the colour (Figure 4.9). Intensity of colour, saturation, contrast and chroma all significantly decreased in the stressed group (Table 4.10). When separated by sex, the results become more interesting as males seem to be more affected compared to females (Figure 4.10). In the females, intensity, saturation, contrast and chroma significantly decreased in the stressed group. In males, the same variables decreased but the differences were more pronounced. Focussing on intensity, the slope of change between control and stressed was steeper in males (-5.61) compared to females (-3.16), however, there was no significant interaction term between treatment group and sex (F = 2.93, p = 0.088).There were no significant changes in hue.

Figure 4.9: Example male wings for a stressed (left) and a control (right) *H. erato*. Photographs were taken under standardised lighting conditions.

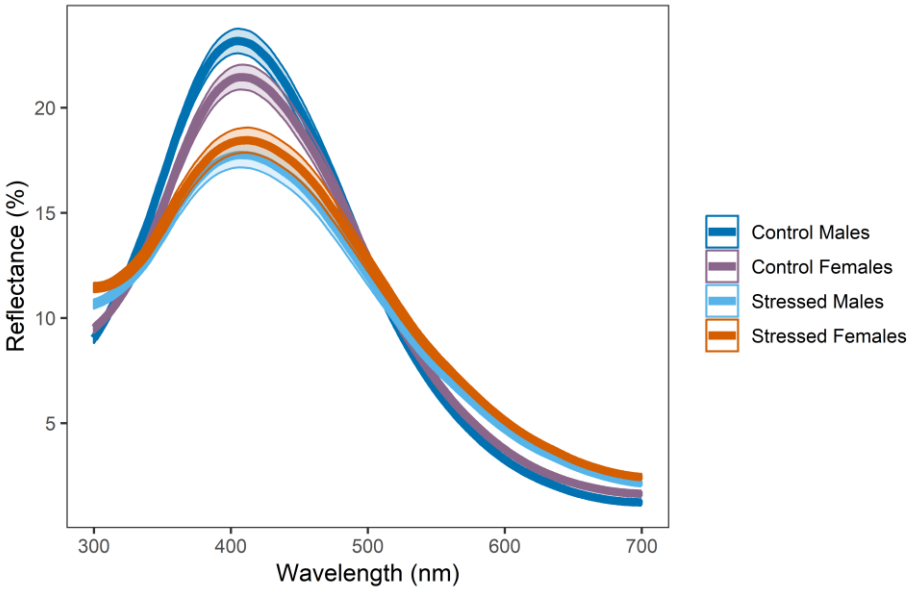

Figure 4.10: Mean relative reflectance (± S.E.) for *H. erato* males and females of the control group and the stressed group.

Table 4.10: Mean ± S.E. colour variables for structural colour in *H. erato* control (n = 111) and stressed (n = 50) groups. T-test results are shown for all individuals together, and males and females separately. Differences between the control and stressed groups were more pronounced in males compared to females.

All individuals	**Control**	**Stressed**	**t**	**df**	**p**
B1	4435 ± 71	4188 ± 134	1.63	8.01	0.107
B3	22.8 ± 0.4	18.3 ± 0.6	6.00	85.61	**<0.001**
S2	33.7 ± 9.4	9.30 ± 0.7	2.60	111.35	**0.011**
S6	21.40 ± 0.4	16.1 ± 0.7	7.00	86.84	**<0.001**
S8	1.93 ± 0.02	1.52 ± 0.03	11.17	85.91	**<0.001**
H1	407 ± 1.4	406 ± 3.3	0.08	66.90	0.933
Female	**Control**	**Stressed**	**t**	**df**	**p**
B1	4364 ± 94	4295 ± 205	0.31	28.77	0.760
B3	21.9 ± 0.4	18.7 ± 1.1	2.76	27.12	**0.010**
S2	20.0 ± 3.6	9.38 ± 1.4	2.73	64.07	**0.008**
S6	20.2 ± 0.4	16.3 ± 1.1	3.31	26.70	**0.003**
S8	1.87 ± 0.02	1.50 ± 0.05	6.64	29.42	**<0.001**
H1	408 ± 2.1	403 ± 6.4	0.70	24.43	0.492
Male	**Control**	**Stressed**	**t**	**df**	**p**
B1	4498 ± 106	4111 ± 178	1.87	48.30	0.068
B3	23.6 ± 0.6	18.0 ± 0.8	5.57	58.12	**<0.001**
S2	45.8 ± 17	9.24 ± 0.7	2.11	58.22	**<0.001**
S6	22.4 ± 0.6	15.9 ± 0.8	6.40	59.67	**<0.001**
S8	1.99 ± 0.03	1.54 ± 0.04	9.26	5256	**<0.001**
H1	405 ± 1.8	408 ± 3.3	-0.83	45.67	0.409

Peak angle did not differ between the control and stressed group (Figure 4.11). Hue was bluer, with less UV reflectance, in the control group at all angles. Within the stressed group there was a slight, but not significant, difference between females (12.5° ± 0.8) and males (13.4° ± 0.8, p = 0.41). Again, hue increased with angle, but females were only bluer (longer peak wavelength) than males when the angle was higher than 18°.

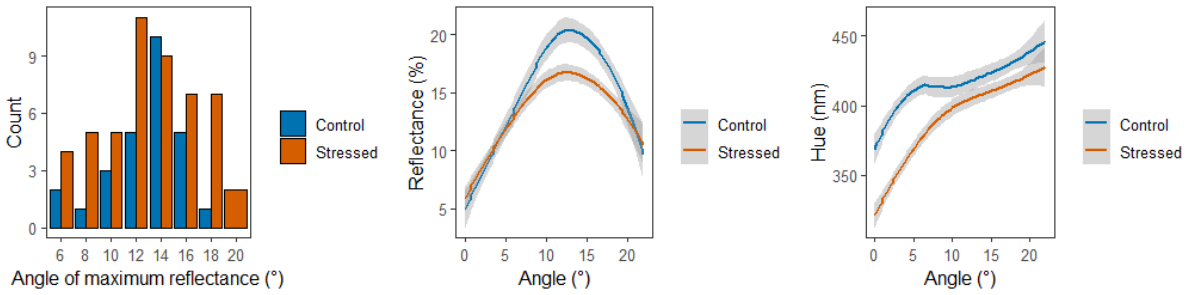

Figure 4.11: **A.** Angle of maximum reflectance for the *H. erato* control group (12.9º) and the treated group (13.0º) did not differ significantly (t = -0.14, df = 65.17, p = 0.889). As there were no sex differences between peak angle, we did not split the treatments by sex. **B**. Effect of angle on reflectance. **C.** Effect of angle on hue.

Wing size decreased in stressed males compared to control males (control = 35.10 ± 0.23, stressed = 33.60 ± 0.39, t = 3.27, df = 48.1, p = 0.002). Female wing size was not significantly different between groups (control = 34.64 ± 0.26, stressed = 33.85 ± 0.46, t = 1.43, df = 30.4, p = 0.163). Size was not correlated with pupal development time (r = -0.18, df = 61, p = 0.165).

Wing size did not correlate with most of the colour variables (Table S4.2). The only correlation was between chroma and control male wing size (r = 0.30, df = 57, p = 0.020), showing larger males had higher colour chroma. There were no correlations within the stressed group.

Structural colour in Heliconius sara

Thermal stress had a larger effect on mortality rate in *H. sara* than was seen in *H. erato* (20.4% for the control group and 39.1% for the stressed group; $x^2 = 5.06$, df = 1, p = 0.025). Developmental time was also significantly longer in the stressed group (control = 7.9 ± 0.1 days, stressed = 8.3 ± 0.1 days, t = -3.51, df = 155.1, p<0.001).

Iridescent colour was greatly affected by the stressful environment in *H. sara* (Figure 4.12; Figure 4.13). Brightness, contrast, saturation and chroma all decreased (Table 4.11) and in the stressed group there was no clear peak of maximum reflectance. Only hue was not significantly affected. Maximum reflectance of males decreased by 5.8% (slope = -5.77) in the stressed group (Table 4.11). Female reflectance decreased slightly more (7.2%, slope = -7.24), perhaps due to being brighter to begin with as there was no significant interaction term between sex and treatment group (F = 1.08, p = 0.300).

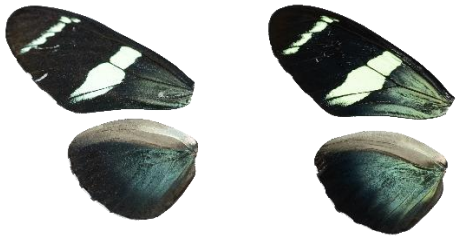

Figure 4.12: Example wings for a stressed (left) and a control (right) *H. sara*. Photographs were taken under standardised lighting conditions.

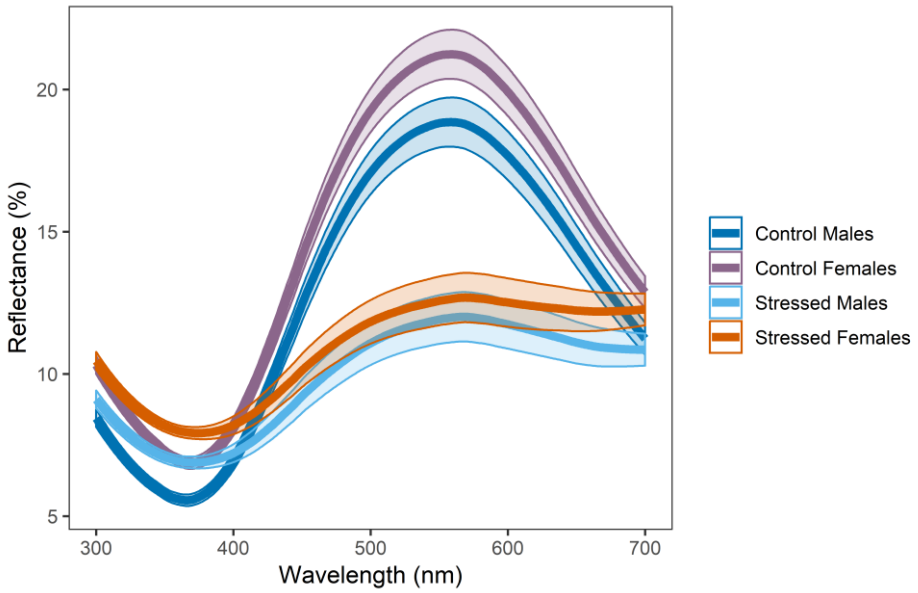

Figure 4.13: Mean relative reflectance (± S.E.) for *H. sara* males and females of the control group and the stressed group.

Table 4.11: Mean ± S.E. colour variables for structural colour in *H. sara* control and stressed groups. T-test results are shown for all individuals, and males and females separately.

All individuals	**Control**	**Stressed**	**t**	**df**	**p**
B1	5521 ± 161	4154 ± 111	6.70	154.10	**<0.001**
B3	20.59 ± 0.7	13.53 ± 0.4	9.31	139.44	**<0.001**
S2	3.56 ± 0.09	1.96 ± 0.05	15.04	136.95	**<0.001**
S6	14.73 ± 0.6	6.45 ± 0.3	12.77	136.95	**<0.001**
S8	1.05 ± 0.02	0.60 ± 0.02	16.66	186.45	**<0.001**
H1	558.3 ± 4.5	569.6 ± 10.6	-0.98	145.85	0.330
Female	**Control**	**Stressed**	**t**	**df**	**p**
B1	5902 ± 236	4359 ± 123	5.80	61.07	**<0.001**
B3	21.89 ± 0.9	14.11 ± 0.4	7.48	56.54	**<0.001**
S2	3.43 ± 0.11	1.89 ± 0.06	11.95	61.64	**<0.001**
S6	15.46 ± 0.8	6.52 ± 0.4	10.12	58.01	**<0.001**
S8	1.03 ± 0.02	0.59 ± 0.02	13.36	87014	**<0.001**
H1	554.1 ± 4.7	574.0 ± 15.7	-1.22	57.70	0.229
Male	**Control**	**Stressed**	**t**	**df**	**p**
B1	5158 ± 207	3984 ± 173	4.34	89.94	**<0.001**
B3	19.35 ± 0.9	13.04 ± 0.6	5.95	80.24	**<0.001**
S2	3.68 ± 0.14	2.01 ± 0.08	10.09	70.56	**<0.001**
S6	14.03 ± 0.8	6.39 ± 0.5	8.18	75.54	**<0.001**
S8	1.06 ± 0.03	0.61 ± 0.03	10.87	95.92	**<0.001**
H1	562.3 ± 7.6	565.9 ± 14.5	-0.22	86.70	0.828

When subject to thermal stress, peak angle for males decreased significantly (control = 5.95° ± 0.3, stressed = 4.17° ± 0.3, t = 4.30, df = 100.6, p<0.001; Figure 4.14). This decrease was not seen in females (control = 4.83° ± 0.3, stressed = 4.24° ± 0.3, t = 1.30, df = 88.2, p = 0.180). The angle dependency of the brightness decreases substantially in the stressed individuals for both males and females. Hue is higher and more variable compared to the controls, and shows greater variation with angle.

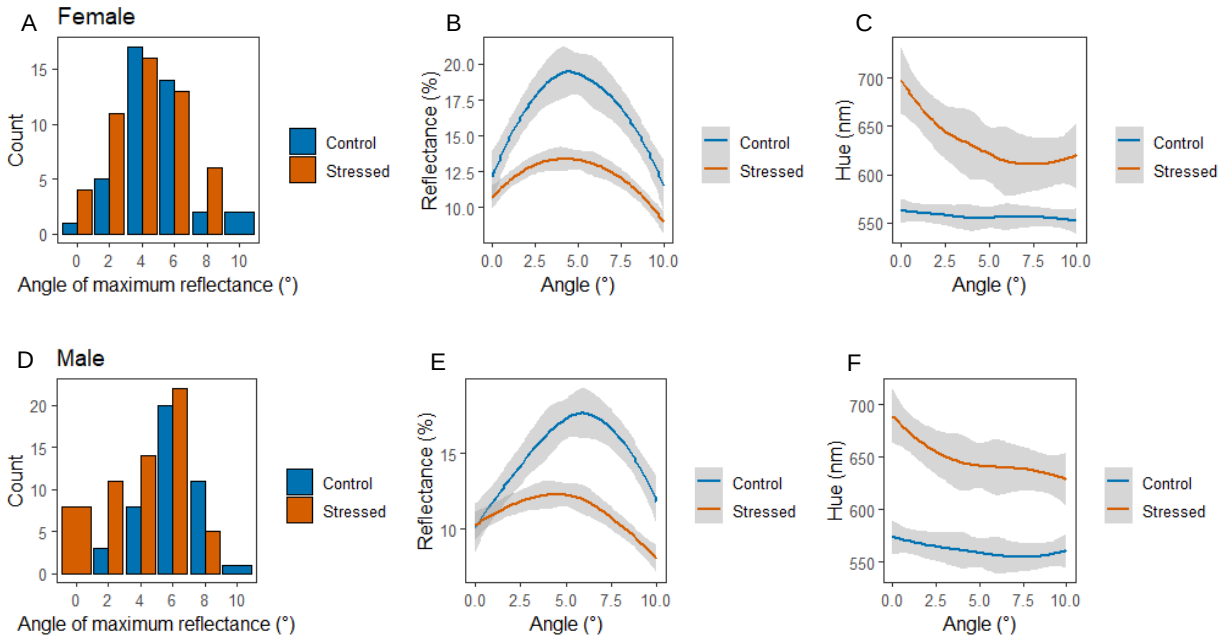

Figure 4.14: Angle of maximum reflectance in control and stressed *H. sara* females (**A**) and males (**D**). **B. E**. Effect of angle on reflectance. The relationship becomes much flatter in the stressed group, showing that the individuals in this group effectively lose the angle dependency of the colour. **C. F.** Effect of angle on hue. Hue moves much further towards the longer wavelengths in the stressed group.

The larger wing size of females was not seen within the stressed group (female = 30.03 ± 0.3mm, males = 29.83 ± 0.3mm, t = 0.49, df = 93.3, p = 0.627), suggesting female size decreases when stressed, although this difference was not significant (control = 30.94 ± 0.4mm, stressed = 30.03 ± 0.3mm, t = 1.80, df = 84.2, p = 0.076), whereas male size is unaffected (control = 29.42 ± 0.4mm, stressed = 29.83 ± 0.3, t = -0.92, df = 78.9, p = 0.360). As in *erato*, wing size did not correlate with developmental time (r = 0.10, df = 142, p = 0.212).

Unlike *H. erato*, wing size was not completely independent to colour. Male wing size correlated with all the colour variables except hue in the control group (Table 4.12), but relationships were less pronounced in the stressed group. This suggests that colour and size are affected to different extents by thermal stress. Similarly, female wing size correlated with some colour variables in the control group but not the stressed group.

Table 4.12: Correlations between *H. sara* wing size and the iridescent colour variables.

	Female Controls		**Male Controls**		**Female Stressed**		**Male Stressed**	
	r (df=39)	p	r (df=47)	p	r (df=47)	p	r (df=58)	p
B1	0.186	0.244	0.410	**0.006**	-0.117	0.424	0.182	0.165
B3	0.239	0.133	0.450	**0.003**	-0.058	0.691	0.230	0.077
S2	0.311	**0.048**	0.371	**0.014**	0.178	0.220	0.290	**0.025**
S6	0.283	0.073	0.450	**0.003**	0.076	0.603	0.286	**0.027**
S8	0.336	**0.032**	0.436	**0.004**	0.156	0.283	0.306	**0.018**
H1	0.312	**0.047**	0.280	0.070	-0.127	0.383	0.100	0.447

Condition dependence of pigment colour

Overall in *H. erato*, brightness of the red reflectance did not decrease in the stressed group compared to the control group (Figure 4.15). However, saturation ($t = 2.91$, $df = 35$, $p = 0.006$), contrast ($t = 2.22$, $df = 66$, $p = 0.030$) and chroma ($t = 4.22$, $df = 65$, $p<0.001$) did decrease in the stressed group. Looking at the sexes separately, saturation, chroma and hue decrease in both stressed males and females, but there are no effects on any of the other variables (Table 4.13).

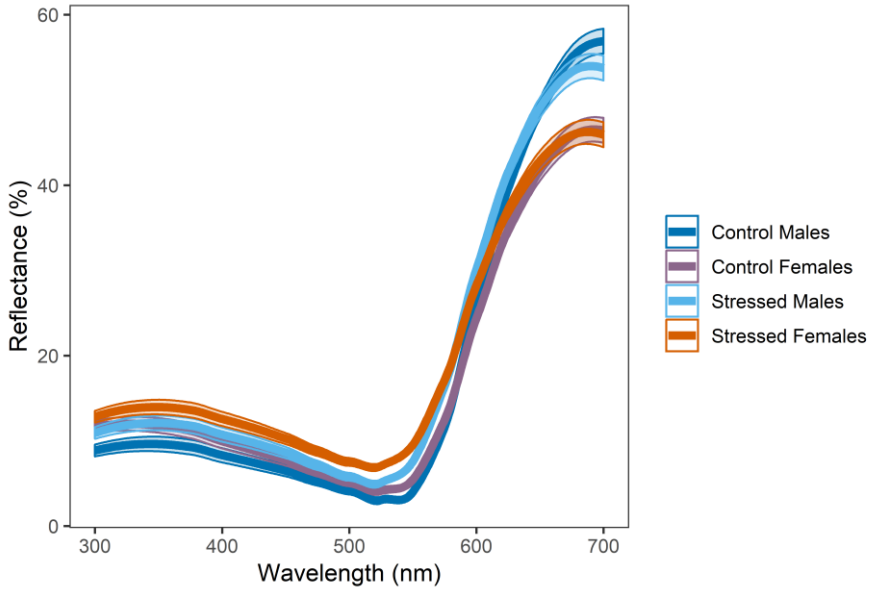

Figure 4.15: Mean relative reflectance (± S.E.) of the red forewing band for *H. erato* males and females of the control group and the stressed group.

Table 4.13: Mean ± S.E. colour variables for *H. erato* red pigment colour in the control and stressed groups. Saturation, chroma and hue were significantly lower in the stressed individuals.

Females	**Control**	**Stressed**	**t**	**df**	**p**
B1	7164 ± 521	7761 ± 524	-0.81	22.60	0.428
B3	49.0 ± 3.5	46.3 ± 2.3	0.65	15.24	0.528
S2	12.8 ± 1.0	8.78 ± 0.9	3.13	20.44	**0.005**
S6	45.0 ± 3.1	39.5 ± 2.1	1.46	15.80	0.165
S8	2.53 ± 0.08	2.14 ± 0.11	2.85	26.86	**0.008**
H1	694 ± 2.2	687 ± 1.4	2.50	15.08	**0.025**
Males					
B1	6886 ± 153	869 ± 401	-2.29	35.53	0.028
B3	55.7 ± 1.3	54.2 ± 1.96	0.64	44.12	0.527
S2	26.1 ± 3.8	15.7 ± 1.7	2.52	23.88	**0.019**
S6	52.8 ± 1.5	49.4 ± 1.8	1.48	44.81	0.147
S8	3.09 ± 0.1	2.60 ± 0.1	3.62	42.84	**<0.001**
H1	698 ± 0.6	690 ± 1.7	4.59	34.82	**<0.001**

Similar to *H. erato*, in *H. sara*, brightness was not affected by thermal stress, but there were decreases in saturation, contrast and chroma (Figure 4.16; Table 4.14). Hue only changed in females, moving into longer orange wavelengths. The reflectance spectrum shows that UV reflectance is higher in the stressed group compared to the controls (Figure 4.16). This provides evidence that there is a decrease in pigment concentration on the band as this allows UV reflectance to become predominant.

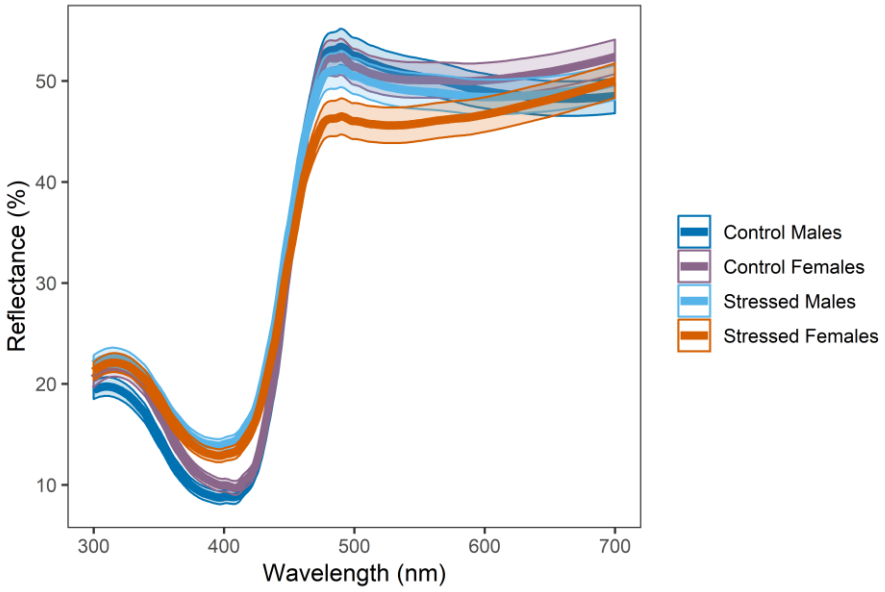

Figure 4.16: Mean (± S.E.) reflectance for *H. sara* yellow forewing band in male and female control and stressed treatments.

Table 4.14: Mean (± S.E.) colour variables for *H. sara* yellow pigment colour in the control and stressed groups. Differences in saturation and related variables are seen in both males and females.

Females	**Control**	**Stressed**	**t**	**df**	**p**
B1	14988 ± 434	14356 ± 432	1.0	87.61	0.300
B3	54.7 ± 1.6	51.1 ± 1.6	1.64	88.26	0.105
S2	6.37 ± 0.4	4.60 ± 0.3	3.92	76.93	**<0.001**
S6	45.2 ± 1.4	38.4 ± 1.5	3.32	88.96	**0.001**
S8	1.21 ± 0.02	1.07 ± 0.03	4.38	86.97	**<0.001**
H1	601 ± 17	649 ± 13	-2.29	78.32	**0.025**
Males	**Control**	**Stressed**	**t**	**df**	**p**
B1	14552 ± 456	15079 ± 406	-0.86	93.20	0.390
B3	54.6 ± 1.7	53.2 ± 1.4	0.64	89.28	0.524
S2	8.11 ± 0.7	4.99 ± 0.3	4.8	59.47	**<0.001**
S6	46.2 ± 1.8	39.8 ± 1.5	2.79	90.04	**0.006**
S8	1.27 ± 0.03	1.07 ± 0.03	4.62	100.39	**<0.001**
H1	533 ± 13	548 ± 13	-0.83	95.94	0.409

Visual modelling

In both bright daylight and forest shade environments, models suggest that the avian and *Heliconius* visual systems could discriminate differences in iridescent colour between control and stressed *H. erato* (Figure 4.17; Table 4.15). However, only the avian model had chromatic JNDs significantly above 3, suggesting they are much more able to see the small differences in hue between the treatment groups. Both avian and *Heliconius* are able to distinguish the differences in brightness (achromatic JNDs). For pigment colour, the avian model was again the most able to discriminate chromatic differences, but *Heliconius* were unable to see these in natural conditions. However, the *Heliconius* model was more able to discriminate achromatic differences compared to the avian model.

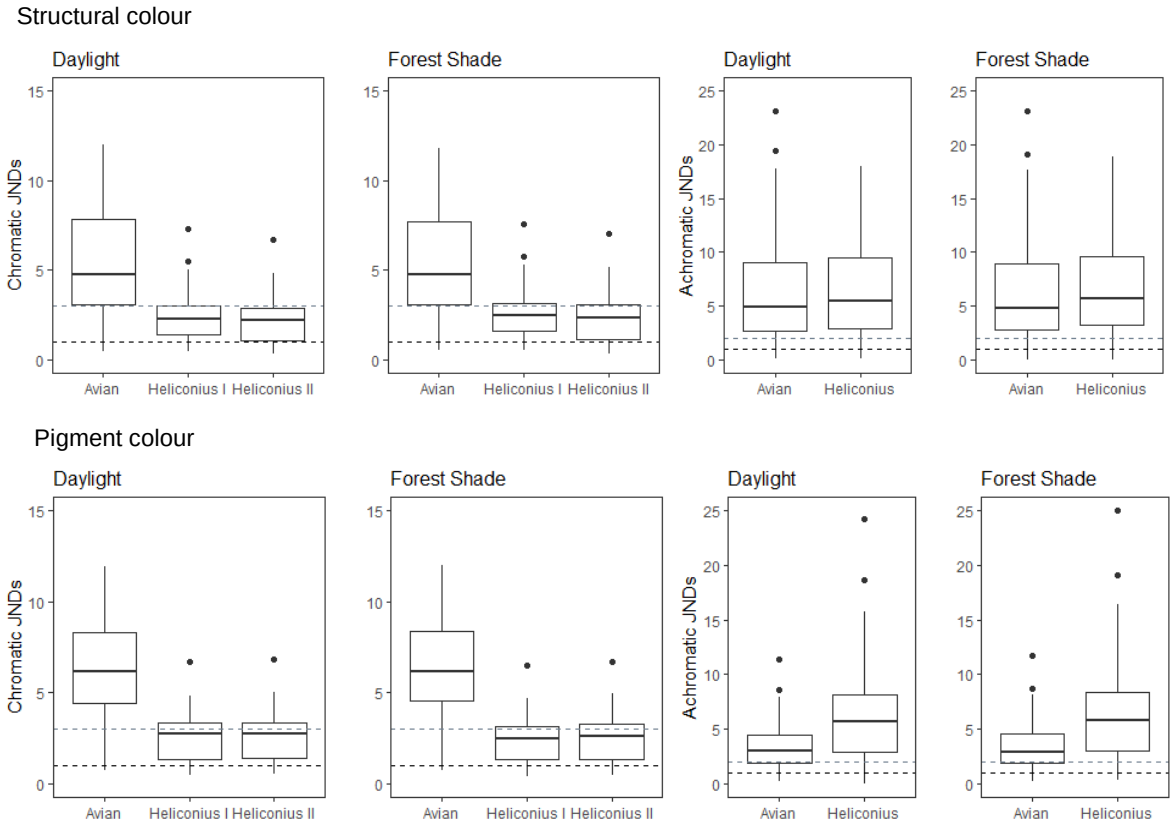

Figure 4.17: Pairwise comparisons between unique pairs of control and stressed *H. erato* wings (n = 50). Ability of the avian, *Heliconius* type I (*erato* female) and *Heliconius* type II (*erato* male) visual models to discriminate chromatic and achromatic differences in structural and pigment colour between control and stressed *H. erato* wings in daylight and forest shade light conditions. The black dotted line shows a JND value of 1, and the grey dotted line a value of 3.

Table 4.15: Mean (± S.E.) chromatic and achromatic Just Noticeable Differences for treatment comparisons under two lighting conditions for structural and pigment colour. Three visual systems are tested - Violet-sensitive avian, *Heliconius* type I (*erato* female), and *Heliconius* type II (*erato* male). Number of comparisons = 50.

Structural colour	**Visual model**	**Chromatic JND**	**Number JNDs >1**	**p**	**Number JNDs >3**	**p**
Daylight	Avian	5.36 ± 0.4	48	**<0.001**	40	**<0.001**
	Heliconius type I	2.46 ± 0.2	43	**<0.001**	12	0.999
	Heliconius type II	2.18 ± 0.2	38	**<0.001**	12	0.999
Forest shade	Avian	5.27 ± 0.4	48	**<0.001**	41	**<0.001**
	Heliconius type I	2.61 ± 0.2	44	**<0.001**	18	0.984
	Heliconius type II	2.32 ± 0.2	39	**<0.001**	13	0.999
		Achromatic JND	**Number JNDs >1**	**p**	**Number JNDs >3**	**p**
Daylight	Avian	6.62 ± 0.7	46	**<0.001**	37	**<0.001**
	Heliconius	6.48 ± 0.6	45	**<0.001**	37	**<0.001**
Forest shade	Avian	6.58 ± 0.7	46	**<0.001**	37	**<0.001**
	Heliconius	6.52 ± 0.6	45	**<0.001**	39	**<0.001**
Red pigment colour		**Chromatic JND**	**Number JNDs >1**	**p**	**Number JNDs >3**	**p**
Daylight	Avian	6.36 ± 0.6	26	**<0.001**	24	**<0.001**
	Heliconius type I	2.56 ± 0.3	23	**<0.001**	11	0.876
	Heliconius type II	2.57 ± 0.3	23	**<0.001**	11	0.876
Forest shade	Avian	6.36 ± 0.6	26	**<0.001**	24	**<0.001**
	Heliconius type I	2.53 ± 0.3	23	**<0.001**	8	0.990
	Heliconius type II	2.52 ± 0.3	25	**<0.001**	11	0.876
		Achromatic JND	**Number JNDs >1**	**p**	**Number JNDs >3**	**p**
Daylight	Avian	3.59 ± 0.5	23	**<0.001**	13	0.695
	Heliconius	6.48 ± 1.1	25	**<0.001**	20	**0.010**
Forest shade	Avian	3.59 ± 0.5	23	**<0.001**	13	0.695
	Heliconius	6.76 ± 1.1	25	**<0.001**	20	**0.010**

In *H. sara*, the large differences in structural colour between stressed and control wings can be discriminated easily by all three models (Figure 4.18; Table 4.16). *Heliconius* type II (males) had the lowest mean chromatic JNDs in both daylight and forest shade conditions, again likely due to the lack of the second UV opsin. While the avian model was most able to discriminate chromatic differences, the *Heliconius* model had higher mean JNDs for achromatic differences. Overall,

differences in pigment colour were much less able to be discriminated by all visual systems in natural environments. While able to see differences in ideal conditions, only the *Heliconius* model for forest shade could discriminate achromatic differences in natural conditions (Table 4.16).

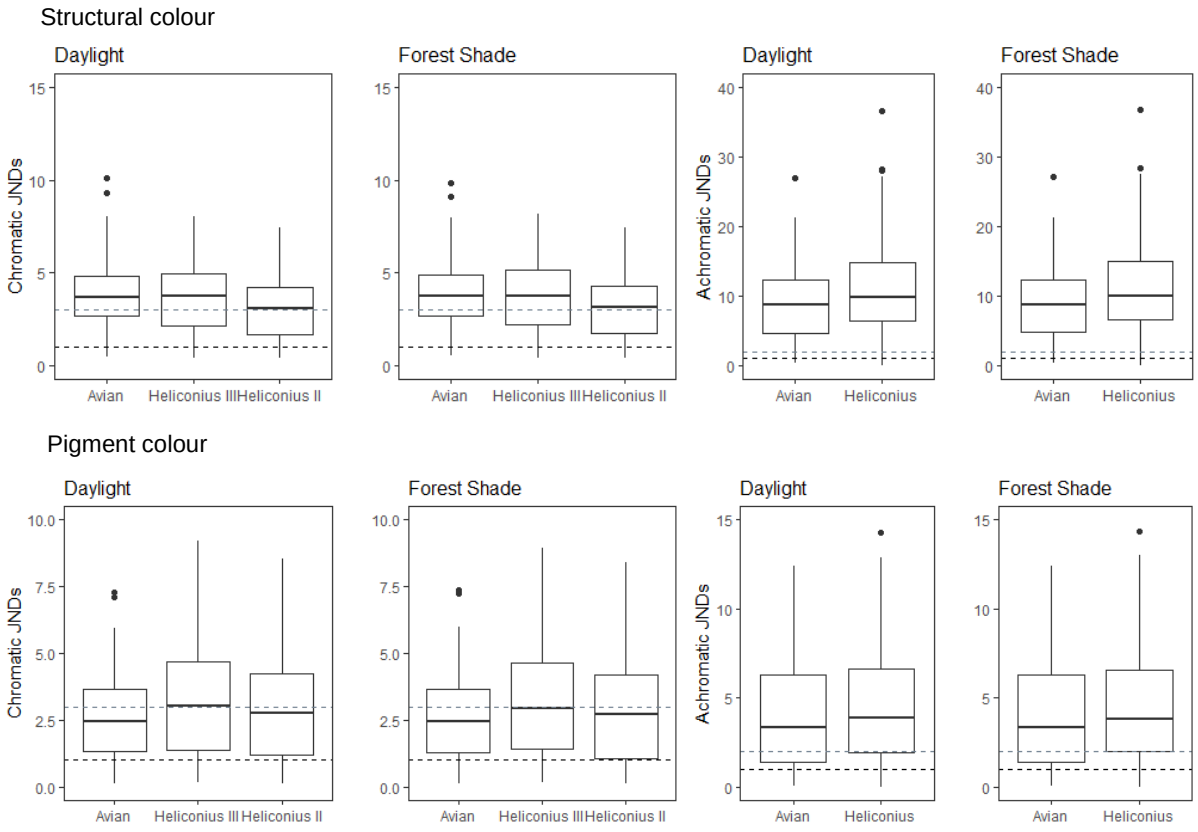

Figure 4.18: Ability of the avian, *Heliconius* type III (*sara* female) and *Heliconius* type II (*sara* male) visual models to discriminate chromatic and achromatic differences between control and stressed *H. sara* wings for structural and pigment colour in daylight and forest shade light conditions. The black dotted line shows a JND value of 1, and the grey dotted line a value of 3. Note the smaller axis used for pigment colour.

Table 4.16: Mean (± S.E.) chromatic and achromatic JNDs for treatment comparisons under two lighting conditions for structural and pigment colour. Three visual systems are tested - Violet-sensitive avian, *Heliconius* type II (*sara* female), and *Heliconius* type III (*sara* male). Number of comparisons = 84.

Structural colour	**Visual model**	**Chromatic JND**	**Number JNDs >1**	**p**	**Number JNDs >3**	**p**
Daylight	Avian	3.88 ± 0.2	80	**<0.001**	57	**<0.001**
	Heliconius type II	3.19 ± 0.2	78	**<0.001**	43	0.457
	Heliconius type III	3.79 ± 0.2	81	**<0.001**	50	**0.051**
Forest shade	Avian	3.89 ± 0.2	80	**<0.001**	57	**<0.001**
	Heliconius type II	3.31 ± 0.2	79	**<0.001**	45	0.293
	Heliconius type III	3.89 ± 0.2	81	**<0.001**	50	**0.051**
		Achromatic JND	**Number JNDs >1**	**p**	**Number JNDs >3**	**p**
Daylight	Avian	8.86 ± 0.6	79	**<0.001**	70	**<0.001**
	Heliconius	11.3 ± 0.8	82	**<0.001**	76	**<0.001**
Forest shade	Avian	8.89 ± 0.6	80	**<0.001**	70	**<0.001**
	Heliconius	11.4 ± 0.8	81	**<0.001**	76	**<0.001**
Yellow pigment colour		**Chromatic JND**	**Number JNDs >1**	**p**	**Number JNDs >3**	**p**
Daylight	Avian	2.59 ± 0.2	69	**<0.001**	27	0.999
	Heliconius type II	3.02 ± 0.2	65	**<0.001**	37	0.885
	Heliconius type III	3.36 ± 0.3	68	**<0.001**	43	0.457
Forest shade	Avian	2.61 ± 0.2	68	**<0.001**	28	0.999
	Heliconius type II	3.01 ± 0.2	66	**<0.001**	37	0.885
	Heliconius type III	3.26 ± 0.2	67	**<0.001**	41	0.683
		Achromatic JND	**Number JNDs >1**	**p**	**Number JNDs >3**	**p**
Daylight	Avian	3.95 ± 0.3	64	**<0.001**	47	0.163
	Heliconius	4.52 ± 0.4	70	**<0.001**	49	0.078
Forest shade	Avian	3.95 ± 0.3	64	**<0.001**	47	0.163
	Heliconius	4.55 ± 0.4	70	**<0.001**	51	**0.031**

4.4.3 Scale morphology

Comparing scanning electron microscopy images for a small number of control and stressed *H. sara* individuals, it seems that the longitudinal ridges in the stressed group are not as uniform as the controls. At high magnification we can see that the ridges do not run perfectly straight down the length of the scale, and some of the lamellae are curved (Figure 4.19). On some stressed scales, the thickness of the ridges themselves are not uniform, e.g. at the point labelled in Figure 4.19, the ridges are thin, and this was seen on a number of the stressed scales (further examples in Figure S4.3).

Longitudinal ridge spacing was measured on a total of 50 scales, comprising of 5 scales from each of 5 control and 5 stressed wings. There were no significant differences in ridge spacing between the groups (control = 682 ± 33nm, stressed = 754 ± 92nm, $t = -1.62$, $df = 5$, $p = 0.159$), although spacing was on average wider and more variable on the stressed scales, suggesting that this could be having some effect on the brightness of the iridescent colour. More samples will be needed to look at the possible effect of thermal stress on ridge spacing and to uncover any differences between sexes.

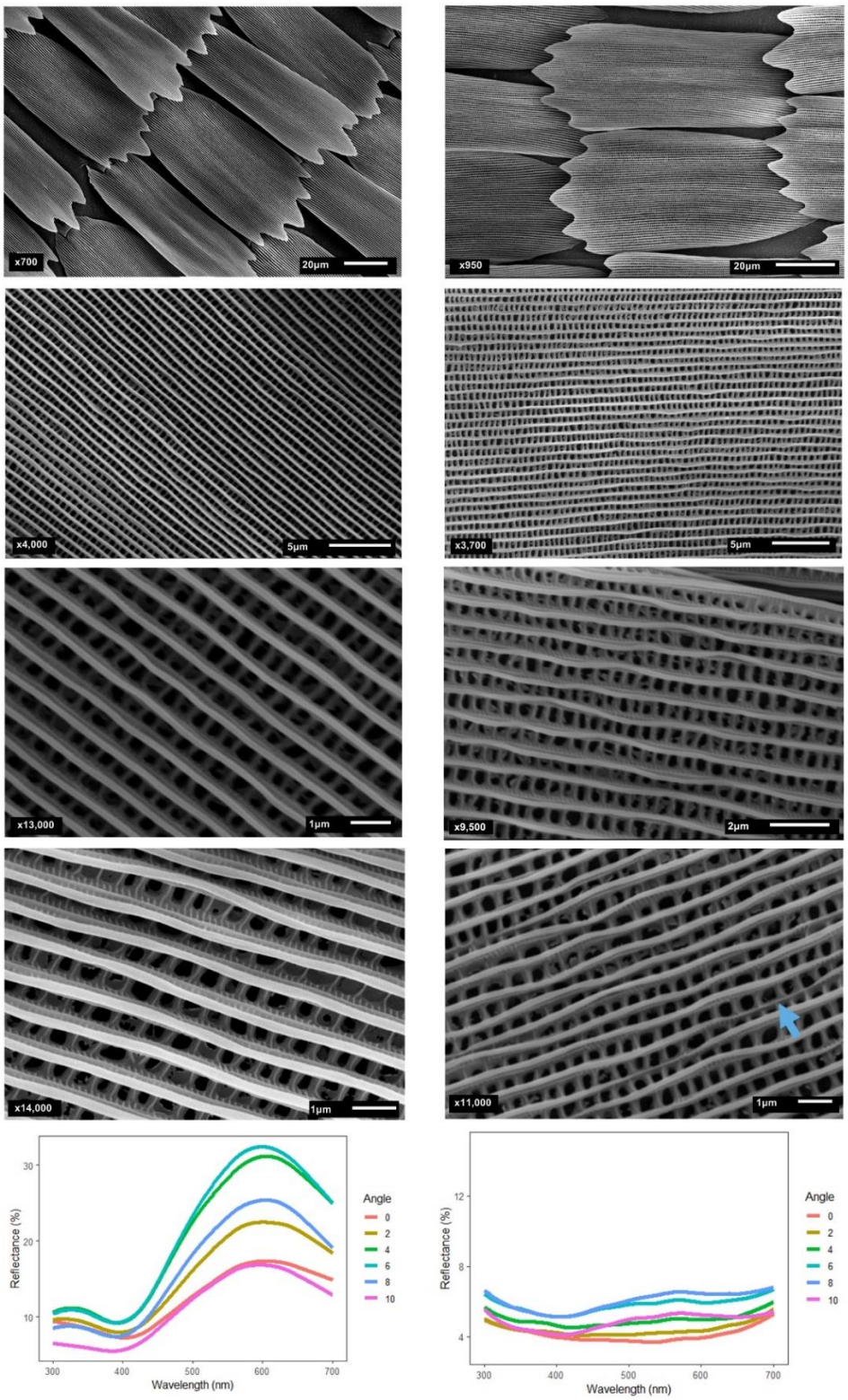

Figure 4.19: Scanning Electron Microscope images at increasing magnification and reflectance spectra for a single control *H. sara* (left images) and a stressed *H. sara* (right images). The blue arrow on the final SEM shows an example of uneven thickness of the longitudinal ridges.

4.5 Discussion

The reduction in iridescence produced by thermal stress shows that structural colour is condition dependent in both *Heliconius erato* and *Heliconius sara.* With *H. erato* iridescence, all colour variables decreased in the stressed group, except total brightness which may be explained by the increased brightness at higher wavelengths (i.e. red became more dominant, resulting in less saturated colour). Colour in males seemed to be more affected than in females, however males were initially brighter so a greater change was possible in this group. In *H. sara*, thermal stress drastically decreased all colour variables except hue, which was highly variable. One sex did not seem to be more affected than the other, although there were slightly larger changes in female brightness.

We also found that pigment colour was condition dependent, but to a lesser extent than iridescence. Both the red pigment colour in *H. erato* and the yellow colour in *H. sara* decreased in saturation and related variables with thermal stress. Brightness of iridescence was independent of pigment colour brightness, suggesting that structural and pigment colours can provide different signals to the viewer. Deposition of yellow pigments during wing development and an increase in concentration of 3-OHK in the haemolymph occurs late in pupal development (Reed et al. 2008), possibly explaining why yellow colour in *sara* was less affected by thermal stress than the *erato* red band.

Sexual dimorphism in colour has likely arisen from differing selection pressures between sexes, the most likely of which is sexual selection. *H. erato* males had higher levels of iridescence, possibly suggesting it may be favoured by females when selecting a mate and could be used to select a high-quality mate. *H. erato* females only mate once and nutrients gained from the males spermatophore are used in egg production, thus females would benefit from choosing to mate with fertile males who can provide the most nutritional ejaculate (Rutowski 1985). If thermal stress affects fecundity, condition dependent colour could act as a signal of fertility. In *Drosophila*, fluctuating temperatures during pupal development were linked to adult male

sterility (Vollmer et al. 2004), suggesting females may be able to use iridescence as an indicator of fertility.

In contrast to *H. erato*, we found that *H. sara* females had brighter iridescent colour than males, although unlike *erato*, there were no differences in chroma or contrast. This suggests that selection for iridescence in this species could be driven by male mate choice. Multiple studies have looked at male choice in *Heliconius* and its role in assortative mating (McMillan et al. 1997; Jiggins et al. 2001; Estrada and Jiggins 2008; Merrill et al. 2019). As with males, iridescence could be used as a signal of female fecundity. In blue tits, UV colouration of females was positively correlated with survival (Doutrelant et al. 2008). *Heliconius* males produce a large spermatophore which provides the female with cyanogenic compounds for protection (Cardoso and Gilbert 2007), as well as being nutrient-rich. This is costly to the male, so could select for male choosiness. Behavioural research on mate choice is needed to determine the importance of structural colour as a sexual signal in *Heliconius*.

Pigment colour has been shown to be used in mate choice and species recognition in *Heliconius*, although within-subspecies variation in colour and its use as a variable sexual signal has not previously been tested. *H. erato* had sexually dichromatic red colour on the forewing which was again more saturated in males. Saturation and hue were sexually dimorphic in the *H. sara* yellow band, with males having more saturated colour than females. These results warrant investigation of the use of pigment colour as a sexually selected signal. However, changes in colour between treatments were more exaggerated in iridescence compared to the pigment colours, which suggest pigment colours are less dependent on developmental conditions and could be providing information about a different factor, e.g. nutrition. Recently, production of red carotenoid pigments was shown to be directly linked to mitochondrial function in finches (Hill et al. 2019). A meta-analysis of sexual dimorphism in avian plumage colour found that structural colour and pigment colour showed different patterns of covariation; structural colour dimorphism was associated with mating strategy while pigment colour dimorphism was linked to parental care

(Owens and Hartley 1998), suggesting that these two types of colour may generally be under different selective pressures.

Life history differences

There are some differences in life history traits between *H. sara* and *H. erato* which may explain some of the differences in sexual dimorphism seen in their colour. Both are within the pupal mating clade (Beltrán et al. 2007), meaning males will mate with females soon after they emerge from the pupa, or even pierce the pupal case to mate before the female has completely emerged. Pupal mating would suggest that female choice is not widespread as males will initiate mating and females cannot actively choose mates. However, in *H. erato* there is a lack of evidence for pupal mating and studies suggest that adult mating is the dominant mating strategy (McMillan et al. 1997; Mallet et al. 1998; Thurman et al. 2018). Using hovering and following behaviours, males will court females who then accept or reject the copulation. We have not observed pupal mating in our stocks of either species, but *sara* have been observed pupal mating in other insectaries (Jiggins 2017). *H. sara* are also gregarious and will lay 15-40 eggs in a group. Larvae in a group will pupate and emerge at similar times, meaning there will be multiple females for males to choose from, and also likely an increase in male-male competition. *H. erato* are solitary and lay only 1-5 eggs together, suggesting that males may not have the same level of choice as with gregarious species.

Although both species are likely to experience the temperatures we tested here in the wild (15-32°), it is the constant fluctuation that makes this a stressful environment in our experiments. Mortality rate in *sara* almost doubled when stressed, but surprisingly there was no effect on mortality in *erato*. Similarly, developmental rate decreased in stressed *sara* but not *erato*. However, smaller differences may have been seen if development times were recorded at more regular intervals. The differences between species may be related to *erato's* larger body size, meaning they are more resistant to temperature changes. On the other hand, *erato* can be found

at higher altitudes and should be better adapted to colder environments. *H. erato cyrbia* in particular is found at high altitudes (up to 2300m above sea level) in the western Andes.

Consistent with previous studies (Hernandez and Benson 1998; Montejo-Kovacevich et al. 2019), we found sexual dimorphism in the wing length of *H. sara*, with males being smaller than females. Hernandez and Benson (1998) found that small male *sara* had an advantage over larger males when defending territory. They hypothesised that large males avoid combat with smaller males as they have more to lose in terms of mating success. Female body size commonly correlates positively with fecundity in insects under constant environmental conditions (Honěk 1993; García-Barros 2000), and in butterflies, females are generally the larger sex as this allows them to carry more eggs (Allen et al. 2010). Therefore, the effect of temperature stress on female size we observed in *sara* may suggest that thermal stress has an impact on fecundity. This could also be consistent with stronger male mate choice operating in *sara.*

Montejo-Kovacevich et al. (2019) found reversed sexual size dimorphism in *H. erato* and other solitary *Heliconius*, with males being larger than females. In our sample, males were on average slightly larger than females, but the difference was not significant. In addition, we found that male size in *erato* decreased with thermal stress, suggesting effects on male fitness. In a study of Swallowtail butterflies, wing length predicted nuptial gift size (Rajyaguru et al. 2013), suggesting females could use wing length as an indicator of potential direct and/or indirect benefits. The reversals in the direction of both sexual dichromatism in iridescent colour and sexual size dimorphism between *erato* and *sara* indicate that sexual selection is operating differently in these two species. In Lepidoptera, adult body size and fecundity are largely determined during the larval stage, so we expect that diet and environment during this period are likely to have further effects on size (Boggs and Freeman 2005).

Structural colour as a private communication channel

Visual modelling showed that there is potential for both the bird and butterfly visual systems to detect and discriminate the colour differences we found. Previous research has shown that violet-

sensitive avian visual systems are less able to distinguish differences between mimetic *Heliconius*, in particular when looking at UV reflectance (Bybee et al. 2012; Llaurens et al. 2014). However, we found no evidence that the differences in structural colour are tuned to the *Heliconius* visual system or act as private communication channels. The avian model is able to discriminate all chromatic differences between sexes and treatments in bright light conditions, in contrary to the prediction that *Heliconius* would be more able to distinguish colours, particularly in lower wavelengths, due to having a UV-sensitive visual system. In *Heliconius*, females were more able than males to discriminate differences, suggesting a possible link to female mate choice. These *Heliconius* species are most likely to be found along forest edges, and the *Heliconius* models were able to discriminate in both forest shade and bright daylight conditions. Models suggest that birds cannot always see achromatic differences which could suggest that brightness of colour could be important for signalling between *Heliconius*. In general, differences in pigment colour were less able to be discriminated by both *Heliconius* and avian models, although *Heliconius* models were more able to see achromatic differences in some cases. Overall this suggests that differences in pigment colour are less likely to be used as a signal of condition, as small differences will not be seen.

Scale morphology

We speculate that thermal stress is affecting the development of longitudinal ridges which are essential for producing bright iridescence (Parnell et al. 2018). Ridges on the brightest control wings seemed to run much straighter down the length of the scales, whereas on the stressed samples, ridges were more uneven and were spaced further apart. Looking at how reflectance changes with angle can tell us something about how the scale structures are changing with stress, especially in *sara* where the reduction in iridescence is more pronounced. Stressed individuals lack an obvious peak angle compared to the controls, showing that the structural colour effectively loses the angle-dependent aspect. Further imaging of scales is needed to determine the precise changes occurring and what is differing between sexes, and whether the changes are in total number of ridges per scale or height of lamellae layering. Prolonged cold stress on

Polyommatus icarus pupae resulted in a change in structural colour caused by the arrangement of scale cells on the wing, rather than changes in the nanostructures (Kertész et al. 2017). Currently, little is known about the development of the particular nanoscale structures which produce structural colours, and at which point during pupal development they are assembled. Uneven thickness of the ridges suggests some problem with the deposition of chitin. Fluctuating temperatures affect metabolic rates, in turn this could affect the insects ability to produce the precise structures needed (Kemp et al. 2006).

Further factors influencing variation in colour

While we have shown that environmental temperature influences variation of iridescence, condition can be linked to many other factors. A further factor to study is diet which is known to affect many sexually selected traits, and diet during *Heliconius* larval stages is likely to have a large effect on adult traits. Diet during the larval stage could influence pigment colours as some chemical pigments are produced from plant compounds in the larval diet, and although many are synthesised during scale development in the pupa, diet may provide the specific amino acids needed (Nijhout 1991). Wing size could be also affected by diet as wing discs begin to form during the larval stage. A previous study showed *Heliconius* larvae which were not reared on their preferred host plant had smaller wing size as adults (Darragh et al. 2019). Manipulating larval diet would show if colour can signal information about larval conditions, as well as the pupal developmental condition which we have shown here. In cowbirds, structural colour, but not melanin-based colour, was indicative of nutritional value of the diet (McGraw et al. 2002). A recent study found that changing the hostplant of *Zerene* larvae did not affect overall UV reflectance of structural colour on adult butterflies, but did result in changes to scale density on the wing (Fenner et al. 2019).

Age is also an important factor, especially in relation to mate choice, as females of the *Heliconius* species studied here will only mate when young. We might expect that structural colours should not decrease over time as much as pigment colour which can fade. For example, red hue was

highly associated with age in *Heliconius melpomene* (Dell'Aglio et al. 2017). On the other hand, nanoscale structures can degrade, and scale loss will decrease overall brightness. Kemp (2006) found that structural colour in *Colias* did degrade over time, but high variance meant that it was not as accurate as pigment colour for predicting male age. UV brightness and chroma were lower in older individuals in studies on birds (Papke et al. 2007; Hegyi et al. 2018).

Many studies have found positive correlations between visual signals and the strength of chemical defences, so this could be another factor influencing colour variation. For example, saturation and contrast of colour on ladybird elytra predicted toxicity (Arenas et al. 2015). *Heliconius* use their bright colour patterns as warning signals of their toxicity to predators, and it is not known if these aposematic signals could be used as a quantitative measure of toxin levels and so explain some of the variation in colour that we see. However, in Lepidoptera, wing colour did not correlate with toxins in 14 species of moths (Briolat et al. 2019), and like *Heliconius*, these species sequester cyanogenic compounds from their host plants, as well as having the ability to synthesise some compounds *de novo* (Fürstenberg-Hägg et al. 2014). Nevertheless, a relationship between colour and chemical defence would be consistent with the visual modelling showing that variation in colour can be distinguished by predators.

Conclusion

In conclusion, our results provide the first evidence that iridescent colour, and to a lesser extent pigment colour, in *Heliconius* are condition dependent traits. Sexual dimorphism in iridescence and differences in the effects of thermal stress between sexes suggest this trait is important in sexual selection, although further study of male and female mate choice is needed to confirm this.

4.6 Supplementary Information

Script 4.1: Python script to convert raw spectral data to the format needed to analyse in R/PAVO.

Standardise spectral data
J Enciso Romero, M Brien
April 2019

load packages

```
import matplotlib as mpl
import matplotlib.pyplot as plt
import numpy as np
import pandas as pd
import os
```

define functions - together these extract text files, standardise spectral data using measurements of a white standard and output the data in the correct format to use in R/PAVO

```
def get_filenames(par_pattern):
    """ get_filenames(str) -> list[str]

    Parameters:
    An extension so that the program can look for files with such extension
    and make a list of those files

    Returns:
    A list with the names of the files containing the data that is going to b
e
    in the plot
    """
    return list(filter(lambda x: par_pattern in x or 'white' in x,
                       os.listdir()))

def transform_name(par_str):
    """
    Simplify file names so for each sample there are files for each angle and
the white standard
    """
    if par_str.startswith("white"):
        return par_str
    elif par_str.startswith("m"):
        return par_str.replace("m", "-")
    elif par_str[0].isnumeric():
        return par_str.split("_")[0]
    else:
        names_ls = par_str.split("_")
        pn = names_ls[0][-1]
        tailnm = "".join(names_ls[3].split("-"))
        new_name = names_ls[1]+pn+tailnm
        new_name = new_name.replace("m", "-")
        return new_name
```

```
def read_data(par_list):
    """
    read_data(list[str]) -> pandas.DataFrame

    Parameters:
    A list of strings corresponding to filenames to process
    Returns:
    A single pandas.DataFrame with the aggregation of the data from the file(
s) in the list
    """
    holder_list = []
    white_df = None
    for i in par_list:
        curr_name = i.strip('.txt')
        curr_name = transform_name(curr_name)
        if i.startswith('white'):
            white_df = pd.read_csv(i, skiprows=50, sep='\t',
                                   names=['wavelength', 'intensity'],
                                   engine='python', skipfooter=1)
            white_df = white_df.assign(name=np.repeat(curr_name,
                                                      white_df.shape[0]))
            # Apply corrections dividing by 1e07
            white_df['wavelength'] = white_df.wavelength.values / 1e07
        else:
            curr_data = pd.read_csv(i, skiprows=50, sep='\t',
                                    names=['wavelength', 'intensity'],
                                    engine='python', skipfooter=1)
            name_col = np.repeat(curr_name, curr_data.shape[0])
            curr_data = curr_data.assign(name=pd.to_numeric(name_col))

            curr_data['wavelength'] = curr_data.wavelength.values / 1e07
            holder_list.append(curr_data)
    transformed_list = []
    for df in holder_list:
        new_intensity = (df.intensity/white_df.intensity)*100
        transformed_list.append(df.assign(n_intensity=new_intensity))
    return pd.concat(transformed_list)


def plot_2d(par_df, savefig=False, showfig=False, fmt="pdf", legend=True):
    """ Plot standardised spectral data for each angle
    plot_2d(pandas.Dataframe, bool, bool) -> None

    Parameters:
    A pandas.DataFrame with 4 columns:
    <float> <float> <int> <float>
    """
    unique_names = list(np.unique(par_df.name.values))
    n_colors = len(unique_names)
    list_colours = np.apply_along_axis(mpl.colors.rgb2hex, 1,
                                       mpl.cm.get_cmap(name='viridis',
                                                       lut=n_colors).colors)
    title = os.getcwd().split("\\")[-1]
    for i,j in zip(unique_names, list_colours):
        my_subset = par_df.loc[par_df['name'] == i]
        plt.scatter(my_subset.wavelength, my_subset.n_intensity,
                    label=i, s=8, color=j)
```

```
    plt.title(title)
    plt.xlabel('Wavelength (nm)')
    plt.ylabel('Reflectance (%)')
    if legend:
        plt.legend(markerscale=2)
    plt.tight_layout()
    if savefig:
        plt.savefig("{}.{}".format(title, fmt), format=fmt)
        print("{}.{} saved".format(title, fmt))
    if not showfig:
        plt.close()

def save_pavo(par_df):
    """
    Saves the data in a format suitable for pavo
    """
    angles = list(np.unique(par_df['name']))
    for angle in angles:
        sub_df = par_df.loc[par_df['name'] == angle][['wavelength',
                            'n_intensity']]
        sub_df.to_csv(
                "{}_{}_PAVO.txt".format(str(angle),
                 os.getcwd().split("\\")[-1]), sep='\t',
                 index=False,
                 float_format='%.3f')
```

Loop through directories to extract spectral data files, run functions and save output files ready for R

```
listdirs = os.listdir()
for dir in listdirs:
    os.chdir(dir)
    ind_name = os.getcwd().split("\\")[-1]
    my_list = get_filenames('.txt')
    all_data = read_data(my_list)
    all_data.to_csv("{}.tsv".format(ind_name), sep='\t', index=False,
                float_format='%.3f')
    all_data = all_data.loc[all_data['wavelength'] > 260]
    all_data = all_data.loc[all_data['wavelength'] < 700]
    plot_2d(all_data, savefig=True, showfig=True, legend=True, fmt='png')
    save_pavo(all_data)
    del all_data
    plt.clf()
    os.chdir("..")
```

Script 4.2: R script for visual modelling using PAVO. Example using *Heliconius* type I visual system. The same method was used for the other *Heliconius* and avian visual systems.

Visual modelling

M Brien, N Nadeau, J Enciso Romero

Load files

```
library(pavo)
# Load file containing spectral data for each individual
spec<-as.rspec(read.csv("spec.csv"))
# File for Heliconius receptor densities with columns for wavelength, UV, VS, M, L
Hcones <- read.csv("HeliconiusVisualSystem.csv")
Hcones <- as.rspec(Hcones)
```

Build visual system models

```
# heliconius type I photoreceptor densities -> UV1, UV2, B, G
i = c(0.09, 0.08, 0.17, 1)
# heliconius type I photoreceptor densities
n <- c(0.09,0.07,0.17,1)
w <- 0.05

# daylight conditions
heli1_daylight <- vismodel(spec, qcatch = "Qi", visual = Hcones, achromatic = "l", illum= "D65", vonkries = T, relative = F)
# forest shade conditions
heli1_forest <- vismodel(spec, qcatch = "Qi", visual = Hcones, achromatic = "l", illum= "forestshade", vonkries = T, relative = F)
# colour distance calculations for daylight and forest shade conditions
heli1_daylight_coldist <- coldist(heli1_daylight, qcatch = "Qi", noise = "neural", achro = T, n=i, weber=w, weber.achro=w)
heli1_forest_coldist <- coldist(heli1_forest, qcatch = "Qi", noise = "neural", achro = T, n=i, weber=w, weber.achro=w)
```

Just Noticeable Difference comparisons

```
# function to extract relevant comparisons - initially runs all pairwise comparisons
compareSpp <- function(Spp1, Spp2, col.distances){
  speciesA1 <- subset(col.distances, subset = grepl(Spp1, patch1))
  speciesA1.B1 <- subset(speciesA1, subset = grepl(Spp2, patch2))
  speciesA2 <- subset(col.distances, subset = grepl(Spp1, patch2))
  speciesA2.B2 <- subset(speciesA2, subset = grepl(Spp2, patch1))
  results <- rbind(speciesA1.B1, speciesA2.B2)
  return(results)
}

# JND differences between males and females
heli1_daylight_sexes <- compareSpp(Spp1="m", Spp2="f", col.distances=heli1_daylight_coldist)
heli1_forest_sexes <- compareSpp(Spp1="m", Spp2="f", col.distances=heli1_forest_coldist)
```

```
# JND differences between control and stressed samples
heli1_daylight_temp <- compareSpp(Spp1="C", Spp2="T", col.distances=heli1_day
light_coldist)
heli1_forest_temp <- compareSpp(Spp1="C", Spp2="T", col.distances=heli1_fores
t_coldist)


# function to extract unique pairs

get_pairs<-function(par_table) {
  # Holds letters that have appeared already
  coll <- list()
  new_df <- par_table[0,]
  for(i in 1:nrow(par_table)){
    # If none of the letters in row was seen already
    if(!(par_table[i, 1] %in% coll) & !(par_table[i, 2] %in% coll)){
      # Add letters to seen collection
      coll[length(coll) + 1] <- par_table[i, 1]
      coll[length(coll) + 1] <- par_table[i, 2]
      # Add row to new dataframe
      new_df[nrow(new_df) + 1,] <- par_table[i,]
    }
  }
  new_df
}
```

Sign tests to determine if differences can be discriminated

```
comparisons <- get_pairs(heli1_forest_temp)
# summarise dS - chromatic differences
summarise(comparisons, mean=mean(dS), se=(sd(dS)/sqrt(length(dS))))
# how many JND comparisons are over 1 or 3?
length(which(comparisons$dS > 1))
length(which(comparisons$dS > 3))
# are a significant number above 1/3?
binom.test(x = length(which(comparisons$dS > 1)), n= length(comparisons$dS),
alternative = "g")$p.value
binom.test(x = length(which(comparisons$dS > 3)), n= length(comparisons$dS),
alternative = "g")$p.value
# summarise dL - achromatic differences
summarise(comparisons, mean=mean(dL), se=(sd(dL)/sqrt(length(dL))))
length(which(comparisons$dL > 1))
length(which(comparisons$dL > 3))
binom.test(x = length(which(comparisons$dL > 1)), n= length(comparisons$dL),
alternative = "g")$p.value
binom.test(x = length(which(comparisons$dL > 3)), n= length(comparisons$dL),
alternative = "g")$p.value
```

Table S4.1: Correlations between colour variables of control *H. erato* iridescent colour and red pigment colour (df = 25), and between *H. sara* iridescent colour and yellow pigment colour (df = 82).

	H. erato		***H. sara***	
	r	p	r	p
B1	0.97	0.339	-0.08	0.475
B3	0.19	0.337	-0.08	0.493
S2	0.45	0.019	-0.64	0.525
S6	0.25	0.213	-0.10	0.355
S8	0.38	0.048	-0.06	0.562

Table S4.2: *H. erato* colour variables did not correlate with wing size, the only exception being chroma in control males.

	Female Controls		**Male Controls**		**Female Stressed**		**Male Stressed**	
	r (df=47)	p	r (df=57)	p	r (df=17)	p	r (df=27)	p
B1	0.005	0.971	0.055	0.680	0.781	0.446	0.086	0.654
B3	0.125	0.392	0.141	0.288	0.112	0.648	0.163	0.340
S2	0.229	0.113	0.003	0.980	-0.048	0.847	0.221	0.258
S6	0.159	0.274	0.161	0.222	0.074	0.764	0.211	0.272
S8	0.255	0.077	0.302	**0.020**	-0.252	0.298	0.271	0.154
H1	-0.246	0.088	-0.061	0.645	0.019	0.938	-0.133	0.490

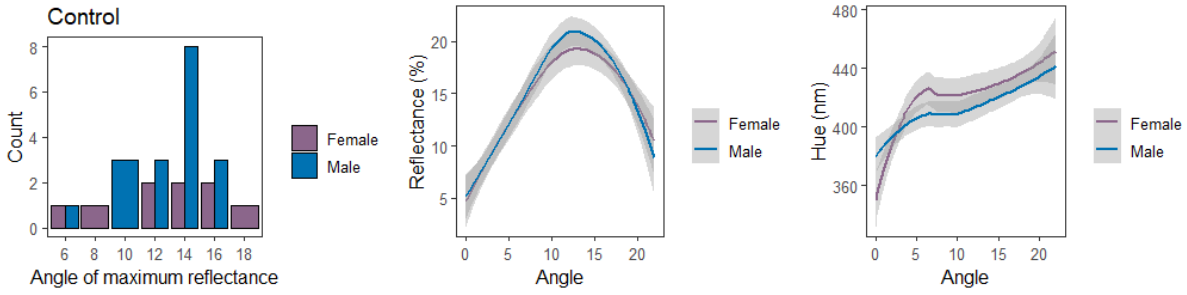

Figure S4.1: Within the *H. erato* control group, peak angle did not differ significantly between males and females. As angle increased, hue moved towards higher wavelengths.

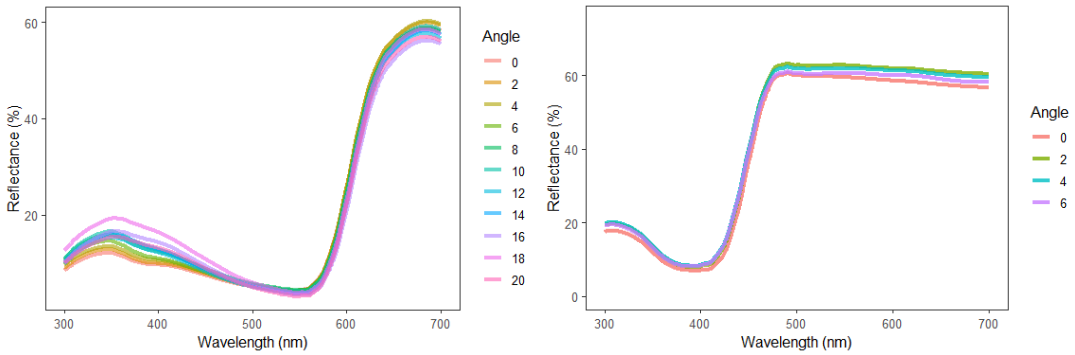

Figure S4.2: An example reflectance spectrum for pigment colour on one *H. erato* (left) and one *H. sara* (right) individual. Measurements of the red and yellow pigment forewing bands did not differ greatly with angle, although the effect of overlying structural colour can be seen in the blue wavelengths in *H. erato*.

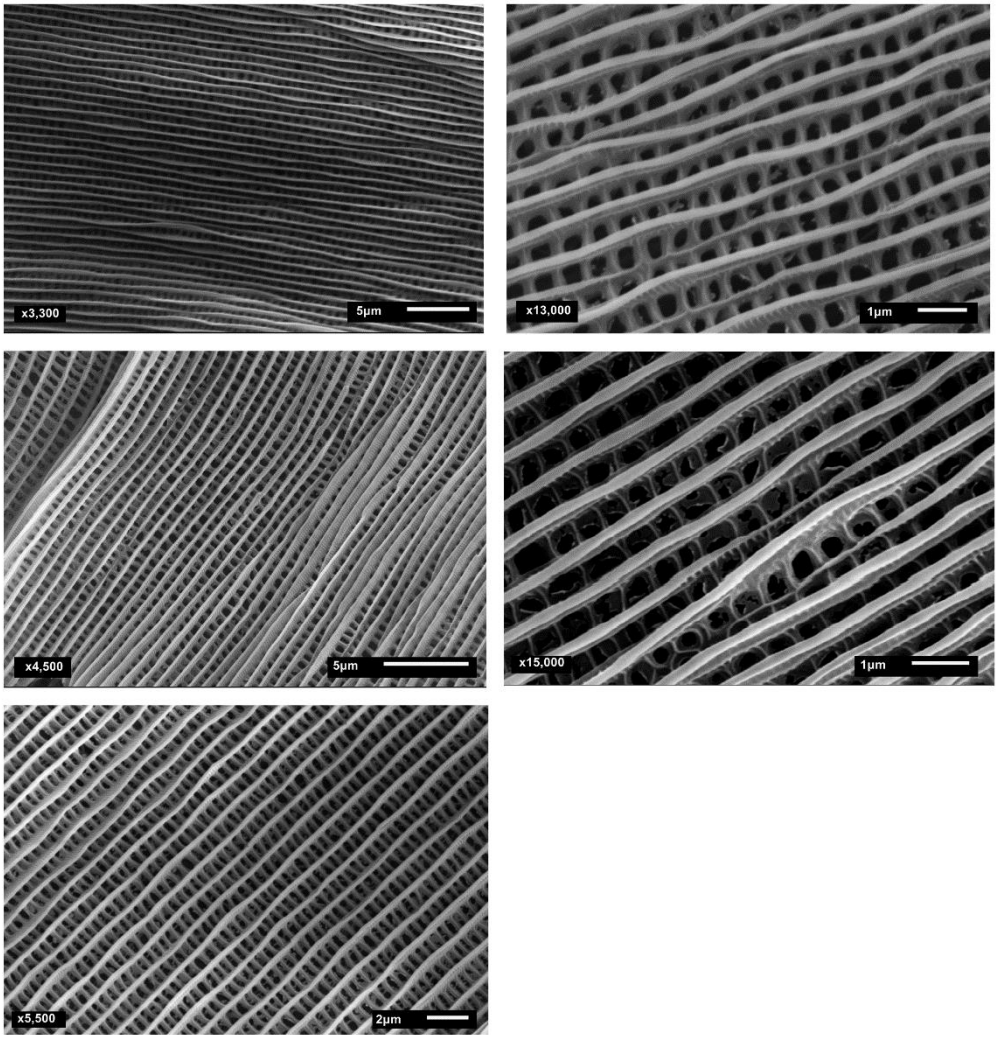

Figure S4.3: Further SEM images for each of the five stressed *H. sara* individuals imaged.

5. General Discussion

5.1 Research summary

In this thesis, I have looked at iridescent colour in *Heliconius* by linking phenotype, genotype and function. With a combination of phenotypic and genotypic data, I have begun to uncover the genetic basis of this complex trait and show that it has a different genetic basis in two mimetic species. It is not an example of gene reuse in distantly related species, suggesting a lack of repeatability of evolution in quantitative traits. This is in contrast to *Heliconius* pigment colour patterns, most of which are controlled by a homologous set of toolkit loci across multiple species (Nadeau 2016). However, there were some similarities between the species – in both, iridescence was controlled by two medium-large effect loci along with a set of small effect loci. The use of genetic crosses allowed the analysis of segregation patterns of Mendelian colour pattern traits and we were able to show that in *H. erato*, iridescent colour loci were not linked to the genes controlling these pigment pattern elements, but that there is some evidence for linkage in *H. melpomene*.

One of the most interesting findings was that iridescence is strongly sex-linked in *H. erato*. Genes on the Z chromosome may therefore be producing the sexual dimorphism in the colour which was shown in Chapter 4. In other species, such as guppies with structurally coloured silver patches, sex-linked traits are only expressed in males (Endler and Houde 1995). As the trait is produced in both sexes, this suggests that there is some difference in the regulation of these genes between sexes. If iridescence emerged at different times in *melpomene* and *erato*, this may explain the differences seen in genetic architecture. There was no sex-linkage of the trait in *melpomene*, and other work did not find any sexual dimorphism of iridescence in *melpomene* (Anna Puttick, *unpublished*).

I then investigated the role of structural colour as a signal in *Heliconius*. Using thermal stress experiments, I showed that the trait is condition dependent, but also crucially, that butterfly visual

systems can see this variation. Sexual dimorphism is often studied in exaggerated traits, but here we focus on smaller differences in a trait which is expressed in both sexes. Differences in the direction of sexual dichromatism in *H. erato* and *H. sara* may reflect differences in life history traits, such as timing of mating. Interestingly, pigment colour was also sexually dimorphic, but not condition dependent to the same extent as iridescence. These results suggest that structural colour could be a sexually selected trait that can be used by potential mates as a phenotypically plastic indicator of an individual's condition.

5.2 Further research on Heliconius structural colour: finding genes and testing the function

The next step with this work is to continue to narrow down the genomic regions controlling iridescence and use gene expression analyses to determine the genes involved. A combination of RNA-seq analyses and the QTL intervals found in this study could provide a list of candidate genes. Next, functional analysis of candidate genes can test whether modification of these genes results in a loss of iridescence. CRISPR/Cas9 gene-editing has already been used to successfully manipulate wing colour patterns in *Heliconius* and other Lepidoptera. *Optix* knockout in *H. erato* resulted in the loss of red pigment colour patterns (Zhang et al. 2017), knockout of *aristaless1* caused white wings to develop as yellow in *H. cydno* (Westerman et al. 2018), and *WntA* modifications disrupted pattern boundaries (Mazo-Vargas et al. 2017). Genome wide association studies (GWAS) have also been carried out to make use of a natural hybrid zone to study iridescence in wild populations of *H. erato* and *H. melpomene* (Curran 2018). QTL and GWAS approaches could be run with other measures of iridescence such as scale structure measurements, e.g. ridge spacing, or reflectance measurements. A combination of these approaches will allow a thorough analysis of this trait.

As we have found that there are differences in the genetic basis of structural colour in two mimetic species, it will be interesting to determine how these results relate to the genetic basis in other *Heliconius* species. Would we expect further differences in an iridescent specialist such as *H. sara*? The lack of non-iridescent *sara* means that other methods would need to be used to answer

this question. Selection experiments would be an interesting route. Differences in scale structure between *sara* and *erato*, e.g. lamellae continuity, suggests there will be some genetic or developmental differences.

To confirm that structural colour is a sexually selected trait in *Heliconius*, we would need to carry out behavioural experiments to test mate choice. Butterflies are an ideal system for testing the functions of adaptive traits as they can be bred in large numbers in the lab, we can manipulate wing colour and run behavioural assays. Previous mate choice experiments with butterflies have involved the use of model wings, on which colour can be manipulated (Ellers and Boggs 2003; Finkbeiner et al. 2014), although iridescent colour is difficult to artificially produce, so real wings will be required, but this has worked successfully in other studies (Merrill et al. 2014). Choice experiments could test female preference for the brightness of iridescence, using a control male against a male with reduced iridescence – either by using a thermally stressed male or by blocking iridescent reflectance using paint or pen. This will need to be tested using live males as it is the males who initiate courtship with females (Klein and de Araújo 2010), thus this could not be tested with models. This factor can also make separating male and female choice difficult as the males initially choose to court a female. Having graded levels of iridescence would allow us to also test sensitivity to the signal by the receiver. UV wavelengths could be blocked with the use of a UV filter, in the way that Sweeney et al. (2003) used depolarising filters to test the role of polarised light as a mating cue. These experiments would provide further evidence for the trait as a sexually selected and honest signal, rather than solely being used for conspecific recognition or assortative mating.

Now that we have shown that structural colour is condition dependent in *Heliconius*, further work can look at what this colour is signalling. Is stress during pupal stages affecting fecundity and does it decrease adult lifespan? Are individuals which have been stressed during development better or less able to cope with stress later in life? Some studies have looked at this in butterflies, known as the predictive-adaptive response, in terms of nutrient stress in larval stages but with

mixed conclusions (Bauerfeind and Fischer 2005; Saastamoinen et al. 2010). The experiments carried out in this thesis could be expanded by looking at whether the level of stress correlates with brightness of the colour, by placing developing pupae into a range of temperature cycles (Cotton et al. 2004). Comparing heat stress to cold stress could also be interesting as these may produce different responses. Kertész et al. (2017) found that cold stress affected the way the scales were arranged on the wing membrane, rather than the nanostructures themselves. In this study, we focussed only on the dorsal side of the wings, but as the ventral side will be visible when butterflies are resting, the colour on these may also be important for signalling. More pronounced effects of cold stress on pigment colour were found on the ventral side of *Polyommatus* butterflies compared to the dorsal side (Kertész et al. 2017).

Previous research with *Heliconius* has looked at which aspects of scale structure influence the reflectance of iridescent colour (Parnell et al. 2018), and in Chapter 4 we start to look at what elements of the structures are changing to reduce reflectance. Other microscopy techniques can be used to give us more details about the changes occurring. Transmission Electron Microscopy (TEM) combined with Atomic Force Microscopy (AFM) would provide measurements of lamellae height and curvature to provide a complete picture of how thermal stress affects scale structure (Vukusic and Stavenga 2009). Because of the sexual dimorphism in colour that we found, we expect that there will be some differences in scale structure between sexes. This has not been investigated in *Heliconius*, but a study on *Bicyclus* found that female wing scales were larger than males, but that this did not impact the colour produced (Matsuoka and Monteiro 2018).

Currently, less is known about the development of these structures. Work in other species suggests that bundles of actin filaments determine where the longitudinal ridges will form, and that scales destined to become iridescent have more of these actin bundles (Dinwiddie et al. 2014). The use of thermal shock experiments could help to determine at which point during development these structures are being laid down.

5.3 Determining the genetic basis of condition dependent traits

In this study, we did not assess whether there is a genetic component to variation in condition dependent colour. Sexually selected traits are predicted to have high genetic variance and determining the genetic basis of condition dependent traits may help to uncover how this genetic variance is maintained when there is strong female preference, the so-called lek paradox (Rowe and Houle 1996). Models assume that condition of such traits will be associated with many small effect QTL (Pomiankowski and Møller 1995). Structural colour is an example of a trait expressed in both sexes but seemingly sexually selected in one, suggesting sex-specific selection or epistasis (Rowe and Houle 1996; Rowe and Bonduriansky 2005). Sexual dimorphism could have evolved by an increase in the frequency of genes for iridescence in the sex with brighter colour, or the presence of modifier genes which restrict expression of iridescence genes in one sex (Rice 2006). Males have 2 copies of genes on the Z chromosome, while females have only one, and so this could be the simplest mechanism to produce sexual dimorphism, especially given the lack of full dosage compensation in *Heliconius* (Walters et al. 2015).

A gene-environment (GxE) interaction, whereby different genotypes respond to environmental changes in different ways, would also be expected under the 'good genes' model of sexual selection. This model assumes that a phenotypic trait is associated with genetic quality and breeding value. If structural colour is a predictor of genetic quality, then it will also be heritable. Rearing families of butterflies in different stress environments should allow us to see if some families are more able to deal with stress than others. Such studies have not found the predicted GxE interactions, and with *Colias* UV reflectance, genetic variance decreased with stress (Papke et al. 2007; Kemp and Rutowski 2007). This suggests that colour is signalling a direct benefit, such as a higher quality spermatophore.

5.4 What next for colour research?

We have seen how animal colouration has been used to study a broad range of concepts. Butterfly wing colouration has allowed us to investigate genetic parallelism between co-mimics, and also

start to uncover the adaptive function. Studies combining genetic mapping, population genetics and mate choice experiments have previously used butterfly colour to study speciation, showing that assortative mating leads to reproductive isolation (Mavárez et al. 2006; Chamberlain et al. 2009). Colour patterns in *Heliconius* have evolved through mimicry and predation, but we have also shown that iridescence is sexually dimorphic and may be sexually selected, which seems contradictory. As iridescence is present in both sexes, further work could look at sexual dimorphism in the context of intralocus sexual conflict (Bonduriansky and Chenoweth 2009). More broadly, future research can continue to investigate how different selection pressures generate diversity in colour, in both visual and morphological terms.

Structural colours in nature have inspired the development of biomimetic materials to artificially replicate their unique properties, although so far these have been costly and difficult to produce (Parker and Townley 2007; Chung et al. 2012). Blue *Morpho* iridescence has inspired highly reflective and anti-fading paints, cosmetics and textiles (Saito 2011), while structures replicated from moth eyes produce anti-reflective glass for solar panels (Forberich et al. 2008). Even biohybrid gels which combine the properties of structural colours with living cells have been developed for use in medical technology (Fu et al. 2018). Uncovering the genetic basis of structural colours and understanding the development of complex morphology will allow researchers to manipulate and select for these colours, and aid artificial production of materials with the same properties.

References

Abramoff, M., Magalhaes, P.J. and Ram, S.J. (2004). Image Processing with ImageJ. *Biophotonics International*. **11**, 36–42.

Allen, C.E., Zwaan, B.J. and Brakefield, P.M. (2010). Evolution of Sexual Dimorphism in the Lepidoptera. *Annual Review of Entomology*. **56**, 445–464.

Andersson, M. (1986). Evolution of Condition-dependent Sex Ornaments and Mating Preferences: Sexual Selection Based On Viability Differences. *Evolution*. **40**, 804–816.

Andersson, M. (1994). *Sexual Selection*. Princeton, New Jersey: Princeton University Press.

Andersson, M. and Simmons, L.W. (2006). Sexual selection and mate choice. *Trends in Ecology and Evolution*. **21**, 296–302.

Andersson, S., Ornborg, J. and Andersson, M. (1998). Ultraviolet sexual dimorphism and assortative mating in blue tits. *Proceedings of the Royal Society B: Biological Sciences*. **265**, 445–450.

Arenas, L.M., Walter, D. and Stevens, M. (2015). Signal honesty and predation risk among a closely related group of aposematic species. *Scientific Reports*. **5**, 1–12.

Arendt, J. and Reznick, D. (2008). Convergence and parallelism reconsidered: what have we learned about the genetics of adaptation? *Trends in Ecology and Evolution*. **23**, 26–32.

Bagnara, J.T., Fernandez, P.J. and Fujii, R. (2007). On the blue coloration of vertebrates. *Pigment Cell Research*. **20**, 14–26.

Bálint, Z., Kertész, K., Piszter, G., Vértesy, Z. and Biró, L.P. (2012). The well-tuned blues: the role of structural colours as optical signals in the species recognition of a local butterfly fauna (Lepidoptera: Lycaenidae: Polyommatinae). *Journal of the Royal Society, Interface*. **9**, 1745–56.

Barton, N.H. and Keightley, P.D. (2002). Understanding Quantitative Genetic Variation. *Nature Reviews Genetics*. **3**, 11–21.

Bates, H.W. (1862). Contributions to an insect fauna of the Amazon valley. Lepidoptera: Heliconidae. *Transactions of the Linnean Society of London*. **23**, 495–566.

Bauerfeind, S.S. and Fischer, K. (2005). Effects of food stress and density in different life stages on reproduction in a butterfly. *Oikos*. **111**, 514–524.

Baxter, S., Johnston, S. and Jiggins, C. (2009). Butterfly speciation and the distribution of gene effect sizes fixed during adaptation. *Heredity*. **102**, 57–65.

Baxter, S.W., Davey, J.W., Johnston, J.S., Shelton, A.M., Heckel, D.G., Jiggins, C.D. and Blaxter, M.L. (2011). Linkage mapping and comparative genomics using next-generation rad sequencing of a non-model organism. *PLoS ONE*. **6**, e19315.

Baxter, S.W., Papa, R., Chamberlain, N., Humphray, S.J., Joron, M., Morrison, C., Ffrench-Constant, R.H., McMillan, W.O. and Jiggins, C.D. (2008). Convergent Evolution in the Genetic Basis of Müllerian Mimicry in *Heliconius* Butterflies. *Genetics*. **180**, 1567–1577.

Van Belleghem, S.M., Rastas, P., Papanicolaou, A., Martin, S.H., Arias, C.F., Supple, M.A., Hanly, J.J., Mallet, J., Lewis, J.J., Hines, H.M., Ruiz, M., Salazar, C., Linares, M., Moreira, G.R.P., Jiggins, C.D., Counterman, B.A., McMillan, W.O. and Papa, R. (2017). Complex modular architecture around a simple toolkit of wing pattern genes. *Nature*

Ecology and Evolution. **1**, 1–12.

Beltrán, M., Jiggins, C.D., Brower, A.V.Z., Bermingham, E. and Mallet, J. (2007). Do pollen feeding, pupal-mating and larval gregariousness have a single origin in *Heliconius* butterflies? Inferences from multilocus DNA sequence data. *Biological Journal of the Linnean Society*. **92**, 221–239.

Bennett, A.T.D., Cuthill, I.C., Partridge, J.C. and Lunau, K. (1997). Ultraviolet plumage colors predict mate preferences in starlings. *Proceedings of the National Academy of Sciences*. **94**, 8618–8621.

Le Boeuf, B.J. (1974). Male-male Competition and Reproductive Success in Elephant Seals. *Integrative and Comparative Biology*. **14**, 163–176.

Boggs, C.L. and Freeman, K.D. (2005). Larval food limitation in butterflies: effects on adult resource allocation and fitness. *Oecologia*. **144**, 353–361.

Bonduriansky, R. (2001). The evolution of male mate choice in insects: a synthesis of ideas and evidence. *Biological reviews of the Cambridge Philosophical Society*. **76**, 305–39.

Bonduriansky, R. and Chenoweth, S.F. (2009). Intralocus sexual conflict. *Trends in Ecology & Evolution*. **24**, 280–288.

Brien, M.N., Enciso-Romero, J., Parnell, A.J., Morochz, C., Chalá, D., Salazar, P.A., Bainbridge, H.E., Zinn, T., Curran, E.V. and Nadeau, N.J. (2018). Phenotypic variation in *Heliconius erato* crosses shows that iridescent structural colour is sex-linked and controlled by multiple genes. *Interface Focus*. **9**, 20180047.

Briolat, E.S., Zagrobelny, M., Olsen, C.E., Blount, J.D. and Stevens, M. (2019). No evidence of quantitative signal honesty across species of aposematic burnet moths (Lepidoptera: Zygaenidae). *Journal of Evolutionary Biology*. **32**, 31–48.

Briscoe, A.D., Bybee, S.M., Bernard, G.D., Yuan, F., Sison-Mangus, M.P., Reed, R.D., Warren, A.D., Llorente-Bousquets, J. and Chiao, C.-C. (2010). Positive selection of a duplicated UV-sensitive visual pigment coincides with wing pigment evolution in *Heliconius* butterflies. *Proceedings of the National Academy of Sciences*. **107**, 3628–3633.

Broman, K., Gatti, D., Simecek, P., Furlotte, N., Prins, P., Sen, S., Yandell, B. and Churchill, G. (2019). R/qtl2: Software for Mapping Quantitative Trait Loci with High-Dimenional Data and Multiparent Populations. *Genetics*. **211**, 495–502.

Broman, K.W., Sen, Ś., Owens, S.E., Manichaikul, A., Southard-Smith, E.M. and Churchill, G.A. (2006). The X chromosome in quantitative trait locus mapping. *Genetics*. **174**, 2151–2158.

Broman, K.W., Wu, H., Sen, Ś. and Churchill, G.A. (2003). R/qtl: QTL mapping in experimental crosses. *Bioinformatics*. **19**, 889–890.

Brunton, C.F.A. and Majerus, M.E.N. (1995). Ultraviolet colours in butterflies: intra- or inter-specific communication? *Proceedings of the Royal Society B: Biological Sciences*. **260**, 199–204.

Burke, M.K., Liti, G. and Long, A.D. (2014). Standing Genetic Variation Drives Repeatable Experimental Evolution in Outcrossing Populations of *Saccharomyces cerevisiae*. *Molecular Biology and Evolution*. **31**, 3228–3239.

Bybee, S.M., Yuan, F., Ramstetter, M.D., Llorente-Bousquets, J., Reed, R.D., Osorio, D. and Briscoe, A.D. (2012). UV Photoreceptors and UV-Yellow Wing Pigments in *Heliconius* Butterflies Allow a Color Signal to Serve both Mimicry and Intraspecific Communication.

The American Naturalist. **179**, 38–51.

Cardoso, M.Z. and Gilbert, L.E. (2007). A male gift to its partner? Cyanogenic glycosides in the spermatophore of longwing butterflies (*Heliconius*). *Naturwissenschaften*. **94**, 39–42.

Cauchard, L., Doucet, S.M., Boogert, N.J., Angers, B. and Doligez, B. (2017). The relationship between plumage colouration, problem-solving and learning performance in great tits *Parus major*. *Journal of Avian Biology*. **48**, 1246–1253.

Chai, P. and Srygley, R.B. (1990). Predation and the Flight, Morphology, and Temperature of Neotropical Rain-Forest Butterflies. *The American Naturalist*. **135**, 748–765.

Chamberlain, N.L., Hill, R.I., Kapan, D.D., Gilbert, L.E. and Kronforst, M.R. (2009). Missing Link in Ecological Speciation. *Science*. **326**, 847–851.

Chapman, R.F. (1998). Visual Signals: Colour and Light Production *In*: *The Insects: Structure and Function*. Cambridge University Press, 655–679.

Chu, T., Henrion, G., Haegeli, V. and Strickland, S. (2001). *Cortex*, a Drosophila gene required to complete oocyte meiosis, is a member of the Cdc20/fizzy protein family. *Genesis*. **29**, 141–152.

Chung, K., Yu, S., Heo, C.-J., Shim, J.W., Yang, S.-M., Han, M.G., Lee, H.-S., Jin, Y., Lee, S.Y., Park, N. and Shin, J.H. (2012). Flexible, Angle-Independent, Structural Color Reflectors Inspired by *Morpho* Butterfly Wings. *Advanced Materials*. **24**, 2375–2379.

Cockerham, C.C. (1986). Modifications in estimating the number of genes for a quantitative character. *Genetics*. **114**, 659–664.

Colosimo, P.F., Hosemann, K.E., Balabhadra, S., Villarreal, G., Dickson, M., Grimwood, J., Schmutz, J., Myers, R.M., Schluter, D. and Kingsley, D.M. (2005). Widespread Parallel Evolution in Sticklebacks by Repeated Fixation of Ectodysplasin Alleles. *Science*. **307**, 1928–1933.

Comeault, A.A., Carvalho, C.F., Dennis, S., Soria-Carrasco, V. and Nosil, P. (2016). Color phenotypes are under similar genetic control in two distantly related species of *Timema* stick insect. *Evolution*. **70**, 1283–1296.

Conte, G.L., Arnegard, M.E., Best, J., Chan, Y.F., Jones, F.C., Kingsley, D.M., Schluter, D. and Peichel, C.L. (2015). Extent of QTL reuse during repeated phenotypic divergence of sympatric threespine stickleback. *Genetics*. **201**, 1189–1200.

Conte, G.L., Arnegard, M.E., Peichel, C.L. and Schluter, D. (2012). The probability of genetic parallelism and convergence in natural populations. *Proceedings of the Royal Society B: Biological Sciences*. **279**, 5039–5047.

Corso, J., Mundy, N.I., Fagundes, N.J.R. and de Freitas, T.R.O. (2016). Evolution of dark colour in toucans (Ramphastidae): a case of molecular adaptation? *Journal of Evolutionary Biology*. **29**, 2530–2538.

Cotton, S., Fowler, K. and Pomiankowski, A. (2004). Do sexual ornaments demonstrate heightened condition-dependent expression as predicted by the handicap hypothesis? *Proceedings of the Royal Society B: Biological Sciences*. **271**, 771–783.

Cotton, S., Fowler, K. and Pomiankowski, A. (2004). Heightened condition dependence is not a general feature of male eyespan in stalk-eyed flies (Diptera: Diopsidae). *Journal of Evolutionary Biology*. **17**, 1310–1316.

Cummings, M.E., Rosenthal, G.G. and Ryan, M.J. (2003). A private ultraviolet channel in visual communication. *Proceedings of the Royal Society B: Biological Sciences*. **270**,

897–904.

Curran, E.V. (2018). *An exploration of the parallel evolution of iridescent structural colour in* Heliconius *butterflies*.[Online] University of Sheffield. Available from: http://etheses.whiterose.ac.uk/id/eprint/22445.

Cuthill, J.H., Charleston, M., Cuthill, J. and Charleston, M. (2012). Phylogenetic codivergence supports coevolution of mimetic *Heliconius* butterflies. *PLoS ONE*. **7**, e36464.

Darragh, K., Byers, K.J.R.P., Merrill, R.M., McMillan, W.O., Schulz, S. and Jiggins, C.D. (2019). Male pheromone composition depends on larval but not adult diet in *Heliconius melpomene*. *Ecological Entomology*. **44**, 397–405.

Darwin, C. (1874). *The Descent of Man, and Selection in Relation to Sex*. London: Murray.

Davey, J.W., Chouteau, M., Barker, S.L., Maroja, L., Baxter, S.W., Simpson, F., Merrill, R.M., Joron, M., Mallet, J., Dasmahapatra, K.K. and Jiggins, C.D. (2016). Major Improvements to the *Heliconius melpomene* Genome Assembly Used to Confirm 10 Chromosome Fusion Events in 6 Million Years of Butterfly Evolution. *G3: Genes, Genomes, Genetics*. **6**, 9–12.

Davey, J.W., Barker, S.L., Rastas, P.M., Pinharanda, A., Martin, S.H., Durbin, R., McMillan, W.O., Merrill, R.M. and Jiggins, C.D. (2017). No evidence for maintenance of a sympatric *Heliconius* species barrier by chromosomal inversions. *Evolution Letters*. **1**, 138–154.

Dell'Aglio, D.D., Akkaynak, D., McMillan, W.O. and Jiggins, C.D. (2017). Estimating the age of *Heliconius* butterflies from calibrated photographs. *PeerJ*. **5**, e3821.

Dinwiddie, A., Null, R., Pizzano, M., Chuong, L., Leigh Krup, A., Ee Tan, H. and Patel, N.H. (2014). Dynamics of F-actin prefigure the structure of butterfly wing scales. *Developmental Biology*. **392**, 404–418.

Doucet, S.M. (2006). Iridescent plumage in satin bowerbirds: structure, mechanisms and nanostructural predictors of individual variation in colour. *Journal of Experimental Biology*. **209**, 380–390.

Doucet, S.M. and Montgomerie, R. (2003). Structural plumage colour and parasites in satin bowerbirds *Ptilonorhynchus violaceus*: implications for sexual selection. *Journal of Avian Biology*. **34**, 237–242.

Douglas, J.M., Cronin, T.W., Chiou, T.-H. and Dominy, N.J. (2007). Light habitats and the role of polarized iridescence in the sensory ecology of neotropical nymphalid butterflies (Lepidoptera: Nymphalidae). *Journal of Experimental Biology*. **210**, 788–799.

Doutrelant, C., Grégoire, A., Grnac, N., Gomez, D., Lambrechts, M.M. and Perret, P. (2008). Female coloration indicates female reproductive capacity in blue tits. *Journal of Evolutionary Biology*. **21**, 226–233.

Ellers, J. and Boggs, C.L. (2003). The evolution of wing color: Male mate choice opposes adaptive wing color divergence in *Colias* butterflies. *Evolution*. **57**, 1100–1106.

Ellers, J. and Boggs, C.L. (2002). The Evolution of Wing Color in *Colias* Butterflies: Heritability, Sex Linkage, and Population Divergence. *Evolution*. **56**, 836–840.

Emsley, M. (1965). The geographical distribution of the color-pattern components of *Heliconius erato* and *Heliconius melpomene* with genetical evidence for the systematic relationship between the two species. *Zoologica*. **49**, 245–286.

Enciso-Romero, J., Pardo-Díaz, C., Martin, S.H., Arias, C.F., Linares, M., McMillan, W.O., Jiggins, C.D. and Salazar, C. (2017). Evolution of novel mimicry rings facilitated by adaptive introgression in tropical butterflies. *Molecular Ecology*. **26**, 5160–5172.

Endler, J.A. (1984). Natural and sexual selection on color patterns in poeciliid fishes *In*: *Evolutionary ecology of neotropical freshwater fishes*. Dordrecht: Springer Netherlands, 95–111.

Endler, J.A. (1980). Natural Selection on Color Patterns in *Poecilia reticulata*. *Evolution*. **34**, 76–91.

Endler, J.A. and Houde, A.E. (1995). Geographic Variation in Female Preferences for Male Traits in *Poecilia reticulata*. *Evolution*. **49**, 456–468.

Estrada, C. and Jiggins, C.D. (2008). Interspecific sexual attraction because of convergence in warning colouration: Is there a conflict between natural and sexual selection in mimetic species? *Journal of Evolutionary Biology*. **21**, 749–760.

Fairbairn, D.J. and Roff, D.A. (2006). The quantitative genetics of sexual dimorphism: assessing the importance of sex-linkage. *Heredity*. **97**, 319–328.

Feder, J.L., Gejji, R., Yeaman, S. and Nosil, P. (2012). Establishment of new mutations under divergence and genome hitchhiking. *Philosophical transactions of the Royal Society of London. Series B, Biological sciences*. **367**, 461–474.

Fenner, J., Rodriguez-Caro, L. and Counterman, B. (2019). Plasticity and divergence in ultraviolet reflecting structures on Dogface butterfly wings. *Arthropod Structure and Development*. **51**, 14–22.

Fernald, R.D. (2006). Casting a genetic light on the evolution of eyes. *Science*. **313**, 1914–1918.

Finkbeiner, S.D., Briscoe, A.D. and Reed, R.D. (2014). Warning signals are seductive: Relative contributions of color and pattern to predator avoidance and mate attraction in *Heliconius* butterflies. *Evolution*. **68**, 3410–3420.

Finkbeiner, S.D., Fishman, D.A., Osorio, D. and Briscoe, A.D. (2017). Ultraviolet and yellow reflectance but not fluorescence is important for visual discrimination of conspecifics by *Heliconius erato*. *The Journal of Experimental Biology*. **220**, 1267–1276.

Fisher, R.A. (1930). *The Genetical Theory of Natural Selection*. Oxford University Press.

Fitzstephens, D.M. and Getty, T. (2000). Colour, fat and social status in male damselflies, *Calopteryx maculata*. *Animal Behaviour*. **60**, 851–855.

Forberich, K., Dennler, G., Scharber, M.C., Hingerl, K., Fromherz, T. and Brabec, C.J. (2008). Performance improvement of organic solar cells with moth eye anti-reflection coating. *Thin Solid Films*. **516**, 7167–7170.

Fu, F., Shang, L., Chen, Z., Yu, Y. and Zhao, Y. (2018). Bioinspired living structural color hydrogels. *Science Robotics*. **3**, 1-8.

Fürstenberg-Hägg, J., Zagrobelny, M., Jørgensen, K., Vogel, H., Møller, B.L. and Bak, S. (2014). Chemical defense balanced by sequestration and de novo biosynthesis in a lepidopteran specialist. *PLoS ONE*. **9**, e108745.

García-Barros, E. (2000). Body size, egg size, and their interspecific relationships with ecological and life history traits in butterflies (Lepidoptera: Papilionoidea, Hesperioidea). *Biological Journal of the Linnean Society*. **70**, 251–284.

Gehring, W.J. and Ikeo, K. (1999). *Pax 6*: Mastering eye morphogenesis and eye evolution. *Trends in Genetics*. **15**, 371–377.

Ghiradella, H. (1989). Structure and Development of Iridescent Butterfly Scales: Lattices and Laminae. *Journal of Morphology*. **202**, 69–88.

Ghiradella, H. and Radigan, W. (1976). Development of Butterfly Scales. *Journal of Morphology*. **150**, 279–297.

Griffiths, A., Wessler, S., Carroll, S. and Doebley, J. (2015). The Inheritance of Complex Traits *In*: *Introduction to Genetic Analyses*. W. H. Freeman, 715–779.

Haldane, J.B.S. (1927). The Comparative Genetics of Colour in Rodents and Carnivora. *Biological Reviews*. **2**, 199–212.

Hart, N.S. (2001). The Visual Ecology of Avian Photoreceptors. *Progress in Retinal and Eye Research*. **20**, 675–703.

Hegyi, G., Laczi, M., Kötél, D., Csizmadia, T., Lőw, P., Rosivall, B., Szöllősi, E. and Török, J. (2018). Reflectance variation in the blue tit crown in relation to feather structure. *The Journal of Experimental Biology*. **221**, 1–9.

Hernandez, M.I.M. and Benson, W.W. (1998). Small-male advantage in the territorial tropical butterfly *Heliconius sara* (Nymphalidae): a paraoxical strategy? *Animal Behaviour*. **56**, 533–540.

Heyduk, K., Moreno-Villena, J.J., Gilman, I.S., Christin, P.-A. and Edwards, E.J. (2019). The genetics of convergent evolution: insights from plant photosynthesis. *Nature Reviews Genetics*. **20**, 485–493.

Hill, G.E., Doucet, S.M. and Buchholz, R. (2005). The effect of coccidial infection on iridescent plumage coloration in wild turkeys. *Animal Behaviour*. **69**, 387–394.

Hill, G.E., Hood, W.R., Ge, Z., Grinter, R., Greening, C., Johnson, J.D., Park, N.R., Taylor, H.A., Andreasen, V.A., Powers, M.J., Justyn, N.M., Parry, H.A., Kavazis, A.N. and Zhang, Y. (2019). Plumage redness signals mitochondrial function in the House Finch. *bioRxiv*, 728873.

Hines, H.M., Counterman, B.A, Papa, R., Albuquerque, P., Moura, D. and Cardoso, M.Z. (2011). Wing patterning gene redefines the mimetic history of *Heliconius* butterflies. *Proceedings of the National Academy of Sciences*. **108**, 19666–19671.

Hoekstra, H.E. (2006). Genetics, development and evolution of adaptive pigmentation in vertebrates. *Heredity*. **97**, 222–234.

Hofreiter, M. and Schöneberg, T. (2010). The genetic and evolutionary basis of colour variation in vertebrates. *Cellular and Molecular Life Sciences*. **67**, 2591–2603.

Honěk, A. (1993). Intraspecific Variation in Body Size and Fecundity in Insects: A General Relationship. *Oikos*. **66**, 483–492.

Horne, C.R., Hirst, A.G. and Atkinson, D. (2018). Insect temperature–body size trends common to laboratory, latitudinal and seasonal gradients are not found across altitudes. *Functional Ecology*. **32**, 948–957.

Hubbard, J.K., Uy, J.A.C., Hauber, M.E., Hoekstra, H.E. and Safran, R.J. (2010). Vertebrate pigmentation: from underlying genes to adaptive function. *Trends in Genetics*. **26**, 231–239.

Huber, B., Whibley, A., Poul, Y.L., Navarro, N., Martin, A., Baxter, S., Shah, A., Gilles, B., Wirth, T., McMillan, W.O. and Joron, M. (2015). Conservatism and novelty in the genetic architecture of adaptation in *Heliconius* butterflies. *Heredity*. **114**, 515–524.

Jiggins, C.D. (2017). *The Ecology & Evolution of* Heliconius *Butterflies*. Oxford, UK: Oxford University Press.

Jiggins, C.D., Naisbit, R.E., Coe, R.L. and Mallet, J. (2001). Reproductive isolation caused by colour pattern mimicry. *Nature*. **411**, 302–305.

Jones, R.T., Salazar, P.A., Ffrench-Constant, R.H., Jiggins, C.D. and Joron, M. (2012). Evolution of a mimicry supergene from a multilocus architecture. *Proceedings of the Royal Society B: Biological Sciences*. **279**, 316–325.

Joron, M., Papa, R., Beltrán, M., Chamberlain, N., Mavárez, J., Baxter, S., Abanto, M., Bermingham, E., Humphray, S.J., Rogers, J., Beasley, H., Barlow, K., H. ffrench-Constant, R., Mallet, J., McMillan, W.O. and Jiggins, C.D. (2006). A Conserved Supergene Locus Controls Colour Pattern Diversity in *Heliconius* Butterflies. *PLoS Biology*. **4**, 1831–1840.

Kapan, D.D. (2001). Three-butterfly system provides a field test of mullerian mimicry. *Nature*. **409**, 18–20.

Kemp, D.J. (2007). Female butterflies prefer males bearing bright iridescent ornamentation. *Proceedings of the Royal Society B: Biological Sciences*. **274**, 1043–1047.

Kemp, D.J. (2006). Heightened phenotypic variation and age-based fading of ultraviolet butterfly wing coloration. *Evolutionary Ecology Research*. **8**, 515–527.

Kemp, D.J. and Rutowski, R.L. (2007). Condition Dependence, Quantitative Genetics, and the Potential Signal Content of Iridescent Ultraviolet Butterfly Coloration. *Evolution*. **61**, 168–183.

Kemp, D.J. and Rutowski, R.L. (2011). The Role of Coloration in Mate Choice and Sexual Interactions in Butterflies. *Advances in the Study of Behavior*. **43**, 55–92.

Kemp, D.J., Vukusic, P. and Rutowski, R.L. (2006). Stress-mediated covariance between nano-structural architecture and ultraviolet butterfly coloration. *Functional Ecology*. **20**, 282–289.

Kertész, K., Piszter, G., Horváth, Z.E., Bálint, Z. and Biró, L.P. (2017). Changes in structural and pigmentary colours in response to cold stress in *Polyommatus icarus* butterflies. *Scientific Reports*. **7**, 1–12.

Kettlewell, H.B. (1955). Selection experiments on industrial melanism in the Lepidoptera. *Heredity*. **97**, 222–234.

Keyser, A.J. and Hill, G.E. (1999). Condition-dependent variation in the blue-ultraviolet coloration of a structurally based plumage ornament. *Proceedings of the Royal Society B: Biological Sciences*. **266**, 771–777.

Keyser, A.J. and Hill, G.E. (2000). Structurally based plumage coloration is an honest signal of quality in male blue grosbeaks. *Behavioural Ecology*. **11**, 202–209.

Klein, A.L. and de Araújo, A.M. (2010). Courtship behavior of *Heliconius erato phyllis* (Lepidoptera, Nymphalidae) towards virgin and mated females: Conflict between attraction and repulsion signals? *Journal of Ethology*. **28**, 409–420.

Klein, A.L. and de Araújo, A.M. (2013). Sexual Size Dimorphism in the Color Pattern Elements of Two Mimetic *Heliconius* Butterflies. *Neotropical Entomology*. **42**, 600–606.

Kottler, M.J. (1980). Darwin, Wallace, and the Origin of Sexual Dimorphism. *Proceedings of the American Philosophical Society*. **124**, 203–226.

Kozak, K.M., Wahlberg, N., Neild, A.F.E., Dasmahapatra, K.K., Mallet, J. and Jiggins, C.D. (2015). Multilocus species trees show the recent adaptive radiation of the mimetic *Heliconius* butterflies. *Systematic Biology*. **64**, 505–524.

Kunte, K. (2009). The diversity and evolution of Batesian mimicry in *Papilio* swallowtail butterflies. *Evolution*. **63**, 2707–2716.

Lande, R. (1981). The minimum number of genes contributing to quantitative variation between and within populations. *Genetics*. **99**, 541–553.

Langmead, B. and Salzberg, S.L. (2012). Fast gapped-read alignment with Bowtie 2. *Nature Methods*. **9**, 357.

Li, H. (2011). A statistical framework for SNP calling, mutation discovery. *Bioinformatics*. **27**, 2987–93.

Lim, M.L.M. and Li, D. (2006). Extreme ultraviolet sexual dimorphism in jumping spiders (Araneae: Salticidae). *Biological Journal of the Linnean Society*. **89**, 397–406.

Little, C.C. (1919). Colour inheritance in cats, with special reference to the colours black, yellow and tortoise-shell. *Journal of Genetics*. **8**, 279–290.

Liu, Y., Cotton, J.A., Shen, B., Han, X., Rossiter, S.J. and Zhang, S. (2010). Convergent sequence evolution between echolocating bats and dolphins. *Current Biology*. **20**, 53–54.

Llaurens, V., Joron, M. and Théry, M. (2014). Cryptic differences in colour among Müllerian mimics: How can the visual capacities of predators and prey shape the evolution of wing colours? *Journal of Evolutionary Biology*. **27**, 531–540.

Lynch, M. and Walsh, B. (1998). Analysis of Line Crosses *In*: *Genetics and Analysis of Quantitative Traits*. Sinauer Associates, Massachusetts, 205–250.

Maia, R., Eliason, C.M., Bitton, P.P., Doucet, S.M. and Shawkey, M.D. (2013). pavo: An R package for the analysis, visualization and organization of spectral data. *Methods in Ecology and Evolution*. **4**, 906–913.

Mallet, J. (1986). Hybrid zones of *Heliconius* butterflies in Panama and the stability and movement of warning colour clines. *Heredity*. **56**, 191–202.

Mallet, J. (1989). The Genetics of Warning Colour in Peruvian Hybrid Zones of *Heliconius erato* and *H. melpomene*. *Proceedings of the Royal Society B: Biological Sciences*. **236**, 163–185.

Mallet, J., Barton, N., Gerardo Lamas, M., Jose Santisteban, C., Manuel Muedas, M. and Eeley, H. (1990). Estimates of selection and gene flow from measures of cline width and linkage disequilibrium in *Heliconius* hybrid zones. *Genetics*. **124**, 921–936.

Mallet, J. and Barton, N.H. (1989). Strong Natural Selection in a Warning-Color Hybrid Zone. *Evoution*. **43**(2), 421–431.

Mallet, J., McMillan, W.O. and Jiggins, C.D. (1998). Estimating the Mating Behavior of a Pair of Hybridizing *Heliconius* Species in the Wild. *Evolution*. **52**, 503.

Manceau, M., Domingues, V.S., Linnen, C.R., Rosenblum, E.B. and Hoekstra, H.E. (2010). Convergence in pigmentation at multiple levels: Mutations, genes and function. *Philosophical Transactions of the Royal Society B: Biological Sciences*. **365**, 2439–2450.

Martin, A., McCulloch, K.J., Patel, N.H., Briscoe, A.D., Gilbert, L.E. and Reed, R.D. (2014). Multiple recent co-options of *Optix* associated with novel traits in adaptive butterfly wing radiations. *EvoDevo*. **5**,7.

Martin, A., Papa, R., Nadeau, N.J., Hill, R.I., Counterman, B.A., Halder, G., Jiggins, C.D., Kronforst, M.R., Long, A.D., McMillan, W.O. and Reed, R.D. (2012). Diversification of complex butterfly wing patterns by repeated regulatory evolution of a *Wnt* ligand.

Proceedings of the National Academy of Sciences. **109**, 12632–12637.

Mason, C.W. (1927). Structural Colours in Insects III. *Journal of Physical Chemistry*. **31**, 1856–1872.

Mather, K. and Jinks, J.L. (1982). *Biometrical Genetics* 3rd ed. Cambridge University Press.

Matsuoka, Y. and Monteiro, A. (2018). Melanin Pathway Genes Regulate Color and Morphology of Butterfly Wing Scales. *Cell Reports*. **24**, 56–65.

Mavárez, J., Salazar, C.A., Bermingham, E., Salcedo, C., Jiggins, C.D. and Linares, M. (2006). Speciation by hybridization in *Heliconius* butterflies. *Nature*. **441**, 868–871.

Mazo-Vargas, A., Concha, C., Livraghi, L., Massardo, D., Wallbank, R.W.R., Zhang, L., Papador, J.D., Martinez-Najera, D., Jiggins, C.D., Kronforst, M.R., Breuker, C.J., Reed, R.D., Patel, N.H., McMillan, W.O. and Martin, A. (2017). Macroevolutionary shifts of *WntA* function potentiate butterfly wing-pattern diversity. *Proceedings of the National Academy of Sciences*. **114**, 10701–10706.

McCulloch, K.J., Osorio, D. and Briscoe, A.D. (2016). Sexual dimorphism in the compound eye of *Heliconius erato*: a nymphalid butterfly with at least five spectral classes of photoreceptor. *The Journal of Experimental Biology*. **219**, 2377–2387.

McCulloch, K.J., Yuan, F., Zhen, Y., Aardema, M.L., Smith, G., Llorente-Bousquets, J., Andolfatto, P. and Briscoe, A.D. (2017). Sexual Dimorphism and Retinal Mosaic Diversification following the Evolution of a Violet Receptor in Butterflies. *Molecular biology and evolution*. **34**, 2271–2284.

McGraw, K.J., Mackillop, E.A., Dale, J. and Hauber, M.E. (2002). Different colors reveal different information: how nutritional stress affects the expression of melanin- and structurally based ornamental plumage. *Journal of Experimental Biology*. **205**, 3747–3755.

McMillan, W.O., Jiggins, C.D. and Mallet, J. (1997). What initiates speciation in passion-vine butterflies? *Proceedings of the National Academy of Sciences*. **94**, 8628–8633.

McRobie, H., Thomas, A. and Kelly, J. (2009). The genetic basis of melanism in the gray squirrel (*Sciurus carolinensis*). *Journal of Heredity*. **100**, 709–714.

Mendel, G. (1865). Experiments in Plant Hybridization. *Verhandlungen des naturforschenden Vereines in Brünn*, 3–47.

Merrill, R.M., Chia, A. and Nadeau, N.J. (2014). Divergent warning patterns contribute to assortative mating between incipient *Heliconius* species. *Ecology and Evolution*. **4**, 911–917.

Merrill, R.M., Dasmahapatra, K.K., Davey, J.W., Dell'Aglio, D.D., Hanly, J.J., Huber, B., Jiggins, C.D., Joron, M., Kozak, K.M., Llaurens, V., Martin, S.H., Montgomery, S.H., Morris, J., Nadeau, N.J., Pinharanda, a. L., Rosser, N., Thompson, M.J., Vanjari, S., Wallbank, R.W.R. and Yu, Q. (2015). The diversification of *Heliconius* butterflies: what have we learned in 150 years? *Journal of Evolutionary Biology*. **28**, 1417–1438.

Merrill, R.M., Rastas, P., Martin, S.H., Melo, M.C., Barker, S., Davey, J., McMillan, W.O. and Jiggins, C.D. (2019). Genetic dissection of assortative mating behavior. *PLoS Biology*. **17**, 1–21.

Merrill, R.M., Wallbank, R.W.R., Bull, V., Salazar, P.C.A., Mallet, J., Stevens, M. and Jiggins, C.D. (2012). Disruptive ecological selection on a mating cue. *Proceedings of the Royal Society B: Biological Sciences*. **279**, 4907–4913.

Montejo-Kovacevich, G., Smith, J.E., Meier, J.I., Bacquet, C.N., Whiltshire-Romero, E., Nadeau, N.J. and Jiggins, C.D. (2019). Altitude and life-history shape the evolution of *Heliconius* wings. *Evolution*. **73**, 2436-2450.

Montgomerie, R. (2006). Analyzing colors *In*: *In Hill, G.E and McGraw, K.J. Bird Coloration Volume 1 Mechanisms and measurements*. Cambridge, Massachusetts: Havard University Press.

Morris, J., Navarro, N., Rastas, P., Rawlins, L.D., Sammy, J., Mallet, J. and Dasmahapatra, K.K. (2019). The genetic architecture of adaptation: convergence and pleiotropy in *Heliconius* wing pattern evolution. *Heredity*. **123**, 138–152.

Mundy, N.I., Badcock, N.S., Hart, T., Scribner, K., Janssen, K. and Nadeau, N.J. (2004). Conserved Genetic Basis of a Quantitative Plumage Trait. *Science*. **303**, 1870–1873.

Nachman, M.W., Hoekstra, H.E. and D'Agostino, S.L. (2003). The genetic basis of adaptive melanism in pocket mice. *Proceedings of the National Academy of Sciences*. **100**, 5268–5273.

Nadeau, N.J. (2016). Genes controlling mimetic colour pattern variation in butterflies. *Current Opinion in Insect Science*. **17**, 24–31.

Nadeau, N.J. and Jiggins, C.D. (2010). A golden age for evolutionary genetics? Genomic studies of adaptation in natural populations. *Trends in Genetics*. **26**, 484–492.

Nadeau, N.J., Pardo-Diaz, C., Whibley, A., Supple, M.A., Saenko, S. V., Wallbank, R.W.R., Wu, G.C., Maroja, L., Ferguson, L., Hanly, J.J., Hines, H., Salazar, C., Merrill, R.M., Dowling, A.J., Ffrench-Constant, R.H., Llaurens, V., Joron, M., McMillan, W.O. and Jiggins, C.D. (2016). The gene *cortex* controls mimicry and crypsis in butterflies and moths. *Nature*. **534**, 106–110.

Nadeau, N.J., Ruiz, M., Salazar, P., Counterman, B., Medina, J.A., Ortiz-Zuazaga, H., Morrison, A., McMillan, W.O., Jiggins, C.D. and Papa, R. (2014). Population genomics of parallel hybrid zones in the mimetic butterflies, *H. melpomene* and *H. erato*. *Genome Research*. **24**, 1316–1333.

Nicholson, A. (1927). *A new theory of mimicry in insects*. Sydney: Royal Zooloigcal Society of New South Wales.

Nijhout, H.F. (1991). *The Development and Evolution of Butterfly Wing Patterns*. Smithsonian Institution Press.

Osorio, D. and Ham, A.D. (2002). Spectral reflectance and directional properties of structural coloration in bird plumage. *The Journal of experimental biology*. **205**, 2017–27.

Otaki, J.M. (2008). Physiologically induced color-pattern changes in butterfly wings: Mechanistic and evolutionary implications. *Journal of Insect Physiology*. **54**, 1099–1112.

Otto, S.P. and Jones, C.D. (2000). Detecting the undetected: estimating the total number of loci inderlying a quantitative trait. *Genetics*. **156**, 2093–2107.

Ouellette, L., Reid, R., Blanchard, S. and Brouwer, C. (2018). LinkageMapView - rendering high-resolution linkage and QTL maps. *Bioinformatics*. **34**, 306–307.

Owens, I.P.F. and Hartley, I.R. (1998). Sexual dimorphism in birds: why are there so many different forms of dimorphism? *Proceedings of the Royal Society B: Biological Sciences*. **265**, 397–407.

Papa, R., Kapan, D.D., Counterman, B.A., Maldonado, K., Lindstrom, D.P., Reed, R.D., Nijhout, H.F., Hrbek, T. and McMillan, W.O. (2013). Multi-Allelic Major Effect Genes

Interact with Minor Effect QTLs to Control Adaptive Color Pattern Variation in *Heliconius erato*. *PLoS ONE*. **8**, e57033.

Papke, R.S., Kemp, D.J. and Rutowski, R.L. (2007). Multimodal signalling: structural ultraviolet reflectance predicts male mating success better than pheromones in the butterfly *Colias eurytheme L.* (Pieridae). *Animal Behaviour*. **73**, 47–54.

Parker, A.R., McKenzie, D.R. and Large, M.C.J. (1998). Multilayer reflectors in animals using green and gold beetles as contrasting examples. *Journal of Experimental Biology*. **201**, 1307–1313.

Parker, A.R. and Townley, H.E. (2007). Biomimetics of photonic nanostructures. *Nature Nanotechnology*. **2**, 347–353.

Parnell, A.J., Bradford, J.E., Curran, E.V., Washington, A.L., Adams, G., Brien, M.N., Burg, S.L., Morochz, C., Fairclough, J.P.A., Vukusic, P., Martin, S.J., Doak, S. and Nadeau, N.J. (2018). Wing scale ultrastructure underlying convergent and divergent iridescent colours in mimetic *Heliconius* butterflies. *Journal of The Royal Society Interface*. **15**, 20170948.

Pinheiro, C.E.G. (2004). Jacamars (Aves, Galbulidae) as selective agents of mimicry in neotropical butterflies. *Ararajuba*. **12**, 69–71.

Pinheiro, C.E.G. (1996). Palatablility and escaping ability in Neotropical butterflies: tests with wild kingbirds (*Tyrannus melancholicus*, Tyrannidae). *Biological Journal of the Linnean Society*. **59**, 351–365.

Pomiankowski, A. and Møller, A.P. (1995). A resolution of the lek paradox. *Proceedings of the Royal Society B: Biological Sciences*. **260**, 21–29.

Pośpiech, E., Draus-Barini, J., Kupiec, T., Wojas-Pelc, A. and Branicki, W. (2011). Gene–gene interactions contribute to eye colour variation in humans. *Journal Of Human Genetics*. **56**, 447.

Prum, R.O. (2006). Anatomically diverse butterfly scales all produce structural colours by coherent scattering. *Journal of Experimental Biology*. **209**, 748–765.

Prum, R.O. (2010). The Lande–Kirkpatrick mechanism is the null model of evolution by intersexual selection: Implications for meaning, honesty, and designin intersexual signals. *Evolution*. **64**, 3085–3100.

Prum, R.O. and Razafindratsita, V.R. (1997). Lek behavior and natural history of the velvet asity (*Philepitta castanea*: Eurylaimidae). *The Wilson Journal of Ornithology*. **109**, 371–392.

Prum, R.O., Torres, R.H., Williamson, S. and Dyck, J. (1998). Coherent light scattering by blue feather barbs. *Nature*. **393**, 12–14.

R Core Team (2018). R: A language and environment for statistical computing. URL: https://www.r-project.org

Rahman, M.H. (2001). Inheritance of petal colour and its independent segregation from seed colour in *Brassica rapa*. *Plant Breeding*. **120**, 197–200.

Rajyaguru, P.K., Pegram, K. V., Kingston, A.C.N.N. and Rutowski, R.L. (2013). Male wing color properties predict the size of nuptial gifts given during mating in the Pipevine Swallowtail butterfly (*Battus philenor*). *Naturwissenschaften*. **100**, 507–513.

Rastas, P. (2017). Lep-MAP3: robust linkage mapping even for low-coverage whole genome sequencing data. *Bioinformatics*. **33**, 3726–3732.

Reed, R.D., McMillan, W.O. and Nagy, L.M. (2008). Gene expression underlying adaptive variation in *Heliconius* wing patterns: Non-modular regulation of overlapping cinnabar and vermilion prepatterns. *Proceedings of the Royal Society B: Biological Sciences*. **275**, 37–45.

Reed, R.D., Papa, R., Martin, A., Hines, H.M., Kronforst, M.R., Chen, R., Halder, G., Nijhout, H.F. and Mcmillan, W.O. (2011). *optix* drives the repeated convergent evolution of butterfly wing pattern mimicry. *Science*. **333**, 1137–1141.

Reinhold, K. (1998). Sex linkage among genes controlling sexually selected traits. *Behavioural Ecology and Sociobiology*. **44**, 1–7.

Rice, W.R. (2006). Sex Chromosomes and the Evolution of Sexual Dimorphism. *Evolution*. **38**, 735.

Rodd, F.H., Hughes, K.A., Grether, G.F. and Baril, C.T. (2002). A possible non-sexual origin of mate preference: Are male guppies mimicking fruit? *Proceedings of the Royal Society B: Biological Sciences*. **269**, 475–481.

Roelants, K., Fry, B.G., Norman, J.A., Clynen, E., Schoofs, L. and Bossuyt, F. (2010). Identical Skin Toxins by Convergent Molecular Adaptation in Frogs. *Current Biology*. **20**, 125–130.

Rosenblum, E.B., Hoekstra, H.E. and Nachman, M.W. (2006). Adaptive Reptile Color Variation and the Evolution of the *Mc1R* Gene. *Evolution*. **58**, 1794.

Rowe and Houle (1996). The lek paradox and the capture of genetic variance. *Proceedings: Biological Sciences*. **263**, 1415–1421.

Rowe, L. and Bonduriansky, R. (2005). Sexual Selection, Genetic Architecture, and the Condition Dependence of Body Shape in the Sexually Dimorphic Fly *Prochyliza xanthostoma* (Piophilidae). *Evolution*. **59**, 138–151.

Rutowski, R.L. (1985). Evidence for Mate Choice in a Sulphur Butterfly (*Colias eurytheme*). *Zeit. Tierpsychol.* **70**, 103–114.

Rutowski, R.L. (1991). The Evolution of Male Mate-Locating Behavior in Butterflies. *The American Naturalist*. **138**, 1121–1139.

Saastamoinen, M., van der Sterren, D., Vastenhout, N., Zwaan, B.J. and Brakefield, P.M. (2010). Predictive Adaptive Responses: Condition-Dependent Impact of Adult Nutrition and Flight in the Tropical Butterfly *Bicyclus anynana*. *The American Naturalist*. **176**, 686–698.

Saito, A. (2011). Material design and structural color inspired by biomimetic approach. *Science and Technology of Advanced Materials*. **12**, 064709.

San-Jose, L.M. and Roulin, A. (2017). Genomics of coloration in natural animal populations. *Philosophical Transactions of the Royal Society B: Biological Sciences*. **372**, 20160337.

Schluter, D., Clifford, E.A., Nemethy, M. and McKinnon, J.S. (2004). Parallel Evolution and Inheritance of Quantitative Traits. *The American Naturalist*. **163**, 809–822.

Seago, A.E., Brady, P., Vigneron, J.-P. and Schultz, T.D. (2009). Gold bugs and beyond: a review of iridescence and structural colour mechanisms in beetles (Coleoptera). *Journal of the Royal Society, Interface*. **6**, 165–184.

Shawkey, M.D., Estes, A.M., Siefferman, L.M. and Hill, G.E. (2003). Nanostructure predicts intraspecific variation in ultraviolet-blue plumage colour. *Proceedings of the Royal Society B: Biological Sciences*. **270**, 1455–1460.

Sheppard, P.M., Turner, J.R.G., Brown, K.S., Benson, W.W. and Singer, M.C. (1985). Genetics and the Evolution of Muellerian Mimicry in Heliconius Butterflies. *Philosophical Transactions of the Royal Society B: Biological Sciences*. **308**, 433–610.

Siefferman, L. and Hill, G.E. (2005). Blue Structural Coloration of Male Eastern Bluebirds *Sialia sialis* Predicts Incubation Provisioning to Females. *Journal of Avian Biology*. **36**, 488–493.

Silberglied, R.E. (1979). Communication in the Ultraviolet. *Annual Review of Ecology and Systematics*. **10**, 373–398.

Silberglied, R.E. (1984). Visual Communication and Sexual Selection *In*: *The Biology of Butterflies*. 207–223.

Silberglied, R.E. and Taylor, O.R. (1978). Ultraviolet Reflection and Its Behavioral Role in the Courtship of the Sulfur Butterflies. *Behavioral Ecology and Sociobiology*. **3**, 203–243.

Slate, J. (2005). Quantitative trait locus mapping in natural populations: Progress, caveats and future directions. *Molecular Ecology*. **14**, 363–379.

Stern, D. and Orgogozo, V. (2009). Is Genetic Evolution Predictable? *Science*. **323**, 746–752.

Sun, J., Bhushan, B. and Tong, J. (2013). Structural coloration in nature. *RSC Advances*. **3**, 14862–14889.

Suomalainen, E., Cook, L. and Turner, J. (1973). Achiasmatic oogenesis in the Heliconiine butterflies. *Hereditas*. **74**, 302–304.

Sweeney, A., Jiggins, C. and Johnsen, S. (2003). Polarized light as a butterfly mating signal. *Nature*. **423**, 31–32.

Taff, C.C., Zimmer, C. and Vitousek, M.N. (2019). Achromatic plumage brightness predicts stress resilience and social interactions in tree swallows (*Tachycineta bicolor*). *Behavioral Ecology*. *30*, 733-745.

Thayer, R.C., Allen, F.I. and Patel, N.H. (2019). Structural color in *Junonia* butterflies evolves by tuning scale lamina thickness. *bioRxiv*. 584532.

Therkildsen, N.O., Wilder, A.P., Conover, D.O., Munch, S.B., Baumann, H. and Palumbi, S.R. (2019). Contrasting genomic shifts underlie parallel phenotypic evolution in response to fishing. *Science*. **365**, 487–490.

Thilbert-Plante, X. and Gavrilets, S. (2013). Evolution of mate choice and the so-called magic traits in ecological speciation. *Ecology Letters*. **16**, 1004–1013.

Thurman, T.J., Brodie, E., Evans, E. and McMillan, W.O. (2018). Facultative pupal mating in *Heliconius erato*: Implications for mate choice, female preference, and speciation. *Ecology and Evolution*. **8**, 1882–1889.

Thurman, T.J. and Seymoure, B.M. (2016). A bird's eye view of two mimetic tropical butterflies: Coloration matches predator's sensitivity. *Journal of Zoology*. **298**, 159–168.

Turner, J. (1977). Butterfly mimicry: the genetical evolution of an adaptation. *Evolutionary Biology*. **10**, 163–206.

Turner, J.R.J. (1981). Adaptation and Evolution in *Heliconius*: A Defense of NeoDarwinism. *Annual Review of Ecology and Systematics*. **12**, 99–121.

van't Hof, A.E., Campagne, P., Rigden, D.J., Yung, C.J., Lingley, J., Quail, M.A., Hall, N., Darby, A.C. and Saccheri, I.J. (2016). The industrial melanism mutation in British

peppered moths is a transposable element. *Nature*. **534**, 102.

Via, S. and West, J. (2008). The genetic mosaic suggests a new role for hitchhiking in ecological speciation. *Molecular Ecology*. **17**, 4334–4345.

Vischer, N. (2013). PeakFinder. *ImageJ macro*., URL: https://imagej.nih.gov/ij/macros/tools/PeakFi.

Vollmer, J.H., Sarup, P., Kærsgaard, C.W., Dahlgaard, J. and Loeschcke, V. (2004). Heat and cold-induced male sterility in *Drosophila buzzatii*: genetic variation among populations for the duration of sterility. *Heredity*. **92**, 257–262.

Vukusic, P. (2001). Now you see it ... *Nature*. **410**, 36.

Vukusic, P., Sambles, J.R., Lawrence, C.R. and Wootton, R.J. (2002). Limited-view iridescence in the butterfly Ancyluris meliboeus. *Proceedings of the Royal Society B: Biological Sciences*. **269**, 7–14.

Vukusic, P., Sambles, J.R., Lawrence, C.R. and Wootton, R.J. (1999). Quantified interference and diffraction in single Morpho butterfly scales. *Proceedings of the Royal Society B: Biological Sciences*. **266**, 1403-1411.

Vukusic, P. and Stavenga, D.G. (2009). Physical methods for investigating structural colours in biological systems. *Journal of The Royal Society Interface*. **6**, S133–S148.

Walters, J.R., Hardcastle, T.J. and Jiggins, C.D. (2015). Sex chromosome dosage compensation in *Heliconius* butterflies: Global yet still incomplete? *Genome Biology and Evolution*. **7**, 2545–2559.

Westerman, E.L., VanKuren, N.W., Massardo, D., Tenger-Trolander, A., Zhang, W., Hill, R.I., Perry, M., Bayala, E., Barr, K., Chamberlain, N., Douglas, T.E., Buerkle, N., Palmer, S.E. and Kronforst, M.R. (2018). *Aristaless* Controls Butterfly Wing Color Variation Used in Mimicry and Mate Choice. *Current Biology*. **28**, 3469-3474.e4.

Wheldale, M. (1907). The inheritance of flower colour in *Antirrhinum majus*. *Proceedings of the Royal Society B: Biological Sciences*. **79**, 288–305.

Whitlock, M.C. and Schluter, D. (2009). *The analysis of biological data*. Roberts & Company Publishers.

Williams, G.C. (1966). *Adaptation and Natural Selection*. Princeton, New Jersey: Princeton University Press.

Wilts, B.D., Vey, A.J.M., Briscoe, A.D. and Stavenga, D.G. (2017). Longwing (*Heliconius*) butterflies combine a restricted set of pigmentary and structural coloration mechanisms. *BMC Evolutionary Biology*. **17**, 1–12.

Wybouw, N., Kurlovs, A.H., Greenhalgh, R., Bryon, A., Kosterlitz, O., Manabe, Y., Osakabe, M., Vontas, J., Clark, R.M. and Van Leeuwen, T. (2019). Convergent evolution of cytochrome P450s underlies independent origins of keto-carotenoid pigmentation in animals. *Proceedings of the Royal Society B: Biological Sciences*. **286**, 20191039.

Xu, S. (2003). Theoretical Basis of the Beavis Effect. *Genetics*. **165**, 2259–2268.

Yeaman, S., Aeschbacher, S. and Bürger, R. (2016). The evolution of genomic islands by increased establishment probability of linked alleles. *Molecular Ecology*. **25**, 2542–2558.

Zahavi, A. (1975). Mate selection - A selection for a handicap. *Journal of Theoretical Biology*. **53**, 205–214.

Zhang, B., Lu, C.M., Kakihara, F. and Kato, M. (2002). Effect of genome composition and cytoplasm on petal colour in resynthesized amphidiploids and sesquidiploids derived from crosses between *Brassica rapa* and *Brassica oleracea*. *Plant Breeding*. **121**, 297–300.

Zhang, L., Mazo-Vargas, A. and Reed, R.D. (2017). Single master regulatory gene coordinates the evolution and development of butterfly color and iridescence. *Proceedings of the National Academy of Sciences*. **114**, 10707-10712.

Appendix

Melanie N. Brien, Juan Enciso-Romero, Andrew J. Parnell, Patricio A. Salazar, Carlos Morochz, Darwin Chalá, Hannah E. Bainbridge, Thomas Zinn, Emma V. Curran and Nicola J. Nadeau (2018). Phenotypic variation in *Heliconius erato* crosses shows that iridescent structural colour is sex-linked and controlled by multiple genes. *Interface Focus*, **9**, 20180047.

INTERFACE FOCUS

rsfs.royalsocietypublishing.org

Research

Cite this article: Brien MN *et al*. 2018 Phenotypic variation in *Heliconius erato* crosses shows that iridescent structural colour is sex-linked and controlled by multiple genes. *Interface Focus* **9**: 20180047.
http://dx.doi.org/10.1098/rsfs.2018.0047

Accepted: 29 October 2018

One contribution of 11 to a theme issue 'Living light: optics, ecology and design principles of natural photonic structures'.

Subject Areas:
biophysics

Keywords:
structural colour, *Heliconius*, butterflies, iridescence, evolution, quantitative genetics

Authors for correspondence:
Melanie N. Brien
e-mail: mnbrien1@sheffield.ac.uk
Nicola J. Nadeau
e-mail: n.nadeau@sheffield.ac.uk

Electronic supplementary material is available online at https://dx.doi.org/10.6084/m9.figshare.c.4302737.

THE ROYAL SOCIETY PUBLISHING

Phenotypic variation in *Heliconius erato* crosses shows that iridescent structural colour is sex-linked and controlled by multiple genes

Melanie N. Brien[1], Juan Enciso-Romero[1,2], Andrew J. Parnell[3], Patricio A. Salazar[1,4], Carlos Morochz[5], Darwin Chalá[5], Hannah E. Bainbridge[1], Thomas Zinn[6], Emma V. Curran[1] and Nicola J. Nadeau[1]

[1]Department of Animal and Plant Sciences, University of Sheffield, Alfred Denny Building, Western Bank, Sheffield S10 2TN, UK
[2]Biology Program, Faculty of Natural Sciences and Mathematics, Universidad del Rosario, Bogotá, Colombia
[3]Department of Physics and Astronomy, University of Sheffield, Hicks Building, Hounsfield Road, Sheffield S3 7RH, UK
[4]Centro de Investigación en Biodiversidad y Cambio Climático (BioCamb), Universidad Tecnológica Indoamérica, Quito, Ecuador
[5]Mashpi Reserve, Ecuador
[6]ESRF — The European Synchrotron, 38043 Grenoble Cedex 9, France

MNB, 0000-0002-3089-4776; JE-R, 0000-0002-4143-3705; AJP, 0000-0001-8606-8644; NJN, 0000-0002-9319-921X

Bright, highly reflective iridescent colours can be seen across nature and are produced by the scattering of light from nanostructures. *Heliconius* butterflies have been widely studied for their diversity and mimicry of wing colour patterns. Despite iridescence evolving multiple times in this genus, little is known about the genetic basis of the colour and the development of the structures which produce it. *Heliconius erato* can be found across Central and South America, but only races found in western Ecuador and Colombia have developed blue iridescent colour. Here, we use crosses between iridescent and non-iridescent races of *H. erato* to study phenotypic variation in the resulting F_2 generation. Using measurements of blue colour from photographs, we find that iridescent structural colour is a quantitative trait controlled by multiple genes, with strong evidence for loci on the Z sex chromosome. Iridescence is not linked to the Mendelian colour pattern locus that also segregates in these crosses (controlled by the gene *cortex*). Small-angle X-ray scattering data show that spacing between longitudinal ridges on the scales, which affects the intensity of the blue reflectance, also varies quantitatively in F_2 crosses.

1. Introduction

Structural colours are bright and highly reflective colours produced by the interaction of light with nanostructures. They can be seen across a range of taxa, including fish, birds, molluscs and insects, and have numerous functions covering visual communication and recognition, mate choice and thermoregulation [1–3]. Despite this, little is known about the genetic basis of structural colour, or how genetic variation translates into developmental differences of the nanostructures.

Examples of the different ways structural colour is produced can be seen across butterfly species. Multilayer reflectors produce the bright blue colour in *Morpho* butterflies [4], while *Callophrys rubi* have a highly connected gyroid structure contained within the upper and lower lamina [5]. Scales on butterfly wings are formed as a long, flattened extension of the cuticle. Generally, they are composed of longitudinal ridges which are linked transversely by cross-ribs (figure 1). These nanostructures make up a variety of repeating elements which can vary in

© 2018 The Author(s) Published by the Royal Society. All rights reserved.

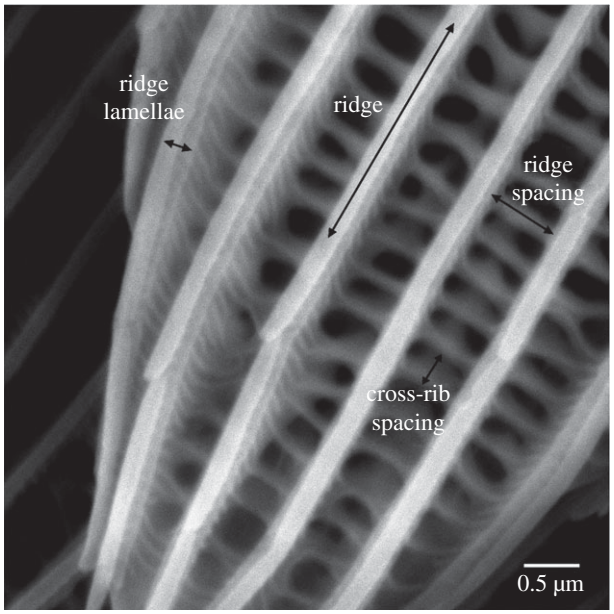

Figure 1. Scanning electron microscope image showing the structures on a *Heliconius* wing scale. Longitudinal ridges, composed of overlapping lamellae, are connected by cross-ribs.

thickness and patterning, producing different visual effects. F-actin filaments are important in the development of wing scale cells and appear to pre-pattern where the ridges will form [6].

The neotropical *Heliconius* butterflies (Nymphalidae) are well known for the diversity in their wing colour patterns and mimicry between species [7]. Many of these colour patterns are formed by chemical pigments, but several species also exhibit structurally produced blue reflectance. *Heliconius* butterflies can produce structural colour by thin film interference using different features on their scales. Longwing *H. doris*, for example, display hindwing colour reflected by their lower lamina; the resulting colour can be blue or green depending on the absence or presence of the yellow pigment 3-OH-kynurenine [8]. Several other species, including *Heliconius erato*, produce iridescent colours, that change in both brightness and wavelength of peak reflectance with angle, using layered lamellae that make up their scale ridges. Density of the ridges, the curvature and layering of the lamellae affect the intensity of the structural colour, with denser ridge spacing producing higher reflectance [9].

Heliconius erato is found across Central and South America and has evolved more than 25 races with a diversity of colour patterns. These aposematic patterns are mimetic with *Heliconius melpomene* and are an example of Müllerian mimicry. Variation in pigment colour patterns has been found to map to a handful of loci that control a diversity of patterns in several distantly related species [10–13]. Despite iridescent colour evolving multiple times in *Heliconius*, the genetics of this trait have not been studied to the same extent as pigment colour patterns, likely due to the difficulty of measuring the trait. Iridescent *H. erato cyrbia* is found on the western slopes of the Andes in Ecuador. *Heliconius erato* races found further north in Panama lack this structural colour, and hybrid zones arise between the iridescent and non-iridescent races, where populations with intermediate levels of iridescence can be found. Previous researchers have noted that levels of iridescence vary in F_2 hybrid crosses and appear to do so in a continuous manner [12,14], but have not attempted to quantify the variation. Continuous variation in the F_2 would suggest that the trait is controlled by multiple loci and therefore not controlled by the 'tool kit' of major effect loci that regulate pigment colour patterns. The genes controlling variation in iridescence may perhaps be those directly controlling the formation of scale structure.

Experimental genetic crosses can be used to estimate the number of genes involved in controlling a trait by investigating the distribution of the phenotype across segregating generations [15]. Traits that are controlled by a single locus of major effect will segregate according to Mendelian ratios, with 50–100% of individuals in the F_2 generation having phenotypes the same as one or other of their parents (depending on dominance of the alleles). The more individuals there are with intermediate phenotypes, the more loci are likely to be involved, as a greater number of allele combinations will be possible. We can also estimate positions of loci in the genome by looking for links to known loci which control other phenotypes and by looking for patterns of sex linkage.

Here, we aim to determine whether iridescence in *H. erato* is a quantitative trait controlled by multiple genes, and if any of these genes are sex-linked or linked to known colour pattern loci, by looking at the segregation of the trait in F_2 crosses between different races. *Heliconius erato demophoon* from Panama is black with red and yellow bands. This race was crossed to *H. erato cyrbia* from Ecuador, which has a similar colour pattern but has an iridescent blue colour instead of being matt black (figure 2). The only major colour pattern differences between these races are the white margin on the hindwing of *H. erato cyrbia* and the yellow bar on the dorsal hindwing of *H. erato demophoon*. Based on previous crosses, these are likely to be controlled by alternative alleles of the *Cr* locus on linkage group 15, which is homologous to three tightly linked loci (*Yb*, *Sb* and *N*) in *H. melpomene* [10] and corresponds to the gene *cortex* [16]. There are also differences in the size and position of the red forewing band between *cyrbia* and *demophoon*, likely controlled by the gene *WntA*, found on chromosome 10 [12,17,18]. We also use small-angle X-ray scattering (SAXS) to quantify ridge spacing in broods. As several aspects of scale morphology are known to vary between the iridescent and non-iridescent races [9], it is possible that apparent continuous variation in the reflectance in the F_2 could be due to independent segregation of these different features, each of which may be controlled by a major effect gene. Therefore, we also test whether ridge spacing shows continuous variation in the F_2 generation.

2. Material and methods

2.1. Crossing experiments

Experimental crosses were performed between geographical races of *H. erato* at the insectary in Mashpi Reserve, Ecuador, over a period of 2 years. *Heliconius erato demophoon* were collected from Gamboa, Panama (9.12° N, 79.67° W) in May 2014, then transported to Mashpi, Ecuador (0.17° N, 78.87° W), where they were kept as stocks. Iridescent *H. erato cyrbia* were collected from the area around Mashpi. *Heliconius erato demophoon* were crossed with *H. e. cyrbia*, and the F_1 generation crossed together, along with the addition of two backcrosses (BC) between the F_1 and *cyrbia* (figure 2). Crosses were reciprocal, so that in roughly half of the first generation crosses the female was the iridescent race and the male non-iridescent, and vice versa. In line with previous studies with intraspecific *Heliconius* hybrids [12,19], races readily

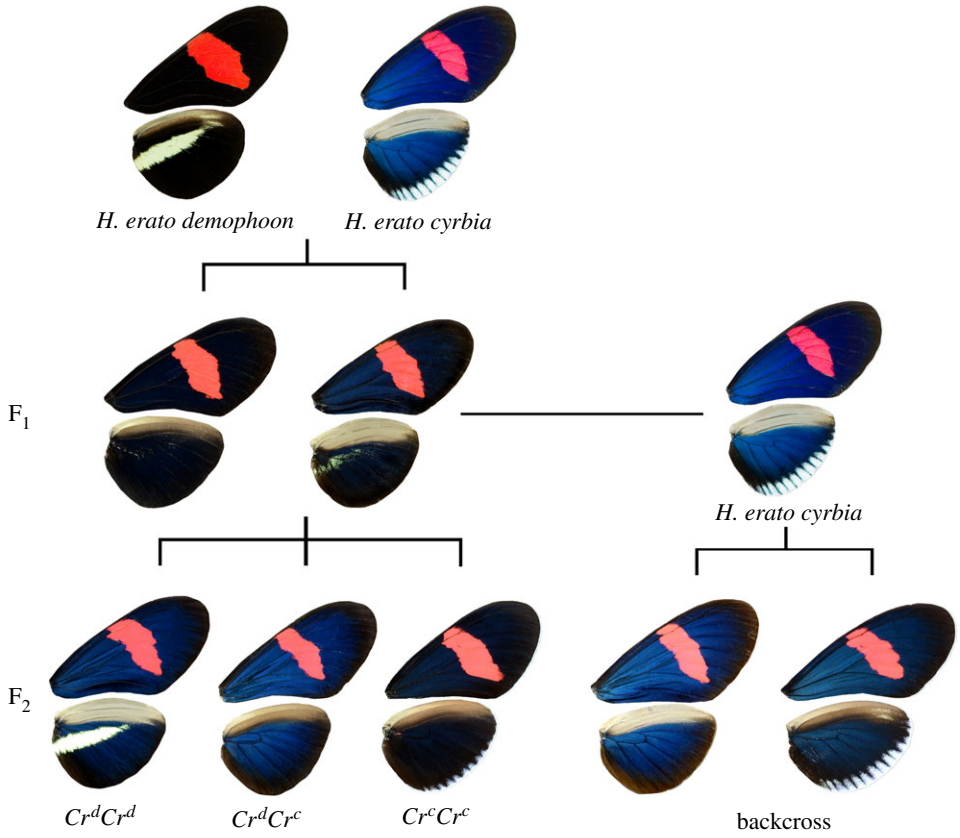

Figure 2. Cross-design and examples of colour pattern variation in *H. erato* F_1, F_2 and backcross generations. Examples of the *Cr* genotypes are shown in the F_2 generation.

Table 1. *Heliconius erato* crosses performed and the number of offspring produced from each. See electronic supplementary material table S2 for details of each cross.

cross type	number of crosses	number of offspring phenotyped for blue values	number of offspring phenotyped for ridge spacing
F_1: *demophoon* ♂ × *cyrbia* ♀	2	37	3
F_1: *cyrbia* ♂ × *demophoon* ♀	3	33	3
F_2: *cyrbia* maternal grandfather	3	100	59
F_2: *demophoon* maternal grandfather	3	14	0
backcross: *cyrbia* ♂ × (*demophoon* ♂ × *cyrbia* ♀)	2	16	0
backcross: *cyrbia* ♀ × (*cyrbia* ♂ × *demophoon* ♀)	1	49	0

hybridized and we did not observe any evidence of hybrid inviability or differing success between the reciprocal crosses. *Passiflora* species were provided as larval food plants and for oviposition, and butterflies were given *Lantana camara* and other locally collected flowers, plus sugar solution (10%) and pollen to feed. The bodies of the parents and offspring were preserved in NaCl saturated 20% dimethyl sulfoxide 0.25 M EDTA solution to preserve the DNA, and the wings stored separately in glassine envelopes. A total of 302 individuals obtained from 14 crosses were used in the analysis (table 1).

2.2. Phenotypic colour analysis

All butterfly wings were photographed flat under standard lighting conditions using a mounted Nikon D7000 DSLR camera with a 40 mm f/2.8 lens set to an aperture of f/10, shutter speed of 1/60 and ISO of 100. Lights were mounted at a fixed angle of 45° to maximize the observed blue reflection from the iridescent wing regions. All photographs also included an X-Rite Colour Checker to help standardize the colour of the images. RAW format images were standardized using the levels tool in Adobe Photoshop CS2 (v. 9.0). Using the colour histogram plugin in ImageJ [20,21], red-green-blue (RGB) values were recorded from two sections of the wings and averaged (figure 3). These areas were chosen because the scales on these sections of the wings close to the body tended to be the least damaged and worn, so a more accurate measurement of the colour could be taken, and the wing venation was used as a marker to allow the same areas to be measured each time.

Blue reflection from the iridescent wing regions was measured as variation in blue-red (BR) colour. This was calculated as $(B - R)/(B + R)$, with -1 being completely red and 1 being completely blue. The level of UV reflectance could not be measured from our photographs. Previous spectral measurements of the wing reflectance show that peak reflectance for *H. erato cyrbia* is just below the visible range at about 360–370 nm, with much of the reflectance being within the human visible range, while *H. erato demophoon* reflects very little but tends to show highest reflectance

Figure 3. RGB values were measured in the hatched areas highlighted on the right wings and averaged for each butterfly. Left wings were used when the right side were too damaged. SAXS measurements were taken along the dotted line shown on the left forewing. (Online version in colour.)

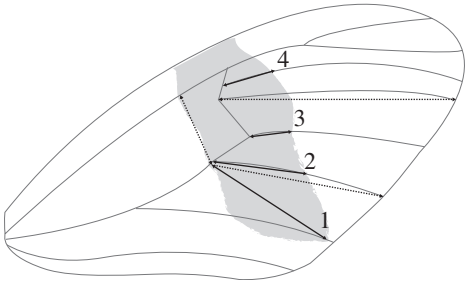

Figure 4. Four measurements of forewing band width were taken (bold arrows) along with three further measurements to standardize wing size (dotted arrows), using wing veins as points of reference.

in the red–infrared range [9]. Therefore, the colour values will allow variation in colour and reflectance to be measured but will not represent butterfly visual systems. Repeatability of the colour measurements was tested using the repeatability equation of Whitlock & Schluter [22] by taking five measurements each on five randomly selected individuals. This estimates the fraction of total variance that is among groups in a random-effects ANOVA. We used the Castle–Wright estimator:

$$n_e = \frac{[\mu(P_1) - \mu(P_2)]^2 - \mathrm{Var}[\mu(P_1)] - \mathrm{Var}[\mu(P_2)]}{8\mathrm{Var}(S)},$$

where $S = \mathrm{Var}(F_2) - \mathrm{Var}(F_1)$, to estimate the effective number of genetic loci (n_e) contributing to variation in the trait [15,23,24]. This is the difference between the mean BR values of the parental races squared, then the subtraction of the two variance terms, which corrects for sampling error of the estimates of the parental means (P_1 and P_2).

The genotype at the *Cr* locus was scored in 286 individuals based on the presence and absence of the white hindwing margin and the dorsal hindwing yellow bar, under the assumption that these pattern elements are controlled by alternative alleles of the *Cr* locus [10,25]. The *demophoon* genotype has the yellow bar present and is scored as Cr^dCr^d, a white margin indicates the *cyrbia* genotype and this is scored as Cr^cCr^c, and the Cr^dCr^c heterozygous genotype has neither of these elements (figure 2). To look for association between variation in the red band and blue colour, we took four measurements of forewing band size in 71 F_2 individuals and three further measurements to adjust for wing size (figure 4), based on methods from Baxter *et al*. [26]. Using ImageJ, band measurements were carried out on the dorsal side of the wing and repeated for both the left and right wings. The average of these two measurements was divided by the average of the three standardizing wing measurements. The three standardizing wing measurements were also used to assess overall size of these individuals.

All statistical analyses were carried out in the R statistical package v. 3.4.2 [27]. Welch's *t*-tests were used for analysis of differences between sexes and reciprocal crosses. ANOVA models were used to compare blue values with *Cr* genotypes. Yellow bar and white margin traits were tested for departures from the expected segregation ratios, based on the above hypothesis of the linkage and Mendelian inheritance, using a χ^2 test. Correlations between BR values and forewing red band measurements, ridge spacing and cross-rib spacing (see below) were tested with the Pearson correlation coefficient.

2.3. Small-angle X-ray scattering data collection

We estimated the size of the spacing between scale ridges and between cross-ribs (figure 1) using SAXS carried out at the ID02 beamline at the European Synchrotron (ESRF), Grenoble, France [28]. The detector was a high-sensitivity FReLon 16 M Kodak CCD with an effective area of 2048 × 2048 pixels (24 µm pixel size). The X-ray wavelength λ was 0.0995 nm (12.45 keV), the beam was collimated to 50 µm × 50 µm and the accessible q-range was from 0.0017 to 0.07 nm^{-1} at 30.7 m sample-to-detector distance. All two-dimensional (2D) images were corrected for dark, spatial distortion, normalized by transmitted flux and masked to account for the beam stop and the edges of the detector. We azimuthally integrated the 2D images to obtain one-dimensional patterns of scattered intensity I as a function of the momentum transfer vector q, where $q = (4\pi \sin\theta)/\lambda$. Here, 2θ is the scattering angle. A typical scattering profile of a *Heliconius* scale is shown in figure 5.

Wings were mounted in a frame that could be rotated to precisely align the samples. We collected between 33 and 113 measurements over 10–20 mm between two of the wing veins on the forewing (figure 3) of 74 *H. erato* individuals: eight *cyrbia*, one *demophoon*, six F_1 (from two crosses in reciprocal directions) and 59 F_2 (all from a single cross). In addition, we measured four *Heliconius erato hydara* individuals to be analysed alongside the *demophoon*. The *H. e. hydara* were also collected in Panama, do not have iridescent colour and differ from *demophoon* only in the lack of yellow hindwing bar. To obtain estimates of the ridge spacing, we fitted the peak positions in the one-dimensional scattered intensity to a composite Lorentzian + linear profile using the lmfit Python module [29]. We then used the centre of each fitted profile to calculate ridge spacing using the expression $d = 2\pi/q$ and averaged these to obtain a single estimate per individual. The average distances between ridges are in good agreement with those previously reported for *H. erato* [9].

3. Results

3.1. Segregation of blue colour

Measurements of blue scores were shown to be repeatable, with 99% of variation due to differences between individuals and 1% due to measurement error ($R^2 = 0.99$, $F_{4,20} = 54159$, $p < 0.001$; electronic supplementary material, table S3). *Heliconius erato demophoon* showed very little blue colour with an average BR value of -0.56 ± 0.08 compared with iridescent *H. erato cyrbia* which had a mean value of 0.97 ± 0.05 (table 2). The mean for the F_2 generation fell midway between the two parental races (figure 6), suggesting additive effects of alleles. The mean of the F_1 was slightly skewed towards *demophoon*, although the median was in a similar position to the F_2 (0.13 and 0.14). The mean BR value of the backcrosses did not fall halfway between that of the F_1 and the

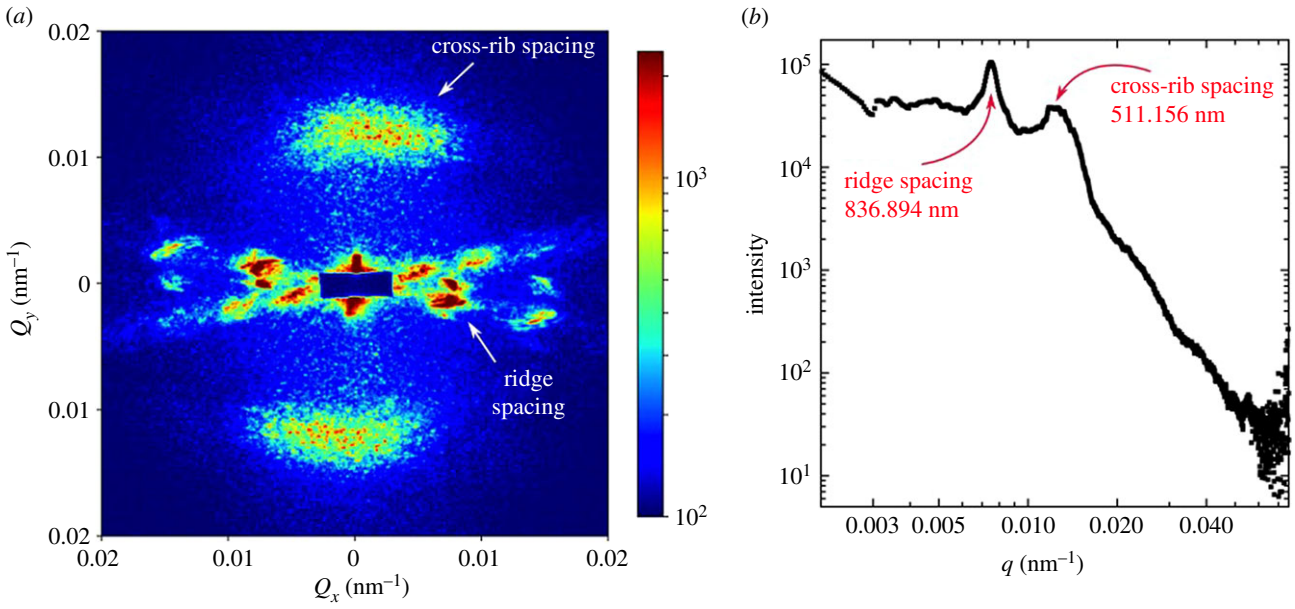

Figure 5. Representative SAXS patterns for a single frame of a male *H. e. cyrbia* parent. (*a*) The 2D pattern reveals approximately perpendicular scattering intensity from scale features. From their orientation, length scales of the scattered intensity and previous interpretations, we infer that they correspond to the spacing between ridges and cross-ribs. (*b*) Full azimuthal integration of the scattered intensity as a function of the magnitude of the momentum transfer vector q. The peaks corresponding to ridge and cross-rib spacing are indicated together with the measurements in real space.

Table 2. Summary statistics for BR values in each generation of *H. erato*.

generation	mean BR value	standard deviation	variance	sample size
demophoon	−0.56	0.08	0.01	12
F_1	0.13	0.23	0.05	60
backcross	0.69	0.28	0.08	65
F_2	0.21	0.30	0.09	114
cyrbia	0.97	0.05	0.00	51

parental race, which they were crossed with, but were skewed towards *cyrbia*, the Ecuadorian race. This suggests that the effects of the alleles are not completely additive, and there may be some dominance of the *cyrbia* alleles or epistatic interactions between loci.

The lack of discrete groups in the F_2 generation suggests that variation in the trait is controlled by more than one locus. Using the Castle–Wright estimator, with mean BR values and variances from only one cross direction to reduce variation due to sex linkage (see subsequent results), we obtained an estimate of 4.6 loci contributing to the trait. While this formula assumes that crosses started with inbred lines, it is generally robust to deviations from the assumptions [30]. However, it likely underestimates the total number of loci as it assumes loci all have equal effects. It is therefore perhaps best interpreted as the likely number of loci with medium to large effects on the phenotype. In addition, the F_1 individual wings that we measured were of varying age and condition, which may have increased the variance and decreased the mean value of blue reflectance seen in these individuals relative to the F_2 individuals, which were all preserved soon after emergence. This could influence the estimation of the number of loci.

3.2. Sex linkage

Sex linkage leads to a difference in the trait between reciprocal crosses in the F_1 generation, which is confined to the heterogametic sex, or a difference between reciprocal crosses in the F_2 generation in the homogametic sex [31]. As in birds, female butterflies are the heterogametic sex; they have ZW sex chromosomes whereas males have ZZ. Differences would occur depending on which parent or grandparent the Z or W is inherited from (figure 7). If the sex difference is present in the parental population, or the pattern is the same in reciprocal crosses, this would indicate a sex-limited trait (i.e. an autosomal trait that is expressed differently between the sexes).

Comparing the F_1 offspring of reciprocal crosses suggested some sex linkage (figure 8 and table 3). Offspring of crosses with a male *cyrbia* parent had significantly higher blue values than those which had a female *cyrbia* parent. Separated by sex, there was no difference between the males from reciprocal F_1 crosses, which had a mean of 0.23 and 0.25, respectively ($t_{11} = -0.19$, $p = 0.85$). The variation was among the female offspring which had means of −0.03 and 0.26 ($t_{44} = -5.55$, $p < 0.001$; table 4). This pattern would be expected if there were one or more loci controlling iridescence on the Z chromosome. In each case, males will be receiving one Z chromosome from an iridescent parent, and the other from a non-iridescent parent. The female offspring, in contrast, will only receive a Z chromosome from their father (figure 7). To confirm that these results were not biased by a particular cross, individual crosses were plotted and the same pattern was found (electronic supplementary material, figure S1). We did not find any difference in blue score between the sexes in pure *H. erato cyrbia* (table 3), demonstrating that the difference between the sexes in the crosses is not due to autosomally mediated sexual dimorphism.

If blue colour was controlled only by genes on the Z chromosome, we would expect that females from crosses with a non-iridescent father would have the same phenotype as *demophoon* females. However, they are significantly bluer

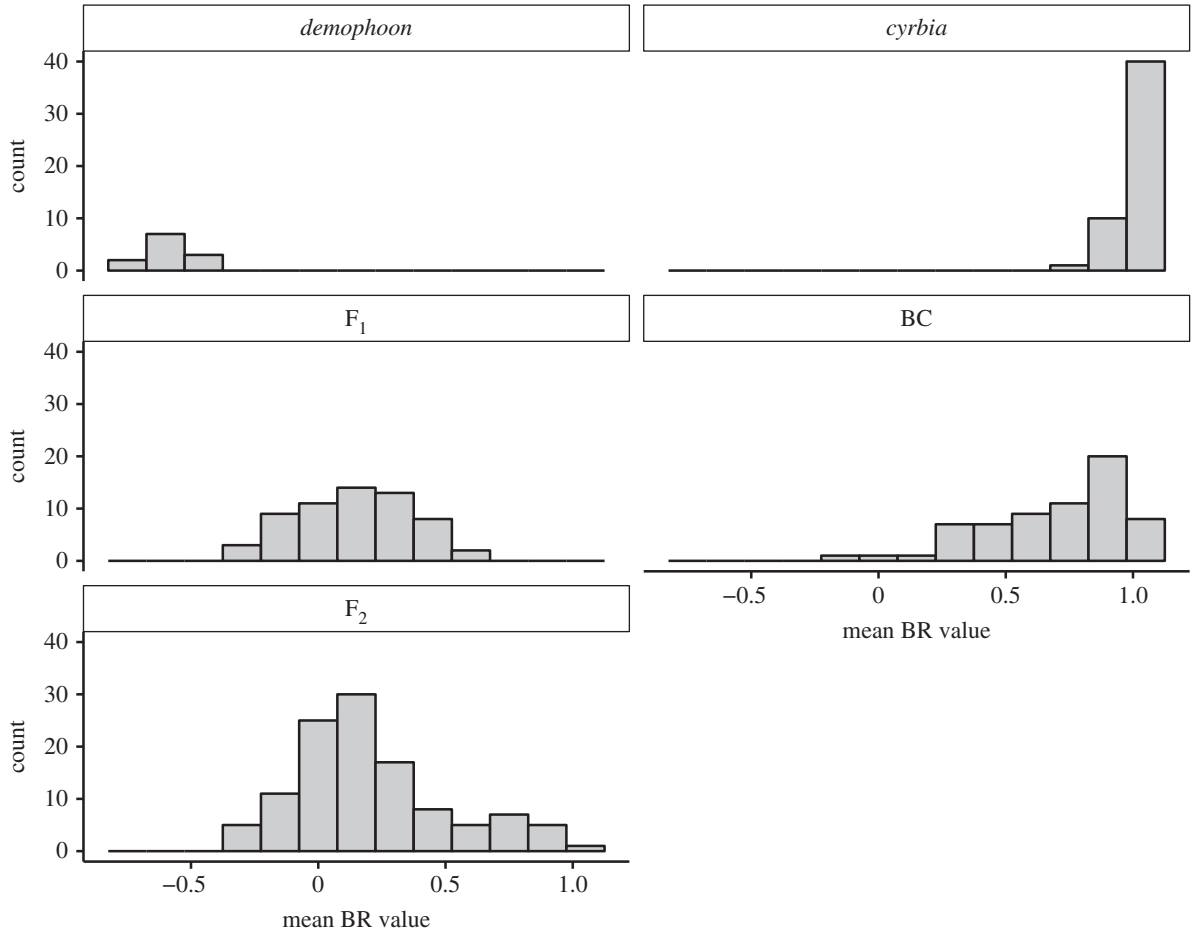

Figure 6. Mean BR values across *H. erato* generations. F_1 and F_2 individuals largely fall between the parental *demophoon* and *cyrbia* races. The backcross generation (BC) are highly skewed towards *cyrbia*, which is the race they were crossed with.

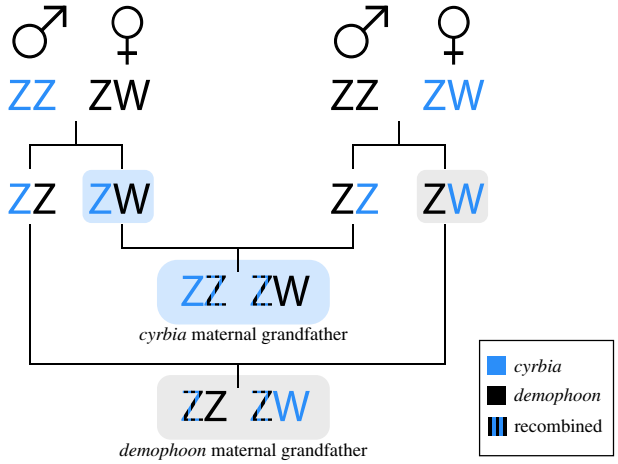

Figure 7. If there are loci of interest on the Z chromosome, F_1 females with an iridescent *cyrbia* father will be bluer than those with a non-iridescent *demophoon* father because they inherit a '*cyrbia*' Z chromosome. In the F_2, males always inherit a complete, non-recombined Z chromosome from their maternal grandfather, so if he is iridescent they will be bluer than offspring from the reciprocal cross.

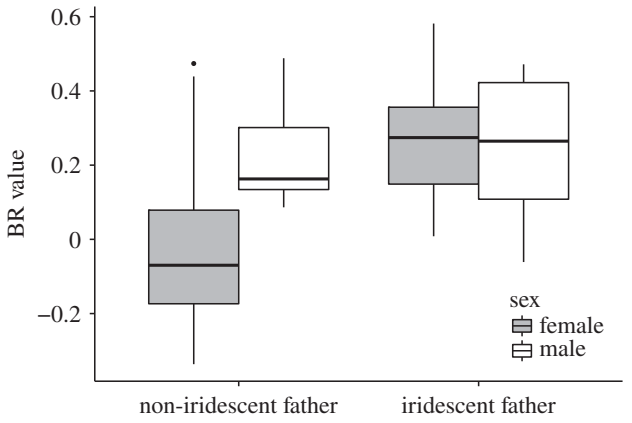

Figure 8. F_1 females with an iridescent *cyrbia* father were significantly bluer than those with a *demophoon* father. There were no differences in males.

than wild *demophoon*, supporting the hypothesis that the colour is controlled by multiple loci on different chromosomes (-0.03 ± 0.2 and -0.56 ± 0.1, $t_{25} = -10.6$, $p < 0.001$).

In the F_2 generation, sex linkage would be shown as males with an iridescent maternal grandfather being more blue than those with an iridescent maternal grandmother. The results point towards this pattern; however, the differences between the male groups are not significant, possibly due to small sample sizes in the first group (figure 9 and table 4). There was little difference in females. Overall, however, offspring with an iridescent maternal grandfather were bluer than those with black maternal grandfather. This is consistent with sex linkage, due to the greater number of '*cyrbia*' Z chromosomes present in the F_2 offspring with an iridescent maternal grandfather (figure 7). Within the offspring with an iridescent maternal grandfather, males were bluer than females, while this was not the case for crosses with a black maternal grandfather, also supporting Z linkage (table 3). In summary, F_1 females were bluer when they had an iridescent father, and

Table 3. Comparison of BR values (±s.d.) between females and males in each *H. erato* generation. Males are bluer than females in crosses with a *demophoon* father or *cyrbia* maternal grandfather (MGF). Males are also bluer in backcrosses with a *cyrbia* MGF. There are no differences in the parental races.

generation	female BR value	female sample size	male BR value	male sample size	*t*-statistic	d.f.	*p*-value
demophoon	−0.56 ± 0.1	6	−0.56 ± 0.1	6	−0.06	9.0	0.955
all F_1	0.10 ± 0.3	46	0.24 ± 0.2	14	−2.37	28.9	0.025
F_1 *cyrbia* father	0.26 ± 0.2	21	0.25 ± 0.2	7	0.17	8.4	0.872
F_1 *demo.* father	−0.03 ± 0.2	25	0.23 ± 0.1	7	−3.80	13.3	0.002
all F_2	0.10 ± 0.3	63	0.33 ± 0.3	51	−4.28	96.4	<0.001
F_2 *cyrbia* MGF	0.12 ± 0.3	53	0.35 ± 0.3	47	4.00	92.1	<0.001
F_2 *demo.* MGF	0.02 ± 0.2	10	0.15 ± 0.4	4	−0.72	3.5	0.512
all BC	0.60 ± 0.3	35	0.79 ± 0.2	30	−2.93	62.9	0.005
BC *cyrbia* MGF	0.58 ± 0.3	24	0.83 ± 0.2	25	−3.86	42.7	<0.001
BC *demo.* MGF	0.65 ± 0.4	11	0.62 ± 0.4	5	0.16	7.6	0.877
cyrbia	0.98 ± 0.2	16	0.97 ± 0.1	35	0.79	48.2	0.431

Table 4. Comparison of BR values for offspring from reciprocal F_1 crosses, which had either an iridescent mother or iridescent father, and for F_2 crosses, which had either an iridescent maternal grandfather or grandmother. Mean values and sample sizes are shown in table 3.

F_1 *cyrbia* or *demophoon* father				F_2 *cyrbia* or *demophoon* maternal grandfather			
	t	d.f.	*p*-value		*t*	d.f.	*p*-value
female	−5.55	43.6	<0.0001	female	−1.64	19.5	0.118
male	−0.19	10.8	0.85	male	−1.06	3.4	0.357
all	−4.67	56.8	<0.0001	all	−2.53	20.2	0.020

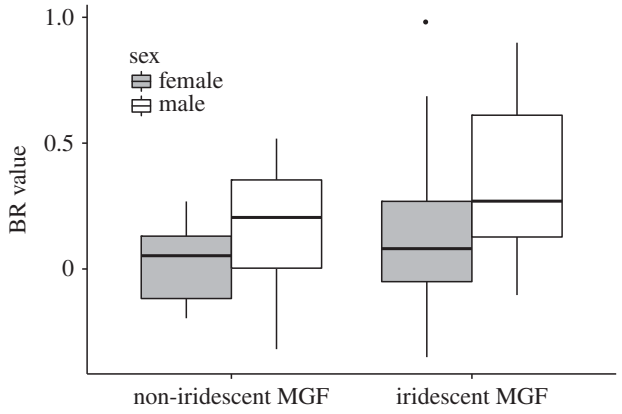

Figure 9. Mean BR values for F_2 males with an iridescent maternal grandfather (MGF) were higher than those with an iridescent maternal grandmother, although not significantly. Females in both groups had similar BR values.

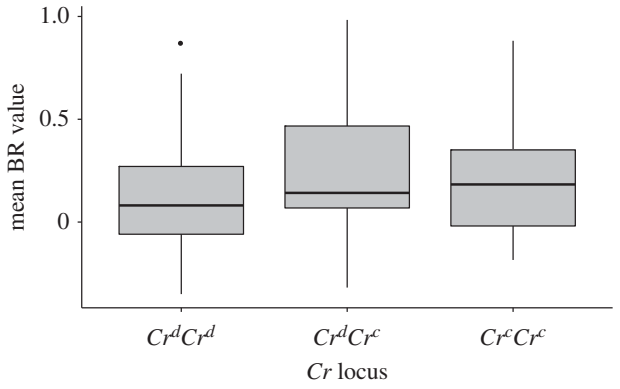

Figure 10. In the F_2 generation, BR values did not differ with the different *Cr* phenotypes. Cr^dCr^d represents the *demophoon* genotype with the yellow bar present on the hindwing, and Cr^cCr^c is the *cyrbia* genotype with the white margin. Cr^dCr^c is heterozygous and has neither of these elements.

males were bluer in the F_2 when they had an iridescent maternal grandfather. There were no differences in BR values between males and females in the parental races, *H. e. demophoon* and *H. e. cyrbia*. These results support the presence of loci controlling iridescence in the Z chromosome.

3.3. Links to other colour pattern loci

In *H. erato*, the *Cr* locus controls the presence of a yellow forewing bar in *demophoon* and a white margin in *cyrbia*. There were three observed phenotypes in the F_2 generation—yellow bar present, white margin present and both absent (figure 2). Consistent with the hypothesis that these two features are controlled by recessive, tightly linked loci or are alternative alleles of the same locus, we did not find any individuals that had both a yellow dorsal bar and a white margin present. The ratio of these traits was also consistent with a 1 : 2 : 1 ratio as expected under the assumption that the individuals lacking both features were heterozygous at this locus ($x^2 = 2.1$, d.f. = 2, $p = 0.35$). There was no significant difference in BR values between individuals with different *Cr* genotypes ($F_{2,107} = 2.05$, $p = 0.133$) (figure 10), suggesting that *cortex* is not one of

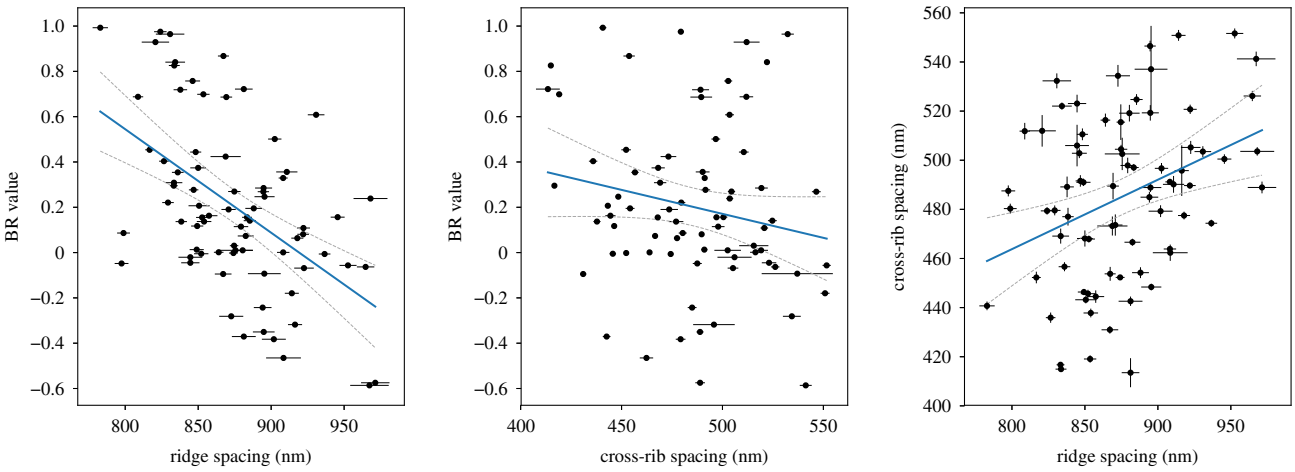

Figure 11. An increase in longitudinal ridge spacing correlated with a decrease in BR values. Blue colour slightly decreased with cross-rib spacing, but ridge spacing and cross-rib spacing were also highly correlated. The cross-hairs show the standard error from the 33 to 133 SAXS point measurements for each individual. Blue lines indicate the fitted linear regression, with the dotted lines showing the 95% confidence interval. (Online version in colour.)

Table 5. There are no significant correlations between the forewing red band measurements and BR colour in the F_2 generation. Measurements are ratios of band measurements to wing size. Degrees of freedom = 69. $N = 71$.

standardized measurement	mean	standard deviation	*t*	*r*	*p*-value
linear 1	0.76	0.08	−1.65	−0.20	0.10
linear 2	0.55	0.06	−1.41	−0.17	0.16
linear 3	0.35	0.05	−1.69	−0.20	0.10
linear 4	0.41	0.05	0.38	0.05	0.71

the genes controlling iridescence, nor are there any major effect loci linked to this region on *Heliconius* chromosome 15. In the F_2, there were also no significant correlations between blue colour and any of the standardized linear measurements used to determine shape of the red forewing band (table 5; electronic supplementary material, figure S2), showing iridescence is unlikely to be linked to *WntA* on chromosome 10.

3.4. Nanostructure variation

As we expected, there was a negative correlation between longitudinal ridge spacing and BR values ($r = -0.52$, $p < 0.001$; figure 11), indicating that blue reflectance increases with increasing density of ridges on the scale. The strength of this correlation shows that ridge spacing is only one factor which is affecting the intensity of iridescence, and that other aspects of scale morphology that determine blue reflectance may segregate somewhat independently in the crosses. BR values also declined with increasing cross-rib spacing, although not significantly ($r = -0.20$, $p = 0.09$; figure 11). Ridge spacing and cross-rib spacing were highly correlated with each other ($r = 0.34$, $p = 0.002$; figure 11) suggesting a genetic correlation between these traits. Therefore, the correlation between cross-rib spacing and BR value is likely due to this association between ridge and cross-rib spacing, as we do not expect the cross-ribs to directly affect colour.

Consistent with previous findings [9], *H. erato cyrbia* had closer ridge spacing than *H. erato demophoon* (table 6). Like the BR values, measurements of ridge spacing in the F_2 generation fell between the parental races (figure 12) and were fairly continuous, consistent with the action of multiple genes.

Table 6. Mean spacing (±s.d.) between longitudinal ridges and between cross-ribs. The narrower ridge spacing in *cyrbia* results in a brighter iridescent colour. The mean values for the F_1 and F_2 generations fell between the values for the parental races.

generation	mean longitudinal ridge spacing (nm)	mean cross-rib spacing (nm)	sample size (male, female)
demophoon/ hydara	926.05 ± 40.1	482.87 ± 37.1	5 (3, 2)
F_1	875.64 ± 57.8	476.66 ± 20.0	6 (4, 2)
F_2	876.25 ± 36.0	484.46 ± 35.0	59 (25, 34)
cyrbia	822.55 ± 30.8	494.82 ± 30.1	8 (5, 3)

Interestingly, ridge spacing in the F_1 generation was highly variable between individuals. This could indicate variation in epistatically acting alleles in the parental populations that segregate in the F_1 generation, or may suggest environmental effects. However, the phenotyped F_1 individuals in this comparison were from two different reciprocal crosses, with apparent differences between these two groups. Therefore, some of the variation that is observed may be due to cross-specific genetic effects and possibly sex linkage, but we have data from too few individuals to fully dissect these effects.

Cross-rib spacing in the F_2 generation appears to extend beyond the range of the parental races (figure 13), again possibly indicating epistatically acting alleles in the parental

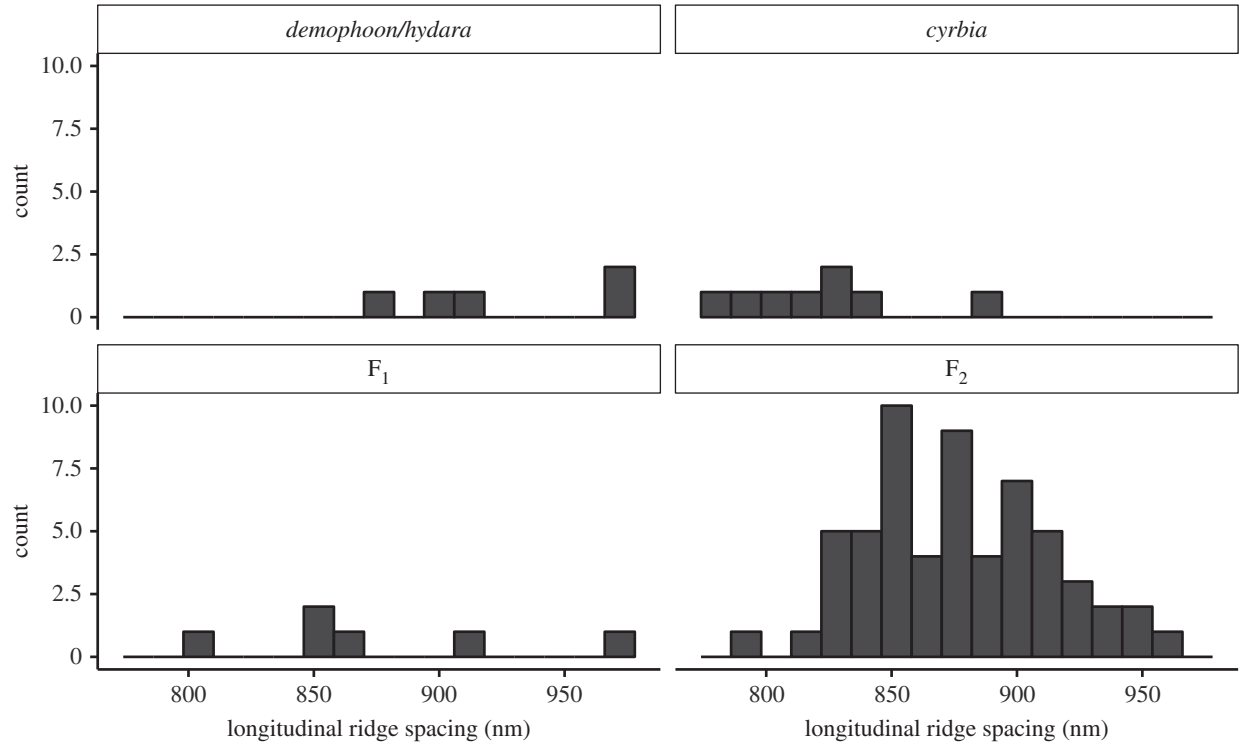

Figure 12. Variation in longitudinal ridge spacing in the F_2 suggests that it is controlled by multiple genes. In the F_1, those with an iridescent father had lower ridge spacing, reflecting the higher BR values seen in this cross.

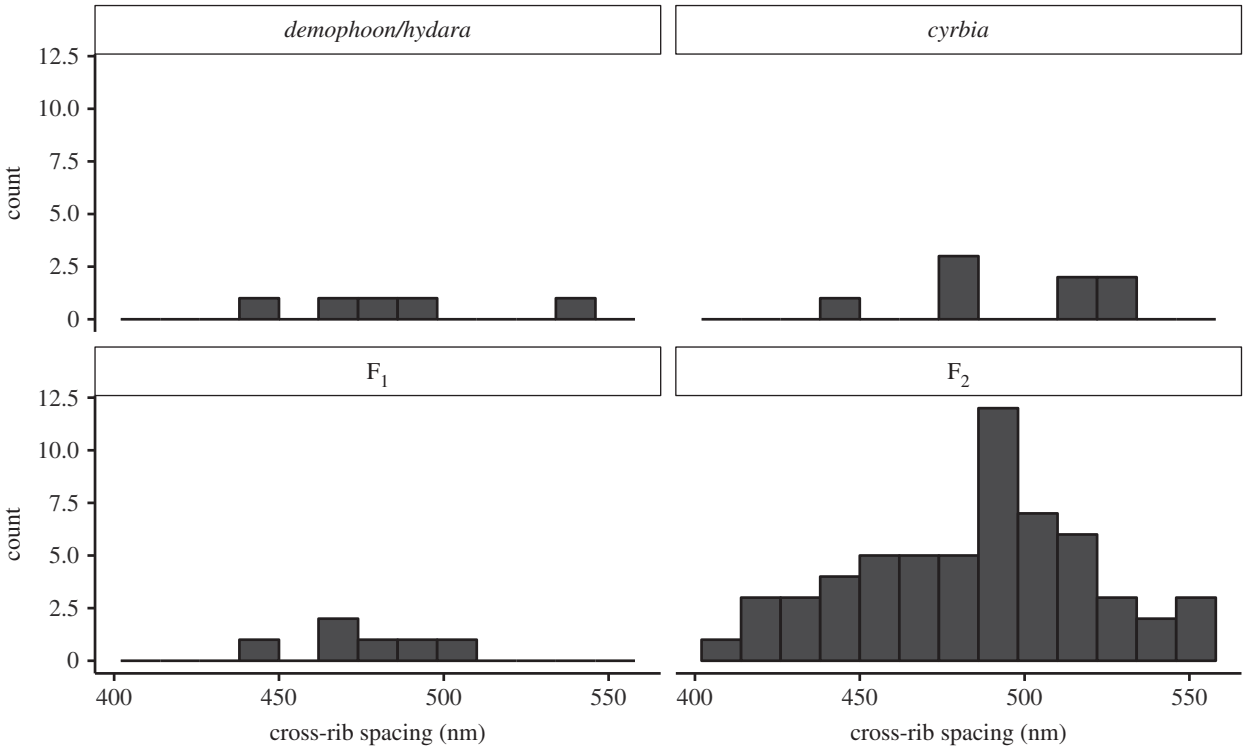

Figure 13. Cross-rib spacing also shows continuous variation in the F_2 generation and extremes extended beyond the values of the few parental individuals which were measured.

populations, although not all parental individuals were measured. Large variation in cross-rib spacing may be expected as it is not predicted to have an effect on colour, so may be under weaker selection. In the F_2 generation, males had narrower longitudinal ridge spacing than females, which was similar to the differences seen in this generation in blue values, and may suggest sex linkage of loci controlling ridge spacing ($t_{57} = 3.80$, $p < 0.001$; figure 14). Cross-rib spacing was also smaller in males ($t_{43} = 4.95$, $p < 0.001$), supporting the idea that ridge spacing and cross-rib spacing may be genetically correlated. However, in this case, we cannot rule out a contribution of autosomally mediated sexual dimorphism because we only have data from one F_2 cross. There was not a significant difference in ridge spacing between sexes in the parental populations (*hydara*/*demophoon* $t_{2.3} = 0.34$, $p = 0.77$; *cyrbia* $t_{4.4} = 0.53$, $p = 0.63$), but this may be due to small sample sizes and the differences were in the same direction as in the F_2, with females having larger

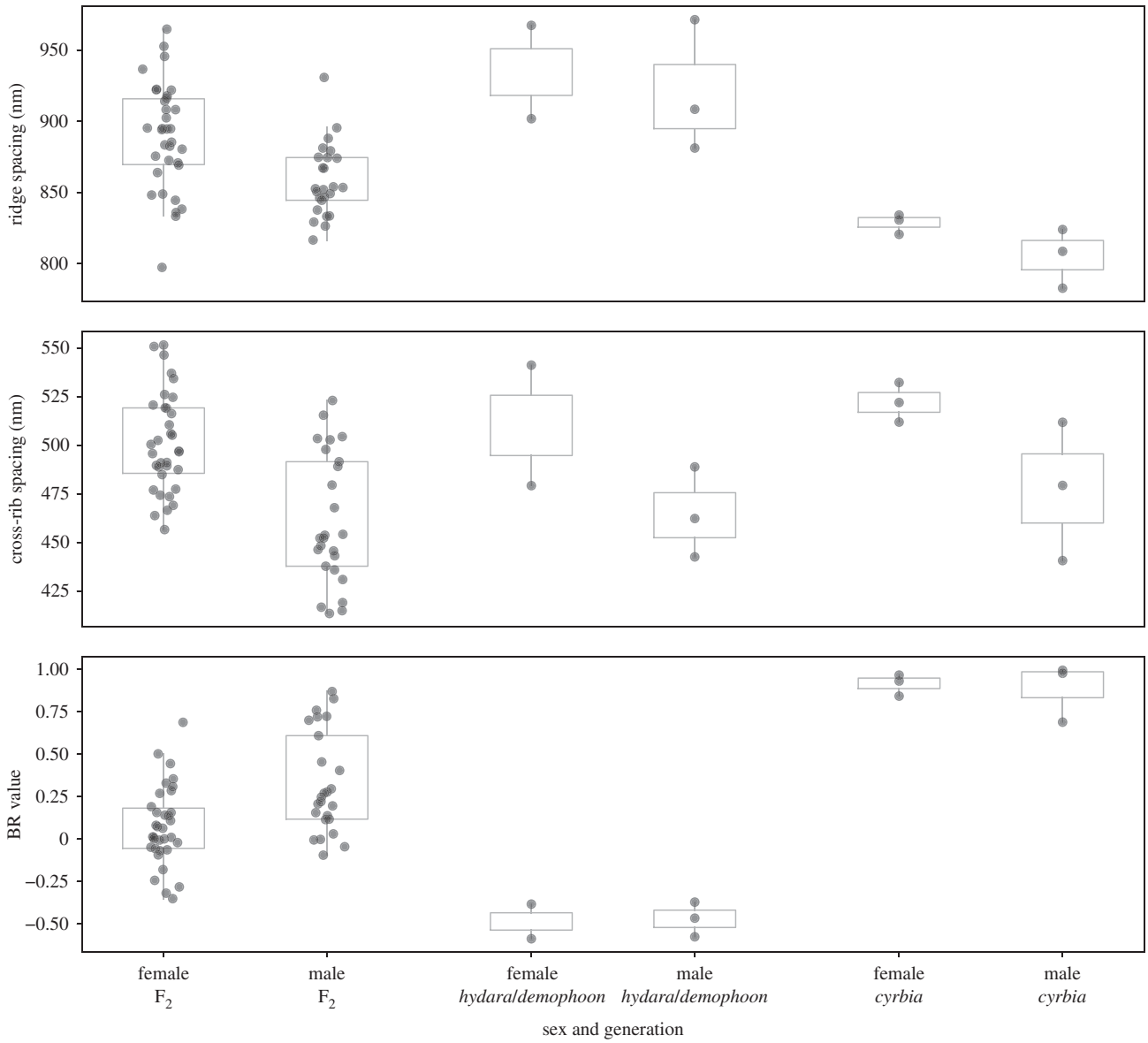

Figure 14. Males have narrower longitudinal ridge spacing than females in the F_2. This difference is less pronounced and not significant in the parental races. Significant differences in cross-rib spacing were seen in *cyrbia* and in the F_2, with males again having narrower spacing. These results are consistent with the finding that males have higher measures of blue colour.

spacing on average (figure 14). There was a significant difference in cross-rib spacing between sexes in *cyrbia* ($t_{5.6} = 3.42$, $p = 0.02$) but not in *hydara/demophoon* ($t_{1.4} = 1.35$, $p = 0.36$). Nevertheless, the differences in ridge spacing seen within the parental races are smaller than those seen in the F_2 generation, supporting a role for sex linkage. Using the wing measurements, there was not a significant difference in wing size between males (11.2 ± 0.5 mm) and females (10.9 ± 0.6 mm) in the F_2 ($t_{68} = -1.82$, $p = 0.07$), and in fact, males tended to be larger, suggesting that the increased ridge and cross-rib spacing in females is not due to overall sexual size dimorphism. Overall, ridge spacing appears to have a very similar genetic architecture to that of the BR colour values, suggesting that it is also controlled by multiple loci.

4. Discussion

Our phenotypic analysis of crosses between iridescent and non-iridescent races shows that iridescence is controlled by multiple loci in *H. erato* with convincing evidence for loci on the Z chromosome. There is an extensive history of using experimental crosses in *Heliconius* to investigate the genes controlling colour and pattern, but although iridescence had been shown to segregate in crosses, the trait has not been investigated due to the difficulty of quantifying the continuous phenotype and measuring the number of different features affecting the colour. We show that standardized photographs and the BR ratio is an effective method of estimating variation in blue iridescent reflectance. As expected, iridescent *H. erato cyrbia* gave the highest blue values, and non-iridescent *H. e. demophoon* the lowest. BR values correlated with longitudinal ridge spacing, which has previously been shown to have an effect on the brightness of the blue iridescent colour [9]. The distribution of blue values in the F_2 generation suggests that variation in the trait is not controlled by a single locus.

The differences in blue values found between sexes in the F_1 reciprocal *erato* crosses suggest that there could be a major effect locus involved in iridescent colour on the Z chromosome. We may expect that genes on the sex chromosomes will control sexually selected traits [32]. Reinhold [33]

calculated that in *Drosophila*, around a third of phenotypic variation in sexually selected traits was caused by X-linked genes, and that X-linked genes only influenced traits classified as under sexual selection. Iridescent structural colours are used as sexual signals in many butterfly species [2,34,35]. Work with *Colias* butterflies has found many wing pattern elements are sex-linked, including melanization, UV reflectance and yellow wing pigmentation [36,37]. These studies found that sex linkage was important in prezygotic isolation and species differentiation. Therefore, sex linkage of iridescence in *Heliconius* may have contributed to the differentiation of this trait between geographical races.

Unlike some Lepidoptera, *Heliconius* do not show complete sex chromosome dosage compensation. Analysis of *H. cydno* and *H. melpomene* gene expression showed a modest dosage effect on the Z chromosome, and overall reduced expression compared to autosomes [38]. Our results are also consistent with a lack of complete dosage compensation, with some evidence for expression of both Z chromosome alleles in males. A lack of dosage compensation could also favour the build-up of sexually selected or sexually antagonistic loci on the Z chromosome, as these will automatically be expressed differently between the sexes.

The three *erato* phenotypes controlled by the *Cr* locus did not show any correlation with iridescent colour values. The gene *cortex*, found in this genomic region, has been shown to underlie these colour pattern differences [16]. There are several reasons why major colour patterning genes could have been hypothesized to also control structural colour variation in *Heliconius*. Knockouts of one of the genes that control colour pattern in *Heliconius*, *optix*, in *Junonia coenia* butterflies resulted in a change in pigmentation, and the gain of structural colour [39], although this was not observed in the same tests with *H. erato*. In addition, linkage between divergently selected loci would be expected under 'divergence hitchhiking', in which genomic regions around key divergently selected loci are protected from recombination during speciation [40]. Hitchhiking regions can be small in natural populations unless recombination is reduced, but in Lepidoptera there is no recombination in the female germline. Furthermore, for highly polygenic traits, we would expect many loci to be distributed throughout the whole genome, so that for any genetic marker there will be some phenotypic association. Individuals with homozygous *Cr* phenotypes, for example, will have inherited an entire chromosome 15 from either an iridescent or non-iridescent grandparent, due to the lack of female recombination. Therefore, any combination of a single major effect locus or multiple smaller effect loci on chromosome 15 would have been seen as a difference in iridescence between individuals with different *Cr* phenotypes. The fact that we find no association with *Cr* suggests that structural colour is not highly polygenic, but controlled by a moderate number of loci, none of which are located on chromosome 15. It is also consistent with it being controlled independently of colour pattern. Similarly, we see no association with variation in forewing red band size, which is largely determined by the gene *WntA*. This region on chromosome 10 controls forewing band shape in multiple races of *H. erato*, as well as other *Heliconius* species [12].

In *Heliconius* pigment colour patterns, a small set of major effect genes have been well studied but a larger set of 'modifier' loci have also been found which adjust colour pattern [12]. It is possible that the iridescence genes have a similar distribution of effect sizes, with a small number of major effect genes, including one on the Z chromosome, and a distribution of other smaller effect genes. This supports the existing evidence of the importance of major effect loci in adaptive change [10–12]. Future work with the co-mimic of *erato*, *Heliconius melpomene*, will allow us to compare the genetic basis of iridescence between the two species. Following the two-step process of Müllerian mimicry described by Turner [41,42], a large effect mutation, such as the one we have found on the Z chromosome, allows an adaptive phenotypic change large enough for the population to resemble those in the mimicry ring and survive, then smaller changes will produce incremental improvements in mimicry.

Longitudinal ridge spacing also appears to have a polygenic architecture. The continuous variation that is observed in blue colour in the F_2 broods does not seem to be due to major effect loci with discrete effects on different aspects of scale structure. Rather it seems that multiple interacting genes are involved in controlling scale morphology. The correlation between ridge and cross-rib spacing suggests that some of these loci produce correlated effects on various aspects of scale morphology. However, the fact that we do not see a perfect correlation between these and blue colour suggests that there is some independent segregation of other aspects of scale morphology that contribute to the colour. Measurements of other aspects of scale morphology, such as ridge curvature and layering, will be needed to confirm this.

5. Conclusion

Crosses are ideal for investigating the genetic basis of colour and pattern as traits will segregate in following generations. Crossing iridescent and non-iridescent *H. erato* has allowed us to quantify variation in the colour and determine that it is sex-linked and controlled by multiple loci.

Data accessibility. SAXS data (doi:10.15131/shef.data.6839315) and accompanying code (doi:10.15131/shef.data.6837905) have been uploaded to an online repository. Colour measurements, repeatability measurements and cross pedigree information can be found as part of the electronic supplementary material.

Authors' contributions. M.N.B. collected the colour data, performed the genetic analysis and wrote the manuscript. J.E.R. analysed the SAXS data under the supervision of A.J.P. A.J.P. coordinated collection of the SAXS data. The crosses were performed by P.A.S., C.M., D.C., M.N.B., N.J.N. and E.V.C. The SAXS data were collected by A.J.P., T.Z., E.V.C., N.J.N. and M.N.B. Wing size and red band measurements were performed by H.E.B. The study was devised and coordinated by N.J.N. All authors read and commented on the manuscript.

Competing interests. We declare we have no competing interests.

Funding. This work was funded by the UK Natural Environment Research Council (NERC) through an Independent Research Fellowship (NE/K008498/1) to N.J.N. M.N.B. and E.V.C. are funded by the NERC doctoral training partnership, ACCE. J.E.R. is funded through the Leverhulme Centre for Advanced Biological Modelling as well as scholarships from Universidad del Rosario and the University of Sheffield.

Acknowledgements. We thank the governments of Ecuador and Panama for permission to collect butterflies. Thanks to Juan López and Gabriela Irazábal for their assistance with the crosses. We are grateful to the European Synchrotron Radiation Facility for provision of X-ray beamtime under proposal LS2720 and to Andrew Dennison for assistance with SAXS data collection.

References

1. Bálint Z, Kertész K, Piszter G, Vértesy Z, Biró LP. 2012 The well-tuned blues: the role of structural colours as optical signals in the species recognition of a local butterfly fauna (Lepidoptera: Lycaenidae: Polyommatinae). *J. R. Soc. Interface* **9**, 1745–1756. (doi:10.1098/rsif.2011.0854)
2. Sweeney A, Jiggins C, Johnsen S. 2003 Insect communication: polarized light as a butterfly mating signal. *Nature* **423**, 31–32. (doi:10.1038/423031a)
3. Hadley NF, Savill A, Schultz TD. 1992 Coloration and its thermal consequences in the New Zealand tiger beetle *Neocicindela perhispida*. *J. Therm. Biol.* **17**, 55–61. (doi:10.1016/0306-4565(92)90020-G)
4. Vukusic P, Sambles JR, Lawrence CR, Wootton RJ. 1999 Quantified interference and diffraction in single *Morpho* butterfly scales. *Proc. R. Soc. B* **266**, 1403–1411. (doi:10.1098/rspb.1999.0794)
5. Winter B, Butz B, Dieker C, Schröder-Turk GE, Mecke K, Spiecker E. 2015 Coexistence of both gyroid chiralities in individual butterfly wing scales of *Callophrys rubi*. *Proc. Natl Acad. Sci. USA* **112**, 12 911–12 916. (doi:10.1073/pnas.1511354112)
6. Dinwiddie A, Null R, Pizzano M, Chuong L, Leigh Krup A, Ee Tan H, Patel NH. 2014 Dynamics of F-actin prefigure the structure of butterfly wing scales. *Dev. Biol.* **392**, 404–418. (doi:10.1016/j.ydbio.2014.06.005)
7. Merrill RM *et al.* 2015 The diversification of *Heliconius* butterflies: what have we learned in 150 years? *J. Evol. Biol.* **28**, 1417–1438. (doi:10.1111/jeb.12672)
8. Wilts BD, Vey AJM, Briscoe AD, Stavenga DG. 2017 Longwing (*Heliconius*) butterflies combine a restricted set of pigmentary and structural coloration mechanisms. *BMC Evol. Biol.* **17**, 226. (doi:10.1186/s12862-017-1073-1)
9. Parnell AJ *et al*. 2018 Wing scale ultrastructure underlying convergent and divergent iridescent colours in mimetic *Heliconius* butterflies. *J. R. Soc. Interface* **15**, 20170948. (doi:10.1098/rsif.2017.0948)
10. Joron M *et al*. 2006 A conserved supergene locus controls colour pattern diversity in *Heliconius* butterflies. *PLoS Biol.* **4**, 1831–1840. (doi:10.1371/journal.pbio.0040303)
11. Baxter SW, Papa R, Chamberlain N, Humphray SJ, Joron M, Morrison C, ffrench-Constant RH, McMillan WO, Jiggins CD. 2008 Convergent evolution in the genetic basis of Mullerian mimicry in *Heliconius* butterflies. *Genetics* **180**, 1567–1577. (doi:10.1534/genetics.107.082982)
12. Papa R, Kapan DD, Counterman BA, Maldonado K, Lindstrom DP, Reed RD, Nijhout HF, Hrbek T, McMillan WO. 2013 Multi-allelic major effect genes interact with minor effect QTLs to control adaptive color pattern variation in *Heliconius erato*. *PLoS ONE* **8**, e57033. (doi:10.1371/journal.pone.0057033)
13. Nadeau NJ. 2016 Genes controlling mimetic colour pattern variation in butterflies. *Curr. Opin. Insect Sci.* **17**, 24–31. (doi:10.1016/j.cois.2016.05.013)
14. Emsley M. 1965 The geographical distribution of the color-pattern components of *Heliconius erato* and *Heliconius melpomene* with genetical evidence for the systematic relationship between the two species. *Zoologica* **49**, 245–286.
15. Lynch M, Walsh B. 1998 Analysis of line crosses. In *Genetics and analysis of quantitative traits*, pp. 205–250. Sunderland, MA: Sinauer Associates.
16. Nadeau NJ *et al*. 2016 The gene *cortex* controls mimicry and crypsis in butterflies and moths. *Nature* **534**, 106–110. (doi:10.1038/nature17961)
17. Martin A *et al*. 2012 Diversification of complex butterfly wing patterns by repeated regulatory evolution of a *Wnt* ligand. *Proc. Natl Acad. Sci. USA* **109**, 12 632–12 637. (doi:10.1073/pnas.1204800109)
18. Mazo-Vargas A *et al*. 2017 Macroevolutionary shifts of *WntA* function potentiate butterfly wing-pattern diversity. *Proc. Natl Acad. Sci. USA* **114**, 10 701–10 706. (doi:10.1073/pnas.1708149114)
19. Mallet J. 1989 The genetics of warning colour in Peruvian hybrid zones of *Heliconius erato* and *H. melpomene*. *Proc. R. Soc. B* **236**, 163–185. (doi:10.1098/rspb.1989.0019)
20. Abramoff, M.D., Magalhaes PJ, Ram SJ. 2004 Image processing with ImageJ. *Biophotonics Int.* **11**, 36–42.
21. Comeault AA, Carvalho CF, Dennis S, Soria-Carrasco V, Nosil P. 2016 Color phenotypes are under similar genetic control in two distantly related species of *Timema* stick insect. *Evolution* **70**, 1283–1296. (doi:10.1111/evo.12931)
22. Whitlock MC. 2007 *The analysis of biological data*, 1st edn. Greenwood Village, CO: Roberts & Company Publishers.
23. Cockerham CC. 1986 Modifications in estimating the number of genes for a quantitative character. *Genetics* **114**, 659–664.
24. Otto SP, Jones CD. 2000 Detecting the undetected: estimating the total number of loci inderlying a quantitative trait. *Genetics* **156**, 2093–2107. (doi:10.1007/s001220050781)
25. Mallet J. 1986 Hybrid zones of *Heliconius* butterflies in Panama and the stability and movement of warning colour dines. *Heredity* **56**, 191–202. (doi:10.1038/hdy.1986.31)
26. Baxter S, Johnston S, Jiggins C. 2009 Butterfly speciation and the distribution of gene effect sizes fixed during adaptation. *Heredity* **102**, 57–65. (doi:10.1038/hdy.2008.109)
27. R Core Team. 2018 *R: a language and environment for statistical computing*. Vienna, Austria: Foundation for Statistical Computing. See https://www.r-project.org.
28. Van Vaerenbergh P, Lonardon J, Sztucki M, Boesecke P, Gorini J, Claustre L, Sever F, Morse J, Narayanan T. 2016 An upgrade beamline for combined wide, small and ultra small-angle x-ray scattering at the ESRF. *AIP Conf. Proc.* **1741**, 030034. (doi:10.1063/1.4952857)
29. Newville M, Stensitzki T, Allen DB, Ingargiola A. 2014 LMFIT: non-linear least-square minimization and curve-fitting for Python. *Zenodo*. (doi:10.5281/zenodo.11813)
30. Lande R. 1981 The minimum number of genes contributing to quantitative variation between and within populations. *Genetics* **99**, 541–553.
31. Mather K, Jinks JL. 1982 *Biometrical genetics*, 3rd edn. Cambridge, UK: Cambridge University Press.
32. Fairbairn DJ, Roff DA. 2006 The quantitative genetics of sexual dimorphism: assessing the importance of sex-linkage. *Heredity* **97**, 319–328. (doi:10.1038/sj.hdy.6800895)
33. Reinhold K. 1998 Sex linkage among genes controlling sexually selected traits. *Behav. Ecol. Sociobiol.* **44**, 1–7. (doi:10.1007/s002650050508)
34. Kemp DJ. 2007 Female butterflies prefer males bearing bright iridescent ornamentation. *Proc. R. Soc. B* **274**, 1043–1047. (doi:10.1098/rspb.2006.0043)
35. Rajyaguru PK, Pegram KV, Kingston ACN, Rutowski RL. 2013 Male wing color properties predict the size of nuptial gifts given during mating in the Pipevine Swallowtail butterfly (*Battus philenor*). *Naturwissenschaften* **100**, 507–513. (doi:10.1007/s00114-013-1046-1)
36. Silberglied RE. 1979 Communication in the ultraviolet. *Annu. Rev. Ecol. Syst.* **10**, 373–398. (doi:10.1146/annurev.es.10.110179.002105)
37. Ellers J, Boggs CL. 2002 The evolution of wing color in *Colias* butterflies: heritability, sex linkage, and population divergence. *Evolution* **56**, 836–840. (doi:10.1111/j.0014-3820.2002.tb01394.x)
38. Walters JR, Hardcastle TJ, Jiggins CD. 2015 Sex chromosome dosage compensation in *Heliconius* butterflies: global yet still incomplete? *Genome Biol. Evol.* **7**, 2545–2559. (doi:10.1093/gbe/evv156)
39. Zhang L, Mazo-Vargas A, Reed RD. 2017 Single master regulatory gene coordinates the evolution and development of butterfly color and iridescence. *Proc. Natl Acad. Sci. USA* **114**, 10 707–10 712. (doi:10.1073/pnas.1709058114)
40. Via S, West J. 2008 The genetic mosaic suggests a new role for hitchhiking in ecological speciation. *Mol. Ecol.* **17**, 4334–4345. (doi:10.1111/j.1365-294X.2008.03921.x)
41. Turner J. 1977 Butterfly mimicry: the genetical evolution of an adaptation. *Evol. Biol.* **10**, 163–206.
42. Turner JRJ. 1981 Adaptation and evolution in *Heliconius*: a defense of NeoDarwinism. *Annu. Rev. Ecol. Syst.* **12**, 99–121. (doi:10.1146/annurev.es.12.110181.000531)